Characterizing the role of Ephrin Eph signaling on tissue separation in Xenopus Laevis

Nazanin Rohani Larijani

Doctorate of philosophy

Department of Biology

McGill University
Montreal, Quebec, Canada
Dec. 11, 2013

A thesis submitted to McGill University in partial fulfillment of the requirements of the degree of Doctor of Philosophy.

Acknowledgments

I have always had this belief that words do not have the capacity to express ones feelings at its entirety. Many people don't agree on that but the truth is that, I feel desperate writing this page, it is really difficult to find appropriate words that would reflect my true gratitude for these great people in my life:

Dr. Francois Fagotto, who is beyond a supervisor for me; he is in addition, like a caring father, a superb friend and an influential mentor in my life. His flourishing thoughts not only toward science but also in life have guided me throughout every step of this path.

Also I want to express my special thanks to Dr.Rudolf Winklbauer for his kindness and bright ideas that has facilitated the fulfilment of this project.

My family and friends, whose support and presence has cheered me up in these years: Minoo, Saeed, Shirin, Matin, Amin, Naghme, Nargess, Matin Mohammad, Ava and my little Tara...

Farhad…..

Anne Sophie & Francois

Mina

Laura, Nadim, Xioyong, Katrina, Zoe, Leily and many other nice people at McGill, whose generous help and guidance have greatly contributed to the realization of this thesis.

In the end, I am thankful of both my supervisors and my committee members Dr. Nathalie Lamarche and Dr. Frieder Schock for being always there for me, without their critical and instructive thoughts this would not have been accomplished.

Contributions

Chapter I: A critical review of the literature relevant to my research on the topics of boundary formation and ephrin-Eph signaling. I researched and wrote this chapter with guidance and consultation from my supervisor, Dr. Francois Fagotto.

Chapter II: "EphrinB/EphB Signaling Controls Embryonic Germ Layer Separation by Contact-Induced Cell Detachment" is published in PloS Biology. Authors: **Rohani N**, Canty L, Luu O, Fagotto F, Winklbauer R 2011. The figures 1(E, F, G), 2 C, 3,4,6,8, S3, S4 (except last column in C), S5 (A, B, C, D), S6 (B) were conducted, analyzed and interpreted by me. Figures 5, S6A, S7 were conducted and analyzed by L.Canty. Figures 7(A, B, C wt meso and ecto was conducted by L.Canty and COMO, EphMO and eprhinMO was done by me), item D is based on the quantification of pulled data by L.Canty and me. Figure S5E is based on the quantification of pulled data from L.Canty and me. O.Luu conducted and analyzed Figure S2. R.Winklbauer conducted and analyzed Figure 2(A, B) and S4C (last column). F.Fagotto conducted experiments for Figure1 (A, B, C, D) and S1. F.Fagotto and R. Winklbauer share the co-last authorship on this paper and participated equally to the writing of the text and design of the experiments. I conducted, designed and interpreted the results and contributed to the writing and preparation of the manuscript.

Chapter III: "Variable combinations of specific ephrin ligand/Eph receptor pairs control embryonic tissue separation" is submitted to PloS Biology and is currently being revised. Authors: **Nazanin Rohani**, Rudolf Winklbauer and François Fagotto 2013. I conducted, analyzed, designed and interpreted all experiments except Figures 1A, 6, S1D and S4 and contributed to the writing and the preparation of the manuscript. The simulation of ephin-Eph signaling (found in figures 6, S4) was conducted by F.Fagotto. R.Winklbauer conducted the experiment for figure 1A and contributed to critical reading and the writing of the text. F.Fagotto designed experiments and wrote the text.

ChapterIV: “A Molecular Base for Cell Sorting at Embryonic Boundaries: Contact Inhibition of Cadherin Adhesion by Ephrin/Eph-Dependent Contractility” is publish in Developmental Cell. Authors: François Fagotto*, **Nazanin Rohani***, Anne-Sophie Touret and Rui Li (2013). Co-first authorship is shared with F.Fagotto who conducted, analyzed and interpreted experiments in figures:1(A,B,D,E), 2(A,B,C), 3,5(D,E),S1,S2,S3,S4(B,C,D,E,F) and wrote the text. I conducted, analyzed and interpreted the experiments in figures: 1(C, F), 2(D, E), 4, 5(F, G), 6, 7B, Table 1, S4A, S5 and contributed to the writing and preparation of the manuscript. A.Touret and R.li conducted the experiments in Figure 5(A, B, C). A.Touret was involved in the critical reading of the text.

ChapterV: A discussion of the core findings in this thesis. I wrote this chapter with the guidance and consultation from my supervisor, Dr. Francois Fagotto.

Table of contents

List of Figures:

Abstract

As they acquire distinct fates, embryonic cell populations become separated by sharp boundaries. Several theories have been proposed to explain this astonishing phenomenon, which remains very poorly understood. This study investigates tissue separation at the cellular and molecular level, using the gastrulating Xenopus embryo as a model. At this developmental stage, boundaries divide the embryo into its basic body structures, starting with separation of the germ layers, followed by the separation of presomitic mesoderm from notochord. Live cell microscopy at these boundaries revealed a contact-mediated repulsion mechanism that is controlled by a combination of several Eph receptors and their ephrin ligands. Loss and gain of function approaches suggest that ephrin-Ephs interact selectively and not promiscuously. They are expressed in a partially complementary pattern on both sides of the boundary. Integration of signals from those pairs reaches maximum intensity at the tissue interface. This phenomenon was simulated computationally based on relative ephrin and Eph concentrations as well as binding affinities. Despite differences in the expression profile of ephrins and Ephs at various boundaries, our model holds true. The underlying cytoskeletal mechanism downstream of ephrin-Eph-mediated cell contraction was investigated further. We found that repulsive events and membrane contraction made the cell membranes less permissive to form stable adhesive bonds, resulting in a state of loose adhesion – as indicated by the smooth appearance of Cadherins at the boundary. This thesis provides a novel understanding of ephrin-Eph control of tissue boundaries. It also has a direct impact on deciphering their intricate role in tumor cell metastasis and invasion.

Résumé

Au cours du développement embryonnaire, la différenciation cellulaire entraîne la mise en place de frontières nettes afin de séparer les différentes populations de cellules qui se dessinent. Plusieurs théories ont tenté d'expliquer ce phénomène fascinant, qui demeure mal compris. La présente étude s'appuie sur la gastrula de Xénope afin d'examiner le processus de séparation des tissus aux niveaux cellulaire et moléculaire. A ce stade du développement, des frontières divisent d'abord l'embryon en trois couches de feuillets embryonnaires, puis séparent la notocorde du mésoderme présomitique. L'imagerie de ces frontières sur des cellules vivantes a révélé un mécanisme de répulsion cellulaire, qui serait contrôlé par une combinaison de plusieurs types de récepteurs Eph et de leurs ligands, les éphrines. Nous montrons à la fois par perte et par gain de fonction que les éphrines interagissent avec les récepteurs Eph de manière sélective, et non pas aléatoire. L'expression de ces protéines de part et d'autre des frontières suit un schéma de complémentarité partielle. L'intégration des signaux générés par les paires d'éphrine-Eph produit une réaction d'amplitude maximale aux interfaces entre les tissus. Nous proposons une simulation numérique de ce phénomène de signalisation intégrée, sur la base des concentrations relatives d'éphrines et d'Ephs, ainsi que de leurs affinités de liaison. Cette simulation semble valide pour modéliser de nombreuses frontières embryonnaires, et ce malgré la variabilité des profils d'expression des éphrines et Ephs à ces différentes frontières. Nous avons également étudié les modifications du cytosquelette en aval de la voie de signalisation éphrine-Eph, qui entraîne la contraction cellulaire. Nos résultats indiquent que les instances de répulsions cellulaires, en conjonction avec la contraction membrannaire, entravent la formation de liaisons adhésives stables entre les cellules. Ceci engendre un état d'adhérance faible, se traduisant par l'apparance lisse des Cadhérines le long des frontières embryonnaires. La présente thèse apporte une compréhension nouvelle du rôle de la voie de signalisation éphrine-Eph dans la régulation des frontières entre différents tissus. Ces trouvailles promettent également d'éclairer l'étude du rôle de ces molécules dans l'invasion et la métastase de tumeurs.

Chapter I: Introduction

The transformation of embryo from an unstructured ball of cells into a well-organized layered body proceeds by successive patterning events that dictate specific fates to progressively smaller and refined regions. Whether transient or permanent, each genetically defined subdivision is almost systematically consolidated by a physical separation. The adjacent cell populations thus become stably delimited by boundaries, which are completely impermeable to cell migration either in form of proliferative events or morphological movements (Krens, & Heisenberg, 2011). Boundaries are found at all developmental stages and throughout metazoans, indicating that they are generally essential for development of multicellular animal organisms. Boundaries can separate distinct tissues, but also divide the plane of a single cell layer. Both cases are found in the simplest example of a diploblastic Hydra, where the outer ectoderm layer and inner endoderm layer must remain separated, and transversal boundaries divide the both layers along the axis of the body column into head and foot structures (Angelika bottger, 2012). The necessity for such separation mechanisms is most obvious during processes that involve massive cell migration, such as vertebrate gastrulation or development of the nervous system (Dahmann, Oates, & Brand, 2011; Lila Solnica-Krezel & Sepich, 2012).

Modes of Boundary Formation

There are two basic modes of boundary formation; boundaries either arise from the partitioning of a region into two new domains, or they appear by apposition of two cell populations brought into proximity by morphogenetic movements (Figure 1.1). As discussed below, the mechanisms preventing cell mixing in each of these two cases may not be fundamentally different. The processes that set the position and properties of the cell types are however quite distinct:

In the former mode, where a field of cells becomes partitioned without any major movement, the position of the interface is typically set by patterning signals emanating from both cell populations, which establish a crosstalk and provide positional information. This mechanism is often extremely precise, and the interface can be, in some cases, marked by a single row of cells with unique gene expression (e.g. Drosophila parasegments and imaginal discs) (Dahmann et al., 2011). The cell genetic identities can either be acquired by inheritable mechanisms transmitted through the lineage or can, on the contrary, depend on the position of the cell. In the first case, each cell stably inherits all the properties of the corresponding cell type, including those required to restrict cell movements and create a boundary. As a consequence, all cells are capable of "sorting", independently of their position, and thus do not need to constantly receive patterning information. The sharp physical boundary is generally formed almost simultaneously to the appearance of the corresponding genetic pattern. These so-called compartment boundaries are frequent in Drosophila. For example, they divide the wing and the leg imaginal discs along the anterior-posterior and the dorsal-ventral axes. They are also found in vertebrates, e.g. in the hindbrain, which becomes segmented in a series of compartments called the rhombomeres. The genetic division into different domains is not always so strict and definitive, but can sometimes be much more plastic. There are indeed cases where cells constantly receive patterning information from neighboring cells. The maintenance of gene expression profile and the separation mechanism is consequently not heritable, at least not until a stable physical separation is established. Until then, if an individual cell happens to be translocated to a new position, it will change its gene expression profile to match its neighbors. An example is the boundary between somitic segments: pre-patterns are first created by Mesoderm Posterior transcription factor, which defines the final position of somitic boundaries. The actual mechanism of separation is acquired later, and the boundary does not appear until cells have established a stable gene expression profile.

A fundamentally different type of boundary forms when two distinct tissues are brought into apposition. This process involves large scale rearrangement of cell populations, and the resulting boundary typically appears as a robust, morphologically visible structure, cleft or fold. A typical example is the separation of the germ layers during gastrulation. Note, as it will be presented later, that morphogenetic movements that lead to this apposition may involve compact masses (e.g. mesoderm involution in amphibians) but also sorting of individual cells (e.g. mesoderm ingression in sea urchin).
Despite this diversity of mode of formation, ultimately all boundaries share the same function of barrier to prevent cell mixing between adjacent cell populations. The molecular mechanisms that determine the location of these boundaries have been studied but the mechanisms that generate them are not quiet understood. Also whether each type of boundary may rely on a specific mechanism, or whether common properties may be identifiable is an important question to which this study has attempted to bring some answers.

Gastrulation: emergence of tissues, necessity for separation

Gastrulation refers to a series of cell movements through which a ball of cells called the blastula is transformed into a multilayered structure, constituted of the three germ layers, ectoderm, mesoderm and endoderm, which are the precursors of all tissues. By the end of gastrulation, these three germ layers have reached the positions characteristic of the typical triploblastic organization, with the ectoderm on the outside, the endoderm in the center, and the mesoderm filling the space between the two other layers. Gastrulation involves a set of cellular movements conserved in all animals, which includes invagination, epiboly and intercalation. Different organisms use various combinations of these basic cell behaviors, which produce an astonishing variety of modes of gastrulation, which all result in one way or the other into the inward translocation of mesoderm and endoderm. For instance, in sea urchin, birds or mammals, single cells ingress to position inside the embryo, while in amphibian and fish embryos, mesoderm cells involute as a

whole mass. In the former case, single ingressing cells must gather together to form the mesoderm mantle, a process that can be qualified as cell sorting. In the latter case, the mesoderm constitutes at all times a coherent tissue and gastrulation positions it directly opposed to inner side of the ectoderm layer. Here tissue separation involves mostly stable maintenance of this new tissue interface. Note that irrespective of the mode of gastrulation, the inward movement of the mesoderm involves a transformation equivalent to epithelial-to-mesenchymal transition (EMT). The high migratory property of mesoderm precursors raises the need for an efficient mechanism of separation that is particularly important compared for example to compartmentalization of a much less dynamic ectoderm sheet, such as the parasegments of the insect blastoderm. Not surprisingly, interference with ectoderm-mesoderm separation has dramatic effects on gastrulation and in consequence on the whole basic organization of the embryo. Besides the fundamental interest of studying morphogenesis of the primordial germ layers, the severity of the phenotypes makes the model particularly attractive (Lila Solnica-Krezel & Sepich, 2012).

The concept of tissue affinities and the models of separation

Tissue affinities

The first hints for how embryonic tissues may separate from each other came from the pioneer experiments of Holtfreter and Towns (Townes & Holtfreter, 1955;Holtfreter, 1939). They had the original idea to reconstitute segregation by mixing cells from different dissociated tissues. Using the germ layers from gastrulating amphibian embryo, they observed that cells would “sort” from the initial mixed aggregates and segregate into distinct populations. Each population developed the typical signs of differentiation of the corresponding tissues and formed histologically recognizable structures very similar to those formed in a normal embryo. Furthermore, the relative position of the tissues was strikingly mimicking the normal organization of the embryo, with cells derived from the

ectoderm and the neuroderm on the outside, endoderm in the center, and mesoderm in between. These results suggested that each cell carries information that dictates which tissue it belongs to and which other cell type it should separate from. In other words cells display different "affinities" for different cell types (Townes & Holtfreter, 1955;Holtfreter, 1939).

The molecular nature of these hypothetical affinities remained unknown, but several studies have attempted to assign them to more specific cellular properties. The most famous interpretation of Holtfreter and Towns experiments was suggested by Steinberg, who stated that these differential affinities could be explained as differences in cell-cell adhesion. The prediction from this model was that the strongest adhering cells would tend to cluster and segregate from less adhering cells (Harris, 1976; M. Steinberg & Takeichi, 1994; M. S. Steinberg, 1970). This notion was then linked to physical properties of cells such as cortical tension, discussed in the next sections (Brodland, 2002; Graner & Glazier, 1992; Harris, 1976).

An alternative explanation would be that the information which directs separation is generated by cell signaling. Specific cell surface receptors would act as sensors which would detect the identity of surrounding cells in the form of soluble secreted molecules (such as EGF, Wnt, Hedgehog) or directly by direct cell-cell contact (Notch, ephrins)(Irvine, 1999; Schilling et al., 2011; Tepass, Godt, & Winklbauer, 2002; Rudolf Winklbauer & Luu, 2009; R. Winklbauer, Medina, Swain, & Steinbeisser, 2001; Zecca & Struhl, 2002). The signal triggered by these molecules would affect cell-cell adhesion or actin cytoskeleton, create differences between cell types and separate them (Tepass et al., 2002; Wacker, Grimm, Joos, & Winklbauer, 2000). It was proposed that Hedgehog (Hh) signaling, which controls anterior/posterior separation of wing disc in Drosophila, modulates cell adhesion indirectly through controlling the level of a cell adhesion molecule called cadherin66 at the transcriptional level (Cheng et al., 2004; Dahmann & Basler, 2000; Irvine, 1999; Tepass et al., 2002). In vertebrate hindbrain, cell intermingling between adjacent segments "rhombomeres" is restricted due to differential ephrin and Eph expression. Furthermore the

differential expression and perhaps differential signaling inside each rhombomere may generate distinct properties for cells on each side of the border.
I briefly review here each of the major hypothetical models for separation.

Differential adhesion hypothesis

In this model cells are considered to behave similar to molecules of fluid, they tend to adhere to each other to minimize their free surface energy (M. S. Steinberg, 1963, 1970). Each type of embryonic tissue has a unique "tissue surface tension" that governs how tissues sort, similar to how fluid surface tension governs de-mixing of immiscible liquids. The level of surface tension is a linear function of adhesion energy. In every system where two adherent tissue cells are mixed, the tissue with lower surface tension and lower adhesion, always envelopes the other tissue. This form of cellular behaviour agrees with the cell sorting observed in Holtfreter's experiments (Ramsey A. Foty, Forgacs, Pfleger, & Steinberg, 1994; R.A. Foty, Steinberg, & . 2004; Phillips, 1978). This so-called Differential Adhesion Hypothesis (DAH) was supported by experiments showing that dissociated tissue cells from different organs of chicken re-aggregated in a manner that would conform to the hierarchy of their adhesiveness (M. Steinberg & Takeichi, 1994; M. S. Steinberg, 1963, 1970).
In the original hypothesis, cell sorting was suggested to depend on differences in the level of adhesiveness. After the discovery of the existence of various adhesion molecules, both differences in the level and types of adhesion were proposed to generate sorting (Redies & Takeichi, 1996; Thiery, Duband, Rutishauser, & Edelman, 1982). This led to the proposal of two distinct variations of the original hypothesis: quantitative and qualitative DAH (Takeichi, 1988; Takeichi, 1995). The qualitative differential adhesion relies on the fact that homophilic adhesion between same adhesion molecules is stronger than heterophilic adhesion between different adhesion molecules. Thus expression of different adhesion molecules would account for sorting of different cell types (Redies & Takeichi, 1996; Takeichi, 1988; Takeichi, 1995). This notion was tested in vitro by expressing E-

and P-cadherins in L cells, a type of mouse fibroblast which is normally non-adherent. Transfected cells preferentially adhered to cells expressing the same cadherin subclass. In vivo support for the qualitative differential adhesion was shown in the mouse brain; the expression of different types of cadherin (cadherin6 and R-cadherin) in the mouse telencephalon was involved in the boundary that forms between the cortex and the striatum (Inoue et al., 2001).

The quantitative DAH however, argued that the observed sorting of cells with different types of adhesion molecules was in fact not due to the particular type of cell adhesion molecule expressed, but to the relative strength of adhesiveness, depending largely on the expression levels. This was tested in vitro: Stably transfected L cells were selected to express different levels of E-cadherin, P-cadherin or N-cadherin. Clones of these cells were then allowed to aggregate. Even a slight difference in the expression level of a given cadherin was sufficient to cause two otherwise identical L cell populations to sort out (Ramsey A. Foty & Steinberg, 2013).Sorting between cells expressing different types of cadherin also depended only on the relative adhesive strength (thus the expression levels) of each cell population. Irrespective of the type of cadherin expressed, the less adhesive cells always enveloped the other cell population (Ramsey A. Foty & Steinberg, 2013; Nose, Nagafuchi, & Takeichi, 1988). These findings were further supported by in vivo experiments in Drosophila, where differences in levels of DE-cadherin between the anterior and posterior part of the wing imaginal disc are required for the formation of the boundary (Ramsey A. Foty & Steinberg, 2013; McNeill, 2000; Schlichting, Demontis, & Dahmann, 2005). Note, however, that these cells failed to sort in an in vitro dissociation assays (Dahmann & Basler, 2000).

Differential cortical tension hypothesis

While the DAH seemed to be capable of explaining the sorting behaviour of different cell types, some aspects of this theory have been subjected to criticism. The leading assumption in the DAH is that cells are considered to sort based on

the same thermodynamic principles that is applied to molecules of liquids. However this cannot be completely accurate for several reasons: The interactions between cells are fundamentally different from molecular interactions in liquids. One of the differences that makes the analogy questionable is the fact that live cellular systems consume energy and are thus not at equilibrium. As a consequence, adhesion and de-adhesion may not be necessarily considered as mirror aspects of a reversible reaction. In addition, while molecules of a fluid are attracted to each other by electrostatic forces of van der waals bonds, the adhesion forces between cells are not necessarily sufficient to bring cells together. In fact some types of adhesion can only form after the cells have made their initial contact. This again supports the idea that de-adhesion energy is not equal to adhesion/attraction energy. Another problem is the difference in the distribution of adhesion molecules: adhesion molecules on cell surface can be either mobile or localized at fixed locations on the cell surface. Thus maximizing contact area does not necessarily translate to maximizing adhesion because adhesion only fills a small fraction of cell surface area (Brodland, 2002; Graner & Glazier, 1992; Harris, 1976).

The above criticisms gave rise to an alternative theory, called the Differential Interfacial Tension Hypothesis (DITH): Harris (Harris, 1976) proposed that surface tension is derived from a contractile layer on the cell surfaces. Cells with different levels of contractility sort accordingly, with the most contractile cell-aggregate engulfed by the least contractile aggregate. In this model, the interface has an intermediate level of contractility. This theory was able to satisfactorily explain Holtfreter's and Steinberg's findings. It was at least indirectly supported by experimental evidence: The in vitro cortical tension measurement of cells, from the three germ layers of the Zebrafish embryo revealed differences which may account for their separation (Beysens, Forgacs, & Glazier, 2000; G. S. Davis, Phillips, & Steinberg, 1997; Krens, Möllmert, & Heisenberg, 2011; Krieg et al., 2008; Maître et al., 2012; Phillips, 1978). Alternatively, one could also conceive a model where the cell contractility would act locally, specifically increasing interfacial tension at the interface of the two cell populations. One has indeed

observed increased actomyosin activity along the dorsal-ventral (D/V) and anterior-posterior (A/P) boundaries in Drosophila wing (Major & Irvine, 2005, 2006), as well as along the early parasegmental boundaries (Monier, Pelissier-Monier, Brand, & Sanson, 2010). Direct experimental interference with myosin at the boundary showed that it is required to maintain straight boundaries (Aliee et al., 2012; Monier et al., 2010).

Some aspects of the in vitro cell sorting experiments that were used to support the DITH were criticized. It was noted in particular that the use of actin depolymerizing drugs to disrupt the contractile network could also interfere with adhesion (Sanger & Holtzer, 1972; M. S. Steinberg & Wiseman, 1972). Cell surface adhesion molecules are indeed directly connected to actin cytoskeleton via catenin complexes. Adhesion appears intimately intertwined with the cytoskeleton, with links in both directions: For instance, adhesion can act as a sensor of mechanical tension (Gumbiner, 2005; Twiss et al., 2012). Thus discrimination between DAH and DITH turned out not to be trivial. Cortical contractility and adhesion may cooperate to orchestrate the processes of adhesion, de-adhesion, contraction and sorting, and the two theories may represent two partial interpretations of a single integrated process (Cavey, Rauzi, Lenne, & Lecuit, 2008; Harris, 1976; Manning, Foty, Steinberg, & Schoetz, 2010; Ninomiya et al., 2012; Nose et al., 1988; Tepass et al., 2002; Rudolf Winklbauer & Kwang, 2009).

Contact inhibition of movement

More than four decades ago Abercombie and Heasman put forward the concept of contact inhibition of movement (Abercrombie, 1970). The phenomenon was discovered in an in vitro experiment where two embryonic chicken heart explants were placed in close proximity. As migrating cells coming from opposite explants collided, they halted. The events were later described at the level of cell behaviour: Upon contact, the expanding protrusions at the front of the migrating cells would rapidly retract (Couchman & Rees, 1979). The first demonstration that this process could mediate cell sorting was made on culture cells expressing ephrins

and Eph receptors (Batson, Astin, & Nobes, 2013; Mellitzer, Xu, & Wilkinson, 1999; Poliakov, Cotrina, & Wilkinson, 2004). Contact between the protrusion of an Eph-expressing cell and an ephrin-expressing cell would cause collapse of the actin cytoskeleton and rapid retraction of the protrusion. Eventually, these repulsions would cause Eph-expressing cells to cluster away from ephrin-expressing cells and sort. A general model based on this type of behavior is an obvious alternative to DAH and DITH. As discussed below, there is a large body of evidence for the participation of ephrins and Ephs at vertebrate boundaries. The fundamental difference between the differential adhesion, tension or contraction hypotheses and the model of contact inhibition is that the former assume that the sorting process depends on intrinsic differences in the biophysical properties of each cell type, while the latter considers local events induced specifically at contacts between different cell types.

Sorting versus boundary formation

Cell sorting and boundary formation have been for long considered conceptually equivalent. Both certainly convey the idea of "separation" of two groups of cells. However it is important to acknowledge that the two terms describe in fact distinct processes, a distinction that may have important consequences for our understanding of the underlying mechanisms. Sorting refers to segregation from an originally mixed population into distinct domains (clustering). This process does not presume absolute isolation of the two cell types and is not necessarily associated with a particular morphology of the resulting interface. A boundary however, refers to a stable interface permanently separating two cell populations. This implies that cell intercalation across the boundary is absolutely inhibited. As a rule, boundaries are sharp and generally smooth interfaces. These properties are not necessarily achieved by cell sorting, although in some cases, including the original Towns and Holtfreter experiments, mix aggregates can resolve into tissues separated by bona fide boundaries (Chen & Gumbiner, 2006; S.-H. Kim,

Jen, De Robertis, & Kintner, 2000; Tepass et al., 2002; Rudolf Winklbauer & Luu, 2009).

Unfortunately the models that have so far attempted to describe the mechanism of separation never clearly distinguish between the two concepts of sorting and boundary formation. I would speculate, however, that those mechanisms which depend on global intrinsic properties of cell populations (like DAH) could drive an initial coarse sorting of cell populations, which would then be more sharply separated by mechanisms that generate local cellular changes at contacts between cells of different types.

Boundary formation in vertebrates

The studies of boundary formation in vertebrates have focused mainly on three models, two of which are segmentation processes: somitogenesis in the paraxial mesoderm (Durbin et al., 1998; Saga & Takeda, 2001) and the formation of the rhombomeres in the hindbrain (J. E. Cooke & Moens, 2002; S. Guthrie & Lumsden, 1991; Sela Donenfeld, Sela Donenfeld, Kayam, & Wilkinson, 2009), the third one being the separation of embryonic germ layers originally studied by Holtfreter, and more recently revisited in Xenopus and in Zebrafish (Krens, et al., 2011; Kühl & Wedlich, 1996; Murakami, Hijikata, Matsukawa, Ishikawa, & Yorifuji, 2006; Townes & Holtfreter, 1955; Wacker et al., 2000;(Holtfreter, 1939). Some work has also been done on the notochord boundary (Keller et al., 1989; Reintsch, Habring-Mueller, Wang, Schohl, & Fagotto, 2005).

Somite boundaries

Somites represent the major segmented pattern that characterizes the body plan of vertebrates. Somite segmentation has been since years a classical model for boundary formation. The process involves three distinct steps: pre-patterning of the paraxial mesoderm, also called presomitic mesoderm (PSM), boundary formation and patterning within the somite itself. The PSM appears as two

parallel elongated cell masses on both sides of the notochord. Pairs of somites synchronously bud off the anterior end of these two structures in a periodic manner (Figure 1.2A). The process of restricting the position of each somite requires well synchronized cycles of gene activation controlled by a crosstalk between FGF, Notch and Wnt pathways (Durbin et al., 1998; Jiang et al., 2000; Yasuo & Lemaire, 2001). Notch activation is further involved in defining the anterior and posterior parts of each somite segments (Jiang et al., 2000; Pourquié, 2001; Saga & Takeda, 2001). Borders of gene expression between cells with anterior and posterior identities become subsequently translated into morphological furrows. The formation of these physical boundaries requires ephrinB2-EphA4 interactions at the interface between the posterior cells of the new somite and the anterior cells of the unsegmented PSM. During segmentation of amniotes and fish, but not amphibians, interface cells undergo mesenchymal to epithelial transition. The subsequent maintenance of sharp boundaries requires integrin α5 and the accumulation of fibronectin at the interface (Dequeant & Pourquie, 2008; Dray et al., 2013; Durbin et al., 1998).

The genetic and molecular detail of the clock that sets the somite pattern has been extensively characterized (Dequeant & Pourquie, 2008). As for the physical separation, the localization and the role of several candidates are known, but the actual cellular mechanisms have not yet been definitively established. All three models for the mechanism of tissue separation were evaluated and evidences for or against each of them was proposed.

Somitic separation was thought to rely on differences of tissue surface tension between the PSM and the forming somite (Grima & Schnell, 2007). The realism of this model was however questioned by biophysical simulations: Given the high viscosities of the somitic tissues, differences in surface tension measured in vitro did not appear sufficient to drive this process (Damon, Mezentseva, Kumaratilake, Forgacs, & Newman, 2008; Grima & Schnell, 2007) .

DAH was tested by Bellairs group, they showed through a series of in vitro cell adhesion assays that somites become more adhesive as they differentiate and proposed that differences in adhesiveness played a role in segmentation (Bellairs,

Curtis, & Sanders, 1978). This model was never directly tested in vivo. However paraxial protocadherin (PAPC) was shown to be segmentally expressed and to be required for proper somite formation (S.-H. Kim et al., 2000; Murakami et al., 2006). The mechanism by which PAPC regulates adhesion and contributes to the formation of boundaries is not clear yet (Chen & Gumbiner, 2006; Chen, Koh, Yoder, & Gumbiner, 2009; Chen, Molino, Liu, & Gumbiner, 2007; S.-H. Kim et al., 2000).

The discovery of a role for ephrins and Ephs suggested that contact inhibition was involved. Several ephrins and Eph receptors are expressed in asymmetric patterns along the anterior-posterior portion of each somite (Kelly Kuan, Tannahill, Cook, & Keynes, 2004). They were shown to be required for proper segmentation, somite differentiation and epithelial to mesenchymal transition (Barrios et al., 2003; Durbin et al., 1998; Nomura-Kitabayashi et al., 2002). Several evidences support their requirement for the formation of the boundary, but a direct function in repulsion at the somite borders has not yet been demonstrated.

Rhombomere boundary

The hindbrain of all vertebrates is subdivided into a series of morphological units, termed rhombomeres. Similar to most compartment boundaries, the segmentation of this structure starts off with building a segmented lineage identity (Figure 1.2B). The segmental expression of a series of homeobox (HOX) genes is induced in response to a cross talk between several signaling pathways such as Wnts, FGF and retinoic acid. This patterning process seems to begin from rhombomere 4 and spreads to the adjacent rhombomeres (Cheng et al., 2004; Sarah Guthrie, 1996; S. Guthrie & Lumsden, 1991; Maves, Jackman, & Kimmel, 2002). Once patterning is completed, the segmental expression of several signaling factors becomes restricted to boundary region. This gives rise to the formation of specialized cells at the borders called “boundary cells”, which are characterized by expression of boundary-restricted genes, an elongated shape, enrichment in extracellular matrix components, and decreased proliferation rate

(Sela Donenfeld et al., 2009). The role of these cells and the mechanism that regulate their formation is not very well understood. What is well established is the fact that ephrins and Ephs are expressed in an alternating pattern in even and odd numbered rhombomeres and that these molecules are directly involved in creating boundaries (S. Guthrie & Lumsden, 1991; Kemp, Cooke, & Moens, 2009; Q Xu, Mellitzer, Robinson, & Wilkinson, 1999). Their interaction across rhombomere interfaces restricts cell mixing and formation of boundaries. Ephrin-Eph signaling system is also required for the formation of boundary cells, but whether this requirement reflects a direct role in cell specification or is a secondary consequence of inhibited cell sorting is not known(J. E. Cooke, Kemp, & Moens, 2005; Kemp et al., 2009).

Segregation of the rhombomeres was also proposed to rely on differential adhesion. In vitro sorting assays showed that dissociated odd and even numbered rhombomeres sorted into distinct populations and that sorting was calcium-dependent, suggesting the involvement of cadherins. No rhombomere-specific adhesion molecule has been identified so far, but the differences in rhombomere cohesion were shown to be dependent on ephrin-Eph signaling. Co-expression of ephrinB2 and EphA4 in the same rhombomere increases its coherence and this effect seems to contribute to the formation of boundary (Theil et al., 1998). Whether increased cohesion was a direct action of ephrins and Ephs or whether ephrin-Eph signaling acted indirectly by affecting other adhesion molecules was not determined.

Note that although ephrin-Eph signaling across the rhombomere interfaces directly contributes to the formation of a sharp boundary, the presence of a repulsive behaviour downstream of ephrin-Eph signaling has not yet been verified, and thus their role in a mechanism that conforms to “contact inhibition” is only inferred from general observations and from the analogy with other ephrin-Eph-dependent systems. Considering the fact that ephrins and Ephs can regulate both repulsion and adhesion, it is possible that the segregation of rhombomeres may be controlled by both mechanisms, but their respective contribution remains unknown.

Boundaries in early developing vertebrate embryos

The issue of formation of the earliest boundaries, which in the vertebrate embryo appear during gastrulation, is even more complicated: They have the difficult task to keep segregated cell masses which have been barely determined to distinct fates and which are undergoing fast and massive movements. How separation is achieved in such a dynamic situations is an important question in the field of morphogenesis. Our current knowledge of the two main boundaries that form during gastrulation phase is reviewed.

Ectoderm-mesoderm boundary

Although the internalization of the mesoderm and its opposition to the ectoderm occurs in various ways in different vertebrates, in all cases mesoderm cells acquires a migratory character, become mesenchymal and lose the ability to mix with ectoderm. The transformation of mesoderm into a migratory unit is thought to be controlled by TGFβ/nodal signaling (Lila Solnica-Krezel & Sepich, 2012). In Xenopus, mesoderm involution on the dorsal marginal zone brings mesoderm and ectoderm opposed to each other. Once inside, the mesoderm migrates on the ectoderm using the inner surface (ectodermal blastocoel roof or BCR in short) as substrate, but despite this intimate contact, the two tissues remain permanently separated. This separation is morphologically visible and was called Brachet's cleft. In the fish, mesodermal progenitor cells coordinately ingress and move toward the anterior. This movement folds the blastoderm into two cellular layers, the epiblast (ectoderm progenitors) and hypoblast (mesoderm and endoderm progenitors). Similar to mesoderm in Xenopus, hypoblast cells use epiblast as a substrate to migrate anteriorly. The two tissues are then separated by a cleft (Montero et al., 2005; Warga & Kimmel, 1990). In both fish and amphibians, preserving a stable interface between the two tissues is necessary for a successful gastrulation (Lilianna Solnica-Krezel, 2005; Lila Solnica-Krezel & Sepich, 2012;

Stern, 2004; Wacker et al., 2000). Many years after Holtfreter's experiments, the system has been recently revisited, both in Xenopus and in Zebrafish. The recent studies have led to the identification of several candidate molecules and to the proposal of mechanistic models (Krens, et al., 2011; Krieg et al., 2008; Maître et al., 2012; Tepass et al., 2002; Wacker et al., 2000; Rudolf Winklbauer & Kwang, 2009; Rudolf Winklbauer & Luu, 2009; R. Winklbauer et al., 2001).

DAH was the first to be tested. In vitro evidence for different levels of cohesiveness, typically higher in the ectoderm, indeed supports DAH (Puech, 2005; Rudolf Winklbauer & Kwang, 2009). In fact several mechanisms were proposed to control the level of adhesive energy in ectoderm and mesoderm.

In Xenopus, TGFβ/nodal signaling induces expression of FLRT3 (transmembrane protein) and Rnd1 (Rho family GTPases) on dorsal marginal zone and controls the levels of cadherin (Chen et al., 2009; Ogata et al., 2007). It has been shown that the mechanism involves formation of a complex containing FLRT3, Rnd1 and the netrin receptor Unc5 (Karaulanov et al., 2009). As a result, surface levels of cadherin are modulated through a dynamin-dependent endocytosis pathway. Similarly in Zebrafish, the small GTPase Rab5c is required for cadherin endocytosis to regulate cohesion in the mesoderm (Ulrich et al., 2005). In both cases, endocytosis seemed to depend on the non-canonical Wnt signaling pathway (Hammerschmidt & Wedlich, 2008; Kraft, Berger, Wallkamm, Steinbeisser, & Wedlich, 2012; Ulrich et al., 2005; Rudolf Winklbauer & Kwang, 2009). All these mechanisms result in decreasing adhesion in the mesoderm and creating a difference with the ectoderm.

In addition, paraxial protocadherin (PAPC), which is specifically expressed in the mesoderm, seems to have an unconventional role in this context. In Xenopus PAPC was shown to act not as an adhesion molecule but by indirectly decreasing C-cadherin adhesion. PAPC interacts with the FLRT3/RND1 pathway to down-regulate adhesiveness. The details of this interaction are not very well understood. It seems that PAPC and FLRT3 are able to reduce adhesion independently, but at the same time they affect each other's function (Chen et al., 2009). Also, PAPC has been shown to function as a signaling molecule. Its interaction with

cytoplasmic effector Ankyrin repeat domain protein 5 (xANR5) is involved in tissue separation (Chung, Yamamoto, & Ueno, 2007).

The above studies examined the effect of differences in levels of adhesion on cell sorting using in vitro assays. However it has been shown that, in the embryo, differences in adhesion are not sufficient to create a sharp boundary between ectoderm and mesoderm ((Ninomiya et al., 2012) and L.Canty and F.Fagotto, unpublished). In fact, gastrulating tissues seem to adjust C-cadherin levels in the mesoderm in order to promote cell migration, but these changes are not sufficient for tissue separation (G. S. Davis et al., 1997; Ninomiya et al., 2012; Phillips, 1978; Rudolf Winklbauer & Kwang, 2009). Note also that qualitative differential adhesion doesn't seem to be involved at this boundary either: In this early stage of Xenopus development, both ectoderm and mesoderm express the same C-cadherin (also called EP-cadherin) and its pseudo allele XB/U cadherin (Münchberg, Spieker, Joos, & Hausen, 1997; Ninomiya et al., 2012; M. S. Steinberg, 2007; Rudolf Winklbauer & Kwang, 2009).

Other reports supported a role for differences in cortical tension DITH: Tissue surface tension of cell aggregates, which results from the combination of tissue adhesion and cortical tension and, reflects tissue cohesiveness, was found to be highest in the ectoderm, intermediate in the mesoderm, and lowest in the endoderm, in both Xenopus and fish embryos (Kalantarian et al., 2009; Luu, David, Ninomiya, & Winklbauer, 2011; Phillips, 1978). The tension/stiffness of the cell cortex was more directly measured using Atomic Force Microscopy (AFM) or a micropipette aspiration system. Again, the same hierarchy was found, and evidence was presented for the predominant role of cortical tension over adhesion in setting the global surface tension (Krens, Möllmert, et al., 2011; Krieg et al., 2008; Maître & Heisenberg, 2011). The authors argued that cortical tension was the leading parameter that controlled germ layer separation (Krieg et al., 2008; Maître & Heisenberg, 2011).

In addition to physical differences, several signaling pathways and their potential downstream effectors have been identified to be involved in the separation process. Most of the information comes from experiments in Xenopus. A non-

canonical Wnt pathway contributes to separation of ectoderm and mesoderm. The molecular determinants of this pathway are partially identified. They include, sequentially, the Wnt receptor frizzeled7 (Fz7), trimeric G proteins, PKC, JNK and Rho (Rudolf Winklbauer & Kwang, 2009; R. Winklbauer et al., 2001). Note that this pathway seems to converge with PAPC signaling: PAPC also regulates Rho, and physically interact with FZ7, but the precise nature and function of this interaction is unclear (Chung et al., 2007; Medina & Steinbeisser, 2000; Rudolf Winklbauer & Luu, 2009).

These pathways converge to the activation of Rho. FZ and PAPC have been shown to fine tune Rho signaling by down-regulation of two Rho GTPase activation proteins (GAPs) in the mesoderm. It is proposed that the regulation occurs at the transcriptional level and that the differential expression of the two GAPs is involved in both migrational behavior of mesoderm and perhaps tissue separation (S. H. Kim, Yamamoto, Bouwmeester, Agius, & Robertis, 1998; Köster, Jungwirth, & Steinbeisser, 2010).

Ephrins and Ephs have also been shown to be required for tissue separation, in parallel to the non-canonical Wnt pathway (Park, Cho, Kim, Choi, & Han, 2011). However the direct evidence for the role of ephrin and Ephs at the boundary is missing.

Despite these molecular evidences, virtually nothing is known about the cellular processes that are regulated by these components, or more generally, about the principles of ectoderm-mesoderm separation.

Notochord boundary

At the end of gastrulation, two boundaries form that separate the most axial dorsal mesoderm, the future notochord, from the paraxial or presomitic mesoderm (PSM). In Xenopus, the initial patterning of the prospective notochord and somitic regions is established at the onset of gastrulation. As notochord-specific transcription factors Xnot and FoxA4 (originally named XFD-1) (Pohl, Pohl, & Knöchel, 2005) become expressed, the somitic muscle-specific transcription

factors like myf-5 and MyoD appear lateral to it (Hopwood, Pluck, Gurdon, & Dilworth, 1992; Knöchel et al., 1992; von Dassow, Schmidt, & Kimelman, 1993). Wnt-β-catenin signaling is particularly important for this patterning: it is required for paraxial fate but inhibits notochord fate (Christian & Moon, 1993; Hoppler, Brown, & Moon, 1996).

The formation of this boundary starts once the trunk mesoderm has involuted and precisely coincides with the onset of convergent extension movements. This boundary is particularly interesting because studies by Keller's group revealed unique aspects of cell behaviour at the boundary, which they named "boundary capture" (Keller et al., 2000; Shih & Keller, 1992). Time-lapse movies of dorsal mesoderm explants showed that when notochord cells reach the boundary, they appeared to "freeze": Protrusive activity ceased along the surface facing the boundary and cells remained permanently located at this interface. These "captured" cells continued however to extend protrusions on the face away from the boundary and to generated traction on neighboring cells, pulling these neighbors toward the boundary. The authors proposed that the mechanism of boundary capture was partially required for proper convergent-extension movements (Keller et al., 2000). These experiments represented the first detailed analysis of cell behaviour at a boundary and shed light on potential cellular mechanisms. Inhibited protrusive activity on the boundary face indeed resembled the classical behavior of contact inhibition of movement (Domingo & Keller, 1995).

The molecular basis of this process had remained however fully unexplored, except for the following observations by Reintsch et al (2005): They showed that the Wnt-β-catenin pathway can act as a switch not only for cell fate, but also for cell sorting: Increased activity leads to cell-autonomous sorting to the somites, and reduced sorting to the notochord. They demonstrated that the process relied on β-catenin transcriptional activity. Surprisingly, levels of cadherin-mediated adhesion did not seem to influence sorting (Reintsch et al., 2005).There is however evidence for the differential expression of other adhesion molecules; axial and paraxial protocadherin on presomitic mesoderm and notochord

respectively. Their inhibition leads to disrupted boundary (M. Frank & Kemler, 2002). It is not clear if the effect of these protocadherins on tissue adhesiveness is direct or indirect.

Xenopus is the ideal model organism to study boundaries

Xenopus development provides an ideal model for the study of cellular and molecular processes involved in the formation of boundaries. One important advantage of this organism is that embryonic cells are large in size, which greatly facilitates investigations at the cellular or even subcellular level. Furthermore the manipulation of cells at early embryonic stages is easier than in any other model system. One can perform a variety of in vivo and in vitro experiments, including complex cell-based analysis and live cell microscopy. Furthermore the large amount of material makes it highly accessible for biochemical analyses. Interference with gene function by knockdown strategy is straightforward: Injection of Morpholino antisense oligonulceotides blocks specifically translation of the targeted mRNA and effectively depletes the corresponding protein. Due to their very low toxicity, multiple Morpholinos can be co-injected, very easily allowing simultaneous knockdowns of multiple gene products. Expression of dominant negative constructs is another effective alternative to inhibit gene function.

Many methods have been developed for the study of developmental processes in Xenopus. In particular, we have exploited here a unique assay where tissue separation is reconstituted in vitro by apposition of tissue explants (Wacker et al., 2000). The assay faithfully reproduces the in vivo situation, while allowing multiple manipulations of each tissue separately, and direct access to the tissue interface. The assay also facilitates visualization of boundary by live cell microscopy, providing a unique opportunity to be able to observe cell behaviour at the boundary.

Ephrins and Eph receptors

The first Eph receptor was discovered in a search for tyrosine kinases involved in cancer (Hirai et al., 1987). It was named after the Erythropoietin Producing Hepatocellular carcinoma cell line from which the gene was isolated. The first clue for its function was derived from its expression in developing and adult nervous system (Tuzi & Gullick, 1994). Ephrins and Ephs are most well known for their role in neural guidance. Initially they were functionally categorized under the broader family of guidance molecules, together with semaphorins and their receptors (neuropilin, plexin), slit and robo, netrins and unc receptors. Several other functions in addition to neural guidance were later discovered: The effect of ephrin-Eph signal can vary from adhesion and attraction to repulsion/de-adhesion (D. Arvanitis & Davy, 2008; Brückner & Klein, 1998; Egea & Klein, 2007a; J. G. Flanagan & Vanderhaeghen, 2003; J.-P. Himanen, Saha, & Nikolov, 2007b). The mechanism by which each of these outcomes is produced will be discussed later. In addition to the functional versatility of these molecules, the context in which they perform is also very wide. Their roles have been studied in several processes such as angiogenesis, vasculogenesis, neural crest cell migration, synaptic plasticity and boundary formation in the brain and in the somites (J. G. Flanagan & Vanderhaeghen, 2003; Kullander & Klein, 2002; Murai & Pasquale, 2003). Ephrins and Ephs have specific characteristics which make them attractive candidates to control cell sorting and boundary formation: Both ligands and receptors are membrane bound, which restricts transduction of signals to those cells which are in direct contact. Resulting reaction can be repulsive or adhesive. Thus the same components may contribute to either efficient detachment under some conditions (e.g. at the boundary), or on the contrary strengthen adhesion (e.g. between cells of the same type). Ephrins and Ephs are widely expressed throughout the development of vertebrate embryos, in patterns that suggest that they are at the right time and right place to play a role in the formation of many different boundaries (Mellitzer et al., 1999; Tepass et al., 2002; Q Xu et al., 1999; Qiling Xu, Mellitzer, & Wilkinson, 2000).

Molecular characteristics of ephrins and Eph receptors

Eph receptors

The Eph family is the largest family of receptor tyrosine kinase (RTK) in the animal kingdom. Eph family and their ligands consist of two groups (A and B) based on sequence conservation and binding affinities. It has been proposed that binding within each group is promiscuous; all EphAs interact with all ephrinAs and EphBs with ephrinBs. In vertebrates, the Eph family consists of 16 receptors (10 As+6 Bs). The domain organization of Eph receptors is very conserved (Figure 1.3). It consists of an N-terminal globular extracellular domain, followed by a cysteine-rich region, a "suchi" and an EGF like domains, two fibronectin type III domains (FN1, FN2), and the last FN domain being immediately followed by the transmembrane domain (TM). The globular domain constitutes the ligand-binding domain (LBD) and the FN and cysteine-rich domains are involved in clustering. The functions of the other domains are not known.

The intracellular part contains sequentially a juxtamembrane region (JM) with two conserved tyrosine residues, the kinase domain, a so-called "sterile alpha motif" (SAM), which is involved in protein-protein interaction and finally a C-terminal domain ending with a PDZ binding motif (Dravis et al., 2004; J.-P.Himanen, & Nikolov, 2003; J.-P. Himanen et al., 2001; Janes, Nievergall, & Lackmann, 2012).

Functionally, the Eph family also distinguishes itself from other RTKs in several aspects: Physiologically most relevant is the fact that both ligands and receptors are membrane bound. In addition they are capable of bi-directional signaling, meaning that both ligand and the receptor are able to generate intracellular signals. "Forward signaling" is directed into the receptor bearing cell, "reverse signaling" is directed into the ligand bearing cell. This unique property allows transduction of mutual signals (D. Arvanitis & Davy, 2008; Brambilla et al., 1996; Dravis et al., 2004; Egea & Klein, 2007a; J. G. Flanagan & Vanderhaeghen,

2003; Harbott, Marston, & Nobes, 2004; J.-P. Himanen et al., 2004; J.-P. Himanen, Saha, & Nikolov, 2007). Another point of difference that distinguishes Eph receptors from other RTKS is at the level of their activation: Unlike other RTKs for which receptor dimerization is sufficient, Ephs require higher order clustering to be able to signal. The size of the cluster contributes to determine the function, influencing the signal to go toward adhesion or repulsion (Gale et al., 1996; J.-P. Himanen et al., 2001; Juha P. Himanen et al., 2010). It has been suggested that Eph cluster size can be controlled by the density of ligands at the membrane of the interacting cells (Bethani, Skanland, Dikic, & Acker-Palmer, 2010; Nikolov, Xu, & Himanen, 2013).

Ephrin ligands

As mentioned above, ephrin ligands are divided into A and B classes, which bind respectively EphA and B isoforms. In vertebrates the ligand family consists of six ephrinAs (A1-A6) and three ephrinBs (B1-B3). All ephrins have a similar globular extracellular domain, but the members of the A and B classes differ significantly by the fact that the former are tethered to the outer leaflet of the plasma membrane by a glycosyl phosphatidy linositol (GPI) linkage, while ephrinBs are classical type I transmembrane proteins (Dravis et al., 2004; J.-P. Himanen et al., 2003; J.-P. Himanen et al., 2001; Janes et al., 2012). Unlike Ephs, the cytoplasmic tail of ephrinBs does not display catalytic activity. Instead, they have a short, highly conserved cytoplasmic tail with five conserved tyrosine residues and a C-terminal PDZ-binding motif. These latter motifs are involved in their membrane localization and reverse signaling (Brückner et al., 1999; Bush & Soriano, 2009; Hock et al., 1998).

Evolutionary aspect

Ephrins and Ephs were first discovered in vertebrates, but the recent analysis of the genomes of invertebrates shows that they are very ancient and present in all

metazoans (Mellott & Burke, 2008). While ephrins were initially thought to have appeared earlier than Ephs (Mellott & Burke, 2008), Eph-like sequences with the exact same domain organization characteristic of vertebrate Ephs are found even in sponges (Reddy, Reddy, Bidaye, & Ghaskadbi, 2011). This suggests that the emergence of this family of receptor tyrosine kinases dates back to before parazoan-eumetazoan evolutionarily split, which is the earliest branch among existing animal phyla. At least three EphA type receptor and one EphB type receptors have been identified in sponges. This suggests that the isoform duplication of Eph receptors perhaps took place before diploblastic –triploblastic split (Drescher, 2002; Mellott & Burke, 2008). In the nematode Caenorhabditis elegans, however, the Eph family consists of one receptor (VAB-1) and four GPI anchored ligands. In Drosophila, a single ephrin and Eph is expressed (Dephrin and DEph) (Drescher, 2002; Mellott & Burke, 2008). Altogether, while the size of the family seem to have undergone reductions throughout evolution, it is clear that the size of the family has further dramatically expanded with the appearance of vertebrates (D. Arvanitis & Davy, 2008; Drescher, 2002; Kullander & Klein, 2002).

As for the ligands, sequence comparison studies indicate that ephrinBs are likely to be more ancient than ephrinAs. The ancestral ephrinB-like ligands had transmembrane domains and the GPI anchorage to the membrane seems to have emerged or been lost at least 3 times (Mellott & Burke, 2008).

While the ephrins and Ephs of higher metazoans are typically categorized as neuronal guidance molecules, their ancestral role has not been identified yet. Sponges do not have a nervous system, yet they do possess tissue-like organizations that are arranged into layers such as epidermis (pinacoderm) on the outside and flagellated cells lining on the interior (Drescher, 2002; Mellott & Burke, 2008; Reddy et al., 2011). As speculated by Drescher's group, it is possible that the ancestral function of the Eph family might be the regulation of cell movements. In order to have a better idea about the possible ancestral roles of ephrins and Ephs, functional data from early metazoans are required (D. Arvanitis & Davy, 2008; Drescher, 2002; Kullander & Klein, 2002).

The large size of the vertebrate Eph family raises the question of whether this evolutionary expansion has been translated into functional diversity or remained restricted to variations of the same function. The functional range of ephrins and Ephs falls systematically into one of the three main categories including regulation of axon guidance (e.g. formation of visual topographic maps), directed cell migration (e.g. neural crest cell path finding), or tissue segregation (e.g. hindbrain segmentation) (Drescher, 2002). A survey of literature reveals that while there are some specific roles unique to each class, on a broader view both A and B classes, despite their sequence divergence, serve essentially the same type of functions. Nonetheless even within a class, the isoforms show highly conserved differences in their sequences, suggesting that each isoform has particularities that are under selective pressure. Thus, although the general functions are shared by all ephrins and Ephs, it is likely that there are subtle yet important functional differences between the isoforms. Expansion in member size of each class could have provided a diversity that was exploited by selection and contributed to the evolutionary increase in the size of the nervous system (Drescher, 2002; Fletcher et al., 1994; Mellott & Burke, 2008).

Promiscuity versus selectivity of interactions

The existence of several ephrins and Eph receptors raises the important question of their specificity. Potentially it is conceivable that, as the number of ligands and receptors increased, some level of specificity was generated. A clear split is already well established between the two classes: ephrinAs have greater affinity for interactions with EphAs than Bs. Note that several exceptions of interclass interactions were reported: EphrinB2 and ephrinB3 have been shown to interact with EphA4 and, ephrinA5 interacts with EphB2. As for intra-class interactions, however, it has been often assumed that they are promiscuous (Pasquale, 2004). Various observations were however not compatible with this simple model of promiscuous interactions: This model predicts that ephrins and Ephs from the same groups are interchangeable and thus could be expressed as random pairs,

however, a subset of ephrin-Eph pairs were repeatedly found to be expressed in striking complementary expression patterns and acted together in many processes (Kullander & Klein, 2002). This apparent coupling of a ligand with a specific receptor suggested some ligand-receptor selectivity. This was supported by in vitro binding measurements, which revealed large differences in affinities between pairs involving members of the same classes. In most cases, those pairs showing a high affinity were the same ones that had been identified based on biological functions (Blits-Huizinga, Nelersa, Malhotra, & Liebl, 2004; J. G. Flanagan & Vanderhaeghen, 2003). This correlation is however far from absolute: There are several cases where pairs with relatively moderate or even weak in vitro affinities have been shown to play important functions in vivo (e.g. ephrinB3 and EphA4) (Fox & Kandpal, 2011; Nikolov et al., 2013; Pasquale, 2004; Qin et al., 2010; Wang, Chen, & Anderson, 1998; G. Zimmer et al., 2011). Conversely, the biological relevance of several high affinity ephrin-Eph pairs has yet to be determined. EphrinB3 and EphB3 is one such example (Blits-Huizinga et al., 2004; J. G. Flanagan & Vanderhaeghen, 2003). There are a number of explanations for these discrepancies: Recombinant proteins used for in vitro measurements may not necessarily have the same activity as the endogenous proteins. Furthermore, binding of membrane-associated proteins is likely to follow different rules than binding in solution (Pabbisetty et al., 2007; Pang & Zhou, 2013). In addition, parameters such as localization to membrane subdomains and clustering, which are expected to enhance binding, may vary between isoforms (Janes et al., 2012). Some studies using Surface Plasmon Resonanse (SPR) were able to refine the previous analysis by comparing monomeric and dimeric binding affinities. They showed that the affinity toward EphB2 was higher for ephrinB2 than for ephrinA5, which perfectly correlates with the biological data on neuronal collapse (Haramis & Perrakis, 2006; J.-P. Himanen et al., 2004; Pabbisetty et al., 2007).This type of experiments should help to establish whether affinities measured in vitro reflect the actual strengths of ephrin-Eph binding in the in vivo situations.

Mechanisms of ephrin-Eph function

Eph activation

The activation mechanism of the Eph receptor consists of several steps that involve ligand recognition, clustering and activation.
The recognition occurs on a hydrophobic cavity of Eph receptor where a long ephrin loop penetrates and initiates the formation of ligand-receptor complex.
In order for the complex to be capable of signaling it requires to form higher order clusters. As mentioned earlier, lateral clustering and expansion of the size of assemblies is critical for the signal to occur. The clustering step involves two separate interfaces of the Eph receptor. The first interface is on the ligand binding domain and is responsible for the formation of receptor dimers. The other interface resides on the cysteine-rich domain and contributes to the formation of higher order clustering. The available data indicate that the dimerization interface becomes exposed upon ligand binding, while the second clustering interface is constitutively present even in the absence of ligand. Eph clustering seems thus to be strongly dependent on receptor local concentration. Several mechanisms can control the local concentration of Ephs: One important factor seems to be the property of ephrins to concentrate in membrane micro-domains and rafts. It is thought that Eph receptors, which are normally sparsely distributed on the cell surface, are being pulled together upon binding to these "pre-clustered" ligands (Egea et al., 2005; Juha P. Himanen et al., 2010; Janes et al., 2012; Seiradake et al., 2013). Note however that high receptor concentration may be sufficient on its own for clustering. This could explain why ligand-independent signaling has been observed on the surface of some tumor cells that express high levels of Eph receptors (Tawadros, Brown, Hart, & Clarke, 2012; S. H. Wimmer-Kleikamp, Janes, Squire, Bastiaens, & Lackmann, 2004). Less common forms of ligand independent Eph "pre-clustering" has been reported for EphA4: It involves the interaction of ligand binding domain LBD of one receptor and Fibronectin domain FNIII of adjacent receptor (J. P. Himanen, 2012). EphA4 receptor

mutants that strengthened the interaction between those domains exhibited increased phosphorylation levels even in the absence of ligand stimulation (K. Xu et al., 2013).

Clustering is followed by Eph activation. Not much is known about the link between the two steps. Activation involves sequential autophosphorylation reactions followed by conformational changes (Singla, Erdjument-Bromage, Himanen, Muir, & Nikolov, 2011). The Singla group revealed the details of this process: They observed that it differs from the mechanism of activation of most other RTKs, in which the activation loop in the kinase domain gets phosphorylated first. In the case of the Ephs, however, the kinase activity is auto-inhibited through interaction with the juxtamembrane (JM) region (Wybenga-Groot et al., 2001). Upon activation, two sequential phosphorylations on the JM tyrosine residues relieve this auto-inhibition and allow the cytoplasmic tail to adopt a new conformation, which is thought to be more permissive for the subsequent phosphorylation of kinase domain (Wiesner et al., 2006). Another study has provided in vivo evidence in support of this model: It has been demonstrated that tyrosine phosphorylation on the JM region of EphA3 triggers a measurable movement of the kinase domain away from the plasma membrane (T. L. Davis et al., 2008; Janes et al., 2005; Janes et al., 2009).

Ephrin activation

Compared to Ephs, much less is known about the ephrin activation process. Both A and B classes are found in glycosylsphingolipid-enriched lipid rafts of the membrane. Since ephrins do not contain a kinase domain, the phosphorylation requires recruitment of other kinases. In fact the Src family of tyrosine kinases (SFK) are recruited to the same rafts through their lipid insertion and are involved in ephrin phosphorylation. Like Eph receptors, the activation of ligands requires multimerization from their basic dimeric configuration to higher order structures. Upon binding to Eph receptors, the ephrin homodimers are disrupted and a circular tetrameric structure constituted of two receptor molecules and two ligand

molecules is formed. The circular tetrameric structure induces conformational changes that are thought to alter the distance between ephrin's transmembrane and cytoplasmic domains (J.-P. Himanen et al., 2001; J.-P. Himanen et al., 2007; Pabbisetty et al., 2007). It has been speculated that this new conformation is more permissive for the phosphorylation of the ephrin cytoplasmic tail by adjacent SFKs (Makarov, 2010). Reverse signaling might be then boosted by the ability of the circular ephrin-Eph tetramers to aggregate into higher order clusters within the lipid rafts to form discrete signaling centers. The cytoplasmic domain of ephrinBs contains five tyrosine residues. The phosphorylation of at least three of these residues is thought to be important in the transduction of reverse signals (C. Cowan, Cowan, & Henkemeyer, 2002; Palmer et al., 2002). EphrinBs can also become phosphorylated in cis, independently of Eph interaction, by pathways downstream of other receptor tyrosine kinases such as PDGF, FGFR, or of cell surface adhesion molecules such as claudins (L. D. Chong, Park, Latimer, Friesel, & Daar, 2000; Semela et al., 2008; Masamitsu Tanaka, Tanaka, Kamata, & Sakai, 2005).

Downstream signaling

The most generic signaling route downstream of ephrins and Ephs that induces relevant consequences for tissue separation goes through activation of Rho GTPases. The main signaling effectors include RhoA, Rac, Cdc42 and Ras (Brückner & Klein, 1998). Each GTPase controls the formation of distinct F-actin based structure. RhoA is involved in formation of stress fibers, Rac in lamellipodia formation and Cdc42 in filopodia formation. Ras modulates multiple aspects of microtubule and microfilaments. The contribution from each GTPase is dictated by the balance between the local concentration of different Guanidine exchange factor (GEFs) or GTPases activating proteins (GAPs) which tips the outcome of signaling towards adhesion or repulsion(Murai & Pasquale, 2003). The major process through which ephrin-Eph signaling promotes cell adhesion involves activation of Rac and Cdc42, which stimulate actin polymerization and

membrane extension, favorable for adhesion (Hall & Nobes, 2000; Noren & Pasquale, 2004; Singh, Winterbottom, & Daar, 2012). The mechanism involves the activation of a classical actin nucleator, the Arp2/3 complex and its activators WASP and SCAR/WAVE (Irie & Yamaguchi, 2002). It also involves the inhibition of actin depolymerisation via Pak and LIM-kinase, which phosphorylates and inactivates the filament severing protein cofilin. Ras activation can act either through MAP kinases to phosphorylate microtubules or modulate the regulators of the actin cytoskeleton, including myosin light chain kinase. It also can modulate integrin mediated cell-substrate adhesion (Groeger & Nobes, 2007; Noren & Pasquale, 2004; Qiling Xu et al., 2000).

Repulsion, on the other hand, is promoted by activation of RhoA and its direct target RhoA-associated kinase (ROCK). ROCK acts through different paths to promote membrane retraction and repulsion: It facilitates formation of leading edge stress fibers by promoting Dia-mediated actin polymerization. It can also decrease actin filament turnover by activating LIM kinase and thus inhibiting cofilin (C. Cowan et al., 2002; Maekawa & Maekawa, 1999). In addition, ROCK modulates myosin function through myosin regulatory light chain (MRLC). Membrane retraction is likely to result from the concerted action of all these reactions to stabilize actin filament and promote actomyosin contractility (Mizutani et al., 2009).

In summary, modulation of different GTPases seems to represent a molecular switch that directs the response to ephrin-Eph signaling: Rac/Cdc42 or Ras activation for membrane extension and RhoA activation for retraction (Kullander & Klein, 2002). It must be noted that regulation of GTPases downstream ephrin-Eph signaling also regulates their endocytosis, which terminates the ephrin-Eph intercellular connection and triggers membrane retraction (Luo & Luo, 2002).

In the next two sections, I describe the specific mechanisms that link activation of ephrins and Eph receptors to these downstream pathways.

Eph forward signaling

After ligand binding, clustering and kinase activation, a series of events downstream of Ephs control the transduction of the signal into the Eph-bearing cell. These reactions are mostly common to other RTKs. However, as mentioned above, the major target here is not nuclear and does not affect gene transcription but it regulates the actin cytoskeleton. Note that the picture of the molecular pathway downstream Ephs is still somewhat fragmentary, because studies have been performed in different model systems and for different Eph isoforms; here I will review some of the most common examples. While the Eph-interacting adaptor proteins seem to be mostly context-specific, some general rules nevertheless apply to most of them: Eph receptors can directly interact with Rho GEFs, which are either recruited or bound constitutively to the phosphorylated juxtamembrane domain, or to the kinase domain. Each class of Eph receptors seem to activate a unique subset of GEFs in neuronal cells. Those that have been frequently identified for EphA receptors are ephexin, Vav and Tiam1, which are all specifically involved in axon guidance (D. Arvanitis & Davy, 2008). Ephexin can activate RhoA, Cdc42, and Rac and affect actin cytoskeleton in different ways. It seems to be constitutively bound to EphA receptor kinase domain and gets phosphorylated upon Eph activation (Bussell, 2001; Shamah et al., 2001; Wahl, Barth, Ciossek, Aktories, & Mueller, 2000). Phosphorylation changes its preference for different substrates: Non-phosphorylated ephexin activates Rac and Cdc42 and thus promotes axonal growth and membrane extension in the absence of ephrin stimulation. Phosphorylation switches ephexin preference toward RhoA, tips the local balance of GTPase activities, thereby causing actin de-polymerization and local retraction (Bussell, 2001; C. W. Cowan et al., 2005; Marquardt et al., 2005; Sahin et al., 2005; Motomasa Tanaka, Chien, Naber, Cooke, & Weissman, 2004; Zhuang, Hunter, Hwang, & Chen, 2007). This pathway appears to be evolutionarily conserved: The single Drosophila Eph receptor mediates synaptic homeostasis at the neuromuscular junction via ephexin (C. A. Frank, Pielage, & Davis, 2009).

EphB receptors interact with a different subset of GEFs, which also activate RhoA, Rac or Cdc42. The most frequently found are intersectin, kalirins and pix

family (Irie & Yamaguchi, 2002; Penzes et al., 2003; Penzes et al., 2001). These are all unrelated to ephexin, and, unlike the latter, do require signal-induced interaction with Eph receptor for activation. For instance, ephrinB1 stimulation of EphB2 activation leads to kalirin phosphorylation, which up-regulates activation of serine/threonine kinase Pak1, a Rac downstream effector, and in turn leads to increase in adhesion and spine maturation (Ma, 2003; May, 2002; Penzes et al., 2003; Penzes et al., 2001). This and a pathway through intersectin and Cdc42 have been recently proposed to regulate the EphB- mediated morphogenesis and spine maturation.

In addition to GEFs, Eph receptors can also associate with GAPs. The Rac-specific GAP α2-chimaerin interacts with EphA4 and, in response to ephrinB3-EphA4 signaling, and inactivates Rac in vivo (Beg, Sommer, Martin, & Scheiffele, 2007; Iwasato et al., 2007b; Wegmeyer et al., 2007). The association of this molecule with Eph receptors is mediated by the Nck2 (Grb4) adaptor protein (Bisson, Poitras, Mikryukov, Tremblay, & Moss, 2007; Fawcett et al., 2007; Iwasato et al., 2007a). Rac inactivation inhibits axonal outgrowth and neural extension.

The other actin-modulating proteins downstream of Eph forward signaling are the Ras GTPases, a subfamily that is also well-known to regulate cell migration and adhesion. The Eph receptors are among the few receptor tyrosine kinases known to negatively regulate Ras and its downstream MAP kinase pathway. It has been shown that EphB2 inhibition of Ras is required for the inhibition of integrin mediated adhesion and for neurite retraction (Dail, Richter, Godement, & Pasquale, 2006; Elowe, Holland, Kulkarni, & Pawson, 2001; I. Kim et al., 2002; Zou et al., 1999). Ras inactivation is achieved in two ways, either directly, through the inhibition of Ras effector domain, or by reduction of its activity through p120 RasGAP. The interaction of EphB and Ras seem to be through SHEP1 (SH2 domain-containing Eph receptor-binding protein 1), which binds directly to both and localizes Ras GTPases to sites of receptor activation.

The C-terminal PDZ-binding motif of Eph receptors mediates their interactions with many PDZ scaffolding proteins. However their role seem to be more

specialized to neuronal guidance contexts. The ones identified in neurons are glutamate receptor interacting protein (GRIP), protein interacting with C-kinase PICK1 and Ras binding protein AF-6 (Brückner & Klein, 1998; Hock et al., 1998; Hoogenraad, Milstein, Ethell, Henkemeyer, & Sheng, 2005; Torres et al., 1998). To summarize, the main signaling effectors downstream of Eph include Rho, Rac, Cdc42, and Ras. Their differential activation or inhibition via activating their corresponding GEFs or GAPs leads to different cellular outcomes, i.e. repulsion/de-adhesion or attraction/adhesion. While the molecular pathway described above are repeatedly found downstream of Ephs in neuronal contexts, their conservation in non-neuronal contexts remains to be addressed.

Ephrin reverse signaling

EphrinB reverse signal is transduced into the cell by recruiting two types of molecules (N.-J. Xu & Henkemeyer, 2012): The phosphorylated tyrosine residues of ephrinBs can recruit SH2/SH3 domain adaptor proteins, while the PDZ domain at the cytoplasmic tail can recruit PDZ domain proteins. These proteins serve as adaptors or scaffolds for signaling complexes.

Among the adaptors binding to the phosphorylated tail, the best known is Grb4, also known as Nck2. Grb4 contains SH2 and SH3 domains, it binds to the ephrinB tail through its SH2 domain, and its SH3 domains recruits GEFs like Dock180 (exchange factor for Rho and Rac and Cdc42) and β-Pix (GEF for Rac). Activation of Rho downstream of ephrinB also requires a formin-homology (FH) protein, Daam1 (disheveled-associated activator of morphogenesis), a component that binds to both Rho and Dishevelled (Dvl). This complex represents a link between reverse signaling and non-canonical Wnt pathway and influence cell contraction and migration (Kida, Sato, Miyasaka, Suto, & Ogura, 2007). Beside GEFs for Rho GTPases, many other molecules are recruited to Grb4, which are all implicated in cytoskeletal regulation, including the Cbl-associated protein (CAP/ponsin), the Abl-interacting protein-1 (Abi-1), dynamin, Pak1, hnRNPK and Axin (Fryer et al., 2006; Kullander & Klein, 2002).

The C-terminal PDZ-binding motif was found to recruit several PDZ domain proteins: Par-3, PDZ-RGS, Syntenin and phosphotyrosine phosphatase PTP-BL (Grootjans et al., 1997; Lu, Sun, & Flanagan, 2004; Lu, Sun, Klein, & Flanagan, 2001; Palmer et al., 2002). These interactions can also regulate the actin cytoskeleton and may be involved in cross talks with other pathways: For instance crosstalk with G-protein coupled receptor, by recruitment of PDZ-RGS, or the Par polarity pathway though recruitment of Par-3. It is not known if the interaction with these molecules is general or context dependant. Except for phosphotyrosine phosphatases that seem to be more general and exert regulatory effect on ephrinB reverse signal:

PTP-BL was found to associate with ephrinB upon activation by EphB receptors. It contains five PDZ domains and can interact with several other cytoplasmic proteins, including a GTPase-activating protein (GAP) with specificity for RhoA that de-activates it. (Brückner et al., 1999; Groeger & Nobes, 2007; Hall & Nobes, 2000; H.-S. Lee et al., 2006; Marston, Dickinson, & Nobes, 2003; Moore, Mood, Daar, & Moody, 2004; Riedl et al., 2005; Saras, 1994; N.-J. Xu & Henkemeyer, 2009; G. Zimmer et al., 2011; M. Zimmer, Palmer, Kohler, & Klein, 2003).

It has been proposed that SFKs and phosphotyrosine phosphatases PTP-BL are required sequentially, which accounts for different phases in ephrin reverse signaling: The first step would be SFK activation and ephrinB phosphorylation. The cytoplasmic domain of ephrinB would now serve as a docking site for adaptor molecules like SH2 domain-containing proteins, which would transduce a phosphotyrosine-dependent signal to the interior of the cell. PTP-BL would be then recruited to the signaling complexes containing ephrinB and SFKs. It would de-phosphorylate ephrinB ligands and inactivates SFKs. Phosphotyrosine-dependent signaling would then be switched off, while the multiple PDZ domains of PTP-BL would allow interaction with other cytoplasmic effectors or potentially generate cross talks with other molecular pathways (Palmer et al., 2002; Sabine H. Wimmer-Kleikamp et al., 2008).

Reverse signaling through ephrinAs is much less understood. Despite lacking intracellular sequences, ephrinAs are also capable of eliciting reverse signal by coupling to co-receptors. They are also targeted to lipid rafts where they assemble into protein complexes that transduce signals. EphrinA reverse signaling involves many downstream effectors (i.e. Src family members, Erk1/2, Rac, AKT, integrin, paxillin, and p75NTR), but the mechanism of activation and the pathways employed still need clarification (Murai & Pasquale, 2003). EphA stimulated ephrinA clustering recruits Src family kinase FYN to the lipid rafts and modulate integrin mediated adhesion. This is accompanied by vinculin redistribution, activation of MAP kinase and increase in cell-substrate adhesion (Mellitzer et al., 1999). In the retinal axons, the p75 neurotrophil receptor and ephrinA form a complex that is required for FYN tyrosine kinase activation and axon repulsion (Lim, Matsuda, & Poo, 2008).

Regulation of function

While ephrin-Eph signaling is mostly known to trigger repulsive reactions, it can also generate the opposite outcome, i.e. cell to cell adhesion. These two antagonistic reactions appear to involve different mechanisms:

Adhesion

To trigger a signal, ephrins and Ephs must bind, creating a direct physical link between the membranes of the two interacting cells. For de-adhesion the ephrin and Eph bond must be disengaged. It is not clear if some ephrin-Eph interactions are by nature adhesive, but it seems that the strength of the signal plays an important role in influencing whether the reaction will be adhesive or repulsive, with adhesive reactions generally requiring lower signal intensity than repulsion. Consistent with this principle, those mechanisms that down-regulate signal usually favour adhesion (Schaupp et al., 2014;Halloran & Wolman, 2006; Sabine H. Wimmer-Kleikamp et al., 2008).

Several factors could in principle control the strength of signal. One parameter would be the ligand and the receptor cell surface densities. Not much is known about the regulation of expression at the transcriptional level. However, a recent study showed that antagonistic effects of different isoforms of Smurf ubiquitin ligases on ephrinB1 control its protein level in the mesoderm of Xenopus embryos (Hwang et al., 2013).

A better understood mechanism is the dampening of the signal by the action of protein tyrosine phosphatases PTPs. This mechanism has been well studied in lymphocytes, where endogenous EphA3 was found to be associated with PTP (Pasquale, 2010). PTP activity efficiently dampened phosphotyrosine-dependant Eph signaling, promoting extension of protrusions and adhesion (Sabine H. Wimmer-Kleikamp et al., 2008). The persisting ephrinA5-EphA3 clusters on these cells were proposed to provide stable tethers between cells. This mechanism appeared to serve as a switch that transforms the non-adherent leukemia cells to adherent and spreading cells (Sabine H. Wimmer-Kleikamp et al., 2008).

Other more specialized mechanisms have been reported, involving for instance splice variants of Eph receptors that are able to induce by default adhesive signals. These splice variants are largely kinase deficient (Holmberg, Clarke, & Frisen, 2000; Truitt & Freywald, 2011). An example is the interaction between kinase deficient EphA7 and ephrinA5 at the tips of neural folds, which is involved in neural tube closure during mouse development (J. Lee, Corcoran, Han, Gardiner, & Muneoka, 2013).

Repulsion

Cell repulsion requires changes in actin and microtubule dynamics, as well as down-regulation of adhesion to other cells and to the extracellular matrix. Ephrin-Eph signaling can initiate an intracellular pathway that directs these changes. To trigger the signal however, ephrin and Eph has to bind, which creates tight links between the cells. These intercellular bonds represent a strong hindrance to de-

adhesion, and must be removed for the repulsion process to start. Two main mechanisms control de-adhesion: Internalization by endocytosis and shedding by proteolytic cleavage.

Detachment by endocytosis

This mode of termination of ephrin-Eph signaling is considered to be the most common mechanism that leads to cell-cell repulsion. Elegant studies have provided evidence for internalization of intact ephrin-Eph complexes. The process is rather peculiar and resembles phagocytosis: Since both ephrins and their receptors are embedded in the plasma membranes, whole patches of the plasma membrane of the adjacent cell are internalized (Groeger & Nobes, 2007; Marston et al., 2003; M. Zimmer et al., 2003). Internalization can be either into the ephrin- or the Eph-bearing cell. The direction is determined by ephrin-Eph-mediated signal transduction. For instance, an EphB variant that lacks the cytoplasmic region directs the internalization of receptor-ligand complex into adjacent ephrinB-expressing cell. Simultaneous truncation of ligand and receptor prolongs adhesion and delays retraction, which is consistent with the importance of intracellular signaling in the process of internalization and more generally in repulsive reactions.

Eph receptors and ephrin ligands endocytosis appears to occur through various routes, involving clathrin, caveolin or dynamin, and to require actin remodeling through activation of small GTPases (Andersson, 2012). Although the details of mechanism are not very well understood, a number of small GTPases have been linked to the trans-endocytosis of ephrin-Eph complex in different contexts. The most common ones are Rho, Rac and Rabs. Rho and Rac are known to be involved in the actin remodeling required for endocytosis, and Rab in the endosomal trafficking. For example ephrinB2-EphB4 dynamin-dependant endocytosis has been shown to require Rac activation (Yoo, Shin, & Park, 2010). Rin1, a GEF for Rab5, is required during endocytosis to target phosphorylated EphA4 to the Rab5 endosomal compartments (Deininger et al., 2008).The role of

some endocytosis regulators seem to be very direct: Vav2, a Rho GEF, physically interacts with Eph and is required for endocytosis in retinal cells (C. W. Cowan et al., 2005; Hunter et al., 2006).

An interesting issue concerns whether sustained signaling from internalized complexes is required during the retraction phase. The endocytosed complexes are indeed thought to include the associated signaling components (Litterst et al., 2007; Sadowski, Sadowski, Pilecka, & Miaczynska, 2009). The ultimate fate of ephrin-Eph complexes is unclear: They have only been tracked as far as the early endosomal compartment (C. W. Cowan et al., 2005; Groeger & Nobes, 2007; Marston et al., 2003; Zhuang et al., 2007; M. Zimmer et al., 2003), it remains to be established if they are degraded in lysosomes or if some components are recycled to the cell surface.

Ephrin/Eph proteolytic cleavage

Two families of membrane-anchored proteases, the ADAM disintegrins and the MPPs (metalloprotease proteins) mediate a wide variety of specific proteolysis events at the cell surface. They catalyze in particular the shedding of the extracellular domain of signaling molecules such as TGF-α, the Notch ligand Delta, and also ephrins and Ephs (Rooke, Pan, Xu, & Rubin, 1996; Seals & Courtneidge, 2003). While ADAMs classically cleave the substrates present on the same cell membrane, in the case of the ephrin/Eph system they act in trans, i.e. they cleave ephrins or Ephs expressed on the opposing cell (Janes et al., 2005). Proteolysis in trans ensures that cleavage occurs only upon ephrin-Eph binding on adjacent cells. Both ligand and receptor cleavages are involved in cell repulsion, but the former case was more extensively studied. Flanagan and colleagues first showed that the inhibition of metalloproteinases impaired axon detachment and led to a delay in repulsion (Hattori, Osterfield, & Flanagan, 2000; Rooke et al., 1996). A role for ADAM metalloproteinases in ephrin-Eph signaling was since confirmed in multiple cases (Janes et al., 2005; Litterst et al., 2007; Solanas, Cortina, Sevillano, & Batlle, 2011). The explanation for why ephrins are

cleaved upon interaction with their receptors came from a study that showed that; prior to ephrin-Eph interaction ADAM10 associate constitutively with the Eph ligand binding domain. Once bound, the activated complex exposes a new recognition motif for the cysteine-rich domain on ADAM10, which positions ADAM10 proteinase domain for effective ephrin cleavage (Janes et al., 2005; Janes et al., 2009; Mancia & Shapiro, 2005). It was shown that the cysteine-rich domain of ADAM10 only recognizes the ephrin-Eph complex and not the individual ligand or receptor (Janes et al., 2005). This is proposed to be due to a change in Eph conformation that occurs during its activation: Indeed, Eph phosphorylation appears to cause the extension of the kinase domain away from the membrane, which transmits in some ways a change to the extracellular part of the ephrin-Eph complex (Janes et al., 2009). This process exposes a novel recognition site for ADAM10 and imposes a correct orientation of protease domain in order to cleave ephrin in trans.

Usually the cleavage of an extracellular domain by metalloproteinase triggers a subsequent cleavage and release of intracellular domain by γ-secretases (Janes et al., 2005; Janes et al., 2009; Mancia & Shapiro, 2005). In Notch signaling pathway this second cleavage translocates the intracellular domain to the nucleus. A similar ADAM/γ -secretase sequential proteolysis occurs upon ephrinB reverse signaling (J.-P. Himanen et al., 2007; Zolkiewska, 2008). However not much is known about the consequences of the intracellular cleavage on cell-cell detachment. There is some evidence that upon ephrinB cleavage an intracellular signaling peptide is released that can bind to Src kinase and prevents its interaction with the inhibitory kinase, therefore keeping it activated. This was suggested to act as a feedback mechanism which would promote reverse signaling (Georgakopoulos et al., 2006; J.-P. Himanen et al., 2007). In another study it was reported that the intracellular domain released by cleavage of ephrinB1 translocates to the nucleus (Tomita, Tomita, Tanaka, Morohashi, & Iwatsubo, 2006). The cytoplasmic tail contains a basic amino acid stretch that seems to serve as nuclear translocation signal (NLS). It is not known whether the cleaved ephrinB1 has any role inside the nucleus.

Note that available data suggest selectivity for the interaction between Eph isoforms and specific ADAM proteins (Janes et al., 2005). Whether the reported mechanisms apply to all cases or are restricted to some specific ligand-receptor pairs remains to be examined.

Ephrin-Eph regulation of expression

The expression of ephrins and Ephs has been studied in many different contexts but the transcriptional control of these molecules has not been analyzed very extensively. There is however an established regulation by homeobox transcription factors (HOX) in the case of the rhombomere segmentation. The segmental expression of ephrins and Ephs suggested indeed an obvious link with the segmented pattern of HOX factors and their well-known role in patterning along the anterior-posterior axis during development. For instance, the homeobox proteins HOXA1 and HOXB1 were shown to activate rhombomere-specific EphA2 expression in the developing mouse brain, and HOXA2 was found to regulate EphA4 in rhombomeres 3 and 5(D. N. Arvanitis & Davy, 2012). Several other transcription factors have been found to regulate ephrin/Eph expression. For instance, chick brain factor 1 (CBF1) regulates ephrinA5 expression during development of the retinotectal map in chicken. EphB2 transcription is controlled by TCF4 and β-catenin in the intestinal epithelium. Valentino (val), a basic leucine zipper bzip transcription factor, was shown to establish the mutually exclusive expression domains of EphB4 and ephrinB2 in the Zebrafish caudal hindbrain, while the zinc-finger transcription factor Zic2 regulates the expression of EphB1 in retinal ganglion cells (D. N. Arvanitis & Davy, 2012).

There is new evidence that ephrin and Eph gene expression could be modulated by mechanical forces in different tissue types, including bone and dental pulp (Diercke, Sen, Kohl, Lux, & Erber, 2011). Periodontal ligament fibroblasts (PDLF) are mechano-responsive cells in these tissues. Members of the ephrin/Eph family might link mechanical forces received by PDLF with the regulation of

osteoblastogenesis on osteoblasts of the alveolar bone. When these cells were subjected to static compressive forces, ephrinA2 expression was induced, while ephrinB2 expression was down-regulated. Note that while these findings suggest an interesting regulatory mechanism, it is not clear if the mechanical effect on ephrin/Eph expression is direct (Diercke et al., 2011).

Another interesting mechanism of regulation utilizes the Ras MAPkinase pathway. A feedback loop mechanism has been deciphered in breast cancer cell line (Macrae et al., 2005). On one hand ligand-induced activation of EphA2 increases its mRNA levels through activation of MAPK pathway (Pratt, 2003). On the other hand the MAPK pathway inhibits ephrinA1 expression, which reciprocally inhibits EphA2 expression. This negative feedback loop regulates Ras activity, which in turn contributes to the receptor-ligand mutually exclusive expression pattern in these cell lines (Macrae et al., 2005; Qian Xu, Lin, Petit, & Groves, 2011; Zhang et al., 2010).

Ephrin and Eph co-expression on the same cell

Although the traditional picture of an ephrin-Eph system considers a complementary expression pattern, with one cell expressing a ligand and the adjacent cell expressing its receptor, the actual situation is often much more complex. The analysis of the nervous system made it soon clear that complementary expression is not the rule, both ephrins and Ephs are most often expressed in overlapping patterns (J. Flanagan, Flanagan, & Vanderhaeghen, 1998). At the cellular levels, this implied that ligands and receptors were present on the same cell surface. In fact, most cells express more than one ephrin and one Eph. This situation was originally described in neurons but now appears to be widespread, including in the embryonic tissues and in tumor cells (Pasquale, 2010; Surawska, Surawska, Ma, & Salgia, 2004). Computation of the final output of the system is thus far from trivial: Firstly, signals triggered through ephrins or Ephs at contacts between cells of the same type can converge to activate a common signal output, or, on the contrary, antagonize each other. Secondly, a cell

may receive simultaneously forward and reverse signals. Potentially, multiple pathways of different nature could be generated in the same cell (e.g. adhesive and repulsive). Different models have been put forward to predict the effect of co-expression of several ephrins and Ephs (D. Arvanitis & Davy, 2008): 1.The formation of cis-interactions can lead to a direct crosstalk between ligands and receptors or between different Eph receptors. 2. Alternatively, ligands and receptors may remain separated by being sequestered into distinct membrane subdomains. Based on this scenario a third situation can also be considered: 3. ephrin-Eph selective interactions may limit the cis-interaction of particular ligands or receptors, depending on the availability of specific partners in the adjacent cell.

Regulation by cis-interactions

Drescher group first reported evidence for an interaction in cis between EphA and ephrinA. They observed that ephrinAs and EphAs exhibited overlapping expression in the retinal cells. By manipulating ephrinA levels in those cells, they observed changes in sensitivity of their axons to exogenous ephrins. FRET analysis confirmed the formation of cis-interaction in neurons between EphA3 and ephrinA5 (Carvalho et al., 2006; Hornberger et al., 1999). A follow-up study mapped the site of cis-interaction on EphA3 to the FNIII domain. This interaction caused a decrease in the phosphorylation levels of EphA3, accounting for the attenuated signaling (Carvalho et al., 2006; Yin et al., 2004). These studies relied mostly on in vitro assays, and the functional significance of this phenomenon in vivo is not very well understood. Note that cis-interaction between the B-classes of ephrins and Ephs have not been determined yet (Kao & Kania, 2011).
In addition to cis-interactions between Ephs and ephrins, the Eph receptors expressed on the same cell can also make hetero-oligomers (Juha P. Himanen et al., 2010; Janes et al., 2011; Janes et al., 2012). It has been demonstrated that different Eph receptors, when activated by compatible ephrin ligands, can cross-phosphorylate each other, which can lead to a cooperative signaling outcome.

Evidence for a crosstalk between Eph receptors was first shown in breast carcinoma cell lines (Fox & Kandpal, 2011). EphB6 expressed in these cell lines is kinase-deficient yet it undergoes ligand-inducible trans-phosphorylation and can initiate specific cytoplasmic signaling events. This activity is due to the fact that EphrinB1 stimulation induces direct EphB1-EphB6 physical interaction, which allows EphB1 to phosphorylate EphB6 (Truitt & Freywald, 2011).
Further studies proposed that the formation of Eph hetero-oligomers may not necessarily depend on their ability to interact with a common ligand, and can be a function of the abundance of those Ephs on the cell surface. Note however that Eph receptors may have different or even antagonistic functions on the same cell. Cases have been shown where Eph heterooligomeres had distinct functions. On those cases the more abundant Eph receptor always dominated the functional outcome (Janes et al., 2011).
These observations revealed that co-expression of ligands and receptors can influence their function in complex ways, via different forms of cis-interaction or lateral inhibitions. Altogether, it is important to always consider the expression of all ephrins and Ephs on cells while studying their role in a given context.

Expression in different membrane domains

A study in motor neurons of the limb showed that ephrinAs and EphAs are sorted into separate membrane microdomains. The ligand and receptor are independently trans-activated and each exerts opposing effect on neuronal growth cone behaviour. EphA proteins trigger growth cone collapse, and ephrinAs promote axon out growth (Marquardt et al., 2005). They show that mis-targeting of the ephrin or Eph to the Eph-enriched, or to ephrin-enriched domains, respectively, lead to cis-interaction and attenuation of the corresponding signal (Marquardt et al., 2005). Basically, segregating ephrins and Ephs to different subdomains allows their signaling in trans without influences from cis-interactions, and thus uncouples them functionally. Mechanistic explanation for how this membrane segregation could occur was missing until a recent study by (Kao & Kania, 2011)

elegantly brought together the two models of cis-inhibition and of sequestration in different microdomains:

The authors revisited the expression pattern and localization of ephrins and Ephs in motor neurons. They showed that ephrin/Eph protein concentration controls the delocalisation of Ephs and ephrins, which in turn controls the balance between cis-attenuation and parallel trans-signaling. In other words, in the absence of trans-interactions, Ephs are very loosely packed, which make them more susceptible to cis-binding by ephrins. Trans-acting ephrin-Eph complexes generate a very compact signaling center that does not allow cis-interactions with adjacent ephrins on the membrane (Brückner et al., 1999). While this study provides appealing evidence for how co-expression of ephrin/Ephs on the same cell is orchestrated, it is not clear if this phenomenon is a general rule that can be applied to other contexts (Egea & Klein, 2007b; Gauthier & Robbins, 2003; J.-P. Himanen et al., 2007).

Alternative uncoupling of ephrins and Ephs by specific trans-activation

An alternate interpretation of the above model can be considered under conditions where selective interactions between individual pairs of ephrin and Eph isoforms are taken into account. It can be speculated that co-expressed ligand and receptor segregate locally on the membrane as a consequence of their specific trans-activation. In other words the availability of a specific ligand and its cognate receptor in trans would be the driving force to separate co-expressed ephrins and Ephs on different membrane domains and reciprocally increase their local concentration on the membrane. For instance one can imagine that Ephs with differential affinities for ephrins in trans accumulate in distinct patches of the membrane. This mechanism is consistent with the model above and can potentially lead to functional separation of different ephrins or Ephs that are expressed on the same cell.

Ephrin/Eph crosstalk with other signaling pathways

Ephrin-Eph signaling together with several other pathways, contributes to regulation of many basic processes such as cell migration, proliferation and tissue boundary formation. Components activated downstream of ephrin/Eph signaling, such as Src, Rac, Rho or Erk, all have a broad range of targets and are common to several other signaling pathways. These pathways can thus engage in synergistic or antagonistic crosstalks with ephrin and Ephs.

The FGF receptor (FGFR), for instance, has been shown to directly influence ephrin-Eph signaling by cross-phosphorylation (L. D. Chong et al., 2000; Jones et al., 1998). It was found that in the early Xenopus embryo, the strong cell dissociation observed upon ephrinB1 overexpression could be inhibited by co-expression of activated FGFR. FGFR binds ephrinB1 in cis and phosphorylates its cytoplasmic tail (L. D. Chong et al., 2000). The relevance of this antagonistic inhibition was shown in the context of the retinotectal mapping, where both pathways coordinately regulate the cell access to the eye field by modulating cell movement (Moore et al., 2004).

Another evidence for the antagonistic crosstalk between ephrin-Eph signaling and FGFR pathway was reported by (Picco, Hudson, & Yasuo, 2007). The study was performed in Ciona, where asymmetric cell division generates notochord and neural precursor cells; it was found that in this system the precursor cells were becoming functionally polarized due to the two signals generated at opposite sides: On one side, activation of Eph at contact with the neighboring ephrin-expressing animal cells caused local Erk inhibition in the mother cells. The broadly expressed FGFs on the other hand activated Erk pathway on those cells. This asymmetry in Erk signaling determined the asymmetric cell division, which in turn created distinct cell fates in the daughter cells (Picco et al., 2007).

The Wnt pathway also establishes cross talk with ephrin-Eph signaling both at the levels of its receptor and other downstream components. The extracellular domain of Wnt receptor RYK has been shown to interact with Eph receptors and modulate their function (D. Arvanitis & Davy, 2008). The relationship between

these two receptors has been examined in several studies on retinotectal mapping (Adam et al., 2006). EphrinB-EphB signaling is involved in positioning retinotectal projections along the medial-lateral axis. Wnt3/RYK pathway acts as a lateral mapping force that counterbalances the ephrinB-EphB medial mapping force in the tectum (Adam et al., 2006; D. Arvanitis & Davy, 2008). Note that it is not clear if the two pathways directly modulate each other. Some evidence suggests on the contrary that their cross talk is modulated through FGF (H.-S. Lee et al., 2009).

Wnt signaling and ephrin-Eph signaling also converge on the downstream components. The Tanaka group showed an interaction of Eph and ephrinB with Dishevelled (Dsh) in Xenopus (Masamitsu Tanaka, Kamo, Ota, & Sugimura, 2003). Dishevelled (Dsh) seems to act as a hub between ephrins and Eph receptors and the Wnt pathway. Dsh is an essential component of the canonical/β-catenin and non-canonical/planar polarity (PCP) pathways. The link with ephrin-Eph signaling seems to involve the latter branch: Dsh can interact with ephrins and Ephs via Daam1(Inoue et al., 2001; Kida et al., 2007; Monschau et al., 1997; Masamitsu Tanaka et al., 2003). The interaction requires the DEP domain of Dsh, consistent with a function in the PCP pathway (Kida et al., 2007). The interaction results in Dsh phosphorylation which in turn activates Rho kinase, leading to the internalization of the ephrin/Eph-Daam1-Dsh complex (Bochenek, Dickinson, Astin, Adams, & Nobes, 2010). The association with Dsh was shown to be functionally relevant for the process of cell sorting: The interference with this interaction disrupted the sorting of ephrinB1 expressing cells from EphB2 expressing cells in vitro and in vivo (Moore et al., 2004). Note that FGF signaling also influences this complex, since ephrin phosphorylation by FGFR reduces the interaction with Dsh (H.-S. Lee et al., 2009).

Finally, G-protein coupled chemokine receptors (CXCR), which regulate among many other processes, cell migration or adhesion, can establish agonistic or antagonistic crosstalks with ephrins and Ephs (Kucia et al., 2004; Salvucci, de la

Luz Sierra, Martina, McCormick, & Tosato, 2006). The crosstalk appears to take place at the level of the small GTPases. The two pathways differentially alter the balance of GTPases and affect cellular migration.

Ephrin-Eph signaling and the control of cell adhesion molecules

In addition to mediating repulsive signal, ephrin and Ephs also modulate positively or negatively, the function of cell-cell and cell-matrix adhesion molecules.

Cell-matrix adhesion

Ephrin-Eph signaling can exert both positive and negative influences on integrin mediated cell-matrix adhesion. An example of cooperative effect was observed at the genetic level in the formation of somites. Both integrin signaling and ephrin-Eph signaling are required for proper somite formation. Inhibition of ephrin-Eph signaling worsened the somite phenotype observed in fibronectin or integrin mutants. Most studies suggest that the convergence of these two pathways is at the level of the cytoplasmic kinases FAK, PI3K, MAPK, or the small GTPases Rho, Rac and Rap (D. Jülich, Julich, Mould, Koper, & Holley, 2009; Koshida, 2005; Prévost et al., 2005; Riedl et al., 2005).

Cell-Cell adhesion

Ephrin-Eph signaling can regulate cell-cell adhesion molecules in different ways. Some evidence for how ephrin-Eph signal modulates adhesion has been reported (Singh et al., 2012): In colorectal cancer, cells that express high levels of EphB2 repulse, pack into compact clusters and sort from ephrinB1 positive cells. Cortina et al (2007) showed that sorting of these two populations was due to the redistribution of E-cadherin from cytoplasm to the basolateral membrane, opposite to the side where EphB2 was activated. This could potentially be a

general mechanism for how EphB signaling may couple cell contraction with cell-to-cell adhesion (Cortina et al., 2007).

More recently, the same group reported a novel mechanism for the control of E-cadherin by ephrin-Eph signaling in epithelial cells. They observed that, when an Eph-expressing cell population is put into contact with ephrinB1-interacting cells, the Eph receptors interact with E-cadherin via the metalloproteinase ADAM10 at the sites of contact with ephrinB-expressing cells. As a result of these interactions, E-cadherin is cleaved locally, resulting in its differential expression on the membranes of the two cell populations (Solanas et al., 2011). This mechanism can well describe what happens at the sites of ephrin-Eph mediated de-adhesion to the adhesion molecules (Herath & Boyd, 2010).

Ephrin-Eph signaling also affects other types of adhesions. Tight junctions for example have been shown to be controlled by ephrin signaling, in particularly via direct interaction between ephrinB1 and the tetraspan membrane proteins claudins (H.-S. Lee, Nishanian, Mood, Bong, & Daar, 2008; Masamitsu Tanaka et al., 2005; M. Tanaka, Tanaka, Kuriyama, & Aiba, 2012). Cis-interaction between claudins and the extracellular domain of ephrinB1 causes phosphorylation of the EphirnB1 cytoplasmic domain, which inhibits the formation of tight junctions. This mechanism can explain the dissociation of epithelial tissue in Xenopus upon overexpression of ephrinB1 (Jones et al., 1998), it may be applied to malignant epithelial cancer cells, which also overexpress ephrinB1 and display weak adhesion.

Biological function

Studies of ephrin-Eph function have focused mostly on their role in differentiated and fairly specialized neuronal cells. Their role in other processes such as boundary formation and cell migration in the developing embryo has been less studied. There are two main difficulties on acquiring more in depth functional analysis for these molecules during the early development: First, the widespread and overlapping expression of ephrins and Ephs makes it difficult to tease their

contribution apart. Their partial functional redundancy or compensation is an additional significant issue. Second, the ability to signal bi-directionally adds another layer of complexity. Thus there remains a great demand to pursue studies on the role of these molecules on aspects other than neuronal guidance. Nevertheless, the fact that ephrins and Eph receptors play an essential role in boundary formation has been firmly established at least for two systems.

The role of ephrin/Eph at the somite boundary

Several ephrins and Eph receptors show conserved segmental expression, including EphA3, EphA4, EphB3, ephrinB1, ephrinB2 and ephrinA5 (Durbin et al., 1998; Fletcher et al., 1994; Kilpatrick et al., 1996). So far, only the role of ephrinB2 and EphA4 have been studied (Bergemann, Cheng, Brambilla, Klein, & Flanagan, 1995; Irving, Nieto, DasGupta, Charnay, & Wilkinson, 1996). These two molecules are expressed sequentially along the antero-posterior axis of the embryo within the somitic and anterior presomitic mesoderm, and seem to play a role in different aspects of somitogenesis: In Zebrafish it has been shown that local de-adhesion within the presomitic mesoderm involved ephrinB2-EphA4 signaling (Wood, Wood, & Thorogood, 1994). Furthermore, they may contribute to the formation of cell polarity during somite segmentation: EphA4 activation has been shown to polarize β-catenin apically and induce de-adhesion at somite boundaries. This process is directly or indirectly linked to morphological changes and epithelialization of the forming somite, which also depends on ephrins and Ephs (Ferrer Vaquer, Ferrer Vaquer, Viotti, & Hadjantonakis, 2010; Kelly Kuan et al., 2004; Nomura-Kitabayashi et al., 2002; Watanabe, Sato, Saito, Tadokoro, & Takahashi, 2009; Winning, Wyman, & Walker, 2001).
The underlying mechanism of somite epithelialization is unclear, but seems to involve parallel regulations by localized secretion of fibronectin at the boundary and ephrin-Eph signaling (Barrios et al., 2003; S.-W. Chong & Jiang, 2005; Dörthe Jülich, Mould, Koper, & Holley, 2009).This conclusion is based on the

increased defects observed upon interference with ephrinB2 in the fibronectin or integrin Zebrafish mutants (Dörthe Jülich et al., 2009).
The role of other ephrins and Ephs has not been yet investigated. Note that ephrin-Eph signaling could be repulsive or adhesive, or be involved in more indirect paths to control the somite boundaries. So far there has been no explicit search for evidence of repulsive reactions along at the boundary. However, examination of published time lapse movies (Kulesa & Fraser, 2002) suggests that cells are indeed pulled apart at the somite boundary.

The role of ephrin/Eph on rhombomere boundaries

The hindbrain develops a segmental pattern consisting of seven segments or rhombomeres (r1–r7). Segmentally expressed transcription factors confer distinct cellular properties of cells in r3/r5 compared to r2/r4/r6 that restrict cell movement between rhombomeres. Ephrins and Ephs are among molecules that are expressed segmentally. Rhombomeres r3-5 show the clearest complementary pattern: EphrinB1, B2 and B3 are expressed in rhombomere r4, and EphA4, A7, B2 and B3 are expressed in r3 and r5. Various manipulations involving ephrinB2/EphA4 depletion or mis-expression and explant transplantation indicate that interaction of these complementarily expressed molecules restrict cell intermingling at the rhombomere interface (J. Cooke et al., 2001; J. E. Cooke et al., 2005; J. E. Cooke & Moens, 2002; S. Guthrie & Lumsden, 1991; Kemp et al., 2009; Sela Donenfeld et al., 2009; Q. Xu, Alldus, Holder, & Wilkinson, 1995). The same molecules may also increase coherence within the segments (J. E. Cooke et al., 2005; Kemp et al., 2009). Again, direct evidence for repulsion is missing. Note also that the complementary expression of ligands and receptors is much less complete in anterior and posterior segments, especially in the late forming rhombomeres r1- r2, where ephrins and Ephs are largely overlapping. These situations are not well understood.

The role of ephrin/Eph in cancer

A variety of ephrins and Ephs are expressed both in tumor cells and tumor micro-environment, and their up- or down- regulation seems to be involved in various aspects of cancer progression (Hafner et al., 2004). EphA2 and EphB4, for example, are up-regulated in many cancers and their expression has been linked to increased malignancy (Surawska et al., 2004). A simple correlation between high ephrin or Eph levels and malignancy cannot be drawn: Decreased Eph or ephrin levels in advanced malignant cancer cell lines and tumor specimens have also been reported (Giannoni et al., 2013). For example, EphA1 is down-regulated in advanced human skin and colorectal cancers and EphB4 in advanced colorectal cancer. Thus it seems that ephrins and Ephs undergo differential expression at different steps during tumor progression.

The reasons for these differences are still unclear, but recent studies have shown reproducible patterns of transcriptional regulation, supporting the idea that these molecules act positively for specific stages of cancer progression, but negatively for others. Specifically, these studies showed that an initial Eph receptor up-regulation, activated by oncogenic signaling pathways, can be followed by epigenetic silencing in more advanced stages owing to promoter hyper-methylation. This regulatory mechanism has been shown for several EphA and EphB receptors in colorectal cancer (D. N. Arvanitis & Davy, 2012; Pasquale, 20100: Such as transcriptional repression of EphB2 by REL (a member of the nuclear factor-κB family), that is involved in Eph silencing.

It has also been shown that different isoforms are expressed at different steps. For instance, a change has been observed in the expression levels of EphB2 to EphB4, during colorectal cancer progression. At the molecular level, this change was attributed to a switch in the association of β-catenin from the co-activator of EphB2 to the co-activator of EphB4 transcription (Kumar et al., 2009). Similar instances have been documented in breast and lung cancer (Brantley-Sieders, 2012). A general picture thus can be speculated: The different level of various ephrin/Ephs in tumors and metastatic states may control repulsive or adhesive signals required for the multiple steps of tumor development and metastasis.

References

Abercrombie, M. (1970). Contact Inhibition in Tissue Culture. *In Vitro, 6*(2), 128-142.

Adam, M. S., Jun, S., Alex, M. W., Chin-Chun, L., Leslie, A. K., & Yimin, Z. (2006). Wnt–Ryk signaling mediates medial–lateral retinotectal topographic mapping. *Nature, 439*(7072), 31-37. doi: 10.1038/nature04334

Aliee, M., Röper, J.-C., Landsberg, Katharina P., Pentzold, C., Widmann, Thomas J., Jülicher, F., & Dahmann, C. (2012). Physical Mechanisms Shaping the Drosophila Dorsoventral Compartment Boundary. *Current biology : CB, 22*(11), 967-976.

Andersson, E. R. (2012). The role of endocytosis in activating and regulating signal transduction. *Cell Mol Life Sci, 69*(11), 1755-1771. doi: 10.1007/s00018-011-0877-1

Angelika bottger, M. H. (2012). Hydra, a model system to trace the emergence of boundaries in developing eumetazoans. *int. J. Dev. Biol, 56*, 583-591. doi: 10.1387/ijdb. 11345ab

Arvanitis, D., & Davy, A. (2008). Eph/ephrin signaling: networks. *Genes & Development, 22*(4), 416-429.

Arvanitis, D. N., & Davy, A. (2012). Regulation and misregulation of Eph/ephrin expression. *Cell Adhesion & Migration, 6*(2), 131-137.

Barrios, A., Poole, R. J., Durbin, L., Brennan, C., Holder, N., & Wilson, S. W. (2003). Eph/Ephrin Signaling Regulates the Mesenchymal-to-Epithelial Transition of the Paraxial Mesoderm during Somite Morphogenesis. *Current biology : CB, 13*(18), 1571-1582.

Batson, J., Astin, J. W., & Nobes, C. D. (2013). Regulation of contact inhibition of locomotion by Eph-ephrin signaling. *J Microsc, 251*(3), 232-241. doi: 10.1111/jmi.12024

Beg, A. A., Sommer, J. E., Martin, J. H., & Scheiffele, P. (2007). α2-Chimaerin Is an Essential EphA4 Effector in the Assembly of Neuronal Locomotor Circuits. *Neuron, 55*(5), 768-778. doi: http://dx.doi.org/10.1016/j.neuron.2007.07.036

Bellairs, R., Curtis, A. S. G., & Sanders, E. J. (1978). Cell adhesiveness and embryonic differentiation. *Journal of Embryology and Experimental Morphology, 46*(1), 207-213.

Bergemann, A. D., Cheng, H.-J., Brambilla, R., Klein, R., & Flanagan, J. G. (1995). ELF-2, a new member of the Eph ligand family, is segmentally expressed in mouse embryos in the region of the hindbrain and newly forming somites. *Molecular and Cellular Biology, 15*(9), 4921-4929.

Bethani, I., Skanland, S. S., Dikic, I., & Acker-Palmer, A. (2010). Spatial organization of transmembrane receptor signaling. *EMBO J, 29*(16), 2677-2688.

Beysens, D. A., Forgacs, G., & Glazier, J. A. (2000). Cell sorting is analogous to phase ordering in fluids. *Proceedings of the National Academy of Sciences of the United States of America, 97*(17), 9467-9471.

Bisson, N., Poitras, L., Mikryukov, A., Tremblay, M., & Moss, T. (2007). EphA4 Signaling Regulates Blastomere Adhesion in the Xenopus Embryo by Recruiting Pak1 to Suppress Cdc42 Function. *Mol. Biol. Cell, 18*(3), 1030-1043. doi: 10.1091/mbc.E06-04-0294

Blits-Huizinga, C. T., Nelersa, C. M., Malhotra, A., & Liebl, D. J. (2004). Ephrins and their Receptors: Binding versus Biology. *IUBMB Life, 56*(5), 257-265. doi: 10.1080/15216540412331270076

Bochenek, M. L., Dickinson, S., Astin, J. W., Adams, R. H., & Nobes, C. D. (2010). Ephrin-B2 regulates endothelial cell morphology and motility independently of Eph-receptor binding. *Journal of cell science, 123*(8), 1235-1246. doi: 10.1242/jcs.061903

Brambilla, R., Brückner, K., Orioli, D., Bergemann, A. D., Flanagan, J. G., & Klein, R. (1996). Similarities and Differences in the Way Transmembrane-Type Ligands Interact with the Elk Subclass of Eph Receptors. *Molecular and Cellular Neuroscience, 8*(2-3), 199-209.

Brantley-Sieders, D. M. (2012). Clinical relevance of Ephs and ephrins in cancer: Lessons from breast, colorectal, and lung cancer profiling. *Seminars in Cell & Developmental Biology, 23*(1), 102-108. doi: http://dx.doi.org/10.1016/j.semcdb.2011.10.014

Brodland, G. W. (2002). The Differential Interfacial Tension Hypothesis (DITH): A Comprehensive Theory for the Self-Rearrangement of Embryonic Cells and Tissues. *Journal of Biomechanical Engineering, 124*(2), 188-197. doi: 10.1115/1.1449491

Brückner, K., & Klein, R. (1998). Signaling by Eph receptors and their ephrin ligands. *Current Opinion in Neurobiology, 8*(3), 375-382. doi: http://dx.doi.org/10.1016/S0959-4388(98)80064-0

Brückner, K., Labrador, J. P., Scheiffele, P., Herb, A., Seeburg, P. H., & Klein, R. (1999). EphrinB Ligands Recruit GRIP Family PDZ Adaptor Proteins into Raft Membrane Microdomains. *Neuron, 22*(3), 511-524. doi: http://dx.doi.org/10.1016/S0896-6273(00)80706-0

Bush, J. O., & Soriano, P. (2009). Ephrin-B1 regulates axon guidance by reverse signaling through a PDZ-dependent mechanism. *Genes & Development, 23*(13), 1586-1599. doi: 10.1101/gad.1807209

Bussell, K. (2001). Eph receptors tip the balance. *Nat Rev Mol Cell Biol, 2*(6), 401-401.

Carvalho, R. F., Beutler, M., Marler, K. J. M., Knoll, B., Becker-Barroso, E., Heintzmann, R., . . . Drescher, U. (2006). Silencing of EphA3 through a cis interaction with ephrinA5. *Nat Neurosci, 9*(3), 322-330. doi: http://www.nature.com/neuro/journal/v9/n3/suppinfo/nn1655_S1.html

Cavey, M., Rauzi, M., Lenne, P.-F., & Lecuit, T. (2008). A two-tiered mechanism for stabilization and immobilization of E-cadherin. *Nature, 453*(7196), 751-756. doi:

http://www.nature.com/nature/journal/v453/n7196/suppinfo/nature06953_S1.html
Chen, X., & Gumbiner, B. M. (2006). Paraxial protocadherin mediates cell sorting and tissue morphogenesis by regulating C-cadherin adhesion activity. *The Journal of Cell Biology, 174*(2), 301-313. doi: 10.1083/jcb.200602062
Chen, X., Koh, E., Yoder, M., & Gumbiner, B. M. (2009). A Protocadherin-Cadherin-FLRT3 Complex Controls Cell Adhesion and Morphogenesis. *PLoS ONE, 4*(12), e8411. doi: 10.1371/journal.pone.0008411
Chen, X., Molino, C., Liu, L., & Gumbiner, B. M. (2007). Structural Elements Necessary for Oligomerization, Trafficking, and Cell Sorting Function of Paraxial Protocadherin. *Journal of Biological Chemistry, 282*(44), 32128-32137. doi: 10.1074/jbc.M705337200
Cheng, Y.-C., Amoyel, M., Qiu, X., Jiang, Y.-J., Xu, Q., & Wilkinson, D. G. (2004). Notch Activation Regulates the Segregation and Differentiation of Rhombomere Boundary Cells in the Zebrafish Hindbrain. *Developmental Cell, 6*(4), 539-550. doi: http://dx.doi.org/10.1016/S1534-5807(04)00097-8
Chong, L. D., Park, E. K., Latimer, E., Friesel, R., & Daar, I. O. (2000). Fibroblast Growth Factor Receptor-Mediated Rescue of x-Ephrin B1-Induced Cell Dissociation in XenopusEmbryos. *Molecular and Cellular Biology, 20*(2), 724-734. doi: 10.1128/mcb.20.2.724-734.2000
Chong, S.-W., & Jiang, Y.-J. (2005). Off limits – Integrins holding boundaries in somitogenesis. *Trends in Cell Biology, 15*(9), 453-457. doi: http://dx.doi.org/10.1016/j.tcb.2005.07.008
Christian, J. L., & Moon, R. T. (1993). Interactions between Xwnt-8 and Spemann organizer signaling pathways generate dorsoventral pattern in the embryonic mesoderm of Xenopus. *Genes & Development, 7*(1), 13-28. doi: 10.1101/gad.7.1.13
Chung, H. A., Yamamoto, T. S., & Ueno, N. (2007). ANR5, an FGF Target Gene Product, Regulates Gastrulation in Xenopus. *Current Biology, 17*(11), 932-939.
Cooke, J., Moens, C., Roth, L., Durbin, L., Shiomi, K., Brennan, C., . . . Holder, N. (2001). Eph signaling functions downstream of Val to regulate cell sorting and boundary formation in the caudal hindbrain. *Development, 128*(4), 571-580.
Cooke, J. E., Kemp, H. A., & Moens, C. B. (2005). EphA4 Is Required for Cell Adhesion and Rhombomere-Boundary Formation in the Zebrafish. *Current Biology, 15*(6), 536-542. doi: http://dx.doi.org/10.1016/j.cub.2005.02.019
Cooke, J. E., & Moens, C. B. (2002). Boundary formation in the hindbrain: Eph only it were simple&. *Trends in neurosciences, 25*(5), 260-267.
Cortina, C., Palomo-Ponce, S., Iglesias, M., Fernandez-Masip, J. L., Vivancos, A., Whissell, G., . . . Batlle, E. (2007). EphB-ephrin-B interactions suppress colorectal cancer progression by compartmentalizing tumor cells. *Nat Genet, 39*(11), 1376-1383. doi: http://www.nature.com/ng/journal/v39/n11/suppinfo/ng.2007.11_S1.html

Couchman, J. R., & Rees, D. A. (1979). The behaviour of fibroblasts migrating from chick heart explants: changes in adhesion, locomotion and growth, and in the distribution of actomyosin and fibronectin. *Journal of cell science, 39*(1), 149-165.

Cowan, C., Cowan, M., & Henkemeyer. (2002). Ephrins in reverse, park and drive. *Trends in Cell Biology, 12*(7), 339-346.

Cowan, C. W., Shao, Y. R., Sahin, M., Shamah, S. M., Lin, M. Z., Greer, P. L., . . . Greenberg, M. E. (2005). Vav Family GEFs Link Activated Ephs to Endocytosis and Axon Guidance. *Neuron, 46*(2), 205-217. doi: http://dx.doi.org/10.1016/j.neuron.2005.03.019

Dahmann, C., & Basler, K. (2000). Opposing Transcriptional Outputs of Hedgehog Signaling and Engrailed Control Compartmental Cell Sorting at the Drosophila A/P Boundary. *Cell, 100*(4), 411-422. doi: http://dx.doi.org/10.1016/S0092-8674(00)80677-7

Dahmann, C., Oates, A. C., & Brand, M. (2011). Boundary formation and maintenance in tissue development. *Nat Rev Genet, 12*(1), 43-55.

Dail, M., Richter, M., Godement, P., & Pasquale, E. B. (2006). Eph receptors inactivate R-Ras through different mechanisms to achieve cell repulsion. *Journal of cell science, 119*(7), 1244-1254. doi: 10.1242/jcs.02842

Damon, B. J., Mezentseva, N. V., Kumaratilake, J. S., Forgacs, G., & Newman, S. A. (2008). Limb bud and flank mesoderm have distinct “physical phenotypes” that may contribute to limb budding. *Developmental Biology, 321*(2), 319-330. doi: http://dx.doi.org/10.1016/j.ydbio.2008.06.018

Davis, G. S., Phillips, H. M., & Steinberg, M. S. (1997). Germ-Layer Surface Tensions and "Tissue Affinities" inRana pipiensGastrulae: Quantitative Measurements. *Developmental Biology, 192*(2), 630-644.

Davis, T. L., Walker, J. R., Loppnau, P., Butler-Cole, C., Allali-Hassani, A., & Dhe-Paganon, S. (2008). Autoregulation by the Juxtamembrane Region of the Human Ephrin Receptor Tyrosine Kinase A3 (EphA3). *Structure, 16*(6), 873-884. doi: http://dx.doi.org/10.1016/j.str.2008.03.008

Deininger, K., Eder, M., Kramer, E. R., Zieglgansberger, W., Dodt, H. U., Dornmair, K., . . . Klein, R. (2008). The Rab5 guanylate exchange factor Rin1 regulates endocytosis of the EphA4 receptor in mature excitatory neurons. *Proc Natl Acad Sci U S A, 105*(34), 12539-12544. doi: 10.1073/pnas.0801174105

Dequeant, M.-L., & Pourquie, O. (2008). Segmental patterning of the vertebrate embryonic axis. *Nat Rev Genet, 9*(5), 370-382.

Diercke, K., Sen, S., Kohl, A., Lux, C. J., & Erber, R. (2011). Compression-dependent Up-regulation of Ephrin-A2 in PDL Fibroblasts Attenuates Osteogenesis. *Journal of Dental Research, 90*(9), 1108-1115. doi: 10.1177/0022034511413926

Domingo, C., & Keller, R. (1995). Induction of notochord cell intercalation behavior and differentiation by progressive signals in the gastrula of Xenopus laevis. *Development, 121*(10), 3311-3321.

Dravis, C., Yokoyama, N., Chumley, M. J., Cowan, C. A., Silvany, R. E., Shay, J., . . . Henkemeyer, M. (2004). Bidirectional signaling mediated by

ephrin-B2 and EphB2 controls urorectal development. *Developmental Biology, 271*(2), 272-290.

Dray, N., Lawton, A., Nandi, A., JÃ¼lich, D. r., Emonet, T., & Holley, ScottÂ A. (2013). Cell-Fibronectin Interactions Propel Vertebrate Trunk Elongation via Tissue Mechanics. *Current Biology, 23*(14), 1335-1341. doi: http://dx.doi.org/10.1016/j.cub.2013.05.052

Drescher, U. (2002). Eph family functions from an evolutionary perspective. *Current Opinion in Genetics & Development, 12*(4), 397-402. doi: http://dx.doi.org/10.1016/S0959-437X(02)00316-7

Durbin, L., Brennan, C., Shiomi, K., Cooke, J., Barrios, A., Shanmugalingam, S., . . . Holder, N. (1998). Eph signaling is required for segmentation and differentiation of the somites. *Genes & Development, 12*(19), 3096-3109. doi: 10.1101/gad.12.19.3096

Egea, J., & Klein, R. (2007a). Bidirectional Eph-ephrin signaling during axon guidance. *Trends in Cell Biology, 17*(5), 230-238.

Egea, J., & Klein, R. (2007b). Bidirectional Eph–ephrin signaling during axon guidance. *Trends in Cell Biology, 17*(5), 230-238. doi: http://dx.doi.org/10.1016/j.tcb.2007.03.004

Egea, J., Nissen, U. V., Dufour, A., Sahin, M., Greer, P., Kullander, K., . . . Klein, R. (2005). Regulation of EphA4 Kinase Activity Is Required for a Subset of Axon Guidance Decisions Suggesting a Key Role for Receptor Clustering in Eph Function. *Neuron, 47*(4), 515-528. doi: http://dx.doi.org/10.1016/j.neuron.2005.06.029

Elowe, S., Holland, S. J., Kulkarni, S., & Pawson, T. (2001). Downregulation of the Ras–Mitogen-Activated Protein Kinase Pathway by the EphB2 Receptor Tyrosine Kinase Is Required for Ephrin-Induced Neurite Retraction. *Molecular and Cellular Biology, 21*(21), 7429-7441. doi: 10.1128/mcb.21.21.7429-7441.2001

Fawcett, J. P., Georgiou, J., Ruston, J., Bladt, F., Sherman, A., Warner, N., . . . Pawson, T. (2007). Nck adaptor proteins control the organization of neuronal circuits important for walking. *Proceedings of the National Academy of Sciences, 104*(52), 20973-20978. doi: 10.1073/pnas.0710316105

Ferrer Vaquer, A., Ferrer Vaquer, M., Viotti, A.-K., & Hadjantonakis. (2010). Transitions between epithelial and mesenchymal states and the morphogenesis of the early mouse embryo. *Cell Adhesion & Migration, 4*(3), 447-457.

Flanagan, J., Flanagan, P., & Vanderhaeghen. (1998). THE EPHRINS AND EPH RECEPTORS IN NEURAL DEVELOPMENT. *Annual Review of Neuroscience, 21*(1), 309-345.

Fletcher, F., Carpenter, M., Shilling, H., Baum, P., Ziegler, S., Gimpel, S., . . . Hjerrild, K. (1994). LERK-2, a binding protein for the receptor-tyrosine kinase ELK, is evolutionarily conserved and expressed in a developmentally regulated pattern. *Oncogene, 9*(11), 3241.

Foty, R. A., Forgacs, G., Pfleger, C. M., & Steinberg, M. S. (1994). Liquid properties of embryonic tissues: Measurement of interfacial tensions. *Physical Review Letters, 72*(14), 2298-2301.

Foty, R. A., & Steinberg, M. S. (2013). Differential adhesion in model systems. *Wiley Interdisciplinary Reviews: Developmental Biology, 2*(5), 631-645. doi: 10.1002/wdev.104

Foty, R. A., Steinberg, M. S., & . (2004). Cadherin-mediated cell-cell adhesion and tissue segregation in relation to malignancy. *Int. J. Dev. Biol., 48*, 397- 409.

Fox, B. P., & Kandpal, R. P. (2011). A Paradigm Shift in EPH Receptor Interaction: Biological Relevance of EPHB6 Interaction with EPHA2 and EPHB2 in Breast Carcinoma Cell Lines. *Cancer Genomics - Proteomics, 8*(4), 185-193.

Frank, C. A., Pielage, J., & Davis, G. W. (2009). A Presynaptic Homeostatic Signaling System Composed of the Eph Receptor, Ephexin, Cdc42, and CaV2.1 Calcium Channels. *Neuron, 61*(4), 556-569. doi: http://dx.doi.org/10.1016/j.neuron.2008.12.028

Frank, M., & Kemler, R. (2002). Protocadherins. *Current Opinion in Cell Biology, 14*(5), 557-562. doi: http://dx.doi.org/10.1016/S0955-0674(02)00365-4

Fryer, B. H., Wang, C., Vedantam, S., Zhou, G.-L., Jin, S., Fletcher, L., . . . Field, J. (2006). cGMP-dependent Protein Kinase Phosphorylates p21-activated Kinase (Pak) 1, Inhibiting Pak/Nck Binding and Stimulating Pak/Vasodilator-stimulated Phosphoprotein Association. *Journal of Biological Chemistry, 281*(17), 11487-11495. doi: 10.1074/jbc.M600279200

Gale, N. W., Holland, S. J., Valenzuela, D. M., Flenniken, A., Pan, L., Ryan, T. E., . . . Yancopoulos, G. D. (1996). Eph Receptors and Ligands Comprise Two Major Specificity Subclasses and Are Reciprocally Compartmentalized during Embryogenesis. *Neuron, 17*(1), 9-19. doi: 10.1016/s0896-6273(00)80276-7

Gauthier, L. R., & Robbins, S. M. (2003). Ephrin signaling: One raft to rule them all? One raft to sort them? One raft to spread their call and in signaling bind them? *Life Sciences, 74*(2–3), 207-216. doi: http://dx.doi.org/10.1016/j.lfs.2003.09.029

Georgakopoulos, A., Litterst, C., Ghersi, E., Baki, L., Xu, C., Serban, G., & Robakis, N. K. (2006). Metalloproteinase/Presenilin1 processing of ephrinB regulates EphB-induced Src phosphorylation and signaling. *EMBO J, 25*(6), 1242-1252. doi: http://www.nature.com/emboj/journal/v25/n6/suppinfo/7601031a_S1.html

Giannoni, E., Taddei, M., Parri, M., Bianchini, F., Santosuosso, M., Grifantini, R., . . . Chiarugi, P. (2013). EphA2-mediated mesenchymal–amoeboid transition induced by endothelial progenitor cells enhances metastatic spread due to cancer-associated fibroblasts. *Journal of Molecular Medicine, 91*(1), 103-115. doi: 10.1007/s00109-012-0941-9

Graner, F., & Glazier, J. A. (1992). Simulation of biological cell sorting using a two-dimensional extended Potts model. *Physical Review Letters, 69*(13), 2013-2016.

Grima, R., & Schnell, S. (2007). Can tissue surface tension drive somite formation? *Developmental Biology, 307*(2), 248-257. doi: http://dx.doi.org/10.1016/j.ydbio.2007.04.032

Groeger, G., & Nobes, C. D. (2007). Co-operative Cdc42 and Rho signaling mediates ephrinB-triggered endothelial cell retraction. *Biochem J, 404*(1), 23-29. doi: 10.1042/bj20070146

Grootjans, J. J., Zimmermann, P., Reekmans, G., Smets, A., Degeest, G., Dürr, J., & David, G. (1997). Syntenin, a PDZ protein that binds syndecan cytoplasmic domains. *Proceedings of the National Academy of Sciences, 94*(25), 13683-13688.

Gumbiner, B. M. (2005). Regulation of cadherin-mediated adhesion in morphogenesis. *Nat Rev Mol Cell Biol, 6*(8), 622-634. doi: 10.1038/nrm1699

Guthrie, S. (1996). Patterning the hindbrain. *Current Opinion in Neurobiology, 6*(1), 41-48. doi: http://dx.doi.org/10.1016/S0959-4388(96)80007-9

Guthrie, S., & Lumsden, A. (1991). Formation and regeneration of rhombomere boundaries in the developing chick hindbrain. *Development, 112*(1), 221-229.

Hafner, C., Schmitz, G., Meyer, S., Bataille, F., Hau, P., Langmann, T., . . . Vogt, T. (2004). Differential Gene Expression of Eph Receptors and Ephrins in Benign Human Tissues and Cancers. *Clinical Chemistry, 50*(3), 490-499. doi: 10.1373/clinchem.2003.026849

Hall, A., & Nobes, C. D. (2000). Rho GTPases: molecular switches that control the organization and dynamics of the actin cytoskeleton. *Philosophical Transactions of the Royal Society of London. Series B: Biological Sciences, 355*(1399), 965-970. doi: 10.1098/rstb.2000.0632

Halloran, M. C., & Wolman, M. A. (2006). Repulsion or adhesion: receptors make the call. *Current Opinion in Cell Biology, 18*(5), 533-540. doi: http://dx.doi.org/10.1016/j.ceb.2006.08.010

Hammerschmidt, M., & Wedlich, D. (2008). Regulated adhesion as a driving force of gastrulation movements. *Development, 135*(22), 3625-3641. doi: 10.1242/dev.015701

Haramis, A.-P. G., & Perrakis, A. (2006). Selectivity and Promiscuity in Eph Receptors. *Structure, 14*(2), 169-171. doi: http://dx.doi.org/10.1016/j.str.2006.01.005

Harbott, L. K., Marston, D. J., & Nobes, C. D. (2004). Ephrin-Regulated Contact Repulsion of Growth Cones. In M. P. P. C. Anne Ridley (Ed.), *Cell Motility* (pp. 61-74).

Harris, A. K. (1976). Is cell sorting caused by differences in the work of intercellular adhesion? A critique of the steinberg hypothesis. *Journal of Theoretical Biology, 61*(2), 267-285. doi: http://dx.doi.org/10.1016/0022-5193(76)90019-9

Hattori, M., Osterfield, M., & Flanagan, J. G. (2000). Regulated cleavage of a contact-mediated axon repellent. *Science, 289*(5483), 1360-1365.

Herath, N. I., & Boyd, A. W. (2010). The role of Eph receptors and ephrin ligands in colorectal cancer. *International Journal of Cancer, 126*(9), 2003-2011. doi: 10.1002/ijc.25147

Himanen, J.-P., Chumley, M. J., Lackmann, M., Li, C., Barton, W. A., Jeffrey, P. D., . . . Nikolov, D. B. (2004). Repelling class discrimination: ephrin-A5 binds to and activates EphB2 receptor signaling. *Nat Neurosci, 7*(5), 501-509. doi: http://www.nature.com/neuro/journal/v7/n5/suppinfo/nn1237_S1.html

Himanen, J.-P., Himanen, D., & Nikolov. (2003). Eph signaling: a structural view. *Trends in neurosciences, 26*(1), 46-51.

Himanen, J.-P., Rajashankar, K. R., Lackmann, M., Cowan, C. A., Henkemeyer, M., & Nikolov, D. B. (2001). Crystal structure of an Eph receptor-ephrin complex. *Nature, 414*(6866), 933-938. doi: http://www.nature.com/nature/journal/v414/n6866/suppinfo/414933a_S1.html

Himanen, J.-P., Saha, N., & Nikolov, D. B. (2007b). Cell–cell signaling via Eph receptors and ephrins. *Current Opinion in Cell Biology, 19*(5), 534-542. doi: http://dx.doi.org/10.1016/j.ceb.2007.08.004

Himanen, J. P. (2012). Ectodomain structures of Eph receptors. *Semin Cell Dev Biol, 23*(1), 35-42. doi: 10.1016/j.semcdb.2011.10.025

Himanen, J. P., Yermekbayeva, L., Janes, P. W., Walker, J. R., Xu, K., Atapattu, L., . . . Dhe-Paganon, S. (2010). Architecture of Eph receptor clusters. *Proceedings of the National Academy of Sciences, 107*(24), 10860-10865. doi: 10.1073/pnas.1004148107

Hirai, H., Hirai, Y., Maru, K., Hagiwara, J., Nishida, F., & Takaku. (1987). A novel putative tyrosine kinase receptor encoded by the eph gene. *Science, 238*(4834), 1717-1720.

Hock, B., Böhme, B., Karn, T., Yamamoto, T., Kaibuchi, K., Holtrich, U., . . . Strebhardt, K. (1998). PDZ-domain-mediated interaction of the Eph-related receptor tyrosine kinase EphB3 and the ras-binding protein AF6 depends on the kinase activity of the receptor. *Proceedings of the National Academy of Sciences, 95*(17), 9779-9784. doi: 10.1073/pnas.95.17.9779

Holmberg, J., Clarke, D. L., & Frisen, J. (2000). Regulation of repulsion versus adhesion by different splice forms of an Eph receptor. *Nature, 408*(6809), 203-206.

Holtfreter, J. (1939). Tissue affinity, a means of embryonic morphogenesis. Arch. Exp. Zellforsch, 23, 169-209.

Hoogenraad, C. C., Milstein, A. D., Ethell, I. M., Henkemeyer, M., & Sheng, M. (2005). GRIP1 controls dendrite morphogenesis by regulating EphB receptor trafficking. *Nat Neurosci, 8*(7), 906-915. doi: http://www.nature.com/neuro/journal/v8/n7/suppinfo/nn1487_S1.html

Hoppler, S., Brown, J. D., & Moon, R. T. (1996). Expression of a dominant-negative Wnt blocks induction of MyoD in Xenopus embryos. *Genes & Development, 10*(21), 2805-2817. doi: 10.1101/gad.10.21.2805

Hopwood, N. D., Pluck, A., Gurdon, J. B., & Dilworth, S. M. (1992). Expression of XMyoD protein in early Xenopus laevis embryos. *Development, 114*(1), 31-38.

Hornberger, M. R., Dütting, D., Ciossek, T., Yamada, T., Handwerker, C., Lang, S., . . . Drescher, U. (1999). Modulation of EphA Receptor Function by Coexpressed EphrinA Ligands on Retinal Ganglion Cell Axons. *Neuron, 22*(4), 731-742. doi: http://dx.doi.org/10.1016/S0896-6273(00)80732-1

Hunter, S. G., Zhuang, G., Brantley-Sieders, D., Swat, W., Cowan, C. W., & Chen, J. (2006). Essential role of Vav family guanine nucleotide exchange factors in EphA receptor-mediated angiogenesis. *Mol Cell Biol, 26*(13), 4830-4842. doi: 10.1128/mcb.02215-05

Hwang, Y.-S., Lee, H.-S., Kamata, T., Mood, K., Cho, H. J., Winterbottom, E., . . . Daar, I. O. (2013). The Smurf ubiquitin ligases regulate tissue separation via antagonistic interactions with ephrinB1. *Genes & Development, 27*(5), 491-503. doi: 10.1101/gad.208355.112

Inoue, T., Tanaka, T., Takeichi, M., Chisaka, O., Nakamura, S., & Osumi, N. (2001). Role of cadherins in maintaining the compartment boundary between the cortex and striatum during development. *Development, 128*(4), 561-569.

Irie, F., & Yamaguchi, Y. (2002). EphB receptors regulate dendritic spine development via intersectin, Cdc42 and N-WASP. *Nat Neurosci, 5*(11), 1117-1118. doi: http://www.nature.com/neuro/journal/v5/n11/suppinfo/nn964_S1.html

Irvine, K. D. (1999). Fringe, Notch, and making developmental boundaries. *Current Opinion in Genetics & Development, 9*(4), 434-441. doi: http://dx.doi.org/10.1016/S0959-437X(99)80066-5

Irving, C., Nieto, M. A., DasGupta, R., Charnay, P., & Wilkinson, D. G. (1996). Progressive Spatial Restriction ofSek-1andKrox-20Gene Expression during Hindbrain Segmentation. *Developmental Biology, 173*(1), 26-38. doi: http://dx.doi.org/10.1006/dbio.1996.0004

Iwasato, T., Katoh, H., Nishimaru, H., Ishikawa, Y., Inoue, H., Saito, Y. M., . . . Itohara, S. (2007). Rac-GAP α-Chimerin Regulates Motor-Circuit Formation as a Key Mediator of EphrinB3/EphA4 Forward Signaling. *Cell, 130*(4), 742-753. doi: http://dx.doi.org/10.1016/j.cell.2007.07.022

Janes, P. W., Griesshaber, B., Atapattu, L., Nievergall, E., Hii, L. L., Mensinga, A., . . . Lackmann, M. (2011). Eph receptor function is modulated by heterooligomerization of A and B type Eph receptors. *The Journal of Cell Biology, 195*(6), 1033-1045. doi: 10.1083/jcb.201104037

Janes, P. W., Nievergall, E., & Lackmann, M. (2012). Concepts and consequences of Eph receptor clustering. *Seminars in Cell & Developmental Biology, 23*(1), 43-50. doi: http://dx.doi.org/10.1016/j.semcdb.2012.01.001

Janes, P. W., Saha, N., Barton, W. A., Kolev, M. V., Wimmer-Kleikamp, S. H., Nievergall, E., . . . Nikolov, D. B. (2005). Adam Meets Eph: An ADAM Substrate Recognition Module Acts as a Molecular Switch for Ephrin Cleavage In trans. *Cell, 123*(2), 291-304. doi: http://dx.doi.org/10.1016/j.cell.2005.08.014

Janes, P. W., Wimmer-Kleikamp, S. H., Frangakis, A. S., Treble, K., Griesshaber, B., Sabet, O., . . . Lackmann, M. (2009). Cytoplasmic Relaxation of Active Eph Controls Ephrin Shedding by ADAM10. *PLoS Biol, 7*(10), e1000215. doi: 10.1371/journal.pbio.1000215

Jiang, Y.-J., Aerne, B. L., Smithers, L., Haddon, C., Ish-Horowicz, D., & Lewis, J. (2000). Notch signaling and the synchronization of the somite segmentation clock. *Nature, 408*(6811), 475-479. doi: http://www.nature.com/nature/journal/v408/n6811/suppinfo/408475a0_S1.html

Jones, T. L., Chong, L. D., Kim, J., Xu, R.-H., Kung, H.-F., & Daar, I. O. (1998). Loss of cell adhesion in Xenopus laevis embryos mediated by the cytoplasmic domain of XLerk, an erythropoietin-producing hepatocellular ligand. *Proceedings of the National Academy of Sciences of the United States of America, 95*(2), 576-581.

Jülich, D., Mould, A. P., Koper, E., & Holley, S. A. (2009). Control of extracellular matrix assembly along tissue boundaries via Integrin and Eph/Ephrin signaling. *Development, 136*(17), 2913-2921. doi: 10.1242/dev.038935

Kalantarian, A., Ninomiya, H., Saad, S. M. I., David, R., Winklbauer, R., & Neumann, A. W. (2009). Axisymmetric Drop Shape Analysis for Estimating the Surface Tension of Cell Aggregates by Centrifugation. *Biophysical journal, 96*(4), 1606-1616. doi: http://dx.doi.org/10.1016/j.bpj.2008.10.064

Kao, T.-J., & Kania, A. (2011). Ephrin-Mediated cis-Attenuation of Eph Receptor Signaling Is Essential for Spinal Motor Axon Guidance. *Neuron, 71*(1), 76-91.

Karaulanov, E., Böttcher, R. T., Stannek, P., Wu, W., Rau, M., Ogata, S., . . . Niehrs, C. (2009). Unc5B Interacts with FLRT3 and Rnd1 to Modulate Cell Adhesion in *Xenopus* Embryos. *PLoS ONE, 4*(5), e5742. doi: 10.1371/journal.pone.0005742

Keller, R., Davidson, L., Edlund, A., Elul, T., Ezin, M., Shook, D., & Skoglund, P. (2000). Mechanisms of convergence and extension by cell intercalation. *Philosophical Transactions of the Royal Society of London. Series B: Biological Sciences, 355*(1399), 897-922. doi: 10.1098/rstb.2000.0626

Keller, R., Keller, M., Cooper, M., Danilchik, P., Tibbetts, P., & Wilson. (1989). Cell intercalation during notochord development inXenopus laevis. *The journal of experimental zoology, 251*(2), 134-154.

Kelly Kuan, C. Y., Tannahill, D., Cook, G. M. W., & Keynes, R. J. (2004). Somite polarity and segmental patterning of the peripheral nervous system. *Mechanisms of Development, 121*(9), 1055-1068. doi: http://dx.doi.org/10.1016/j.mod.2004.05.001

Kemp, H. A., Cooke, J. E., & Moens, C. B. (2009). EphA4 and EfnB2a maintain rhombomere coherence by independently regulating intercalation of progenitor cells in the zebrafish neural keel. *Developmental Biology, 327*(2), 313-326.

Kida, Y. S., Sato, T., Miyasaka, K. Y., Suto, A., & Ogura, T. (2007). Daam1 regulates the endocytosis of EphB during the convergent extension of the zebrafish notochord. *Proceedings of the National Academy of Sciences, 104*(16), 6708-6713. doi: 10.1073/pnas.0608946104

Kilpatrick, T. J., Brown, A., Lai, C., Gassmann, M., Goulding, M., & Lemke, G. (1996). Expression of theTyro4/Mek4/Cek4Gene Specifically Marks a Subset of Embryonic Motor Neurons and Their Muscle Targets. *Molecular and Cellular Neuroscience, 7*(1), 62-74. doi: http://dx.doi.org/10.1006/mcne.1996.0005

Kim, I., Ryu, Y. S., Kwak, H. J., Ahn, S. Y., Oh, J.-L., Yancopoulos, G. D., . . . Koh, G. Y. (2002). EphB ligand, ephrinB2, suppresses the VEGF- and angiopoietin-1-induced Ras/mitogen-activated protein kinase pathway in venous endothelial cells. *The FASEB Journal*. doi: 10.1096/fj.01-0805fje

Kim, S.-H., Jen, W.-C., De Robertis, E. M., & Kintner, C. (2000). The protocadherin PAPC establishes segmental boundaries during somitogenesis in Xenopus embryos. *Current Biology, 10*(14), 821-830. doi: http://dx.doi.org/10.1016/S0960-9822(00)00580-7

Kim, S. H., Yamamoto, A., Bouwmeester, T., Agius, E., & Robertis, E. M. (1998). The role of paraxial protocadherin in selective adhesion and cell movements of the mesoderm during Xenopus gastrulation. *Development, 125*(23), 4681-4690.

Knöchel, S., Lef, J., Clement, J., Klocke, B., Hille, S., Köster, M., & Knöchel, W. (1992). Activin A induced expression of a fork head related gene in posterior chordamesoderm (notochord) of Xenopus laevis embryos. *Mechanisms of Development, 38*(2), 157-165. doi: http://dx.doi.org/10.1016/0925-4773(92)90007-7

Koshida, S. (2005). Integrinα5-dependent fibronectin accumulation for maintenance of somite boundaries in zebrafish embryos. *Developmental Cell, 8*(4), 587.

Köster, I., Jungwirth, M. S., & Steinbeisser, H. (2010). xGit2 and xRhoGAP 11A regulate convergent extension and tissue separation in Xenopus gastrulation. *Developmental Biology, 344*(1), 26-35. doi: http://dx.doi.org/10.1016/j.ydbio.2010.03.025

Kraft, B., Berger, C. D., Wallkamm, V., Steinbeisser, H., & Wedlich, D. (2012). Wnt-11 and Fz7 reduce cell adhesion in convergent extension by sequestration of PAPC and C-cadherin. *The Journal of Cell Biology, 198*(4), 695-709. doi: 10.1083/jcb.201110076

Krens, S. F. G., Möllmert, S., & Heisenberg, C.-P. (2011). Enveloping cell-layer differentiation at the surface of zebrafish germ-layer tissue explants. *Proceedings of the National Academy of Sciences, 108*(3), E9-E10. doi: 10.1073/pnas.1010767108

Krieg, M., Arboleda-Estudillo, Y., Puech, P. H., Kafer, J., Graner, F., Muller, D. J., & Heisenberg, C. P. (2008). Tensile forces govern germ-layer organization in zebrafish. *Nat Cell Biol, 10*(4), 429-436.

Kucia, M., Jankowski, K., Reca, R., Wysoczynski, M., Bandura, L., Allendorf, D. J., . . . Ratajczak, M. Z. (2004). CXCR4-SDF-1 signaling, locomotion, chemotaxis and adhesion. *J Mol Histol, 35*(3), 233-245.

Kühl, M., & Wedlich, D. (1996). *Xenopus* cadherins: Sorting out types and functions in embryogenesis. *Developmental Dynamics, 207*(2), 121-134.

Kulesa, P. M., & Fraser, S. E. (2002). Cell Dynamics During Somite Boundary Formation Revealed by Time-Lapse Analysis. *Science, 298*(5595), 991-995. doi: 10.1126/science.1075544

Kullander, K., & Klein, R. (2002). Mechanisms and functions of Eph and ephrin signaling. *Nature reviews, 3*, 475-485.

Kumar, S. R., Scehnet, J. S., Ley, E. J., Singh, J., Krasnoperov, V., Liu, R., . . . Gill, P. S. (2009). Preferential Induction of EphB4 over EphB2 and Its Implication in Colorectal Cancer Progression. *Cancer Research, 69*(9), 3736-3745. doi: 10.1158/0008-5472.can-08-3232

Lee, H.-S., Bong, Y.-S., Moore, K. B., Soria, K., Moody, S. A., & Daar, I. O. (2006). Dishevelled mediates ephrinB1 signaling in the eye field through the planar cell polarity pathway. *Nat Cell Biol, 8*(1), 55-63.

Lee, H.-S., Mood, K., Battu, G., Ji, Y. J., Singh, A., & Daar, I. O. (2009). Fibroblast Growth Factor Receptor-induced Phosphorylation of EphrinB1 Modulates Its Interaction with Dishevelled. *Molecular Biology of the Cell, 20*(1), 124-133. doi: 10.1091/mbc.E08-06-0662

Lee, H.-S., Nishanian, T. G., Mood, K., Bong, Y.-S., & Daar, I. O. (2008). EphrinB1 controls cell-cell junctions through the Par polarity complex. *Nat Cell Biol, 10*(8), 979-986. doi: http://www.nature.com/ncb/journal/v10/n8/suppinfo/ncb1758_S1.html

Lee, J., Corcoran, A., Han, M., Gardiner, D. M., & Muneoka, K. (2013). Dlx5 and Msx2 regulate mouse anterior neural tube closure through ephrinA5-EphA7. *Development, Growth & Differentiation, 55*(3), 341-349. doi: 10.1111/dgd.12044

Lim, B. K., Matsuda, N., & Poo, M.-m. (2008). Ephrin-B reverse signaling promotes structural and functional synaptic maturation in vivo. *Nat Neurosci, 11*(2), 160-169. doi: http://www.nature.com/neuro/journal/v11/n2/suppinfo/nn2033_S1.html

Litterst, C., Georgakopoulos, A., Shioi, J., Ghersi, E., Wisniewski, T., Wang, R., . . . Robakis, N. K. (2007). Ligand Binding and Calcium Influx Induce Distinct Ectodomain/γ-Secretase-processing Pathways of EphB2 Receptor. *Journal of Biological Chemistry, 282*(22), 16155-16163. doi: 10.1074/jbc.M611449200

Lu, Q., Sun, E. E., & Flanagan, J. G. (2004). Analysis of PDZ-RGS3 Function in Ephrin-B Reverse Signaling. In P. S. David (Ed.), *Methods in Enzymology* (Vol. Volume 390, pp. 120-128): Academic Press.

Lu, Q., Sun, E. E., Klein, R. S., & Flanagan, J. G. (2001). Ephrin-B Reverse Signaling Is Mediated by a Novel PDZ-RGS Protein and Selectively Inhibits G Protein Coupled Chemoattraction. *Cell, 105*(1), 69-79.

Luo, L., & Luo. (2002). ACTINCYTOSKELETONREGULATION INNEURONALMORPHOGENESIS ANDSTRUCTURALPLASTICITY. *Annual Review of Cell and Developmental Biology, 18*(1), 601-635.

Luu, O., David, R., Ninomiya, H., & Winklbauer, R. (2011). Large-scale mechanical properties of Xenopus embryonic epithelium. *Proceedings of the National Academy of Sciences, 108*(10), 4000-4005. doi: 10.1073/pnas.1010331108

Ma, X. M. (2003). Kalirin, a multifunctional Rho guanine nucleotide exchange factor, is necessary for maintenance of hippocampal pyramidal neuron dendrites and dendritic spines. *The Journal of Neuroscience, 23*(33), 10593.

Macrae, M., Neve, R. M., Rodriguez-Viciana, P., Haqq, C., Yeh, J., Chen, C., . . . McCormick, F. (2005). A conditional feedback loop regulates Ras activity through EphA2. *Cancer Cell, 8*(2), 111-118. doi: http://dx.doi.org/10.1016/j.ccr.2005.07.005

Maekawa, M., & Maekawa. (1999). Signaling from Rho to the Actin Cytoskeleton Through Protein Kinases ROCK and LIM-kinase. *Science, 285*(5429), 895-898.

Maître, J.-L., Berthoumieux, H., Krens, S. F. G., Salbreux, G., Jülicher, F., Paluch, E., & Heisenberg, C.-P. (2012). Adhesion Functions in Cell Sorting by Mechanically Coupling the Cortices of Adhering Cells. *Science, 338*(6104), 253-256. doi: 10.1126/science.1225399

Maître, J.-L., & Heisenberg, C.-P. (2011). The role of adhesion energy in controlling cell–cell contacts. *Current Opinion in Cell Biology, 23*(5), 508-514. doi: http://dx.doi.org/10.1016/j.ceb.2011.07.004

Major, R. J., & Irvine, K. D. (2005). Influence of Notch on dorsoventral compartmentalization and actin organization in the Drosophila wing. *Development, 132*(17), 3823-3833. doi: 10.1242/dev.01957

Major, R. J., & Irvine, K. D. (2006). Localization and requirement for Myosin II at the dorsal-ventral compartment boundary of the Drosophila wing. *Developmental Dynamics, 235*(11), 3051-3058. doi: 10.1002/dvdy.20966

Makarov, R. (2010). *Expression and functional analysis of EFNB1 mutations in craniofrontonasal syndrome.* Magdeburg, Univ., Diss., 2010.

Mancia, F., & Shapiro, L. (2005). ADAM and Eph: How Ephrin-Signaling Cells Become Detached. *Cell, 123*(2), 185-187. doi: http://dx.doi.org/10.1016/j.cell.2005.10.004

Manning, M. L., Foty, R. A., Steinberg, M. S., & Schoetz, E.-M. (2010). Coaction of intercellular adhesion and cortical tension specifies tissue surface tension. *Proceedings of the National Academy of Sciences*. doi: 10.1073/pnas.1003743107

Marquardt, T., Shirasaki, R., Ghosh, S., Andrews, S. E., Carter, N., Hunter, T., & Pfaff, S. L. (2005). Coexpressed EphA Receptors and Ephrin-A Ligands Mediate Opposing Actions on Growth Cone Navigation from Distinct Membrane Domains. *Cell, 121*(1), 127-139. doi: 10.1016/j.cell.2005.01.020

Marston, D. J., Dickinson, S., & Nobes, C. D. (2003). Rac-dependent trans-endocytosis of ephrinBs regulates Eph-ephrin contact repulsion. *Nat Cell Biol, 5*(10), 879-888.

Maves, L., Jackman, W., & Kimmel, C. B. (2002). FGF3 and FGF8 mediate a rhombomere 4 signaling activity in the zebrafish hindbrain. *Development, 129*(16), 3825-3837.

May, V. (2002). Kalirin Dbl-homology guanine nucleotide exchange factor 1 domain initiates new axon outgrowths via RhoG-mediated mechanisms. *The Journal of Neuroscience, 22*(16), 6980.

McNeill, H. (2000). Sticking together and sorting things out: adhesion as a force in development. *Nat Rev Genet, 1*(2), 100-108.

Medina, A., & Steinbeisser, H. (2000). Interaction of Frizzled 7 and Dishevelled in *Xenopus*. *Developmental Dynamics, 218*(4), 671-680.

Mellitzer, G., Xu, Q., & Wilkinson, D. G. (1999). Eph receptors and ephrins restrict cell intermingling and communication. *Nature, 400*(6739), 77-81.

Mellott, D., & Burke, R. (2008). The molecular phylogeny of eph receptors and ephrin ligands. *BMC Cell Biology, 9*(1), 27.

Mizutani, T., Mizutani, K., Kawabata, Y., Koyama, M., Takahashi, H., & Haga. (2009). Regulation of cellular contractile force in response to mechanical stretch by diphosphorylation of myosin regulatory light chain via RhoA signaling cascade. *Cell motility and the cytoskeleton, 66*(7), 389-397.

Monier, B., Pelissier-Monier, A., Brand, A. H., & Sanson, B. (2010). An actomyosin-based barrier inhibits cell mixing at compartmental boundaries in Drosophila embryos. *Nat Cell Biol, 12*(1), 60-65. doi: http://www.nature.com/ncb/journal/v12/n1/suppinfo/ncb2005_S1.html

Monschau, B., Kremoser, C., Ohta, K., Tanaka, H., Kaneko, T., Yamada, T., . . . Drescher, U. (1997). Shared and distinct functions of RAGS and ELF-1 in guiding retinal axons. *EMBO J, 16*, 1258 - 1267.

Montero, J.-A., Carvalho, L., Wilsch-Bräuninger, M., Kilian, B., Mustafa, C., & Heisenberg, C.-P. (2005). Shield formation at the onset of zebrafish gastrulation. *Development, 132*(6), 1187-1198. doi: 10.1242/dev.01667

Moore, K. B., Mood, K., Daar, I. O., & Moody, S. A. (2004). Morphogenetic Movements Underlying Eye Field Formation Require Interactions between the FGF and ephrinB1 Signaling Pathways. *Developmental Cell, 6*(1), 55-67. doi: http://dx.doi.org/10.1016/S1534-5807(03)00395-2

Münchberg, F. E., Spieker, T. P., Joos, T. O., & Hausen, P. (1997). A paired oocyte adhesion assay reveals the homophilic binding properties of the Xenopus maternal cadherins, XBU- and EP-cadherin. *Mechanisms of Development, 64*(1-2), 87-94.

Murai, K., & Pasquale, E. (2003). 'Eph'ective signaling: forward, reverse and crosstalk. *J Cell Sci, 116*, 2823 - 2832.

Murakami, T., Hijikata, T., Matsukawa, M., Ishikawa, H., & Yorifuji, H. (2006). Zebrafish protocadherin 10 is involved in paraxial mesoderm development and somitogenesis. *Developmental Dynamics, 235*(2), 506-514. doi: 10.1002/dvdy.20622

Nikolov, D. B., Xu, K., & Himanen, J. P. (2013). Eph/ephrin recognition and the role of Eph/ephrin clusters in signaling initiation. *Biochimica et Biophysica Acta (BBA) - Proteins and Proteomics*(0). doi: http://dx.doi.org/10.1016/j.bbapap.2013.04.020

Ninomiya, H., David, R., Damm, E. W., Fagotto, F., Niessen, C. M., & Winklbauer, R. (2012). Cadherin-dependent differential cell adhesion in Xenopus causes cell sorting in vitro but not in the embryo. *Journal of cell science, 125*(8), 1877-1883. doi: 10.1242/jcs.095315

Nomura-Kitabayashi, A., Takahashi, Y., Kitajima, S., Inoue, T., Takeda, H., & Saga, Y. (2002). Hypomorphic Mesp allele distinguishes establishment of rostrocaudal polarity and segment border formation in somitogenesis. *Development, 129*(10), 2473-2481.

Noren, N. K., & Pasquale, E. B. (2004). Eph receptor-ephrin bidirectional signals that target Ras and Rho proteins. *Cellular Signaling, 16*(6), 655-666.

Nose, A., Nagafuchi, A., & Takeichi, M. (1988). Expressed recombinant cadherins mediate cell sorting in model systems. *Cell, 54*(7), 993-1001. doi: 10.1016/0092-8674(88)90114-6

Ogata, S., Morokuma, J., Hayata, T., Kolle, G., Niehrs, C., Ueno, N., & Cho, K. W. Y. (2007). TGF-Î² signaling-mediated morphogenesis: modulation of cell adhesion via cadherin endocytosis. *Genes & Development, 21*(14), 1817-1831.

Pabbisetty, K. B., Yue, X., Li, C., Himanen, J.-P., Zhou, R., Nikolov, D. B., & Hu, L. (2007). Kinetic analysis of the binding of monomeric and dimeric ephrins to Eph receptors: Correlation to function in a growth cone collapse assay. *Protein Science, 16*(3), 355-361. doi: 10.1110/ps.062608807

Palmer, A., Zimmer, M., Erdmann, K. S., Eulenburg, V., Porthin, A., Heumann, R., . . . Klein, R. (2002). EphrinB Phosphorylation and Reverse Signaling: Regulation by Src Kinases and PTP-BL Phosphatase. *Molecular Cell, 9*(4), 725-737. doi: http://dx.doi.org/10.1016/S1097-2765(02)00488-4

Pang, X., & Zhou, H. X. (2013). Activation of signaling receptors: do ligands bind to receptor monomer, dimer, or both? *BMC Biophys, 6*, 7. doi: 10.1186/2046-1682-6-7

Park, E. C., Cho, G.-S., Kim, G.-H., Choi, S.-C., & Han, J.-K. (2011). The involvement of Eph–Ephrin signaling in tissue separation and convergence during Xenopus gastrulation movements. *Developmental Biology, 350*(2), 441-450. doi: 10.1016/j.ydbio.2010.12.012

Pasquale, E. B. (2004). Eph-ephrin promiscuity is now crystal clear. *Nat Neurosci, 7*(5), 417-418.

Pasquale, E. B. (2010). Eph receptors and ephrins in cancer: bidirectional signaling and beyond. *Nat Rev Cancer, 10*(3), 165-180.

Penzes, P., Beeser, A., Chernoff, J., Schiller, M. R., Eipper, B. A., Mains, R. E., & Huganir, R. L. (2003). Rapid Induction of Dendritic Spine Morphogenesis by trans-Synaptic EphrinB-EphB Receptor Activation of the Rho-GEF Kalirin. *Neuron, 37*(2), 263-274. doi: http://dx.doi.org/10.1016/S0896-6273(02)01168-6

Penzes, P., Johnson, R. C., Sattler, R., Zhang, X., Huganir, R. L., Kambampati, V., . . . Eipper, B. A. (2001). The Neuronal Rho-GEF Kalirin-7 Interacts with PDZ Domain–Containing Proteins and Regulates Dendritic Morphogenesis. *Neuron, 29*(1), 229-242. doi: http://dx.doi.org/10.1016/S0896-6273(01)00193-3

Phillips, H. M. (1978). Liquid-Tissue Mechanics in Amphibian Gastrulation: Germ-Layer Assembly in Rana Pipiens. *American Zoolology, 18*(1), 81-93. doi: 10.1093/icb/18.1.81

Picco, V., Hudson, C., & Yasuo, H. (2007). Ephrin-Eph signaling drives the asymmetric division of notochord/neural precursors in Ciona embryos. *Development, 134*, 1491 - 1497.

Pohl, B., Pohl, W., & Knöchel. (2005). Of Fox and Frogs: Fox (fork head/winged helix) transcription factors in Xenopus development. *Gene, 344*, 21-32.

Poliakov, A., Cotrina, M., & Wilkinson, D. G. (2004). Diverse Roles of Eph Receptors and Ephrins in the Regulation of Cell Migration and Tissue Assembly. *Developmental Cell, 7*(4), 465-480.

Pourquié, O. (2001). VERTEBRATE SOMITOGENESIS. *Annual Review of Cell and Developmental Biology, 17*(1), 311-350. doi: doi:10.1146/annurev.cellbio.17.1.311

Pratt, R. L. (2003). Ligand Binding Up-Regulates EphA2 Messenger RNA through the Mitogen-Activated Protein/Extracellular Signal-Regulated Kinase Pathway. *Molecular cancer research, 1*(14), 1070-1076.

Prévost, N., Woulfe, D. S., Jiang, H., Stalker, T. J., Marchese, P., Ruggeri, Z. M., & Brass, L. F. (2005). Eph kinases and ephrins support thrombus growth and stability by regulating integrin outside-in signaling in platelets. *Proceedings of the National Academy of Sciences of the United States of America, 102*(28), 9820-9825. doi: 10.1073/pnas.0404065102

Puech, P. H. (2005). Measuring cell adhesion forces of primary gastrulating cells from zebrafish using atomic force microscopy. *Journal of cell science, 118*(18), 4199-4206.

Qin, H., Noberini, R., Huan, X., Shi, J., Pasquale, E. B., & Song, J. (2010). Structural Characterization of the EphA4-Ephrin-B2 Complex Reveals New Features Enabling Eph-Ephrin Binding Promiscuity. *Journal of Biological Chemistry, 285*(1), 644-654. doi: 10.1074/jbc.M109.064824

Reddy, P. C., Reddy, S., Bidaye, S., & Ghaskadbi. (2011). Genome-wide screening reveals the emergence and divergence of RTK homologues in basal Metazoan Hydra magnipapillata. *Journal of Biosciences, 36*(2), 289-296.

Redies, C., & Takeichi, M. (1996). Cadherins in the Developing Central Nervous System: An Adhesive Code for Segmental and Functional Subdivisions. *Developmental Biology, 180*(2), 413-423. doi: http://dx.doi.org/10.1006/dbio.1996.0315

Reintsch, W. E., Habring-Mueller, A., Wang, R. W., Schohl, A., & Fagotto, F. (2005). β-Catenin controls cell sorting at the notochord–somite boundary independently of cadherin-mediated adhesion. *The Journal of Cell Biology, 170*(4), 675-686. doi: 10.1083/jcb.200503009

Riedl, J., Riedl, D., Brandt, E., Batlle, L., Price, H., Clevers, J., & Bos. (2005). Down-regulation of Rap1 activity is involved in ephrinB1-induced cell contraction. *Biochemical journal, 389*(2), 465.

Rooke, J., Pan, D., Xu, T., & Rubin, G. M. (1996). KUZ, a Conserved Metalloprotease-Disintegrin Protein with Two Roles in Drosophila Neurogenesis. *Science, 273*(5279), 1227-1231. doi: 10.1126/science.273.5279.1227

Sadowski, L., Sadowski, I., Pilecka, M., & Miaczynska. (2009). Signaling from endosomes: Location makes a difference. *Experimental cell research, 315*(9), 1601-1609.

Saga, Y., & Takeda, H. (2001). The making of the somite: molecular events in vertebrate segmentation. *Nat Rev Genet, 2*(11), 835-845.

Sahin, M., Greer, P. L., Lin, M. Z., Poucher, H., Eberhart, J., Schmidt, S., . . . Greenberg, M. E. (2005). Eph-Dependent Tyrosine Phosphorylation of Ephexin1 Modulates Growth Cone Collapse. *Neuron, 46*(2), 191-204.

Salvucci, O., de la Luz Sierra, M., Martina, J. A., McCormick, P. J., & Tosato, G. (2006). EphB2 and EphB4 receptors forward signaling promotes SDF-1–induced endothelial cell chemotaxis and branching remodeling. *Blood, 108*(9), 2914-2922. doi: 10.1182/blood-2006-05-023341

Sanger, J. W., & Holtzer, H. (1972). Cytochalasin B: Effects on Cell Morphology, Cell Adhesion, and Mucopolysaccharide Synthesis. *Proceedings of the National Academy of Sciences, 69*(1), 253-257.

Saras, J. (1994). Cloning and characterization of PTPL1, a protein tyrosine phosphatase with similarities to cytoskeletal-associated proteins. *Journal of Biological Chemistry, 269*(39), 24082-24089.

Schilling, S., Willecke, M., Aegerter-Wilmsen, T., Cirpka, O. A., Basler, K., & von Mering, C. (2011). Cell-Sorting at the A/P Boundary in the *Drosophila* Wing Primordium: A Computational Model to Consolidate Observed Non-Local Effects of Hh Signaling. *PLoS Comput Biol, 7*(4), e1002025. doi: 10.1371/journal.pcbi.1002025

Schlichting, K., Demontis, F., & Dahmann, C. (2005). Cadherin Cad99C is regulated by Hedgehog signaling in Drosophila. *Developmental Biology, 279*(1), 142-154. doi: http://dx.doi.org/10.1016/j.ydbio.2004.12.008

Seals, D. F., & Courtneidge, S. A. (2003). The ADAMs family of metalloproteases: multidomain proteins with multiple functions. *Genes & Development, 17*(1), 7-30. doi: 10.1101/gad.1039703

Seiradake, E., Schaupp, A., del Toro Ruiz, D., Kaufmann, R., Mitakidis, N., Harlos, K., . . . Jones, E. Y. (2013). Structurally encoded intraclass differences in EphA clusters drive distinct cell responses. *Nat Struct Mol Biol, 20*(8), 958-964. doi: 10.1038/nsmb.2617 http://www.nature.com/nsmb/journal/v20/n8/abs/nsmb.2617.html#supplementary-information

Sela Donenfeld, D., Sela Donenfeld, G., Kayam, D., & Wilkinson. (2009). Boundary cells regulate a switch in the expression of FGF3 in hindbrain rhombomeres. *BMC developmental biology, 9*(1), 16.

Semela, D., Das, A., Langer, D., Kang, N., Leof, E., & Shah, V. (2008). Platelet-Derived Growth Factor Signaling Through Ephrin-B2 Regulates Hepatic Vascular Structure and Function. *Gastroenterology, 135*(2), 671-679.e672. doi: http://dx.doi.org/10.1053/j.gastro.2008.04.010

Shamah, S. M., Lin, M. Z., Goldberg, J. L., Estrach, S., Sahin, M., Hu, L., . . . Greenberg, M. E. (2001). EphA Receptors Regulate Growth Cone Dynamics through the Novel Guanine Nucleotide Exchange Factor Ephexin. *Cell, 105*(2), 233-244. doi: http://dx.doi.org/10.1016/S0092-8674(01)00314-2

Schaupp, A., Sabet, O., Dudanova, I., Ponserre, M., Bastiaens, P., & Klein, R. d. (2014). The composition of EphB2 clusters determines the strength in the cellular repulsion response. *The Journal of Cell Biology, 204*(3), 409-422. doi: 10.1083/jcb.201305037

Shih, J., & Keller, R. (1992). Cell motility driving mediolateral intercalation in explants of Xenopus laevis. *Development, 116*(4), 901-914.

Singh, A., Winterbottom, E., & Daar, I. O. (2012). Eph/ephrin signaling in cell-cell and cell-substrate adhesion. *Front Biosci (Landmark Ed), 17*, 473-497.

Singla, N., Erdjument-Bromage, H., Himanen, Juha P., Muir, Tom W., & Nikolov, Dimitar B. (2011). A Semisynthetic Eph Receptor Tyrosine Kinase Provides Insight into Ligand- Induced Kinase Activation. *Chemistry & Biology, 18*(3), 361-371. doi: http://dx.doi.org/10.1016/j.chembiol.2011.01.011

Solanas, G., Cortina, C., Sevillano, M., & Batlle, E. (2011). Cleavage of E-cadherin by ADAM10 mediates epithelial cell sorting downstream of EphB signaling. *Nat Cell Biol, 13*(9), 1100-1107. doi: http://www.nature.com/ncb/journal/v13/n9/abs/ncb2298.html#supplementary-information

Solnica-Krezel, L. (2005). Conserved Patterns of Cell Movements during Vertebrate Gastrulation. *Current Biology, 15*(6), R213-R228. doi: http://dx.doi.org/10.1016/j.cub.2005.03.016

Solnica-Krezel, L., & Sepich, D. S. (2012). Gastrulation: Making and Shaping Germ Layers. *Annual Review of Cell and Developmental Biology, 28*(1), 687-717. doi: 10.1146/annurev-cellbio-092910-154043

Steinberg, M., & Takeichi, M. (1994). Experimental specification of cell sorting, tissue spreading, and specific spatial patterning by quantitative differences in cadherin expression. *Proc natl Acad Sci USA, 86*, 7043-7047.

Steinberg, M. S. (1963). Reconstruction of tissues by dissociated cells. *Science, 141*, 401-408.

Steinberg, M. S. (1970). Does differential adhesion govern self-assembly processes in histogenesis? Equilibrium configurations and the emergence of a hierarchy among populations of embryonic cells. *J. Exp. Zool., 173*, 395–434.

Steinberg, M. S. (2007). Differential adhesion in morphogenesis: a modern view. *Current Opinion in Genetics & Development, 17*(4), 281-286.

Steinberg, M. S., & Wiseman, L. L. (1972). DO MORPHOGENETIC TISSUE REARRANGEMENTS REQUIRE ACTIVE CELL MOVEMENTS?: The Reversible Inhibition of Cell Sorting and Tissue Spreading by Cytochalasin B. *The Journal of Cell Biology, 55*(3), 606-615. doi: 10.1083/jcb.55.3.606

Stern, C. e. (2004). *Gastrulation. From cells to embryo. Cold Spring Harbor Laborat. Press, New York*.

Surawska, H., Surawska, P., Ma, R., & Salgia. (2004). The role of ephrins and Eph receptors in cancer. *Cytokine & growth factor reviews, 15*(6), 419-433.

Takeichi, M. (1988). The cadherins: cell-cell adhesion molecules controlling animal morphogenesis. *Development, 102*(4), 639-655.

Takeichi, M., & Takeichi. (1995). Morphogenetic roles of classic cadherins. *Current Opinion in Cell Biology, 7*(5), 619-627.

Tanaka, M., Chien, P., Naber, N., Cooke, R., & Weissman, J. S. (2004). Conformational variations in an infectious protein determine prion strain differences. *Nature, 428*(6980), 323-328. doi: http://www.nature.com/nature/journal/v428/n6980/suppinfo/nature02392_S1.html

Tanaka, M., Kamo, T., Ota, S., & Sugimura, H. (2003). Association of Dishevelled with Eph tyrosine kinase receptor and ephrin mediates cell repulsion. *EMBO J, 22*(4), 847-858.

Tanaka, M., Tanaka, R., Kamata, R., & Sakai. (2005). Phosphorylation of ephrin-B1 via the interaction with claudin following cell–cell contact formation. *EMBO journal, 24*(21), 3700-3711.

Tanaka, M., Tanaka, S., Kuriyama, N., & Aiba. (2012). Nm23-H1 regulates contact inhibition of locomotion, which is affected by ephrin-B1. *Journal of cell science, 125*(18), 4343-4353.

Tawadros, T., Brown, M. D., Hart, C. A., & Clarke, N. W. (2012). Ligand-independent activation of EphA2 by arachidonic acid induces metastasis-like behaviour in prostate cancer cells. *Br J Cancer, 107*(10), 1737-1744. doi: http://www.nature.com/bjc/journal/v107/n10/suppinfo/bjc2012457s1.html

Tepass, U., Godt, D., & Winklbauer, R. (2002). Cell sorting in animal development: signaling and adhesive mechanisms in the formation of tissue boundaries. *Current Opinion in Genetics & Development, 12*(5), 572-582.

Theil, T., Frain, M., Gilardi-Hebenstreit, P., Flenniken, A., Charnay, P., & Wilkinson, D. G. (1998). Segmental expression of the EphA4 (Sek-1) receptor tyrosine kinase in the hindbrain is under direct transcriptional control of Krox-20. *Development, 125*(3), 443-452.

Thiery, J. P., Duband, J. L., Rutishauser, U., & Edelman, G. M. (1982). Cell adhesion molecules in early chicken embryogenesis. *Proceedings of the National Academy of Sciences, 79*(21), 6737-6741.

Tomita, T., Tomita, S., Tanaka, Y., Morohashi, T., & Iwatsubo. (2006). Presenilin-dependent intramembrane cleavage of ephrin-B1. *Molecular neurodegeneration, 1*(1), 2.

Torres, R., Firestein, B. L., Dong, H., Staudinger, J., Olson, E. N., Huganir, R. L., . . . Yancopoulos, G. D. (1998). PDZ Proteins Bind, Cluster, and Synaptically Colocalize with Eph Receptors and Their Ephrin Ligands. *Neuron, 21*(6), 1453-1463. doi: http://dx.doi.org/10.1016/S0896-6273(00)80663-7

Townes, P. L., & Holtfreter, J. (1955). Directed movements and selective adhesion of embryonic amphibian cells. *Journal of Experimental Zoology, 128*(1), 53-120.

Truitt, L., & Freywald, A. (2011). Dancing with the dead: Eph receptors and their kinase-null partnersThis paper is one of a selection of papers published in a Special Issue entitled CSBMCB 53rd Annual Meeting — Membrane Proteins in Health and Disease, and has undergone the Journal's usual peer review process. *Biochemistry and Cell Biology, 89*(2), 115-129. doi: 10.1139/O10-145

Tuzi, N. L., & Gullick, W. J. (1994). eph, the largest known family of putative growth factor receptors. *Br J Cancer, 69*(3), 417-421.

Twiss, F., Le Duc, Q., Van Der Horst, S., Tabdili, H., Van Der Krogt, G., Wang, N., . . . De Rooij, J. (2012). Vinculin-dependent Cadherin mechanosensing regulates efficient epithelial barrier formation. *Biol Open, 1*(11), 1128-1140. doi: 10.1242/bio.20122428

Ulrich, F., Ulrich, M., Krieg, E.-M., Schötz, V., Link, I., Castanon, V., . . . Heisenberg. (2005). Wnt11 Functions in Gastrulation by Controlling Cell Cohesion through Rab5c and E-Cadherin. *Developmental Cell, 9*(4), 555-564.

von Dassow, G., Schmidt, J. E., & Kimelman, D. (1993). Induction of the Xenopus organizer: expression and regulation of Xnot, a novel FGF and activin-regulated homeo box gene. *Genes Dev, 7*(3), 355-366.

Wacker, S., Grimm, K., Joos, T., & Winklbauer, R. (2000). Development and control of tissue separation at gastrulation in Xenopus. *Dev. Biol., 224*, 428-439.

Wahl, S., Barth, H., Ciossek, T., Aktories, K., & Mueller, B. K. (2000). Ephrin-A5 Induces Collapse of Growth Cones by Activating Rho and Rho Kinase. *The Journal of Cell Biology, 149*(2), 263-270. doi: 10.1083/jcb.149.2.263

Wang, H., Chen, Z., & Anderson, D. (1998). Molecular distinction and angiogenic interaction between embryonic arteries and veins revealed by ephrin-B2 and its receptor Eph-B4. *Cell, 93*, 741 - 753.

Warga, R. M., & Kimmel, C. B. (1990). Cell movements during epiboly and gastrulation in zebrafish. *Development, 108*(4), 569-580.

Watanabe, T., Sato, Y., Saito, D., Tadokoro, R., & Takahashi, Y. (2009). EphrinB2 coordinates the formation of a morphological boundary and cell epithelialization during somite segmentation. *Proceedings of the National Academy of Sciences, 106*(18), 7467-7472. doi: 10.1073/pnas.0902859106

Wegmeyer, H., Egea, J., Rabe, N., Gezelius, H., Filosa, A., Enjin, A., . . . Betz, A. (2007). EphA4-Dependent Axon Guidance Is Mediated by the RacGAP α2-Chimaerin. *Neuron, 55*(5), 756-767. doi: http://dx.doi.org/10.1016/j.neuron.2007.07.038

Wiesner, S., Wybenga-Groot, L. E., Warner, N., Lin, H., Pawson, T., Forman-Kay, J. D., & Sicheri, F. (2006). A change in conformational dynamics underlies the activation of Eph receptor tyrosine kinases. *EMBO J, 25*(19), 4686-4696. doi: http://www.nature.com/emboj/journal/v25/n19/suppinfo/7601315a_S1.html

Wimmer-Kleikamp, S. H., Janes, P. W., Squire, A., Bastiaens, P. I., & Lackmann, M. (2004). Recruitment of Eph receptors into signaling clusters does not require ephrin contact. *J Cell Biol, 164*(5), 661-666. doi: 10.1083/jcb.200312001

Wimmer-Kleikamp, S. H., Nievergall, E., Gegenbauer, K., Adikari, S., Mansour, M., Yeadon, T., . . . Lackmann, M. (2008). Elevated protein tyrosine phosphatase activity provokes Eph/ephrin-facilitated adhesion of pre-B leukemia cells. *Blood, 112*(3), 721-732. doi: 10.1182/blood-2007-11-121681

Winklbauer, R., & Kwang, W. J. (2009). Chapter 5 Cell Adhesion in Amphibian Gastrulation *International Review of Cell and Molecular Biology* (Vol. Volume 278, pp. 215-275): Academic Press.

Winklbauer, R., & Luu, O. (2009). Frizzled-7-dependent Tissue Separation in the Xenopus Gastrula *Wnt Signaling* (pp. 485-492).

Winklbauer, R., Medina, A., Swain, R. K., & Steinbeisser, H. (2001). Frizzled-7 signaling controls tissue separation during Xenopus gastrulation. *Nature, 413*(6858), 856-860.

Winning, R. S., Wyman, T. L., & Walker, G. K. (2001). EphA4 Activity Causes Cell Shape Change and a Loss of Cell Polarity in Xenopus laevis embryos. *Differentiation, 68*(2–3), 126-132. doi: http://dx.doi.org/10.1046/j.1432-0436.2001.680206.x

Wood, A., Wood, P., & Thorogood. (1994). Patterns of cell behaviour underlying somitogenesis and notochord formation in intact vertebrate embryos. *Developmental Dynamics, 201*(2), 151-167.

Wybenga-Groot, L. E., Baskin, B., Ong, S. H., Tong, J., Pawson, T., & Sicheri, F. (2001). Structural Basis for Autoinhibition of the EphB2 Receptor Tyrosine Kinase by the Unphosphorylated Juxtamembrane Region. *Cell, 106*(6), 745-757. doi: http://dx.doi.org/10.1016/S0092-8674(01)00496-2

Xu, K., Tzvetkova-Robev, D., Xu, Y., Goldgur, Y., Chan, Y.-P., Himanen, J. P., & Nikolov, D. B. (2013). Insights into Eph receptor tyrosine kinase activation from crystal structures of the EphA4 ectodomain and its complex with ephrin-A5. *Proceedings of the National Academy of Sciences*. doi: 10.1073/pnas.1311000110

Xu, N.-J., & Henkemeyer, M. (2009). Ephrin-B3 reverse signaling through Grb4 and cytoskeletal regulators mediates axon pruning. *Nat Neurosci, 12*(3),

268-276. doi: http://www.nature.com/neuro/journal/v12/n3/suppinfo/nn.2254_S1.html
Xu, N.-J., & Henkemeyer, M. (2012). Ephrin reverse signaling in axon guidance and synaptogenesis. *Seminars in Cell & Developmental Biology, 23*(1), 58-64. doi: http://dx.doi.org/10.1016/j.semcdb.2011.10.024
Xu, Q., Alldus, G., Holder, N., & Wilkinson, D. G. (1995). Expression of truncated Sek-1 receptor tyrosine kinase disrupts the segmental restriction of gene expression in the Xenopus and zebrafish hindbrain. *Development, 121*(12), 4005-4016.
Xu, Q., Lin, W.-C., Petit, Rebecca S., & Groves, Jay T. (2011). EphA2 Receptor Activation by Monomeric Ephrin-A1 on Supported Membranes. *Biophysical journal, 101*(11), 2731-2739.
Xu, Q., Mellitzer, G., Robinson, V., & Wilkinson, D. (1999). In vivo cell sorting in complementary segmental domains mediated by Eph receptors and ephrins. *Nature, 399*, 267 - 271.
Xu, Q., Mellitzer, G., & Wilkinson, D. G. (2000). Roles of Eph receptors and ephrins in segmental patterning. *Philosophical Transactions of the Royal Society of London. Series B: Biological Sciences, 355*(1399), 993-1002.
Yasuo, H., & Lemaire, P. (2001). Role of Goosecoid, Xnot and Wnt antagonists in the maintenance of the notochord genetic programme in Xenopus gastrulae. *Development, 128*(19), 3783-3793.
Yin, Y., Yamashita, Y., Noda, H., Okafuji, T., Go, M. J., & Tanaka, H. (2004). EphA receptor tyrosine kinases interact with co-expressed ephrin-A ligands in cis. *Neuroscience Research, 48*(3), 285-295. doi: http://dx.doi.org/10.1016/j.neures.2003.11.009
Yoo, S., Shin, J., & Park, S. (2010). EphA8-ephrinA5 signaling and clathrin-mediated endocytosis is regulated by Tiam-1, a Rac-specific guanine nucleotide exchange factor. *Mol Cells, 29*(6), 603-609. doi: 10.1007/s10059-010-0075-2
Zecca, M., & Struhl, G. (2002). Subdivision of the Drosophila wing imaginal disc by EGFR-mediated signaling. *Development, 129*(6), 1357-1368.
Zhang, W., Zeng, X., Briggs, K. J., Beaty, R., Simons, B., Chiu Yen, R. W., . . . Watkins, D. N. (2010). A potential tumor suppressor role for Hic1 in breast cancer through transcriptional repression of ephrin-A1. *Oncogene, 29*(17), 2467-2476. doi: http://www.nature.com/onc/journal/v29/n17/suppinfo/onc201012s1.html
Zhuang, G., Hunter, S., Hwang, Y., & Chen, J. (2007). Regulation of EphA2 Receptor Endocytosis by SHIP2 Lipid Phosphatase via Phosphatidylinositol 3-Kinase-dependent Rac1 Activation. *Journal of Biological Chemistry, 282*(4), 2683-2694. doi: 10.1074/jbc.M608509200
Zimmer, G., Rudolph, J., Landmann, J., Gerstmann, K., Steinecke, A., Gampe, C., & Bolz, J. (2011). Bidirectional EphrinB3/EphA4 Signaling Mediates the Segregation of Medial Ganglionic Eminence- and Preoptic Area-Derived Interneurons in the Deep and Superficial Migratory Stream. *The Journal of Neuroscience, 31*(50), 18364-18380. doi: 10.1523/jneurosci.4690-11.2011

Zimmer, M., Palmer, A., Kohler, J., & Klein, R. (2003). EphB-ephrinB bi-directional endocytosis terminates adhesion allowing contact mediated repulsion. *Nat Cell Biol, 5*(10), 869-878.

Zolkiewska, A. (2008). ADAM proteases: ligand processing and modulation of the Notch pathway. *Cellular and Molecular Life Sciences, 65*(13), 2056-2068. doi: 10.1007/s00018-008-7586-4

Zou, J. X., Wang, B., Kalo, M. S., Zisch, A. H., Pasquale, E. B., & Ruoslahti, E. (1999). An Eph Receptor Regulates Integrin Activity through R-Ras. *Proceedings of the National Academy of Sciences of the United States of America, 96*(24), 13813-13818. doi: 10.2307/121304

Figure legends

Figure 1.1:

Modes of boundary formation in the embryo:

The causes of boundary formation are categorized in two: Boundaries that do and those that do not depend on cellular translocation. The boundaries that do not require cellular translocation, divide a field of cells into partitions. This type is divided into linage or none linage boundaries. The non-linage boundaries are more plastic. In this case if a cell is placed on a wrong cell population it can change its identity. The linage boundaries (compartment boundaries) are more rigid, cells in this case sort at the interface. In both cases boundary formation mechanisms straighten the boundary. The boundaries that form as a result of cellular translocation: morphological movements bring two formerly mixed cell population in apposition. Cells can either move in a group or singly. Boundary is shown by dashed line

Figure 1.2:

A. Somite segmentation: The paraxial mesoderm PSM appears as two parallel elongated cell masses on both sides of the notochord. The paraxial mesoderm is progressively segmented into somites. Each somite has distinct genes expressed in the anterior and posterior halves, an example of which is EphA4 on the anterior and ephrinB2 on the posterior half. The boundary forms specifically at the interface between the posterior cells of the last formed somite and the anterior cells of the posterior unsegmented mesoderm. **B.** Rhombomere boundaries: Once separated from the midbrain, the hindbrain undergoes segmentation into seven rhombomeres (r1-r7). Their separation is controlled by alternate gene expression in even and odd segments. Their expression on the first two rhombomeres is overlapping. The segmented expression pattern of ephrin and Ephs is showed by the two colors.

Figure 1.3:

The molecular domains of ephrins and Ephs are depicted in this diagram. Dashed line shows the boundary.

Figure 1.1

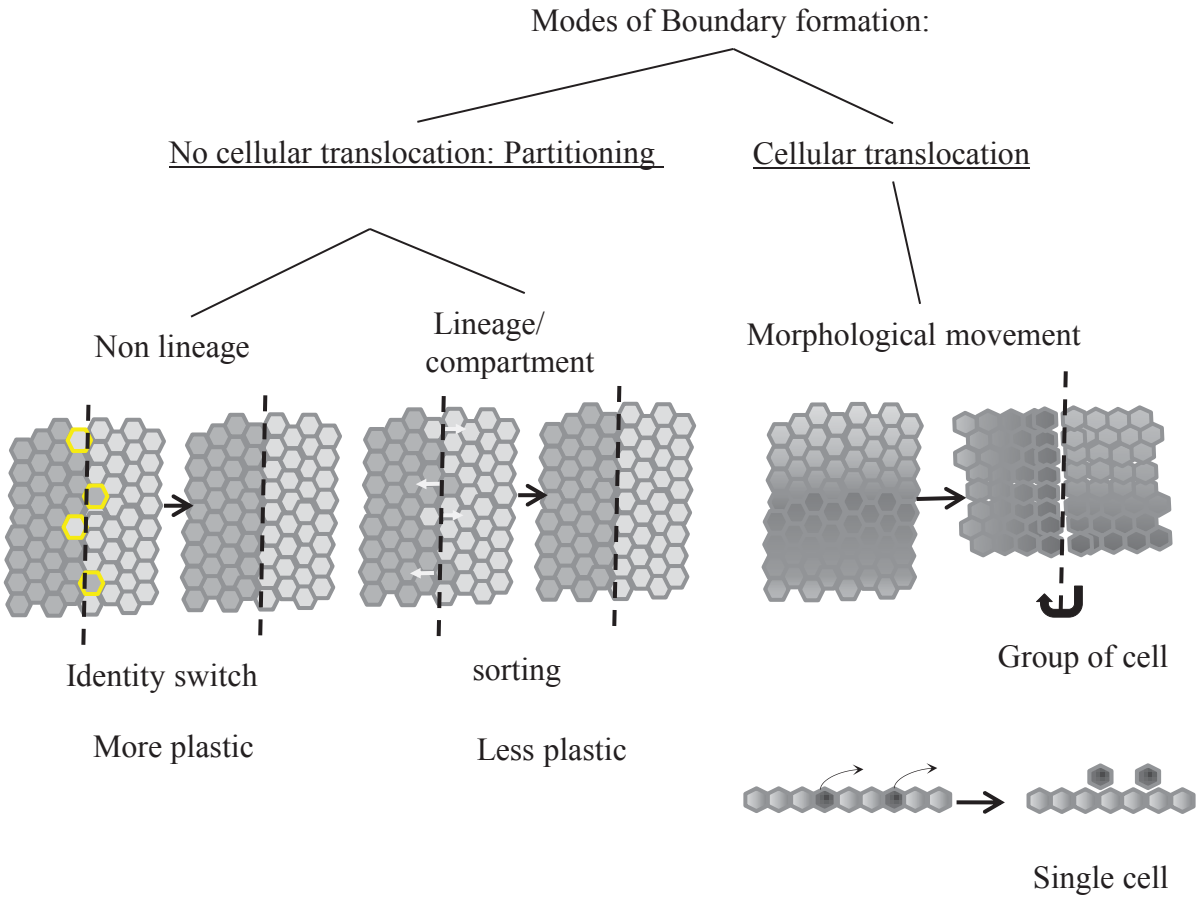
Modes of Boundary formation:
No cellular translocation: Partitioning
Cellular translocation
Non lineage
Lineage/
compartment
Morphological movement
Identity switch
sorting
Group of cell
More plastic
Less plastic
Single cell

Figure 1.2

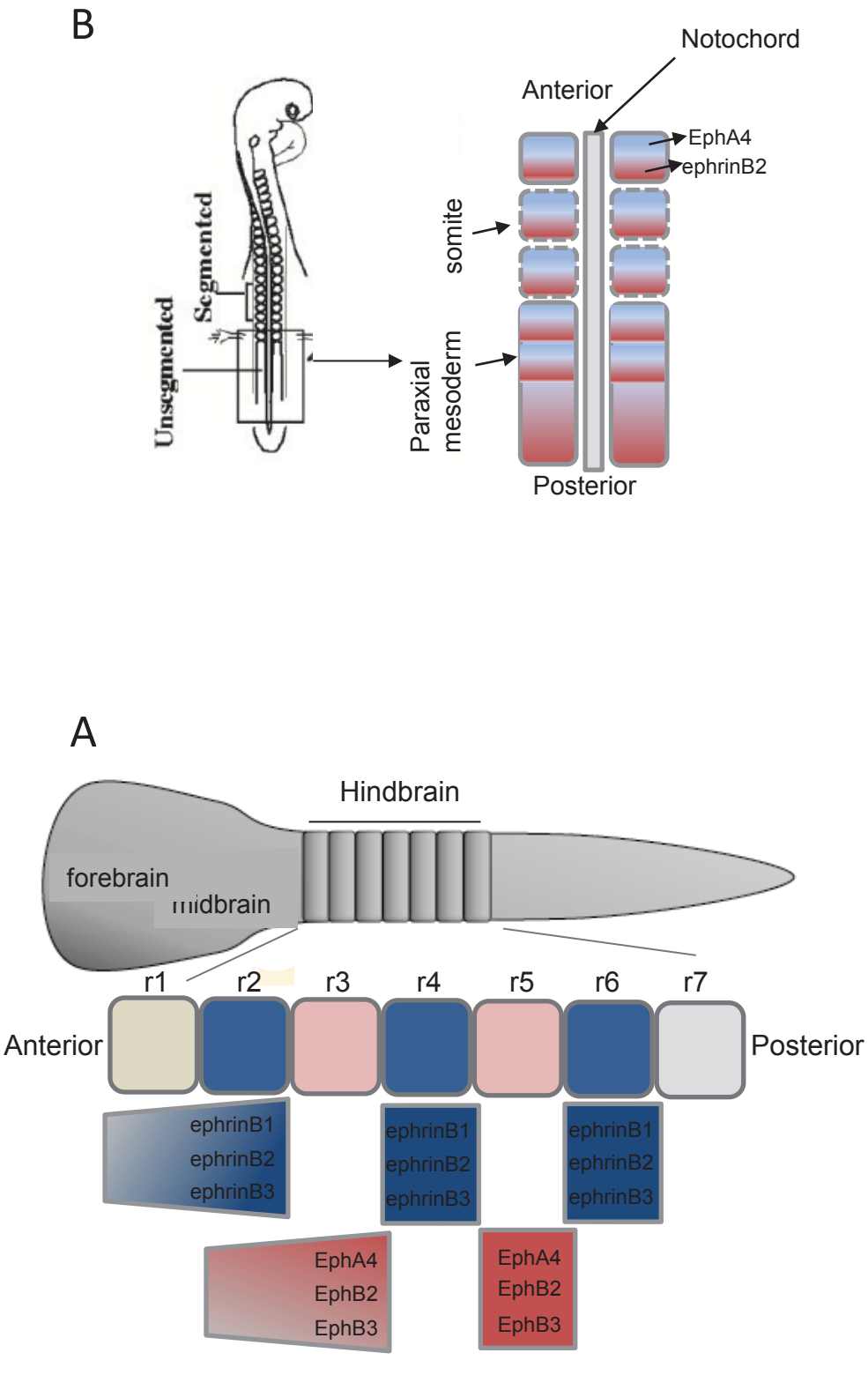
B
Notochord
Anterior
EphA4
ephrinB2
somite
Segmented
Unsegmented
Paraxial mesoderm
Posterior
A
Hindbrain
forebrain
midbrain
r1
r2
r3
r4
r5
r6
r7
Anterior
Posterior
ephrinB1
ephrinB2
ephrinB3
ephrinB1
ephrinB2
ephrinB3
ephrinB1
ephrinB2
ephrinB3
EphA4
EphB2
EphB3
EphA4
EphB2
EphB3

Figure 1.3

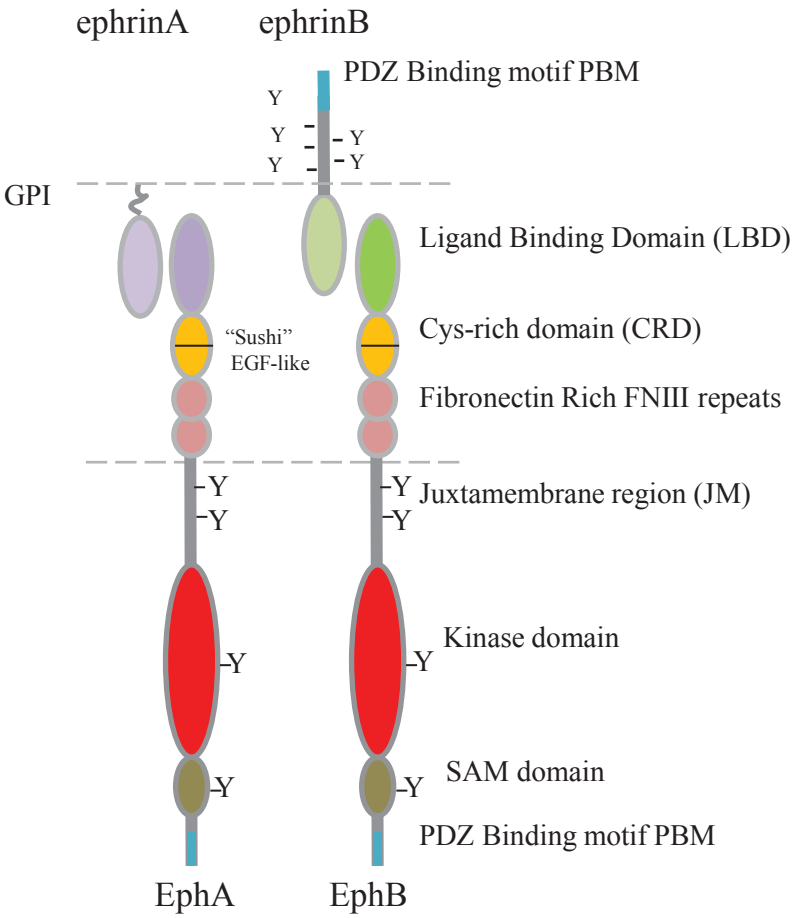
ephrinA
ephrinB
PDZ Binding motif PBM
Y
Y
Y
Y
Y
GPI
Ligand Binding Domain (LBD)
"Sushi"
EGF-like
Cys-rich domain (CRD)
Fibronectin Rich FNIII repeats
Y
Y
Y
Y
Juxtamembrane region (JM)
Y
Kinase domain
Y
Y
SAM domain
Y
PDZ Binding motif PBM
EphA
EphB

Thesis objectives

Chapter1: This chapter contains a literature review of the relevant areas of research. It begins with introduction to tissue separation and reviews involved mechanisms, then it focuses on the role and mechanism of function of ephrins and Ephs with a focus on their role at developmental boundaries.

Chapter2: This section identifies the mechanism that separate ectoderm and mesoderm cell at Brachet's cleft. My results suggested that the formation of this boundary relies on a dynamic process of contact-repulsion that is controlled by antiparallel signals from ephrin and Eph receptors on both sides of the boundary.

Chapter3: Ectoderm and mesoderm cells co-express several ephrins and Ephs yet separation occurs at the interface of the two tissues. I propose that the confinement of separation to the boundary relies on selective interactions between specific ephrin and Ephs and on their asymmetrical expression. Integration of signals from asymmetrically expressed pairs creates the zone of stronger repulsion at the boundary. Such mechanism is able to induce separation across three boundaries that are formed during Xenopus gastrula: dorsal and ventral ectoderm-mesoderm boundary and nototchord somite boundary.

Chapter4: This section focuses on the boundary formed between the notochord and somite. We show Ephrin-Eph mediated local actomyosin activity creates a region of increased contractility that does not allow stable cadherin bonds to form. These data represent a potential mechanism for ephrin-Eph mediated de-adhesion at in vivo boundaries.

Chapter5: This chapter revisits the current views in the field of tissue separation and discuss them in the light of current findings to propose that, tissue separation at its core relies on ephrin-Ephs signaling. Also our understanding of how ephrin-Ephs functions in this context is discussed and analyzed by revisiting existing data about ephrin-Ephs at other studied boundaries.

Bridge to Chapter II

In the previous chapter, a survey of literature showed that while several models for cell sorting are proposed there are very little in vivo studies about the cellular mechanism controlling tissue separation. In the following chapter we investigate the mechanism of tissue separation at the ectoderm-mesoderm boundary in Xenopus leavis. We demonstrate that separation is a contact mediated mechanism that is controlled by antiparallel ephrin-Eph signaling at ectoderm and mesoderm boundary. Ephrin-Ephs signaling and activation of Rho and Rac downstream of them generates a special local cellular behaviour that has not been documented before at the boundaries. This cellular behaviour consists of cycles of detachment followed by attachments. Such dynamic retraction behaviour indeed supports the existence of repulsive signals at the boundary. The following chapter is a reproduction of the paper below that is published in PloS Biology:
EphrinB/EphB Signaling Controls Embryonic Germ Layer Separation by Contact-Induced Cell Detachment. Rohani N, Canty L, Luu O, Fagotto F, Winklbauer R (2011) PLoS Biol 9(3): e1000597. doi:10.1371/journal.pbio.100059

Chapter II: EphrinB/EphB-signaling controls embryonic germ layer separation by contact-induced cell detachment

Abstract

Background: The primordial organization of the metazoan body is achieved during gastrulation by the establishment of the germ layers. Adhesion differences between ectoderm, mesoderm and endoderm cells could in principle be sufficient to maintain germ layer integrity and prevent intermixing. However, in organisms as diverse as fly, fish or amphibian, the ectoderm-mesoderm boundary not only keeps these germ layers separated: the ectoderm also serves as substratum for mesoderm migration, and the boundary must be compatible with repeated cell attachment and detachment. Principal findings: We show that localized detachment resulting from contact-induced signals at the boundary is at the core of ectoderm-mesoderm segregation. Cells alternate between adhesion and detachment, and detachment requires ephrinB/EphB signaling. Multiple ephrinB ligands and EphB receptors are expressed on each side of the boundary, and tissue separation depends on forward signaling across the boundary in both directions, involving partially redundant ligands and receptors and activation of Rac and RhoA. Conclusion: This mechanism differs from a simple differential adhesion process of germ layer formation. Instead, it involves localized responses to signals exchanged at the tissue boundary, and an attachment/detachment cycle which allows for cell migration across a cellular substratum.

Introduction

When Townes and Holtfreter (Townes & Holtfreter, 1955) observed the sorting of mixed embryonic ectoderm, mesoderm and endoderm cells, they proposed that this segregation of germ layers and the consequent self-assembly of the basic body structure was based on mutual 'tissue affinities'. This concept was later refined into Steinberg's (Steinberg, 1963) Differential Adhesion Hypothesis, which posited that simple adhesion differences between cell populations are sufficient for their separation and their positioning relative to each other, explaining, for example, the arrangement of germ layers in amphibian embryos (Davis, Phillips, & Steinberg, 1997; Phillips, 1978) However, if the boundary between two germ layers also serves for tissue translocation, more specialized tissue separation mechanisms may be required.

In the Xenopus gastrula, mesoderm translocates across the ectodermal blastocoel roof (BCR), and the boundary between these two germ layers, Brachet's cleft, must permit this movement yet prevent invasion of the BCR by the migratory mesoderm (Fig.2.1A). Interaction with a sparse network of fibronectin fibrils controls the motility of mesoderm cells, but their adhesion to the BCR is fibronectin-independent (Winklbauer & Keller, 1996). In fact, BCR and mesoderm cells are in direct contact (Nakatsuji, 1976), and the same adhesion molecules, C- and XB/U-cadherin, are expressed in both tissues (reviewed in (Kühl & Wedlich, 1996)).

This ectoderm-mesoderm boundary has been established as a model for tissue separation. Properties of the mesoderm and the BCR that underlie their separation can be studied in an in vitro assay (Fig.2.1A) (Wacker, Grimm, Joos, & Winklbauer, 2000; Winklbauer & Keller, 1996). The molecular control of separation behavior is partly known. Non-canonical Wnt signaling downstream of the Wnt receptor Xfz7 (Winklbauer, Medina, Swain, & Steinbeisser, 2001), interaction of Xfz7 with paraxial protocadherin (PAPC) and with the ankyrin

repeat domain protein 5 (xANR5), and activation of RhoA and Rho kinase(Chung, Yamamoto, & Ueno, 2007; Hukriede et al., 2003; Medina, Swain, Kuerner, & Steinbeisser, 2004) are involved in the implementation of a proximal, yet still unknown cellular mechanism that actually generates the boundary.

A candidate for this proximal mechanism is ephrin/Eph signaling. Eph receptor tyrosine kinases are subdivided into EphA and EphB subclasses and their membrane-linked ephrin ligands correspondingly into ephrinAs and ephrinBs. Within subclasses, binding appears promiscuous, although some Eph receptors have a higher affinity for specific ephrins. Receptor ligation and clustering initiates 'forward signaling', but receptor-ligand interaction can also stimulate 'reverse signaling' downstream of the ephrin ligand. Ephrin/Eph signaling has been implicated in boundary formation under conditions where receptor and ligand are expressed in complementary patterns (Blits-Huizinga, Nelersa, Malhotra, & Liebl, 2004; Kullander & Klein, 2002; Murai & Pasquale, 2003; Pasquale, 2005; Poliakov, Cotrina, & Wilkinson, 2004; Tepass, Godt, & Winklbauer, 2002). In particular, a model was proposed for rhombomere-boundary formation based on repulsive Eph-ephrin signaling, acting in parallel with an Eph-dependent regulation of adhesion within the rhombomeres (Cooke, Kemp, & Moens, 2005; Sela-Donenfeld & Wilkinson, 2005). However, direct observation of repulsive behavior at the boundary, similar to what is classically seen during neuron guidance, has not been attempted. In the early Xenopus embryo, expression of several Eph receptors and ephrins has been reported (reviewed in (Winklbauer & Luu, 2009)). Their in vivo functions during gastrulation have not yet been established, although gain-of-function experiments indicate that they can regulate cell adhesion, migration and sorting (Jones et al., 1998; Lee et al., 2006; Tanaka, Kamo, Ota, & Sugimura, 2003). Thus, ephrin signaling is a prime candidate to mediate tissue separation in the early Xenopus embryo.

Results

Cells display sustained attachment-repulsion cycles at the ectoderm-mesoderm boundary

To examine cell contact dynamics at the boundary in living tissues, membrane-labeled mesoderm explants and ectodermal blastocoel roofs (BCRs) were combined, and the reconstituted boundary was observed by confocal microscopy (Fig.2.1 and Suppl. movies). Contacts within each tissue appeared tight, as cells remained apposed and moved in concert. (Fig.2.1C,D, arrowheads, Suppl. movies 1 and 2). The same behavior was seen at the boundary between BCR and ectoderm explants: cells re-established contacts within minutes and remained stably apposed throughout the experiments (up to 2 hours) (Fig.2.1D, G, arrows, Suppl. movies 2 and 6). In contrast, contacts between mesoderm and BCR cells appeared dynamic (Fig.2.1C arrow, E, Suppl. movies 1 and 3) with frequent detachments followed by re-establishment of contacts (Fig.2.1G).

The frequency and length of detachment phases was variable. Also, separation was not uniform over the length of the boundary (see e.g. Fig.2.1B,E, Suppl. Movie1 and 3). While in close contact, mesodermal cells appeared to adhere to the BCR. They moved in concert with BCR cells, and during subsequent detachment, taut retraction fibers often spanned the gaps between cells (Fig.2.1C, frame insert#34a, Fig.2.1F frame#2a, Suppl. movies 1 and 3). A detachment event typically spread along the boundary, where existing contacts seemed to resist retraction (see e.g. Suppl. movie 1, and Fig.2.1C and E). Detached cells from either side of the boundary can emit protrusions which probe the cleft (Fig.2.1C, frame#34, Fig.2.1E insert frame #9, Suppl. movies 1 and 3). While repeatedly retracting and attaching, mesoderm cells can move along the BCR into gaps produced by other retracting mesoderm cells (Suppl. movie 3). This suggests a mechanism for the normal collective migration of mesoderm on the BCR substratum, and is consistent with the co-existence of close adhesive contacts and gaps between mesoderm cells and the BCR at the ultrastructural level (Nakatsuji, 1976). Altogether, it appears that contact-induced detachment between

ectodermal and mesodermal cells is at the base of a tissue separation mechanism supportive of cell movement at the interface.

In vitro activation of EphB signaling is sufficient to induce tissue separation
We tested the role of ephrins and Ephs on tissue separation in an in vitro assay (Fig.2.1A). This assay is scored by determining the percentage of test explants placed on a dissected blastocoel roof that remain separate after 1hr. Wild type ectoderm explants all sink into the BCR, while the majority of wild type mesoderm explants remain distinctly separated, i.e. on the surface of the BCR (Fig.2.2B). Note that after 45-60 min, the reaction is complete: explants have either fully integrated (usually within 15 min for wild type ectoderm) or will remain definitively separated, implying that for individual explants the response is all or none. However, when the percentage of explants remaining separated in a given experiment is counted, the overall outcome is graded, which can be shown by increasing concentrations of interfering reagents (e.g. Suppl. Fig.2.S3) and/or increasing incubation times with activating Fc fragments (e.g. Fig.2.2A).
We first performed gain-of-function experiments on ectoderm tissues by treating them with activating pre-clustered extracellular ephrin-Fc fusion polypeptides. While untreated ectodermal BCR explants readily reintegrated into BCRs, test explants incubated with ephrinB2-Fc tended to remain separate (Fig.2.2A). The same result was obtained by treating the substrate BCR instead of the test explants. Separation increased with incubation time, but could be detected as soon as 2 min after treatment (Fig.2.2A), indicating a rapid and direct cellular response. Activation was reversible, as a 30 min wash significantly decreased separation behaviour (not shown). Separation was strongest when both the substrate BCR and BCR test explants were treated with ephrinB-Fc, over the whole duration of the assay, suggesting that the effect is not due to the establishment of a difference between two cell population, but rather to a change in cell contact behaviour. The response is specific for ephrinBs; ephrinA-Fc had very little effect (Fig.2.2A). These results imply that an EphB receptor is present on ectodermal cells, and that its stimulation by ephrinB can immediately induce tissue separation.

Consequently, we determined the expression pattern of all known ephrinB and EphB receptor isoforms in the gastrula by RT-PCR (Suppl. Fig.2.S1): all isoforms were expressed in all germ layers, although at different levels; as an exception, ephrinB3 was restricted to the ectoderm. Eph receptor-ephrin ligand binding is largely promiscuous, providing ample opportunity for redundancy. Moreover, Eph/ephrin signaling has previously been implicated in boundary formation in situations where receptor and ligand are expressed in complementary patterns in vivo (e.g. (Durbin et al., 1998; Q. Xu, Alldus, Holder, & Wilkinson, 1995; Qiling Xu, Mellitzer, Robinson, & Wilkinson, 1999)) or under experimental conditions (e.g. (Mellitzer, Xu, & Wilkinson, 1999; Tanaka et al., 2003)). With co-expression of receptors and ligands in each of two adjacent tissues, the question arises whether Eph/ephrin signaling can nevertheless be employed for their separation.

EphrinBs and EphB function are required for tissue separation

To address this issue, we performed loss-of-function experiments using antisense morpholino oligonucleotides (MOs) against ephrinBs and EphBs to knock down putative crucial factors for boundary formation. Interfering with ephrin/Eph signaling led to severe developmental defects (Suppl. Fig.2.S2). Most strikingly, analysis of early gastrulae revealed a strong reduction of Brachet's cleft (Suppl. Fig.2.S2a-c). While disruption of the cleft alone will affect gastrulation movements and produce shorter tadpoles (Suppl. Fig.2.S2e), ephrin/Eph signaling appears to disturb additional processes (EphB depleted embryos die before hatching, Suppl. Fig.2.S2f). By using the in vitro assay (Fig.2.1A) and by directly examining cell behavior, we isolated its specific function in tissue separation. Ephrin B1 and B2 MOs indeed inhibited tissue separation when injected either in the mesoderm or in the BCR (Fig.2.2 B,C, Suppl. Fig.2.S3), showing that both ephrins are required on both sides of the boundary. EphrinB1 MO was slightly more efficient in the BCR (not shown) and ephrinB2 MO in the mesoderm (Suppl. Fig.2.S3), consistent with relative expression levels of the two ligands (Suppl. Fig.2.S1). Inhibition of separation shows dose-dependence before

reaching a plateau at around 30-40% (Suppl. Fig.2.3B). Knock down of ectoderm specific ephrinB3 caused a similar partial inhibition (Suppl. Fig.2.S4A). In all cases, separation was rescued by co-injection of corresponding wild type ephrinB mRNA (Fig.2.2C and Suppl. Fig.2.S4A). Inhibition was not significantly increased in double knock-down of ephrinB1 and B2 in the mesoderm (Suppl. Fig.2.S3), and the same was true for triple knock-down of all ephrinB1-3 in the BCR (Suppl. Fig.2.S4A). We conclude that all ephrinBs expressed in a given tissue are required to a degree related to their relative expression levels, but simultaneous depletion is not sufficient for complete inhibition of separation.

We next tested whether ephrinB2, which is enriched in the mesoderm, could induce separation when overexpressed in the ectoderm. We found indeed that a significant number (~40%) of ectoderm explants now remained separated from wild type BCR (Suppl. Fig.2.S4B). However, overexpression of ephrinB1, which is already abundant in the ectoderm, had no effect (Suppl. Fig.2.S4B). Both constructs are strongly expressed (data not shown) and effectively rescue normal separation between the mesoderm and the BCR (Fig.2.2C). These results show that increasing ephrinB2 levels is sufficient to trigger separation, and suggests that formation of the ectoderm-mesoderm boundary relies at least partly on the differences in ephrin composition observed between these two tissues (Suppl. Fig.2.S1).

Since ephrinB2 is required in the mesoderm, overexpression in the BCR of a cytoplasmically truncated form of the cognate receptor EphB4 (ΔC-EphB4) should compete for ephrin B2 binding with all endogenous Eph receptors and inhibit forward signaling in this tissue. Expression of ΔC-EphB4 in the BCR did indeed diminish separation, to a degree very similar to that obtained by ephrinB loss-of-function in the mesoderm (Fig.2.2C). EphB4 MO mimicked this effect, both in the BCR and in the mesoderm (Fig.2.2C), demonstrating that EphB4 is required. We conclude that the B family ligands and receptors are required in both ectoderm and mesoderm for tissue separation.

In the Xenopus gastrula, PDGF-A is expressed in the ectoderm and its receptor, PDGFR-α, in a complementary pattern the mesoderm. However, inhibition of PDGF signaling, by inhibiting PDGFR isoforms, does not affect formation of the boundary (Damm and Winklbauer, submitted) or separation behavior in the BCR assay (Suppl. Fig.2. S4B). Likewise, interaction with the fibronectin-rich matrix on the surface of the BCR, which together with PDFG-A signaling determines the direction of mesoderm cell movement across the BCR (Nagel, Tahinci, Symes, & Winklbauer, 2004), is not required for tissue separation (Winklbauer & Keller, 1996), emphasizing the dominant role of EphB/ephrinB signaling in this process.

Evidence for two anti-parallel ephrinB/EphB pathways signaling across the ectoderm-mesoderm boundary

Our results suggest that ephrinB-EphB signaling occurs within each tissue on either side of the boundary, or that two anti-parallel pathways signal across the boundary. To distinguish between these alternatives, we performed a series of systematic ephrinB/EphB double knock down/inhibition/rescue experiments. We first established that we maximally inhibited ligand or receptor activities: Coinjection of ephrinB1 and B2 MOs indicated saturation of ephrinB inhibition (Suppl. Fig.2.S3). Moreover, the degree of inhibition upon expression of ΔC-EphB could not be increased by increasing mRNA levels (Suppl. Fig.2. S3C). Thus, even when a pathway was maximally inhibited on one side, separation was only partially impaired. However, separation could be further reduced by interfering with ΔC-EphB4 on both sides of the boundary (Fig.2.3A and Suppl. Fig.2.S3C). Increased inhibition was also obtained by downregulating ephrinB and EphB activity simultaneously in the mesoderm (Suppl. Fig.2.S3A) or in the BCR (data no shown), but not by downregulating ephrinBs in one tissue and Eph receptor in the other (Fig.2.2C). Since these double inhibition experiments were preformed under conditions of maximal EphB interference (Suppl. Fig.2.S3), ephrinB inhibition should not have had an effect if in the same EphB pathway. Thus, the simplest interpretation of our results was that separation is controlled by the additive activity of two antiparallel pathways signaling across the boundary.

Each pathway involves ephrin ligands on one side and Eph receptors on the other side.

We tested this hypothesis more directly using ephrinB-Fc fragments (Fig.2.3B,C), which allowed us to stimulate these pathways specifically at the tissue surface, i.e. at the boundary. The rationale was to deplete ephrins in one of the interacting tissues, and then restore the forward signal by treating the other tissue with ephrin-Fc fragments to trigger activation of Eph receptors at its surface (Fig.2.3B). When we activated EphB signaling in mesoderm explants by treatment with ephrinB2-Fc (which binds to all EphB receptors), and placed them on ephrinB1/B2 depleted BCR, robust separation occurred (Fig.2.3C). Thus, direct activation of EphB receptors at the mesoderm surface can rescue separation from ephrin-depleted ectoderm, implicating forward signaling from the ectoderm to the mesoderm in tissue separation. The complementary experiment - ephrinB2 depletion in the mesoderm and EphB activation at the surface of the BCR - also resulted in a rescue of separation (Fig.2.3C), indicating that forward signaling from the mesoderm to the ectoderm is similarly active during tissue separation. The experiments show that separation can be restored by activating forward signaling directly at the surface of adjacent tissues. Thus, the separation phenotype induced by ephrinB loss-of-function can be fully accounted for by an inhibition of signaling across the boundary. Altogether, full tissue separation requires two forward signals, one triggered by mesodermal ephrins binding to the EphB receptors at the surface of the ectoderm, and a second one depending on ectodermal ephrins interacting with Eph receptors of the mesoderm.

EphrinB/EphB signaling is required for cell detachment at the boundary

EphrinB or EphB knockdown impedes cell detachment at the boundary (Fig.2.4). EphrinB2 MOs in the mesoderm dramatically decreased the frequency of attachment/detachment events (Fig.2.4B,G). Often, mesoderm cells remained apposed to BCR cells for the whole duration of the recording (Fig.2.4B, Suppl. movie 4), similar to ectoderm aggregates (Fig.2.4E, Suppl. movie 6). Mesoderm

and BCR cells moved in concert, indicating stable contacts (Suppl. movie 4). Detachment was similarly inhibited when ephrinB1 was depleted from the BCR, or EphB4 from the mesoderm (Fig.2.4D,C, Suppl. movie 5). Thus, signaling in both tissues is required for cell detachment at the interface.
Attachment/detachment cycles were also rescued after ephrinB1 depletion in the BCR by incubating wild type mesoderm test explants with increasing doses of soluble ephrinB1-Fc fragments (Fig.2.4F,G), demonstrating that this behavior is an immediate reaction to ephrin-Eph signaling at the boundary.

The experiments above show that direct ephrin activation at the tissue interface accounts for repulsion between ectoderm and mesoderm. In our time lapse recordings, repulsion is never observed within the tissues, but ephrin/Eph signals may nevertheless affect cell-cell adhesion (Cooke et al., 2005; Jones et al., 1998; Pasquale, 2005; Sela-Donenfeld & Wilkinson, 2005). We evaluated the effect of Eph/ephrin loss- and gain-of –function on adhesion of ectoderm and mesoderm cells, using a classical reaggregation assay. Aggregation of dissociated cells started within minutes (not shown), and mesoderm cells formed smaller aggregates than ectoderm after 1 hour (Suppl. Fig.2.S5), consistent with mesoderm being less cohesive (Brieher & Gumbiner, 1994; Kalantarian et al., 2009). EphrinB2 or EphB4 depletion had no effect on mesoderm cell aggregation, suggesting that ephrinB/EphB activity does not contribute to mesoderm tissue cohesion. In the ectoderm, however, corresponding ephrinB1/EphB4 depletion diminished aggregation. Overexpression of ephrinB2 had a similar, although more variable effect. Thus, while ephrinB2 overexpression induces tissue separation and ephrin/Eph depletion inhibits separation, both treatments reduce cohesion within the ectodermal tissue. Altogether, putative effects of ephrins and Eph receptors on cell-cell adhesion within tissues are not correlated with their roles in cell detachment at the tissue boundary.

RhoA and Rac GTPase mediate tissue separation downstream of Ephrin/Eph in both mesoderm and BCR

RhoA and Rac are well established downstream effectors of Ephrin/Eph signaling that modulate cytoskeletal dynamics. RhoA activity in the mesoderm had been implicated in separation behavior (Medina et al., 2004), but the role of RhoA in the BCR and of Rac in both tissues has not yet been addressed. We systematically tested the effects of manipulating RhoA or Rac function. Dominant negative N19RhoA and N17Rac both inhibited separation when expressed in either of the two tissues (Fig.2.5A,B). Because expression of constructs interfering with RhoA and Rac function may also have long term indirect effects, we complemented these data with experiments using specific soluble inhibitors of Rac and of Rho-associated kinase, a direct target of RhoA (Fig.2.5C). A short incubation with these inhibitors was sufficient to cause mesoderm test explants to integrate into the BCR, thus mimicking the effect of the dominant negative GTPases. This immediate response to the inhibitors suggests that RhoA and Rac activities are directly required during the separation process.

We next asked if RhoA/Rac activation could rescue separation when ephrin/Eph signaling is impaired. Since we had demonstrated forward signaling in both directions, we inhibited signaling on the Eph receptor side, by injection of EphB4 MO in the mesoderm and ΔC-EphB4 in the BCR, and tested the effect of constitutively active forms of RhoA and Rac (V14RhoA ,V12Rac), expressed at low levels in the same tissue. In both cases, separation could be efficiently rescued by both V14RhoA and V12Rac (Fig.2.5D,E). A weak rescue was also observed upon overexpression of wild type RhoA and Rac (Suppl. Fig.2.S6B). Constitutively active Cdc42 was unable to rescue separation (Fig.2.5D). We conclude that RhoA and Rac, but not Cdc42, function downstream of Eph signaling on both sides of Brachet's cleft. Since RhoA has also been proposed to act downstream of Xfz7/PAPC/xANR5 in the mesoderm to regulate tissue separation (Medina et al., 2004), we asked whether co-expression of Xfz7 and PAPC could rescue separation in ephrinB2+EphB4 MO-injected mesoderm. We did not observe any rescue (Suppl. Fig.2.S4C), indicating that ephrinB/EphB signaling acts downstream of or in parallel to Xfz7/PAPC.

We next examined the effect of RhoGTPases activity on repulsion at the cleft by live confocal microscopy (Fig.2.6). When dominant negative forms of RhoA or Rac were expressed in the BCR or in the mesoderm, the frequency of attachment/detachment was strongly reduced in all cases (Fig.2.6H). Most cells established stable contacts between ectoderm and mesoderm that were indistinguishable from contacts within tissues (Fig.2.6E,F). Conversely, when activated forms of RhoA or Rac were co-expressed with dominant negative EphB receptor, the rescue of tissue separation (Fig.2.5) was paralleled by a rescue of detachment at the boundary (Fig.2.6A-D, G; Suppl. movies #7,8). However, compared to controls, repulsion at the boundary appeared more transient. Although the membranes of abutting cells often remained close to each other for prolonged periods, they were clearly detached, and cells were able to slide along the boundary (Fig.2.6B), indicating that they had failed to re-establish contacts. It appeared as if cells were locked in a detached state by active RhoA or Rac, but could not fully retract under these conditions.

Our results imply that RhoA and Rac should be locally activated at ectoderm-mesoderm contacts in an Eph signaling-dependent manner. We investigated the subcellular localization of active, GTP-bound GTPases in the mesoderm by expressing the GTPase-binding domains (GBD) of N-Wasp (a target of Cdc42/Rac) or Rhothekin (a target of RhoA) fused to GFP. These test explants were combined with BCRs expressing mCherry and examined by spinning disk confocal microscopy. While these constructs can act as inhibitors of their respective GTPases, at low expression levels they are expected to accumulate at sites of high concentrations of active GTPases (Bement, Benink, & von Dassow, 2005; Benink & Bement, 2005; Berger, März, Kitzing, Grosse, & Steinbeisser, 2009).

We observed accumulation of both GBDs at the ectoderm-mesoderm boundary (Fig.2.7A,B, large arrows). Signal intensity was generally higher there than at cell

contacts within the explants. We quantified the GBD distribution in all cells which were in contact with BCR cells (Fig.2.7D). While in controls, BCR-BCR contacts showed accumulation in less than 20% of the cells, about 60-80% of mesoderm cells contacting the BCR scored positive for a high fluorescent signal, for both Wasp and Rhothekin GDBs. This was a significant increase ($p<0.001$) compared to GFP alone. EphB4 MO seemed to inhibit GBDs accumulation at boundary contacts (arrowheads): the frequency of accumulation decreased to 30-40% ($p<0.001$). A similar frequency was obtained for mesoderm cells expressing dominant negative GTPases (Fig.2.7D). We also observed a dramatic decrease in Wasp/Rhothekin-GBD boundary localization when ephrin B1 was depleted in the adjacent BCR (frequency around 20%, $p<0,0001$ compared to control MO). We have not yet been successful in performing the reciprocal experiment, i.e. imaging GBDs in the BCR. This tissue appears to tolerate expression of GBDs less. However, the data from mesoderm explants demonstrate an Eph signaling-dependent activation of GTPases at the boundary.

Time lapse microscopy of mesoderm cells expressing Wasp/Rhothekin-GBDs revealed that accumulation at the boundary was highly dynamic. As expected from the large variation in contact time and area (see above), and from the superposition of detachment and protrusion formation, we observed fluctuations that spanned a large range of intensities and were highly variable in frequency (Suppl. movies S9 and S10). Drastic changes often occurred between 2 frames, i.e. in less than 2min, in agreement with a fast dynamics of GTPase signaling. Despite this variation, a correlation could nevertheless be seen between retraction and signal decay. We analyzed cells for which we could unambiguously determine a transition from intimate contact with the BCR to detachment. In almost all cases (14/16 cells for WaspGBD and 13/14 cells for RtknGBD, from 4 independent experiments) the membranes of mesoderm cells contacting the BCR showed significant accumulation of the GFP construct, which decreased once the cell had detached (Fig.2.8). Generally, retractions and GFP decay both happened from one frame to the next (e.g. Fig.2.8A). In some cases, retractions spanned

several frames, which then correlated with a slower decay of the GFP signal (e.g. Fig.2.8B). Some of the changes in signal intensity that were observed in non-retracting cells may be due to small detachments not detectable at the resolution of the GFP-GBD signal. Also, GTPase activation events may simply not be successful in triggering detachment. Note that the fluctuations occurring asynchronously in neighboring areas (Fig.2.8A, small arrows) and the signal from mesoderm-mesoderm (Fig.2.8B, thin arrows) contacts served an internal control for the absence of photobleaching in these recordings.

As for putative downstream targets of the GTPases, we visualized cytoskeletal F-actin, phospho-nonmuscle-myosinII, and microtubules (Suppl. Fig.2.S7 and not shown). We did not detect any significant accumulations or depletions at the boundary for microtubules and P-myosin (not shown). F-actin was enriched at the boundary, and this was dependent on ephrin-signaling (supplemental Fig.2.S7). However, the pattern did not fully correlate with separation behavior, as a significant decrease was observed in the presence of N17Rac but not of N19Rho. These data indicate that the cytoskeleton is indeed modulated at the boundary, although tissue separation must be mediated by processes that cannot be distinguished at the level of global F-actin distribution. They also suggest that Rac and RhoA have distinct effects downstream of ephrin signaling, although we did not detect evidence for synergy between RhoA and Rac at the level of separation behavior (Suppl. Fig.2.S6).

Discussion

Previous attempts to explain the separation of ectoderm and mesoderm (Davis et al., 1997; Krieg et al., 2008; Phillips, 1978; M. Steinberg & M. Takeichi, 1994) have been based on a thermodynamic model involving the minimization of tissue surface free energy. It assumes that two respective cell types are intrinsically different in terms of cell adhesiveness or cortical tension, and that this difference can drive cell sorting, boundary formation and tissue positioning, analogous to the phase separation of immiscible fluids (Beysens, Forgacs, & Glazier, 2000; Krieg

et al., 2008; M. S. Steinberg & M. Takeichi, 1994; Steinberg, 1963). Here we have shown evidence for a different model, in which signaling across the ectoderm-mesoderm boundary is crucial to locally regulate cell detachment and eventually tissue separation. Thus, although all cells of the two populations have the potential to form a cleft-like boundary if juxtaposed, acute separation behavior is not based on permanent adhesion differences between cells, but on transient contact-dependent reactions. The resulting, alternating phases of adhesion and repulsion appear to be part of a self-regulating loop (Fig.2.9). The spreading of an adhesion zone brings ephrins and Ephs in contact, inducing a repulsion signal. Once cells are apart, the signal decays, cells start to explore the intercellular space created at the boundary, and eventually re-establish adhesion. This mechanism prevents mesoderm cells from intruding into the BCR while providing necessary substratum contacts for migration.

Cell detachment is restricted to the tissue interface, and although various ephrins and their cognate receptors are coexpressed within each tissue, they do not lead to overall mutual cell repulsion and hence tissue dissociation. This could be explained by several mechanisms. First, Eph/ephrin interaction between adjacent cells can not only mediate repulsion, but also cell adhesion, depending on the levels of receptors and ligands expressed. At low levels, adhesion is often promoted, while high levels induce cell repulsion e.g. (Hansen, Dallal, & Flanagan, 2004) (McLaughlin, Hindges, Yates, & O'Leary, 2003), reviewed by Poliakov et al. (Poliakov et al., 2004). Moreover, evidence for a relative binding specificity of various pairs of ephrinB/EphB subtypes has been accumulating (Blits-Huizinga et al., 2004). In fact, our observation that ectopic overexpression of the mesodermally enriched ephrinB2 in the ectoderm is sufficient to trigger separation, but that ephrinB1 is unable to do so, suggests a surprising degree of specificity of ligand-receptor interaction, and leads us to propose that the type and the level of ephrins and Eph receptors expressed in each of the two tissues may be the main determinant for tissue separation. Since a mixture of receptors and ligands is expressed in the ectoderm, and a similar, but distinctly different mixture

in the mesoderm, it is conceivable that the sum of interactions within each tissue is adhesive, while interactions across the boundary result in repulsion. Thus, quantitative effects, such as expression levels and binding affinities, and qualitative differences, for example ephrinB3 expression in ectoderm but not mesoderm, could be integrated in the form of overall signal intensity, and eventually result in a decision between stable contacts and repulsion. Second, in addition to expression levels of receptors and ligands that interact with specific affinities in trans, coexpression of Eph receptors and ligands in the same cell can also modulate tissue cohesion. Cis-interaction between ephrinsA and EphA receptors can inhibit forward signaling (Carvalho et al., 2006), and coactivation of EphB and ephrinB within the same cell can induce an adhesive instead of a repulsive response (Dravis et al., 2004). Again, this effect may be different within and between separating tissues.

The decreased reaggregation of ectoderm cells upon Eph/ephrin-depletion supports the possibility that Eph/ephrin interaction within this tissue upregulates cell-cell adhesion (Suppl. Fig.2.S5). For the mesoderm, a similar mechanism may work, although no obvious effect of Eph/ephrin function on tissue cohesion was observed; perhaps the adhesive function is miminal here, but sufficient to balance repulsion. Third, parallel mechanisms could further attenuate EphB/ephrinB-driven repulsion within the mesoderm or enhance it at the boundary. A candidate would be Xfz7/PAPC signaling, which is sufficient to induce separation in the ectoderm (Medina et al., 2004), and functions upstream or in parallel to EphB. Importantly, regulation of tissue cohesion by EphB/ephrinB function seems to be independent of the control of tissue separation. In the ectoderm, ephrinB2 overexpression which triggers separation, and ephrin/Eph depletion which inhibits it, both decreased reaggregation, and in the mesoderm, inhibition of separation behavior is not associated with a change in cell-cell adhesion. This is consistent with other results indicating that changes in global adhesive strength do not necessarily affect tissue separation (Jørgensen et al., 2009; Reintsch, Habring-Mueller, Wang, Schohl, & Fagotto, 2005). The results indicate also that ectoderm-

mesoderm separation is sensitive to the detailed expression pattern of Eph receptors and ligands, which is more complex than the classical complementary pattern, but may determine boundary formation in an essentially similar manner.

Ephrin/Eph-mediated boundary formation often involves the complementary expression of receptors and ligands in adjacent tissues, and bidirectional signaling e.g. (Mellitzer et al., 1999). This leads to rapid, large-scale asymmetric changes in downstream pathways in forward- and reverse-signaling cells (Barrios et al., 2003). Nevertheless, unidirectional signaling can be sufficient for cell segregation. Thus, in the zebrafish embryo, formation of the gap between adjacent somites depends on Eph forward signaling, while the ephrin reverse signal is dispensable (Watanabe, Sato, Saito, Tadokoro, & Takahashi, 2009). Surprisingly, the same process using the same receptor and ligand isoforms requires ephrin reverse signaling, but not an Eph forward signal, in the chick embryo (Zimmer, Palmer, Kohler, & Klein, 2003). We found that similar to zebrafish somite segmentation, forward signaling is essential for ectoderm-mesoderm separation, and that two antiparallel forward signals are sufficient for complete repulsion at the boundary.

The demonstrated requirement for both RhoA and Rac in tissue separation is consistent with their known functions in Eph/ephrin mediated repulsion. Thus, the termination of EphB-ephrinB interaction required for repulsion involves endocytosis of receptor and ligand (Zimmer et al., 2003), which in turn depends on Rac function downstream of EphB (Marston, Dickinson, & Nobes, 2003). RhoA and Rho kinase activation downsteam of an EphB receptor can be mediated by the adaptor protein, Dishevelled, and underlies experimentally induced cell sorting of Xenopus gastrula ectoderm cells (Tanaka et al., 2003). The local activation of Rac and RhoA at the ectoderm-mesoderm interface agrees with an above-threshold activation of Eph/ephrin signaling at the boundary only, despite the widespread co-expression of receptors and ligands.

It is worth noting that despite the very low levels used in our experiments, each of the constitutively active RhoA and Rac construct could efficiently rescue separation. While this is likely due in part to the potency of these forms, the cellular phenotypes produced by their overexpression appeared relatively mild. This was illustrated by the fact that even though the boundaries often appeared locked in a separated state upon rescue, attachment/detachment cycles were still observed occasionally. We hypothesize that in our inhibition experiments, ephrin/Eph signaling is decreased below the threshold required to maintain separation, but not completely abolished. Low amounts of active GTPases are then sufficient to boost the process and restore repulsion, while still allowing subsequent re-attachment. Alternatively, low levels of residual ephrin/Eph signaling may be sufficient to deliver exogenous active RhoA and Rac to their respective targets, though not to activate the endogenous GTPases sufficiently. The weak rescuing effects of wild type Rac and RhoA are consistent with both possibilities. In any case, the process of tissue separation appears particularly sensitive to small positive or negative changes in RhoGTPase activity, while larger alterations are required to affect other processes known to depend of such activities, in particular cell-cell adhesion.

Cleft-like boundaries based on attachment/repulsion cycles could generally be a requirement for the migration of cells across the surface of an adjacent tissue. A cleft-like ectoderm-mesoderm boundary is also seen in the zebrafish gastrula (Kimmel et al., 1995), and migration of mesoderm cells across the ectodermal layer occurs in Drosophila gastrulation (McMahon, McMahon, Supatto, Fraser, & Stathopoulos, 2008). It would be interesting to see whether the ephrinB/EphB mechanism of tissue separation is conserved in these cases. In contrast to the sparse, cell-permeable network of fibronectin fibrils that covers the ectodermal BCR of Xenopus, mouse or chicken gastrulae possess a well-developed basal lamina which physically separates ectoderm from mesoderm, possibly rendering germ layer separation independent of a cell repulsion mechanism (Brown & Brown, 2011). Indeed, mouse ephrinB1, ephrinB2 and EphB4 null mutants

apparently gastrulate normally (Adams et al., 1999; Compagni, Logan, Klein, & Adams, 2003; Gerety, Wang, Chen, & Anderson, 1999; Wang, Chen, & Anderson, 1998). After gastrulation, numerous mass cell migration events take place, for example neural crest migration, which in principle could also employ the mechanism presented here. Finally, deposition of an extracellular matrix seems to require free tissue surface (Dzamba, Jakab, Marsden, Schwartz, & DeSimone, 2009; Winklbauer, 1998), and initially separating rhombomeres or somites by a repulsion cleft could be the first step in the boundary maturation process which ends with a matrix-filled space between tissue blocks.

Experimental Procedures

Recombinant proteins

Recombinant mouse EphrinB2/FC chimera (R & D systems) comprising the extracellular domain of mouse ephrinB2 fused to C-terminal 6X histidin tagged Fc region of human IgG were pre-clustered with anti-human Fc antibody (Jackson ImmunoResearch Laboratories) at a 1:2 ratio in MBSH (Winklbauer & Keller, 1996) and incubated 1 h before application.

Injections

mRNAs were synthesized according to manufacturer instructions (mMessage mMachine kit, Ambion). MOs and mRNAs were injected animally in the two blastomeres of 2-cell stage embryos for ectoderm/BCR tissues, and equatorially in the two dorsal blastomeres of 4-cell stage embryos for mesoderm explants, at amounts listed in supplementary materials.

In vitro separation assay

The assay was performed as described (Winklbauer & Luu, 2009). Mesoderm explants were dissected from the lower lip region before the start of involution, as described (Winklbauer et al., 2001). For in vitro activation of Eph receptors, explants or BCRs were pre-incubated with preclustered ephrinB2-Fc fragments (40nM in MBSH) for 15 min at room temperature. For the statistical analysis, results were compared using the paired sample Student's t-test, taking each assay as an experimental unit. Thus each experiment was scored based on the percentage of test explants remaining separate (i.e. it is a graded response).

Confocal microscopy

Explants from embryos injected respectively with 2x200-400pg mGFP, mYFP or mCherry mRNA were mounted in a dish with a bottom cover slip. For figure 2.1A-C and suppl. movies 1 and 2, time lapse recordings were acquired using a Zeiss LSM510 with a 40x Neofluar NA=1.3 oil objective. GFP and YFP were excited with the 477 and 514 argon laser lines. Dicroïc and emission filters were HFT477, BP500/20 for GFP, and HFT514, LP530 for YFP. In other experiments,

a Quorum technologies WaveFX spinning disc confocal mounted on an automated DMI6000B Leica microscope was used, with a 40x HCX PL APO CS, NA = 1.25 oil objective. GFP and Cherry were excited with 491 and 561nm diode lasers. Images were collected with EM CCD 512X512 BT camera and controlled with Improvision Volocity 3DM software. Image processing was performed with Metamorph (Universal Imaging Corporation) and Adobe Photoshop7 software. For phalloidin staining, explants were fixed in 4% formaldehyde in MBSX for 10min, followed by permeabilization (1% formaldehyde, 0.1% TritonX100),1 hr incubation with blocking buffer (10% sheep serum), and overnight incubation with 2U/ml Alexa488-phalloidin (Invitrogen) in 10% sheep serum. After three washes in PBS and addition of antifade reagent (Slowfade® Gold, Invitrogen), sample were examined using the spinning disc microscope.

Re-aggregation assay

Mesoderm and inner layer ectoderm were dissociated in alkaline calcium-free buffer (88mM NaCl, 1mM KCl, 10mM NaHCO3, pH 9.3). Dissociated cells were transferred to agarose-coated Petri-dishes in normal MBSH, and incubated for 1 hr under mild rotation (10rpm) on an orbital shaker. Images of the whole area where aggregation occurred, i.e. including all single cells and all aggregates, were taken under a dissecting microscope at a 12.5xmagnification using a Micropublished RTV3.3 camera (Qimaging) and were analyzed for object size using ImageJ software. Two parameters were measured, average object area and area/perimeter ratio. Results of 5 independent experiments were normalized using wild type ectoderm as reference (=1.0).

Acknowledgements

We thank the McGill Biology Dpt. CIAN for technical support with the confocal microscopes. We also thank A. Brandli, I. Daar, , K. Cho, E. DeRobertis, H. Steinbeisser, K. Symes, and D. Wilkinson for reagents, and U. Tepass for critical reading of the manuscript. N.R. was recipient of a Canderell McGill Cancer Centre student award. This work was supported by grants CIHR# MOP-62898

and CCSRI #017162 to F.F. and by grant# 019355 from the Canadian Cancer Society – Ontario Division to R.W.

References

Adams, RH, Wilkinson, GA, Weiss, C, Diella, F, Gale, NW, Deutsch, U, . . . Klein, R. (1999). Roles of ephrinB ligands and EphB receptors in cardiovascular development: demarcation of arterial/venous domains vascular morphogenesis and sprouting angiogenesis. *Genes Dev, 13*, 295 - 306.

Angelika bottger, Monika Hassel. (2012). Hydra, a model system to trace the emergence of boundaries in developing eumetazoans. *int. J. Dev. Biol, 56*, 583-591. doi: 10.1387/ijdb. 11345ab

Barrios, Arantza, Poole, Richard J., Durbin, Lindsey, Brennan, Caroline, Holder, Nigel, & Wilson, Stephen W. (2003). Eph/Ephrin Signaling Regulates the Mesenchymal-to-Epithelial Transition of the Paraxial Mesoderm during Somite Morphogenesis. *Current biology : CB, 13*(18), 1571-1582.

Bement, William M., Benink, Helene A., & von Dassow, George. (2005). A microtubule-dependent zone of active RhoA during cleavage plane specification. *The Journal of Cell Biology, 170*(1), 91-101.

Benink, Helene A., & Bement, William M. (2005). Concentric zones of active RhoA and Cdc42 around single cell wounds. *The Journal of Cell Biology, 168*(3), 429-439.

Berger, Corinna D., März, Martin, Kitzing, Thomas M., Grosse, Robert, & Steinbeisser, Herbert. (2009). Detection of activated Rho in fixed *Xenopus* tissue. *Developmental Dynamics, 238*(6), 1407-1411.

Beysens, D. A., Forgacs, G., & Glazier, J. A. (2000). Cell sorting is analogous to phase ordering in fluids. *Proceedings of the National Academy of Sciences of the United States of America, 97*(17), 9467-9471.

Blits-Huizinga, Carla T., Nelersa, Claudiu M., Malhotra, Arun, & Liebl, Daniel J. (2004). Ephrins and their Receptors: Binding versus Biology. *IUBMB Life, 56*(5), 257-265. doi: 10.1080/15216540412331270076

Brieher, W M, & Gumbiner, B M. (1994). Regulation of C-cadherin function during activin induced morphogenesis of Xenopus animal caps. *The Journal of Cell Biology, 126*(2), 519-527. doi: 10.1083/jcb.126.2.519

Brown, N. H., & Brown. (2011). Extracellular Matrix in Development: Insights from Mechanisms Conserved between Invertebrates and Vertebrates. *Cold Spring Harbor perspectives in biology, 3*(12), a005082-a005082.

Carvalho, Ricardo F., Beutler, Martin, Marler, Katharine J. M., Knoll, Bernd, Becker-Barroso, Elena, Heintzmann, R., . . . Drescher, Uwe. (2006). Silencing of EphA3 through a cis interaction with ephrinA5. *Nat Neurosci, 9*(3), 322-330. doi: http://www.nature.com/neuro/journal/v9/n3/suppinfo/nn1655_S1.html

Chung, Hyeyoung A., Yamamoto, Takamasa S., & Ueno, Naoto. (2007). ANR5, an FGF Target Gene Product, Regulates Gastrulation in Xenopus. *Current Biology, 17*(11), 932-939.

Compagni, Amelia, Logan, Malcolm, Klein, Rüdiger, & Adams, Ralf H. (2003). Control of Skeletal Patterning by EphrinB1-EphB Interactions. *Developmental Cell, 5*(2), 217-230. doi: http://dx.doi.org/10.1016/S1534-5807(03)00198-9

Cooke, Julie E., Kemp, Hilary A., & Moens, Cecilia B. (2005). EphA4 Is Required for Cell Adhesion and Rhombomere-Boundary Formation in the Zebrafish. *Current Biology, 15*(6), 536-542. doi: http://dx.doi.org/10.1016/j.cub.2005.02.019

Dahmann, Christian, Oates, Andrew C., & Brand, Michael. (2011). Boundary formation and maintenance in tissue development. *Nat Rev Genet, 12*(1), 43-55.

Davis, Grayson S., Phillips, Herbert M., & Steinberg, Malcolm S. (1997). Germ-Layer Surface Tensions and "Tissue Affinities" inRana pipiensGastrulae: Quantitative Measurements. *Developmental Biology, 192*(2), 630-644.

Dravis, Christopher, Yokoyama, Nobuhiko, Chumley, Michael J., Cowan, Chad A., Silvany, Robert E., Shay, Jennifer, . . . Henkemeyer, Mark. (2004). Bidirectional signaling mediated by ephrin-B2 and EphB2 controls urorectal development. *Developmental Biology, 271*(2), 272-290.

Durbin, Lindsey, Brennan, Caroline, Shiomi, Kensuke, Cooke, Julie, Barrios, Arantza, Shanmugalingam, Shantha, . . . Holder, Nigel. (1998). Eph signaling is required for segmentation and differentiation of the somites. *Genes & Development, 12*(19), 3096-3109. doi: 10.1101/gad.12.19.3096

Dzamba, Bette J., Jakab, Karoly R., Marsden, Mungo, Schwartz, Martin A., & DeSimone, Douglas W. (2009). Cadherin Adhesion, Tissue Tension, and Noncanonical Wnt Signaling Regulate Fibronectin Matrix Organization. *Developmental Cell, 16*(3), 421-432. doi: http://dx.doi.org/10.1016/j.devcel.2009.01.008

Gerety, SS, Wang, HU, Chen, ZF, & Anderson, DJ. (1999). Symmmetrical mutant phenotypes of the receptor EphB4 and its specific transmembrane ligand ephrin-B2 in cardiovascular development. *Mol Cell, 4*, 403 - 414.

Hansen, Michael J., Dallal, Gerard E., & Flanagan, John G. (2004). Retinal Axon Response to Ephrin-As Shows a Graded, Concentration-Dependent Transition from Growth Promotion to Inhibition. *Neuron, 42*(5), 717-730. doi: http://dx.doi.org/10.1016/j.neuron.2004.05.009

Hukriede, Neil A., Tsang, Tania E., Habas, Raymond, Khoo, Poh-Lynn, Steiner, Kirsten, Weeks, Daniel L., . . . Dawid, Igor B. (2003). Conserved Requirement of Lim1 Function for Cell Movements during Gastrulation. *Developmental Cell, 4*(1), 83-94.

Jones, Teri L., Chong, Lisa D., Kim, Jaebong, Xu, Ren-He, Kung, Hsiang-Fu, & Daar, Ira O. (1998). Loss of cell adhesion in Xenopus laevis embryos mediated by the cytoplasmic domain of XLerk, an erythropoietin-producing hepatocellular ligand. *Proceedings of the National Academy of Sciences of the United States of America, 95*(2), 576-581.

Jørgensen, Claus, Sherman, Andrew, Chen, Ginny I., Pasculescu, Adrian, Poliakov, Alexei, Hsiung, Marilyn, . . . Pawson, Tony. (2009). Cell-Specific Information Processing in Segregating Populations of Eph Receptor Ephrin–Expressing Cells. *Science, 326*(5959), 1502-1509. doi: 10.1126/science.1176615

Kalantarian, Ali, Ninomiya, Hiromasa, Saad, Sameh M. I., David, Robert, Winklbauer, Rudolf, & Neumann, A. Wilhelm. (2009). Axisymmetric Drop Shape Analysis for Estimating the Surface Tension of Cell Aggregates by Centrifugation. *Biophysical Journal, 96*(4), 1606-1616. doi: http://dx.doi.org/10.1016/j.bpj.2008.10.064

Kimmel, Charles, Kimmel, William, Ballard, Seth, Kimmel, Bonnie, Ullmann, Thomas, & Schilling. (1995). Stages of embryonic development of the zebrafish. *Developmental dynamics, 203*(3), 253-310.

Krieg, M., Arboleda-Estudillo, Y., Puech, P. H., Kafer, J., Graner, F., Muller, D. J., & Heisenberg, C. P. (2008). Tensile forces govern germ-layer organization in zebrafish. *Nat Cell Biol, 10*(4), 429-436.

Kühl, Michael, & Wedlich, Doris. (1996). *Xenopus* cadherins: Sorting out types and functions in embryogenesis. *Developmental Dynamics, 207*(2), 121-134.

Kullander, Klas, & Klein, Rudiger. (2002). Mechanisms and functions of eph and ephrin signaling. *Nat Rev Mol Cell Biol, 3*(7), 475-486.

Lee, Hyun-Shik, Bong, Yong-Sik, Moore, Kathryn B., Soria, Kathleen, Moody, Sally A., & Daar, Ira O. (2006). Dishevelled mediates ephrinB1 signaling in the eye field through the planar cell polarity pathway. *Nat Cell Biol, 8*(1), 55-63.

Marston, Daniel J., Dickinson, Sarah, & Nobes, Catherine D. (2003). Rac-dependent trans-endocytosis of ephrinBs regulates Eph-ephrin contact repulsion. *Nat Cell Biol, 5*(10), 879-888.

McLaughlin, Todd, Hindges, Robert, Yates, Paul A., & O'Leary, Dennis D. M. (2003). Bifunctional action of ephrin-B1 as a repellent and attractant to control bidirectional branch extension in dorsal-ventral retinotopic mapping. *Development, 130*(11), 2407-2418. doi: 10.1242/dev.00467

McMahon, A., McMahon, W., Supatto, S. E., Fraser, A., & Stathopoulos. (2008). Dynamic Analyses of Drosophila Gastrulation Provide Insights into Collective Cell Migration. *Science, 322*(5907), 1546-1550.

Medina, A., Swain, R., Kuerner, K.-M., & Steinbeisser, H. (2004). Xenopus paraxial protocadherin has signaling functions and is involved in tissue separation. *EMBO J., 23*, 3249–3258.

Mellitzer, Georg, Xu, Qiling, & Wilkinson, David G. (1999). Eph receptors and ephrins restrict cell intermingling and communication. *Nature, 400*(6739), 77-81.

Murai, Keith K., & Pasquale, Elena B. (2003). Eph'ective signaling: forward, reverse and crosstalk. *Journal of Cell Science, 116*(14), 2823-2832.

Nagel, Martina, Tahinci, Emilios, Symes, Karen, & Winklbauer, Rudolf. (2004). Guidance of mesoderm cell migration in the Xenopus gastrula requires PDGF signaling. *Development, 131*(11), 2727-2736. doi: 10.1242/dev.01141

Nakatsuji, N. (1976). Studies on gastrulation of amphibian embryos - ultrastructure of migrating cells of anurancs. *Wilhelm Rouxs Archives of Developmental Biology 180* (3), 229-240.

Pasquale, Elena B. (2005). Eph receptor signaling casts a wide net on cell behaviour. *Nat Rev Mol Cell Biol, 6*(6), 462-475.

Phillips, Herberi M. (1978). Liquid-Tissue Mechanics in Amphibian Gastrulation: Germ-Layer Assembly in Rana Pipiens. *American Zoolology, 18*(1), 81-93. doi: 10.1093/icb/18.1.81

Poliakov, Alexei, Cotrina, Marisa, & Wilkinson, David G. (2004). Diverse Roles of Eph Receptors and Ephrins in the Regulation of Cell Migration and Tissue Assembly. *Developmental Cell, 7*(4), 465-480.

Reintsch, Wolfgang E., Habring-Mueller, Anette, Wang, Renee W., Schohl, Anne, & Fagotto, François. (2005). β-Catenin controls cell sorting at the notochord–somite boundary independently of cadherin-mediated adhesion. *The Journal of Cell Biology, 170*(4), 675-686. doi: 10.1083/jcb.200503009

Sela-Donenfeld, Dalit, & Wilkinson, David G. (2005). Eph Receptors: Two Ways to Sharpen Boundaries. *Current Biology, 15*(6), R210-R212. doi: http://dx.doi.org/10.1016/j.cub.2005.03.013

Solnica-Krezel, Lila, & Sepich, Diane S. (2012). Gastrulation: Making and Shaping Germ Layers. *Annual Review of Cell and Developmental Biology, 28*(1), 687-717. doi: 10.1146/annurev-cellbio-092910-154043

Steinberg, M. S., & Takeichi, M. (1994). Experimental specification of cell sorting, tissue spreading, and specific spatial patterning by quantitative differences in cadherin expression. *Proceedings of the National Academy of Sciences of the United States of America, 91*(1), 206-209.

Steinberg, M.S. (1963). Reconstruction of tissues by dissociated cells. *Science, 141*, 401-408.

Steinberg, MS, & Takeichi, M. (1994). Experimental specification of cell sorting, tissue spreading, and specific spatial patterning by quantitative differences in cadherin expression. *Proc natl Acad Sci USA, 86*, 7043-7047.

Tanaka, Masamitsu, Kamo, Takaharu, Ota, Satoshi, & Sugimura, Haruhiko. (2003). Association of Dishevelled with Eph tyrosine kinase receptor and ephrin mediates cell repulsion. *EMBO J, 22*(4), 847-858.

Tepass, Ulrich, Godt, Dorothea, & Winklbauer, Rudolf. (2002). Cell sorting in animal development: signaling and adhesive mechanisms in the formation of tissue boundaries. *Current Opinion in Genetics & Development, 12*(5), 572-582.

Townes, Philip L., & Holtfreter, Johannes. (1955). Directed movements and selective adhesion of embryonic amphibian cells. *Journal of Experimental Zoology, 128*(1), 53-120.

Wacker, S., Grimm, K., Joos, T., & Winklbauer, R. (2000). Development and control of tissue separation at gastrulation in Xenopus. *Dev. Biol., 224*, 428-439.

Wang, HU, Chen, ZF, & Anderson, DJ. (1998). Molecular distinction and angiogenic interaction between embryonic arteries and veins revealed by ephrin-B2 and its receptor Eph-B4. *Cell, 93*, 741 - 753.

Watanabe, Tadayoshi, Sato, Yuki, Saito, Daisuke, Tadokoro, Ryosuke, & Takahashi, Yoshiko. (2009). EphrinB2 coordinates the formation of a morphological boundary and cell epithelialization during somite segmentation. *Proceedings of the National Academy of Sciences, 106*(18), 7467-7472. doi: 10.1073/pnas.0902859106

Winklbauer, Rudolf. (1998). Conditions for fibronectin fibril formation in the early Xenopus embryo. *Developmental Dynamics, 212*(3), 335-345. doi: 10.1002/(SICI)1097-0177(199807)212:3<335::AID-AJA1>3.0.CO;2-I

Winklbauer, Rudolf, & Keller, Ray E. (1996). Fibronectin, Mesoderm Migration, and Gastrulation in Xenopus. *Developmental Biology, 177*(2), 413-426.

Winklbauer, Rudolf, & Luu, Olivia. (2009). Frizzled-7-dependent Tissue Separation in the Xenopus Gastrula *Wnt Signaling* (pp. 485-492).

Winklbauer, Rudolf, Medina, Araceli, Swain, Rajeeb K., & Steinbeisser, Herbert. (2001). Frizzled-7 signaling controls tissue separation during Xenopus gastrulation. *Nature, 413*(6858), 856-860.

Xu, Q., Alldus, G., Holder, N., & Wilkinson, D.G. (1995). Expression of truncated Sek-1 receptor tyrosine kinase disrupts the segmental restriction of gene expression in the Xenopus and zebrafish hindbrain. *Development, 121*(12), 4005-4016.

Xu, Qiling, Mellitzer, Georg, Robinson, Vicky, & Wilkinson, David G. (1999). In vivo cell sorting in complementary segmental domains mediated by Eph receptors and ephrins. *Nature, 399*(6733), 267-271.

Zimmer, Manuel, Palmer, Amparo, Kohler, Jenny, & Klein, Rudiger. (2003). EphB-ephrinB bi-directional endocytosis terminates adhesion allowing contact mediated repulsion. *Nat Cell Biol, 5*(10), 869-878.

Figure legends

Figure 2.1:

Cell repulsion at ectoderm-mesoderm boundary

A) Tissue separation assay. Test explants are placed on blastocoel roofs (BCR), and the percent remaining separate are scored after 45-60 min. Cell behavior at the boundary between tissues is examined by live confocal microscopy using explants expressing membrane-targeted Cherry into BCRs with GFP-labeled membranes. B-F) Live confocal microscopy. Test explants expressing mYFP (B-D) or mCherry (E, F) were combined with mGFP-expressing BCRs. Time between frames was 1 min for B-D, 5 min for E,F, frame # indicated. B) Overview, mesoderm explant on BCR (Suppl. movie 1). Arrows show retractions. C) Area indicated (arrow, asterisk) in B. Simultaneous retraction of mesoderm and BCR; a gap appears (#14), spreads to upper right (#26), then to opposite side (#34). Protrusions extend into gap (#26, short arrow). Insert #34a, double arrowheads: retraction fibers. Stealth arrowheads: stable contacts within the tissues. D) Ectoderm aggregate on BCR (Suppl. movie 2), showing stable contacts within the tissues (stealth arrowheads) and at the interface between the two ectoderm explants (arrows). E) Attachment/detachment of 3 mesoderm cells at BCR. Contact is first established by upper cell (long arrow #9), then spreads through all cells (between long arrows #10). Cells detach again from sides of frame (arrowheads #16), central cell (*) (long arrow #16) seems to resist and is last to detach (#18). Arrow, insert in frame #9: cell protrusions. F) Mesoderm on BCR. Initially in close contact (frame #1), cells from both tissues retract (frame #2) leaving retraction fibers behind (arrowheads #2a). 4 focal planes merged to capture entire fibers. G) Quantification of attachment/detachment events. Numbers on top indicate total #events/#cells.

Figure 2.1

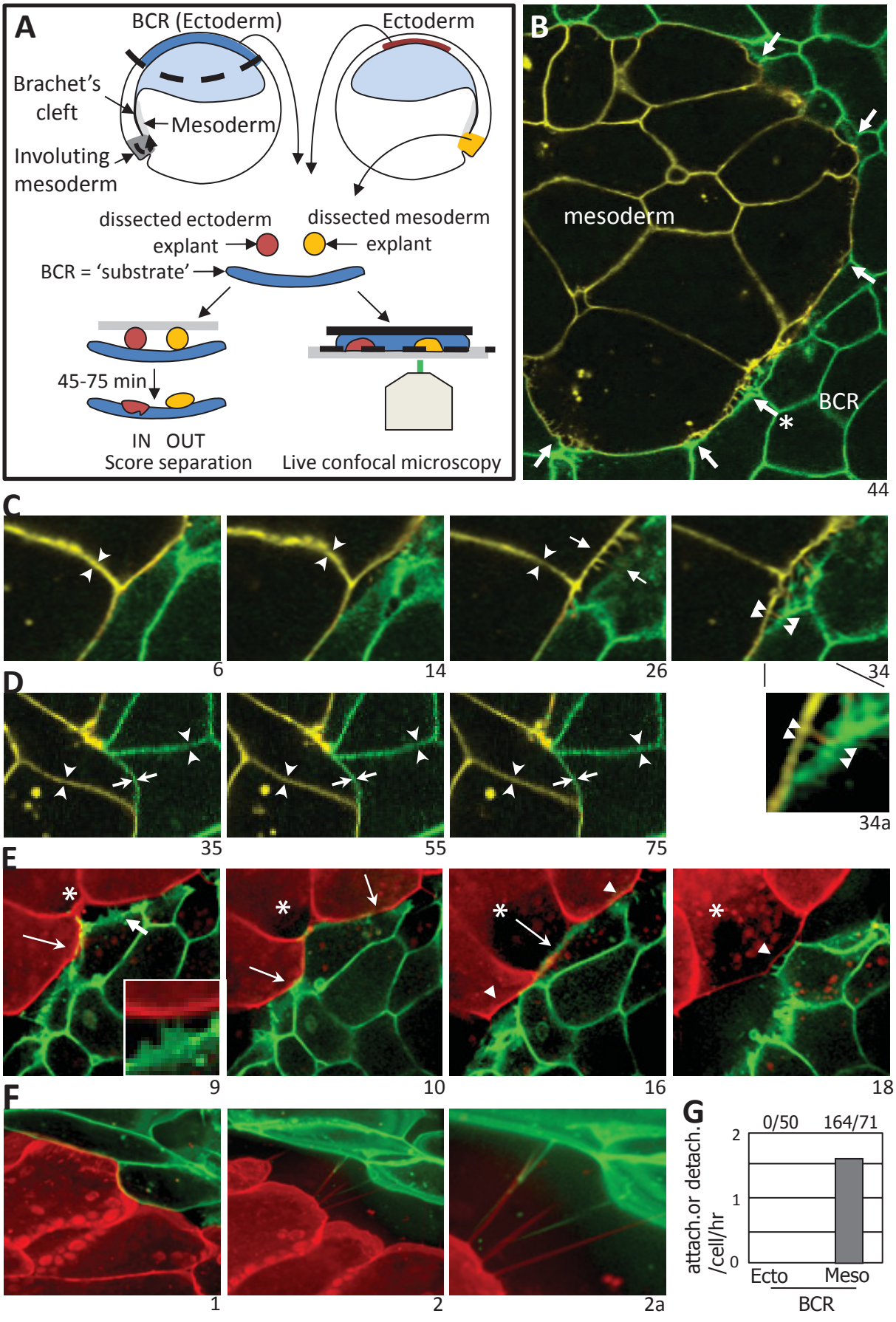
A
BCR (Ectoderm)
Ectoderm
Brachet's cleft
Mesoderm
Involuting mesoderm
dissected ectoderm explant
dissected mesoderm explant
BCR = 'substrate'
45-75 min
IN OUT
Score separation
Live confocal microscopy
B
mesoderm
BCR
44
C
6
14
26
34
D
35
55
75
34a
E
9
10
16
18
F
1
2
2a
G
0/50
164/71
attach.or detach. /cell/hr
Ecto
Meso
BCR

Figure 2.2:

EphrinB/EphB signaling controls tissue separation

A) Soluble ephrin B fragments induce tissue separation between ectodermal cells. Separation assay was performed after a short pre-treatment of the ectodermal aggregates (ecto) or of the BCR substrate with soluble, pre-clustered ephrin A/B-Fc fragments (eA*/eB*). Unless stated otherwise, pre-treatment was for 15 min. Untreated mesoderm aggregates (meso) on untreated BCR were used as positive controls for maximal separation behaviour. Untreated ectoderm explants rapidly sunk into untreated BCR. Strong separation was induced when either ectodermal aggregates or BCR were treated with eB*. Separation was particularly strong when both the test aggregates and the BCR were treated by performing the assay in eB* solution. eA* had no effect. B,C) EphrinB/EphB signaling is required for tissue separation. B) Separation assay: EphrinB depletion inhibits separation. Mesoderm test explants injected with control MO (COMO) remained out of BCR (arrowheads), those injected with ephrinB2 MO (eB2 MO), 2 out of 4 invaded the BCR in the example shown (arrows). C) Quantification of loss-of-function (LOF) experiments for ephrinBs and EphBs. Injections in mesoderm (Meso) or ectodermal BCR are indicated below bars for each tissue combination; wt, uninjected, ephrinB1,2 MO (eB1,2MO), EphB4 MO (EphMO), cytoplasmically deleted EphB (ΔCEph). Numbers of test explants remaining separated/total number of explants on top of bars. ** indicates $p<0.01$ compared to controls. Simultaneous depletion/inhibition in the mesoderm and the BCR (eB2MO/ΔCEph) did not increase the phenotype compared to eB2MO or ΔCEph alone ($p=0.2$ and 0.3).

Figure 2.2

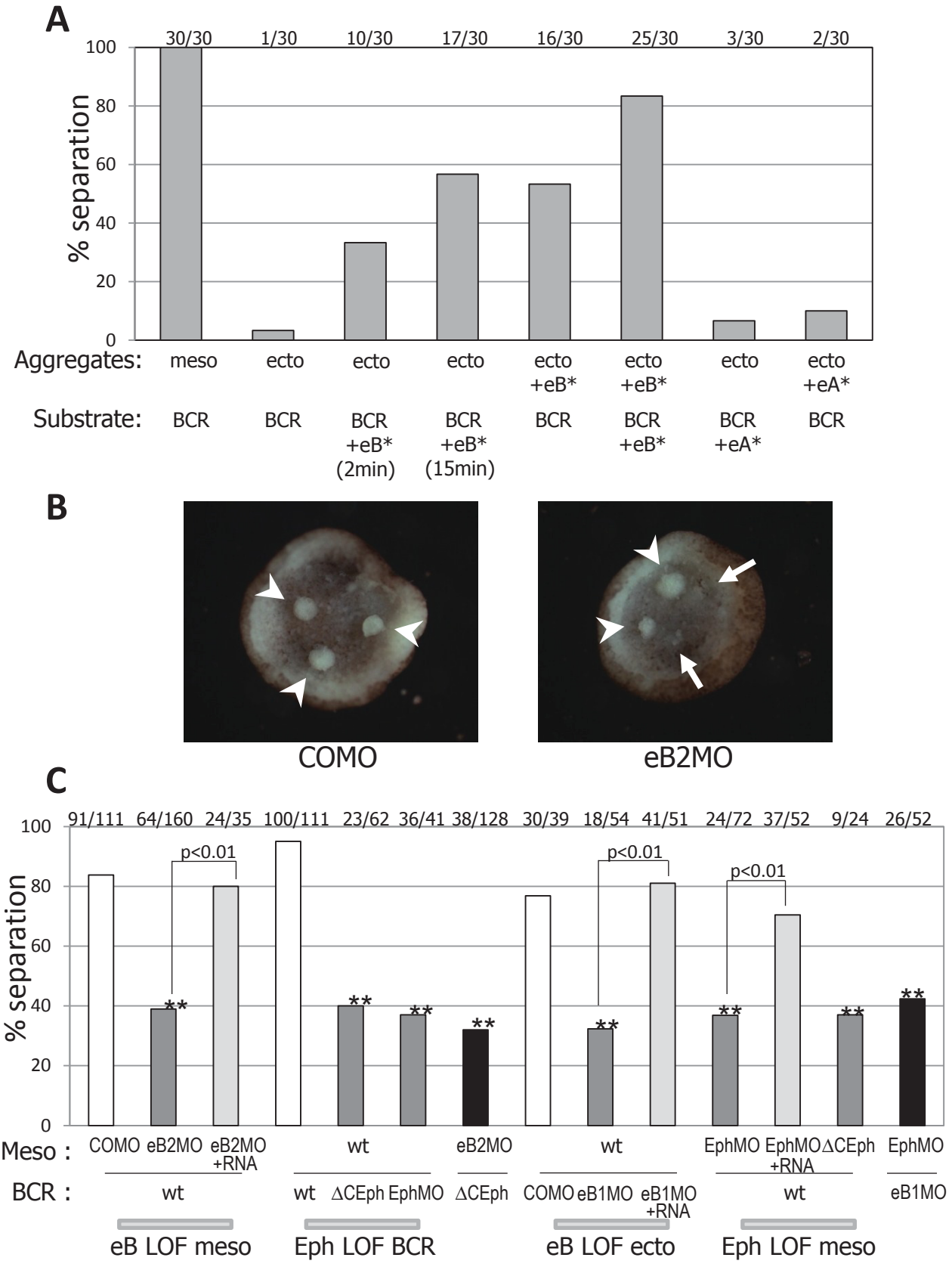
A
30/30
1/30
10/30
17/30
16/30
25/30
3/30
2/30
% separation
Aggregates:
meso
ecto
ecto
ecto
ecto +eB*
ecto +eB*
ecto
ecto +eA*
Substrate:
BCR
BCR
BCR +eB* (2min)
BCR +eB* (15min)
BCR
BCR +eB*
BCR +eA*
BCR
B
COMO
eB2MO
C
91/111
64/160
24/35
100/111
23/62
36/41
38/128
30/39
18/54
41/51
24/72
37/52
9/24
26/52
p<0.01
p<0.01
p<0.01
% separation
Meso :
COMO
eB2MO
eB2MO +RNA
wt
eB2MO
wt
EphMO
EphMO +RNA
ΔCEph
EphMO
BCR :
wt
wt
ΔCEph
EphMO
ΔCEph
COMO
eB1MO
eB1MO +RNA
wt
eB1MO
eB LOF meso
Eph LOF BCR
eB LOF ecto
Eph LOF meso

Figure 2.3:

Forward signaling across the boundary is required in both apposed tissues

A) Enhanced inhibition of separation by interference with EphB signaling in both tissues. ΔC-EphB was expressed in the mesoderm, in the BCR, or in both. Symbols as in Fig.2.2.

B-C) Rescue of separation by soluble ephrinB2-Fc fragment after ephrinB depletion. B) Diagram of the experiment. Ephrins in one tissue and their cognate Eph receptors in the other tissue are represented as green and red plasma membranes, respectively. Ephrins were depleted in one of the tissues (eB1+eB2 in the BCR and eB2 in the mesoderm, depletion symbolized by black membranes), and the signal was then restored at the surface of the other tissue by a 15min treatment with ephrin-Fc fragment (eB2*, green dots) before assembly of the assay. Fc, control Fc fragments. Otherwise, symbols as in B).

Figure 2.3

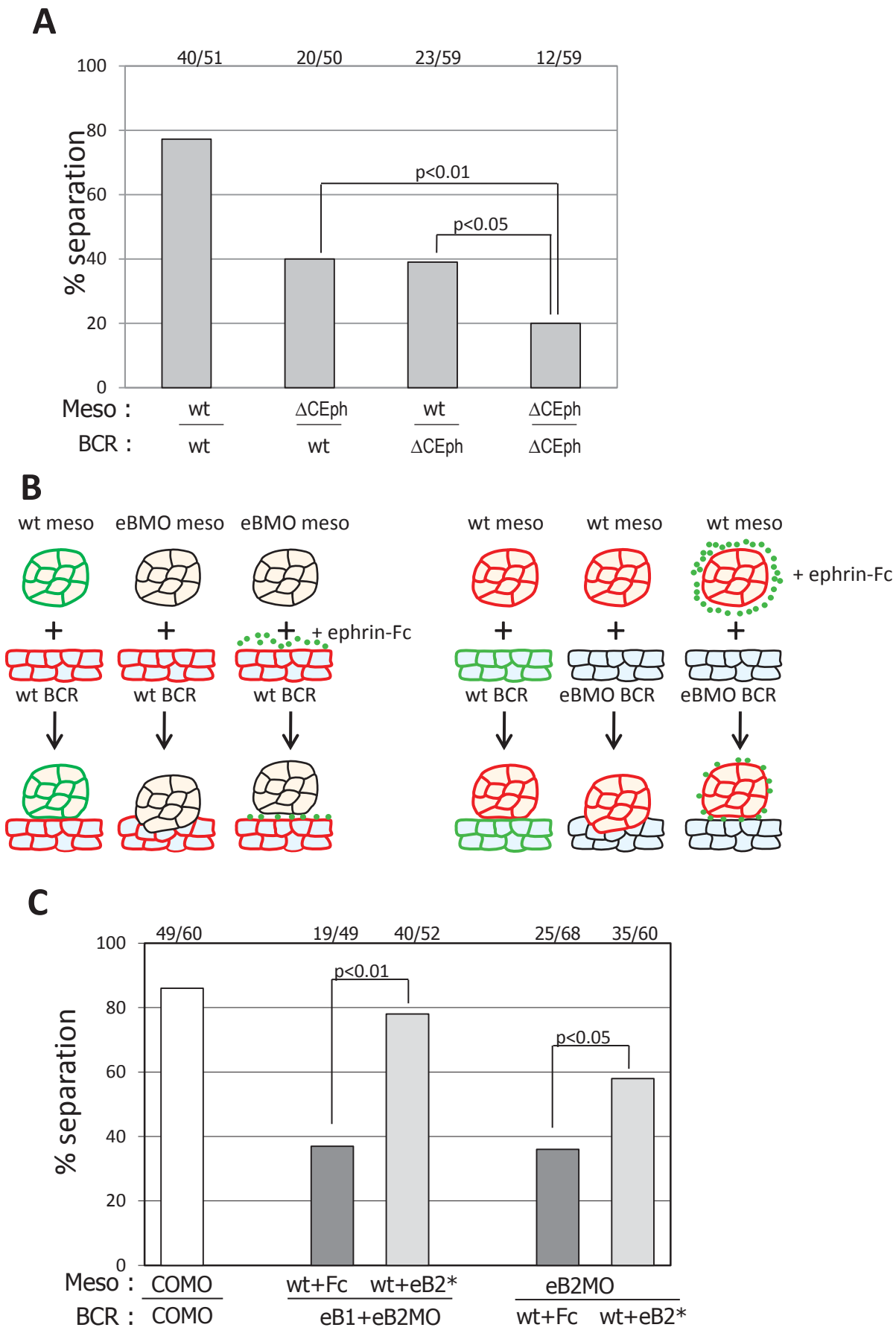
A
40/51
20/50
23/59
12/59
100
80
60
40
20
0
% separation
p<0.01
p<0.05
Meso :
BCR :
wt
ΔCEph
wt
ΔCEph
wt
wt
ΔCEph
ΔCEph
B
wt meso
eBMO meso
eBMO meso
+ ephrin-Fc
wt meso
wt meso
wt meso
+ ephrin-Fc
wt BCR
wt BCR
wt BCR
wt BCR
eBMO BCR
eBMO BCR
C
49/60
19/49
40/52
25/68
35/60
100
80
60
40
20
0
% separation
p<0.01
p<0.05
Meso :
BCR :
COMO
COMO
wt+Fc
wt+eB2*
eB1+eB2MO
eB2MO
wt+Fc
wt+eB2*

Figure 2.4:

Ephrin/Eph loss-of-function inhibits repulsion at the boundary

A-E) Effect of ephrin/Eph MO on repulsion. Time lapse spinning disc confocal microscopy using mesoderm explants expressing mCherry on mGFP-expressing BCRs. EphrinB2 MO or EphB4 MO in mesoderm (B,C), or ephrinB1 MO in BCR (D) inhibited repulsion compared to control MO, A). The interface between inhibited mesoderm explants and BCR resembled ectoderm-ectoderm contacts (E). F) Incubation of mesoderm test explants with ephrinB1-Fc fragments rescues repulsion from ephrinB1-depleted BCR in a dose dependent manner. G) Quantification of attachment/detachment events per cell per hour. Numbers on top indicate total #events/#cells.

Figure 2.4

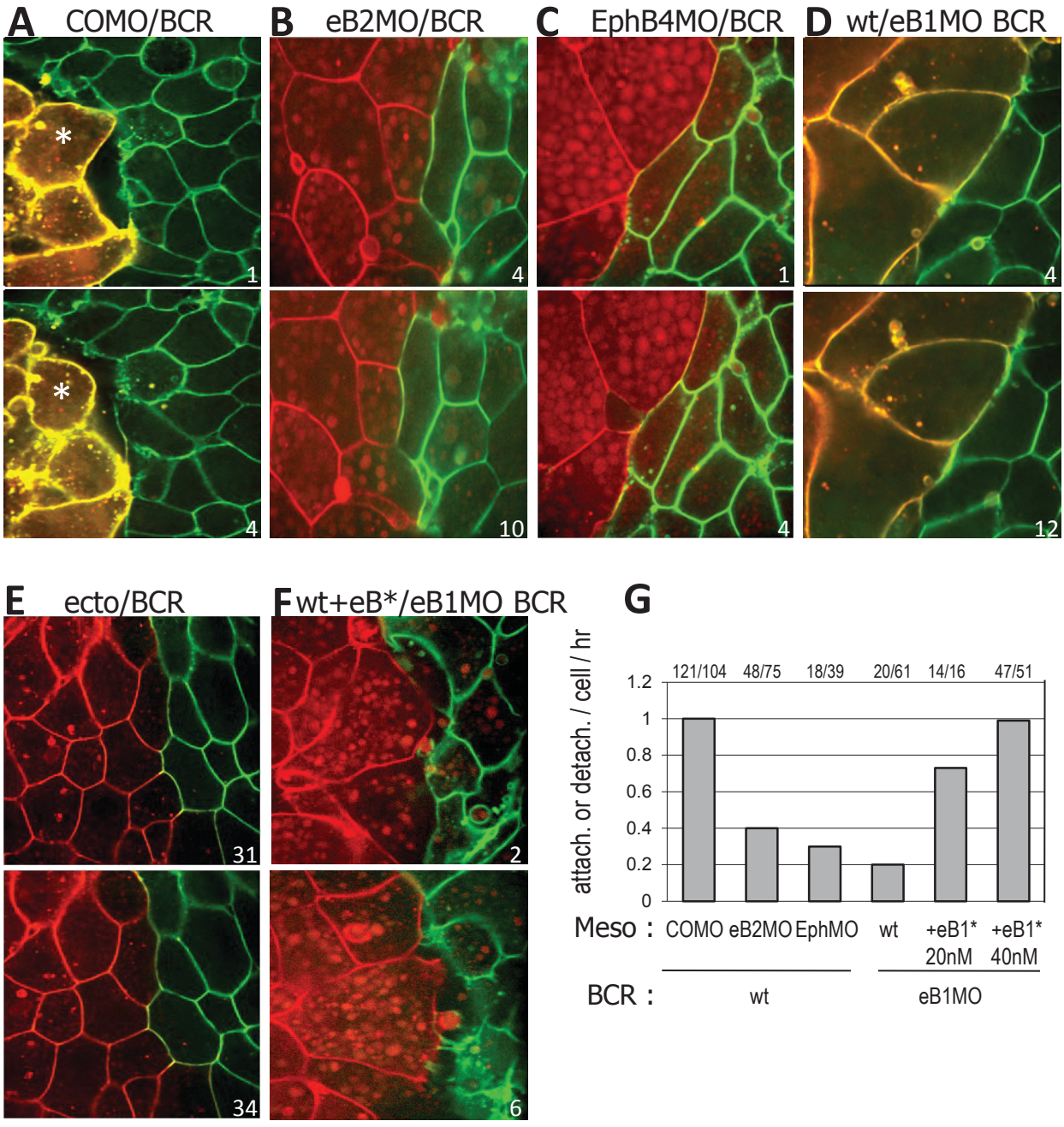
A COMO/BCR
B eB2MO/BCR
C EphB4MO/BCR
D wt/eB1MO BCR
E ecto/BCR
F wt+eB*/eB1MO BCR
G
attach. or detach. / cell / hr
121/104
48/75
18/39
20/61
14/16
47/51
1.2
1
0.8
0.6
0.4
0.2
0
Meso :
COMO
eB2MO
EphMO
wt
+eB1* 20nM
+eB1* 40nM
BCR :
wt
eB1MO

Figure 2.5:

Involvement of RhoA and Rac downstream of ephrin/Eph signaling

A-C) Rac and RhoA activities are required for tissue separation. A, B) Expression of dominant negative forms N17Rac and N19RhoA either in the mesoderm test aggregates or in the BCR blocked separation. C) Separation was strongly inhibited when assays with wt mesoderm and wt BCR were performed in the presence of the Rac inhibitor NSC23766 (18μM) or the Rok inhibitor Y26732 (50μM).

D-E) Rac or RhoA activation can rescue loss of ephrin signaling. Signaling was inhibited by injecting EphB4 MO (D) in the mesoderm or expressing ΔCEphB in the BCR (E). In both cases, separation was rescued by co-expression of constitutively active V12Rac or V14RhoA. Constitutively active cdc42 (V14cdc42) had no effect (D).

Figure 2.5

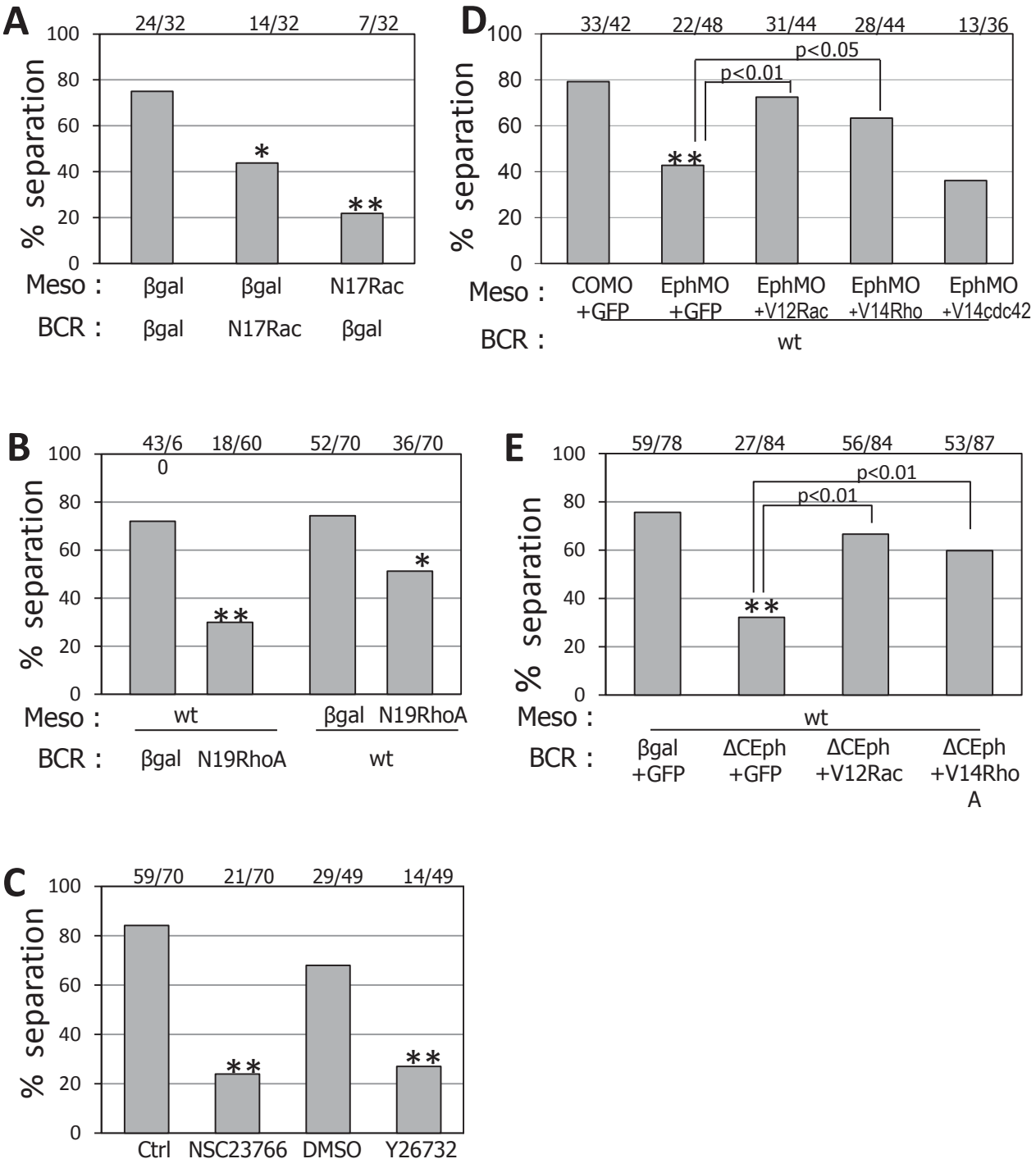
A
24/32
14/32
7/32
% separation
Meso :
βgal
βgal
N17Rac
BCR :
βgal
N17Rac
βgal
D
33/42
22/48
31/44
28/44
13/36
p<0.05
p<0.01
Meso :
COMO +GFP
EphMO +GFP
EphMO +V12Rac
EphMO +V14Rho
EphMO +V14cdc42
BCR :
wt
B
43/6
0
18/60
52/70
36/70
Meso :
wt
βgal
N19RhoA
BCR :
βgal
N19RhoA
wt
E
59/78
27/84
56/84
53/87
p<0.01
p<0.01
Meso :
wt
BCR :
βgal +GFP
ΔCEph +GFP
ΔCEph +V12Rac
ΔCEph +V14RhoA
C
59/70
21/70
29/49
14/49
Ctrl
NSC23766
DMSO
Y26732

Figure 2.6:

Effect of Rho/Rac activation/inhibition on cell behavior at the boundary
Live confocal microscopy of mesoderm explants expressing mCherry combined with mGFP-expressing BCRs. A-F) Selected frames from time lapse movies (Suppl. movies 7 and 8). G, H) Quantification of attachment/detachment events per cell per hour. Numbers on top indicate total #events/#cells. A-D) Inhibition of repulsion by ΔCEph in the BCR (A) is recued upon co-expression of constitutively active forms of RhoA (V14Rho) (B) and Rac (V12Rac) (C). D) Control wild type mesoderm and BCR. Arrowheads in C and D point at mesoderm cells that were initially in contact with BCR cells and detached during in subsequent frames. The arrow in frame 12 of panel C points to a protrusion emanating from the BCR cell after detachment. In the example shown in B) cells remain detached for a prolonged period (compare the two parallel but separated membranes in the enlarged field B1a and B7a with the merged signals from the closely apposed membranes for ΔCEph alone, A3a and A12a). Asterisks indicate the relative positions of two mesoderm and ectoderm cells sliding along the boundary, and the antiparallel arrows shows the relative translation of these cells. This phenotype is observed in both V14RhoA and V12Rac rescues. E-F) Inhibition of repulsion by dominant negative forms of RhoA and Rac. N19RhoA and N17Rac caused ectoderm and mesoderm cells to remain stably attached. Note disruption of the boundary through intercalation of cells from both tissues (F, arrows).

Figure 2.6

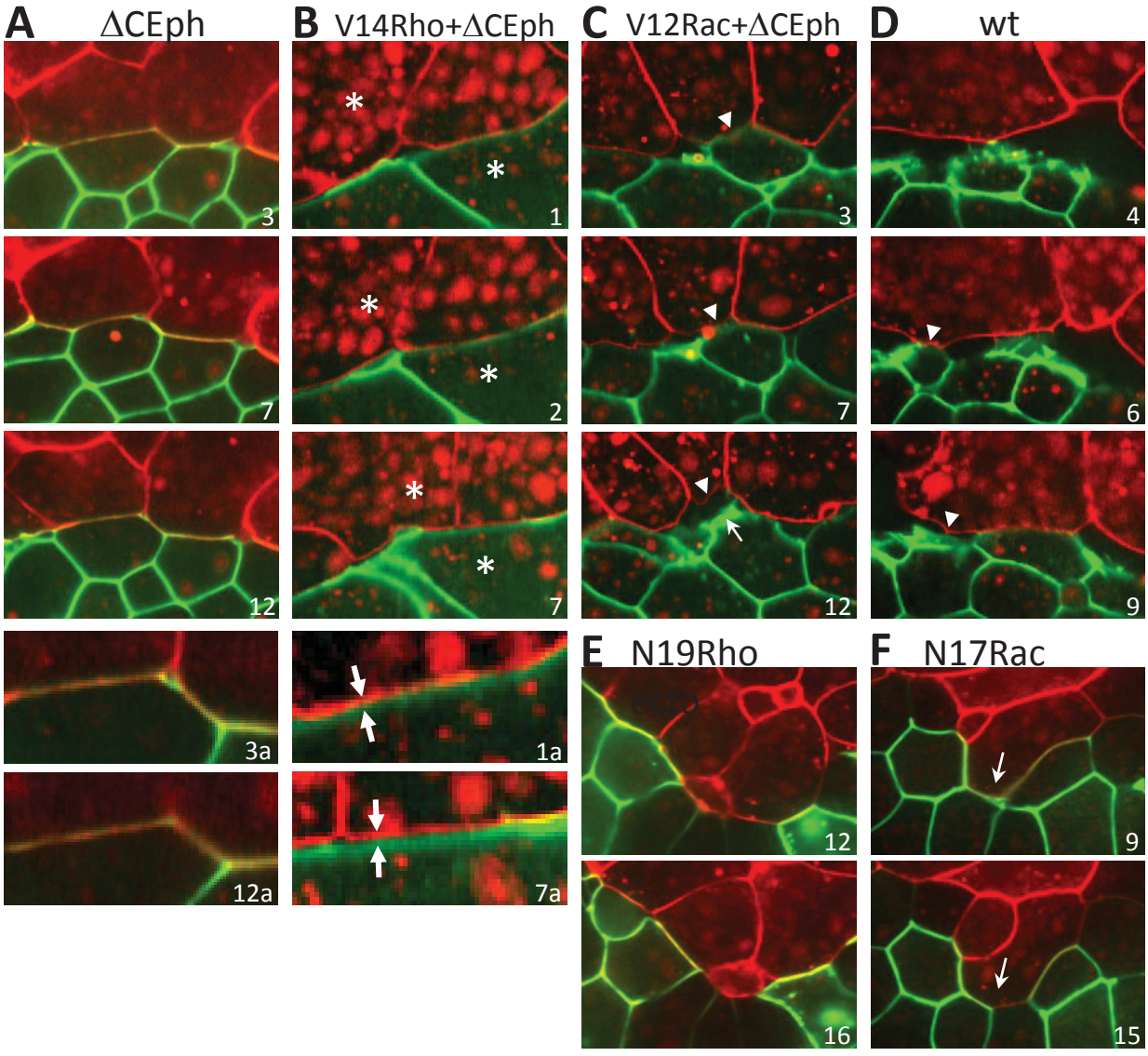
A ΔCEph
B V14Rho+ΔCEph
C V12Rac+ΔCEph
D wt
E N19Rho
F N17Rac
3
1
3
4
7
2
7
6
12
7
12
9
3a
1a
12
9
12a
7a
16
15

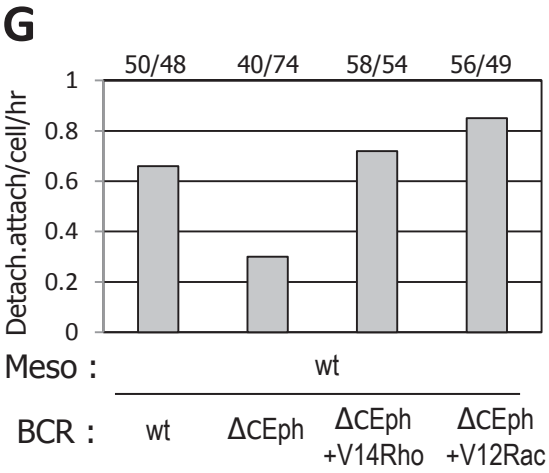
G
50/48
40/74
58/54
56/49
Detach.attach/cell/hr
1
0.8
0.6
0.4
0.2
0
Meso :
wt
BCR :
wt
ΔCEph
ΔCEph +V14Rho
ΔCEph +V12Rac

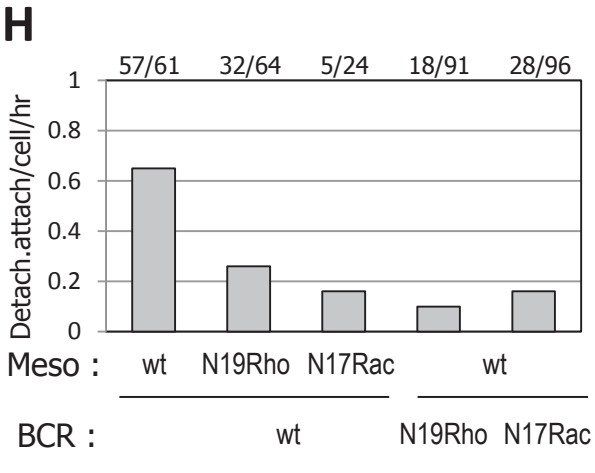
H
57/61
32/64
5/24
18/91
28/96
Detach.attach/cell/hr
1
0.8
0.6
0.4
0.2
0
Meso :
wt
N19Rho
N17Rac
wt
BCR :
wt
N19Rho
N17Rac

Figure 2.7:

Subcellular localization of activated GTPases at the boundary.
Explants expressing GFP-Rhothekin-GBD (A), GFP-Wasp-GBD (B), or control GFP (C) were combined with mCherry expressing BCRs and analyzed by live confocal microscopy. D) Quantification: % cells showing accumulation at contact sites with the BCR. Both GDBs accumulated preferentially at sites of contact with the BCR in wt mesoderm (large arrows), but not in wt ectoderm (arrowheads). Control GFP in wt mesoderm did not accumulate at the boundary. EphB4 depletion (EphMO) in the mesoderm or ephrinB1 depletion (eB1 MO) in the BCR both strongly decreased accumulation at most contact sites (arrowheads), similar to expression of dominant negative forms of RhoA (N19Rho) for GFP-Rhothekin-GBD or Rac (N17Rac) for GFP-Wasp-GBD. Small arrows: residual accumulation.

Figure 2.7

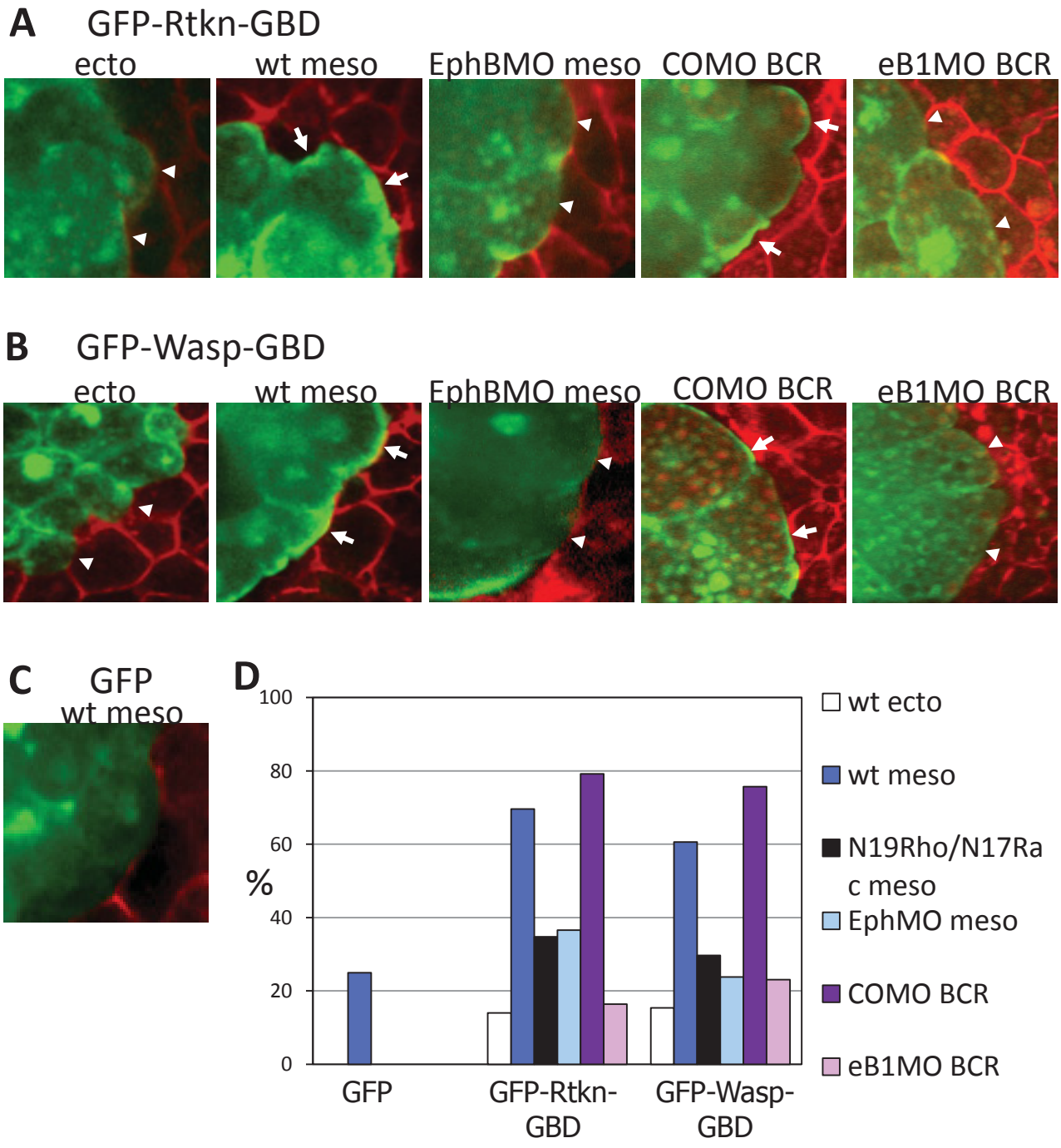
A
GFP-Rtkn-GBD
ecto
wt meso
EphBMO meso
COMO BCR
eB1MO BCR
B
GFP-Wasp-GBD
ecto
wt meso
EphBMO meso
COMO BCR
eB1MO BCR
C
GFP
wt meso
D
100
80
60
40
20
0
%
GFP
GFP-Rtkn-GBD
GFP-Wasp-GBD
wt ecto
wt meso
N19Rho/N17Rac meso
EphMO meso
COMO BCR
eB1MO BCR

Figure 2.8:

Dynamic activation of RhoGTPases at the ectoderm-mesoderm boundary. Explants expressing GFP-Rhothekin-GBD (A) and GFP-Wasp-GBD (B) were combined to mCherry expressing BCRs. Selected frames from time lapse movies (Suppl. Movies 9,10). Time between frames was 2 min for A and 1 min for B. A',B': pseudocolors for the GFP signal. A, A': The mesoderm cell labeled with a star establishes contact with a BCR cell in frames 14 and 15 (arrow), then retracts in frame16. GFP-Rhothekin-GBD concentrates near the site of contact in frames 14and 15, and the signal decreases after detachment (frame16). A second cell in the lower part of the field accumulates progressively high levels of GFP-Rhothekin-GBD but fails to retract during this sequence. B,B': Two cells are initially in close contact with the BCR. While the upper cell maintains the contact throughout this sequence (frame13, thin arrow), the lower cell (thick arrow) detaches progressively starting from the lower edge (arrowheads). The intense GFP-Wasp-GBD signal at the sites of contact (frame 8) dissipates in both cells (frames 9-13), while the signal in the cytoplasm and near the membrane separating both cells (small arrows) remains relatively constant (small arrow frames 8 and 13).

Figure 2.8

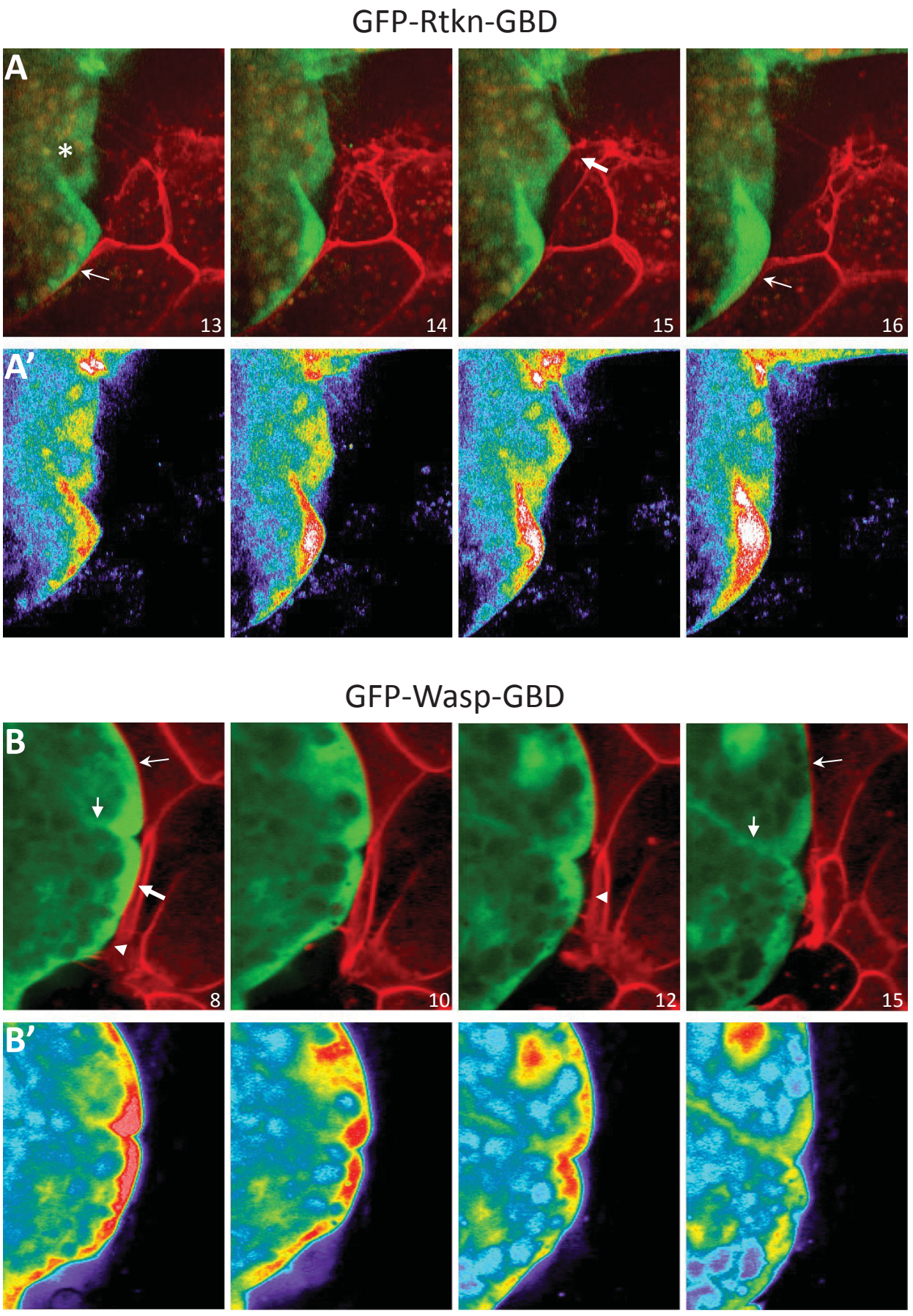

Figure 2.9:

Model for tissue separation

Cells at boundary alternate between attachment and detachment: contact at boundary triggers signaling through membrane-bound ephrinB and EphB receptors, which induces repulsion. Once cells are apart, the signal decays, cells emit protrusions and re-establish contacts. This prevents mesoderm cells from invading the BCR, but allows them to use the BCR as substrate for migration.

Figure 2.9

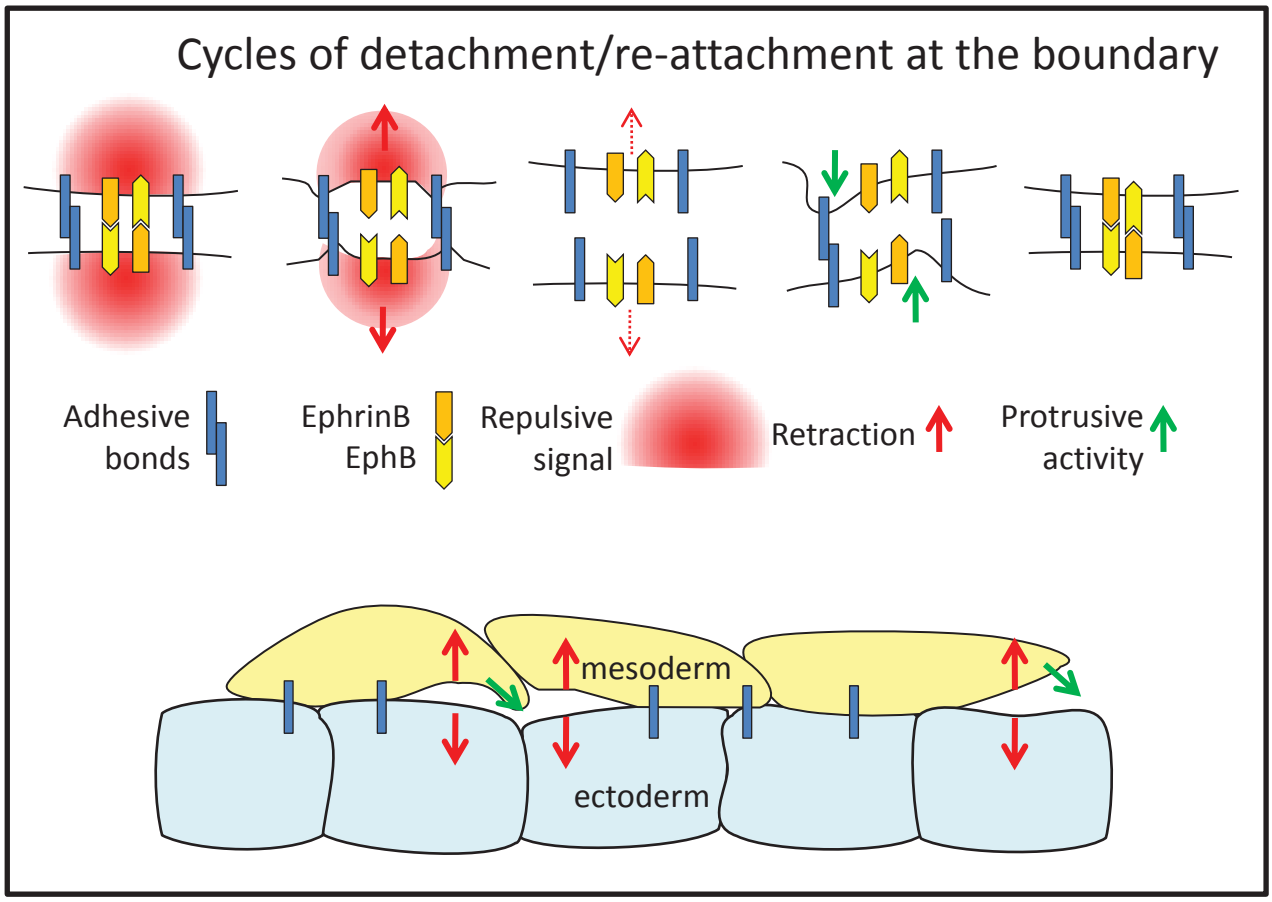
Cycles of detachment/re-attachment at the boundary
Adhesive bonds
EphrinB
EphB
Repulsive signal
Retraction
Protrusive activity
mesoderm
ectoderm

Supplementary Figure legends

Figure 2.S1:

EphrinBs and EphBs expression pattern in the three germ layers at early gastrula stage.

RT-PCR was performed using mRNA extracted from ectoderm, dorsal mesoderm and endoderm tissues dissected at stage 10.5. Loading was equalized by comparing levels of FGFR in the three tissues (not shown). Two independent experiments showed identical patterns of expression.

Figure 2.S2:

Whole embryo phenotypes for ephrinB2 and EphB4 depletion:

EphrinB2 (eB2) and EphB4 MOs were injected in the two blastomeres of the 2-cell stage embryo. Embryos were fixed at the early gastrula stage and bisected sagitally (A-C), or allowed to develop until early tadpole stages (D-F). (A-C) Arrows point to both ends of Brachet's cleft.

Figure 2.S3:

Multiple interference with ephrinB1, B2 and EphB

A) Single and double EphrinB1 and B2 knockdowns in the mesoderm by injection of various amounts of eB1 and eB2 MOs. Single MOs caused significant separation, demonstrating that both ephrins are required. Inhibition was dose dependent. The phenotype was not increased by double injections of eB1 and eB2 MOs, even with the highest MO amounts, indicating that ephrins from the mesoderm contribute only partly to tissue separation. B) Simultaneous injection of EphB4 MO with eB2 MO or eB1+eB2 MO causes stronger inhibition of separation compared to single EphB4 or eB2 or eB1+eb2 MO injections. C) EphB interference by expression of dominant negative ΔC-EphB. EphB activity is required in both ectoderm and mesoderm. Inhibition by ΔC-EphB was dose dependent but reaches a maximum at 400pg. A significantly stronger phenotype

was obtained by simultaneous interference in both tissues, both with levels yielding maximal (400pg) or submaximal inhibition (150pg).

Figure 2.S4:

Ephrin-Eph gain and loss of function and interaction with other pathways. A) Interference with ephrin B3 in the BCR. Injection of eB3 MO (40ng) in the BCR caused inhibition of separation (p=7.40E-07). The degree of inhibition upon triple injection of eB1, eB2 and eB3 MO was similar to eB1 MO alone (Fig. 2C). Separation was rescued by co-injection of eB3 mRNA.

B) EphrinB2 overexpression is sufficient to induce separation behaviour in the ectoderm.

Embryos were injected with ephrinB1 or ephrinB2 mRNA (500pg/injection). EphrinB2 induced separation (p=0.01) while ephrinB1 had no effect (p=0.24).

C) Effect of PDGF and Fz/PAPC signaling. Treatment of mesoderm explants with PDGF receptor kinase inhibitor AG1296 (10μM) does not inhibit separation. Expression of Fz7 and PAPC does not rescue separation when co-injected with eB1 and EphB4 MOs.

Figure 2.S5:

The effect of ephrin-Ephs on tissue cohesion: Dissociated cells from ectoderm and mesoderm tissues were left to re-aggregate for one hour (see Materials and Methods). A-D) Representative examples of re-aggregated wild type ectoderm (A), wild type mesoderm (B), ephrinB1-depleted ectoderm (C) and ephrinB2 overexpressing ectoderm (D). E) The degree of re-aggregation was determined using two criteria: the average particle size, reflecting the extent of aggregation, and the total area/perimeter ratio, which integrates both the size of the aggregates and their degree of compaction (single cells and small aggregates have a large area/perimeter ratio, and large round aggregates have a minimal perimeter, thus a higher area/perimeter ratio). Results of individual experiments were normalized using wild type ectoderm as reference (=1.0) to account for embryo batch to batch variation. Both parameters gave similar results, and the same trend for each of the condition was observed at earlier time points (data not shown): mesoderm re-aggregated less than ectoderm. EphrinB1 and EphB4 depletions decreased

ectoderm re-aggregation. EphrinB2 overexpression lead to a similar, although more variable inhibition. EphrinB2 and EphB4 depletions had no effect on mesoderm (p value for Area = 0.5 and 0.8. p value for A/P = 0.6/0.8).

Figure 2.S6:

Combined RhoA/Rac interference and rescue with wild type RhoA and Rac.
A) Dominant negative N19RhoA and N17Rac (100pg mRNA) were expressed alone or in combination in the BCR. Double inhibition of RhoA and Rac did not significantly enhance inhibition of separation. Data are from 6 independent experiments. B) ΔCEph was expressed alone or with wild type RhoA and Rac. Inhibition of separation by ΔCEph is very partially rescued by wild type RhoA and Rac. Rescue was not enhanced by simultaneous expression of both RhoA and Rac. Data were pooled from 3 experiments with doses of 100pg and 3 experiments with doses of 200 pg RhoA or Rac mRNA. The strength of rescue was similar at both doses.

Figure 2.S7:

Ephrin-signaling-dependent F-actin accumulation at the mesoderm/BCR boundary
Wild type mesoderm explants were combined to BCRs manipulated by injection of ΔCEph, N17Rac, N19RhoA mRNAs or eB1 MO. Sample were fixed and stained with Alexa488-phalloidin and analyzed by confocal microscopy. Stacks of 5 focal planes (2μm) were merged, and relative intensity levels were compared using pseudocolors. A) Example of boundary between mesoderm and control BCR. F-actin is concentrated in a cortical network all around the cells. BCR cells had a stronger signal than mesoderm cells. The boundary (arrows) showed irregular staining with accumulations (thick arrows) reaching the high levels typically found at some of the "tri-cellular junctions" of the BCR (arrowheads).
B) Mesoderm cells mixed with ΔCEph-expressing cells (arrows). F-actin at the mesoderm/BCR interface was weaker than in controls.
C) Quantitation of F-actin accumulation at the boundary. Using pseudocolors, BCR cells were scored for stronger signal at the boundary compared to intra-

tissue contacts. A significant decrease was observed for ΔCEph, eB1 MO and dominant negative Rac (*: $p<0.05$; **: $p<0.01$).

Figure 2.S1

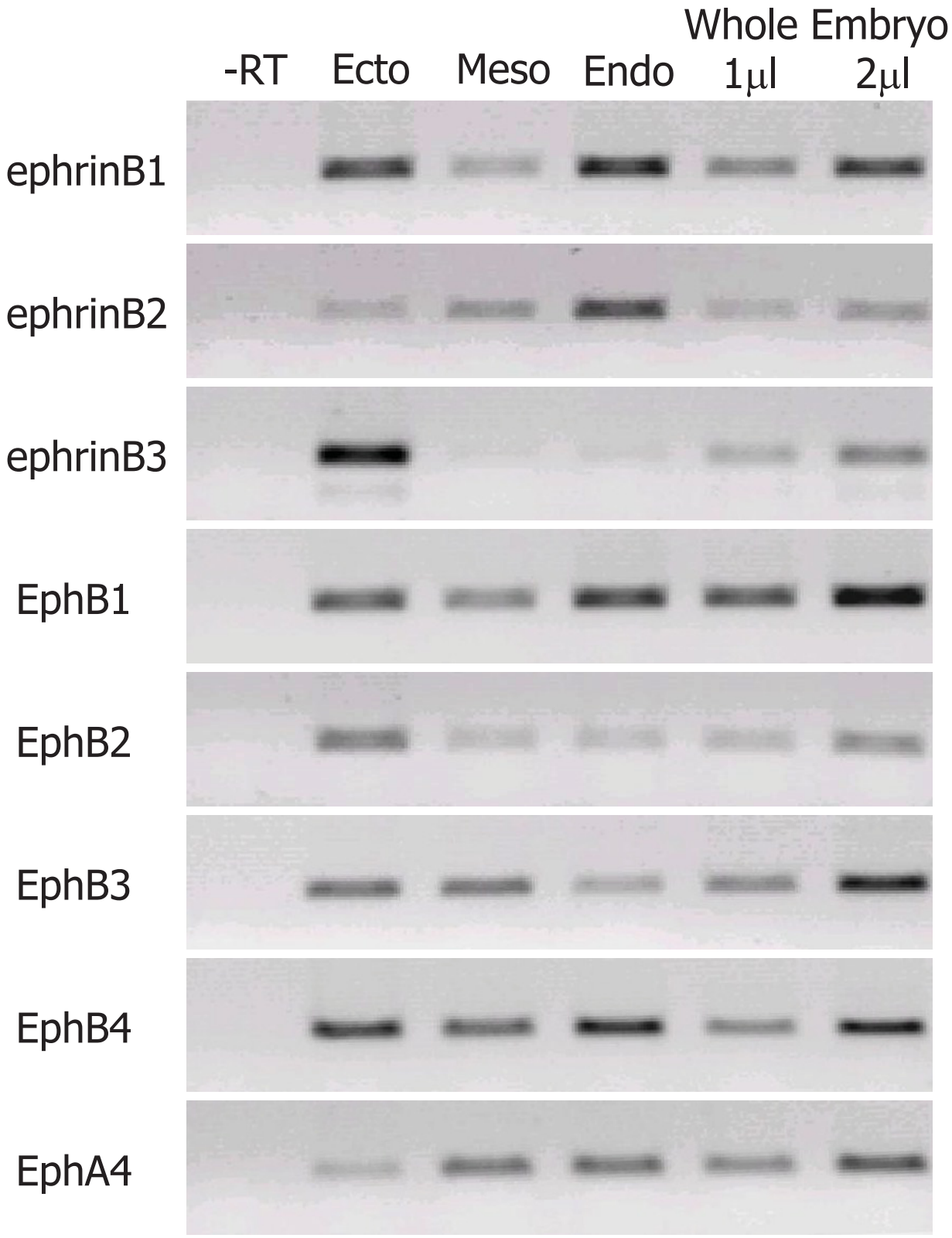
Whole Embryo
-RT
Ecto
Meso
Endo
1μl
2μl
ephrinB1
ephrinB2
ephrinB3
EphB1
EphB2
EphB3
EphB4
EphA4

Figure 2.S2

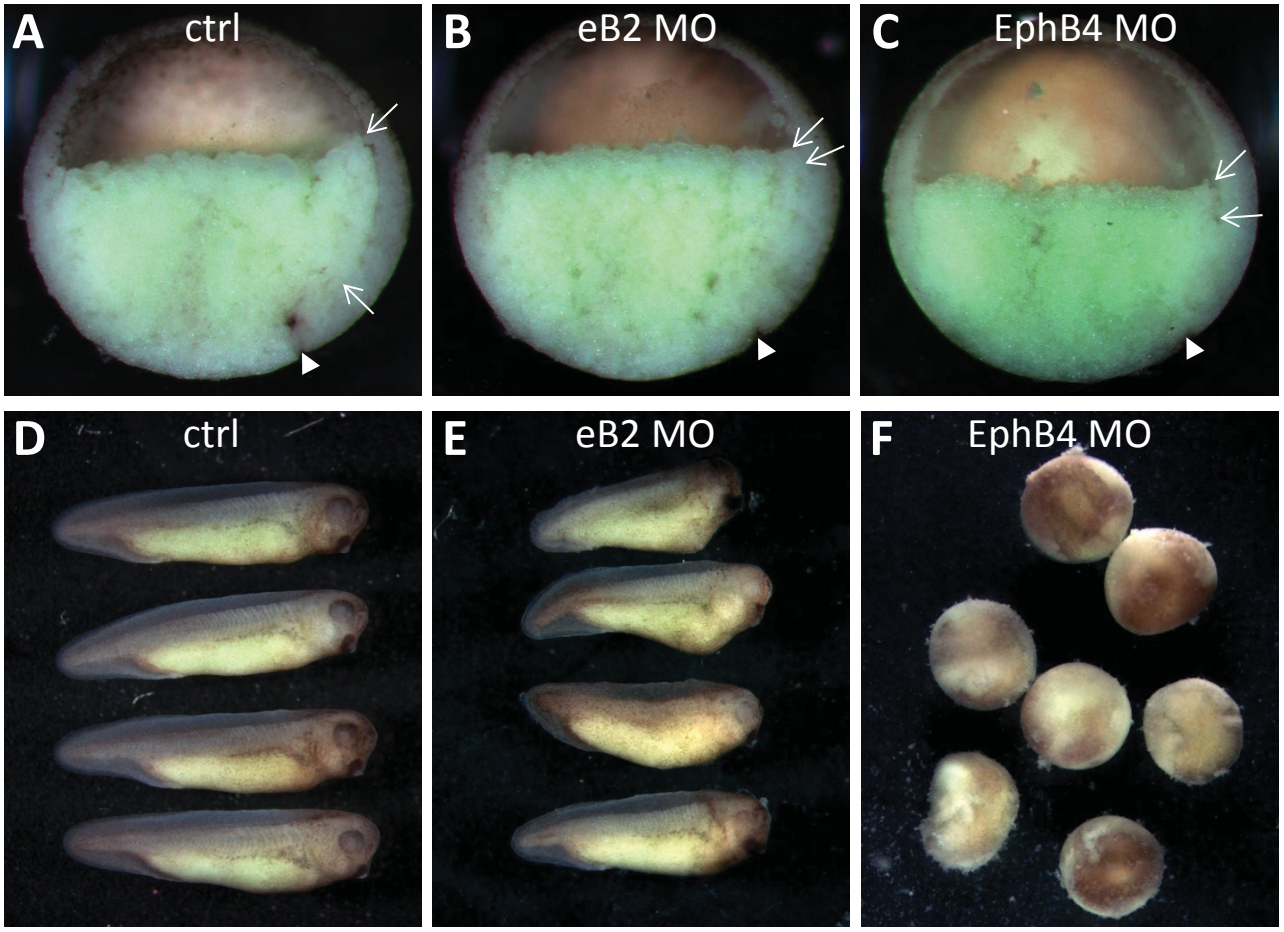

Figure 2.S3

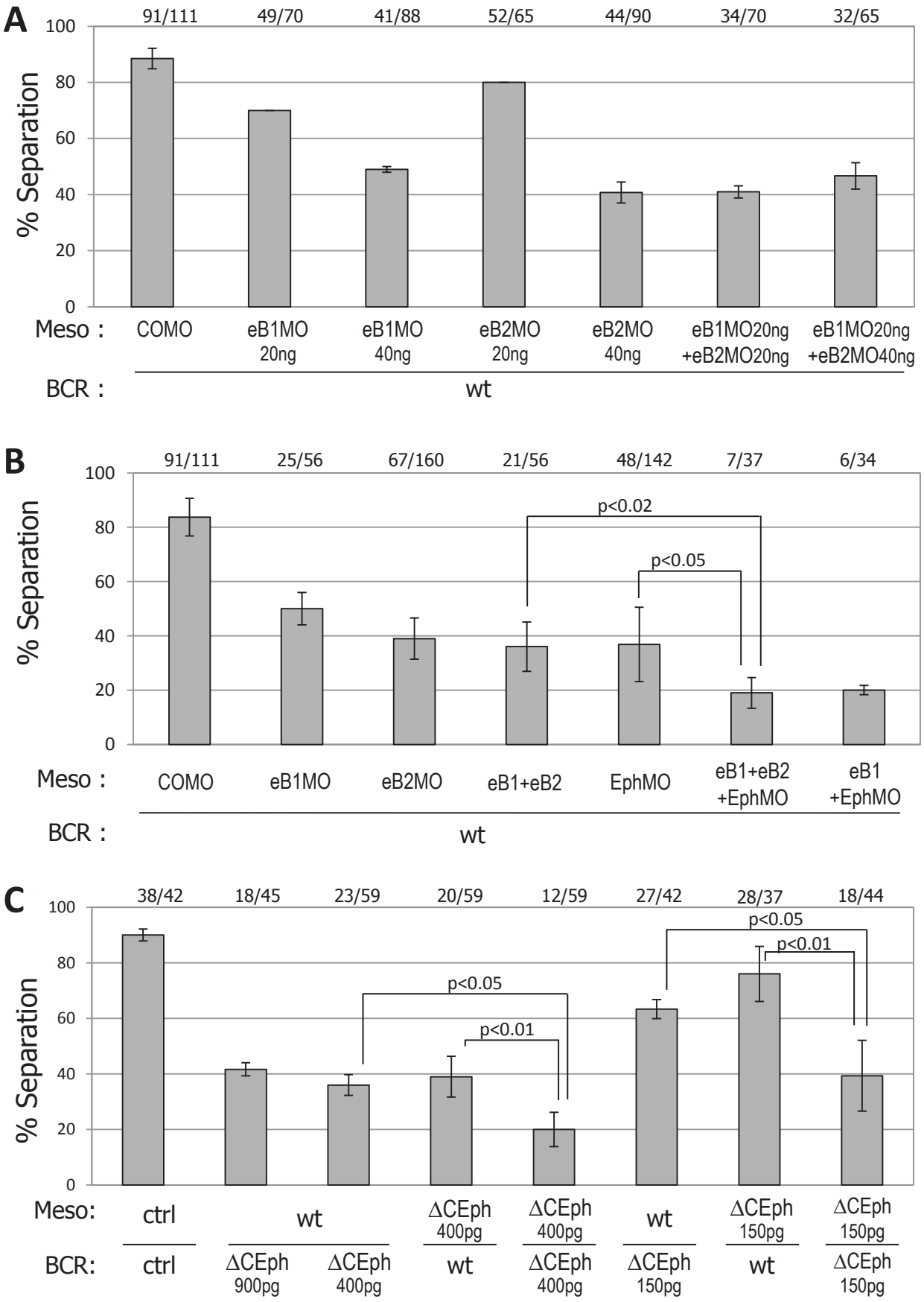
A
91/111
49/70
41/88
52/65
44/90
34/70
32/65
% Separation
Meso :
COMO
eB1MO 20ng
eB1MO 40ng
eB2MO 20ng
eB2MO 40ng
eB1MO20ng +eB2MO20ng
eB1MO20ng +eB2MO40ng
BCR :
wt
B
91/111
25/56
67/160
21/56
48/142
7/37
6/34
p<0.02
p<0.05
% Separation
Meso :
COMO
eB1MO
eB2MO
eB1+eB2
EphMO
eB1+eB2 +EphMO
eB1 +EphMO
BCR :
wt
C
38/42
18/45
23/59
20/59
12/59
27/42
28/37
18/44
p<0.05
p<0.01
p<0.05
p<0.01
% Separation
Meso:
ctrl
wt
ΔCEph 400pg
ΔCEph 400pg
wt
ΔCEph 150pg
ΔCEph 150pg
BCR:
ctrl
ΔCEph 900pg
ΔCEph 400pg
wt
ΔCEph 400pg
ΔCEph 150pg
wt
ΔCEph 150pg

Figure 2.S4

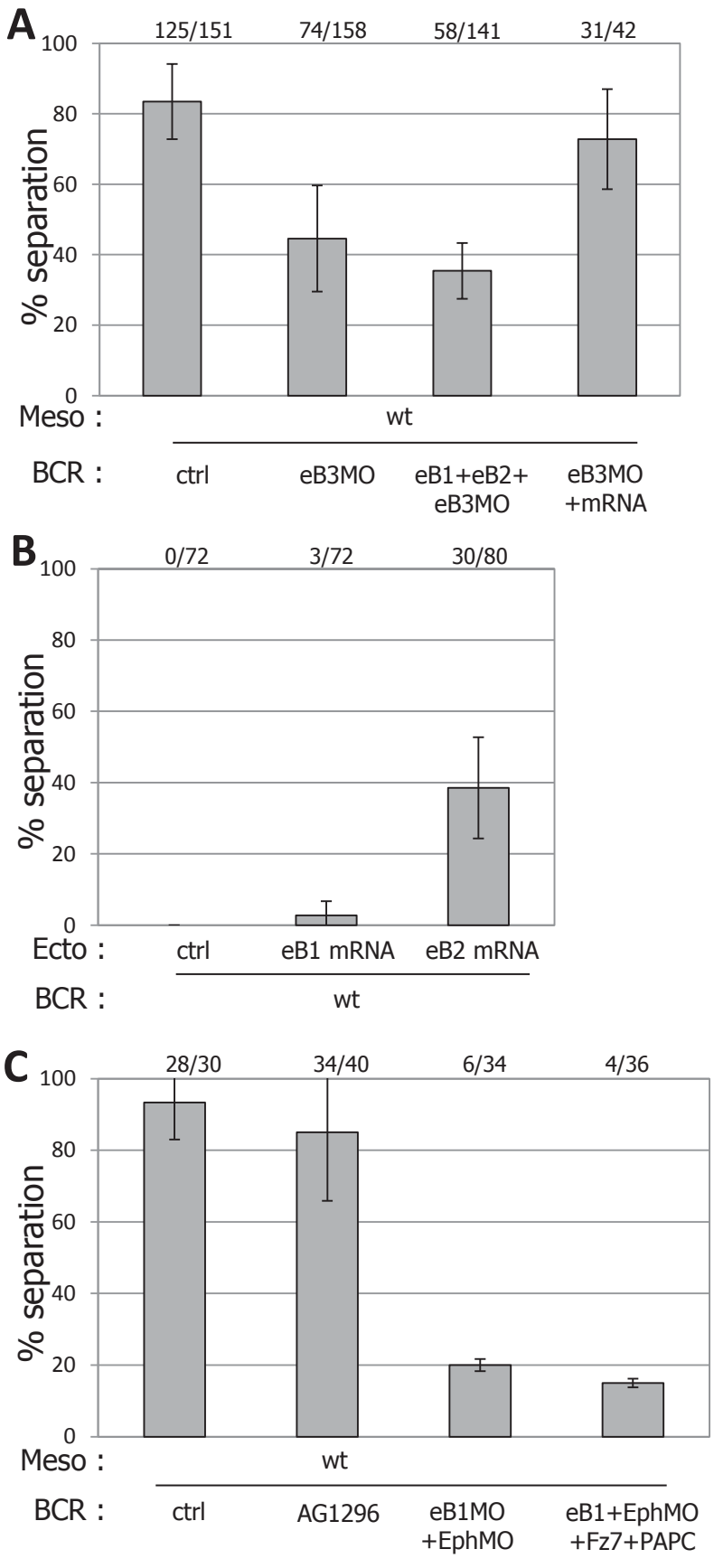
A
125/151
74/158
58/141
31/42
100
80
60
40
20
0
% separation
Meso :
wt
BCR :
ctrl
eB3MO
eB1+eB2+
eB3MO
eB3MO
+mRNA
B
0/72
3/72
30/80
100
80
60
40
20
0
% separation
Ecto :
ctrl
eB1 mRNA
eB2 mRNA
BCR :
wt
C
28/30
34/40
6/34
4/36
100
80
60
40
20
0
% separation
Meso :
wt
BCR :
ctrl
AG1296
eB1MO
+EphMO
eB1+EphMO
+Fz7+PAPC

Figure 2.S5

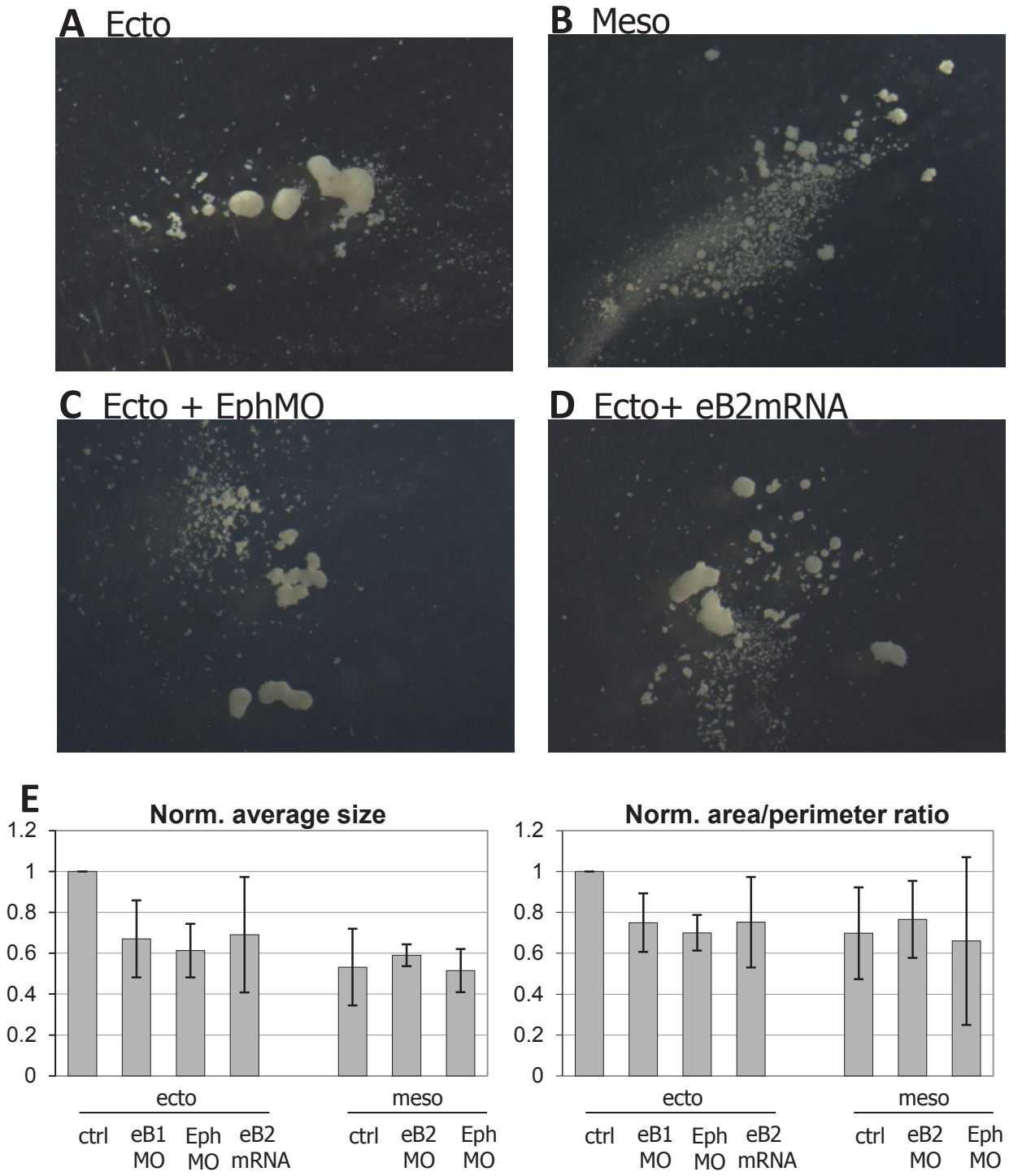
A Ecto
B Meso
C Ecto + EphMO
D Ecto+ eB2mRNA
E
Norm. average size
Norm. area/perimeter ratio
1.2
1
0.8
0.6
0.4
0.2
0
ecto
meso
ctrl
eB1 MO
Eph MO
eB2 mRNA
eB2 MO

Figure 2.S6

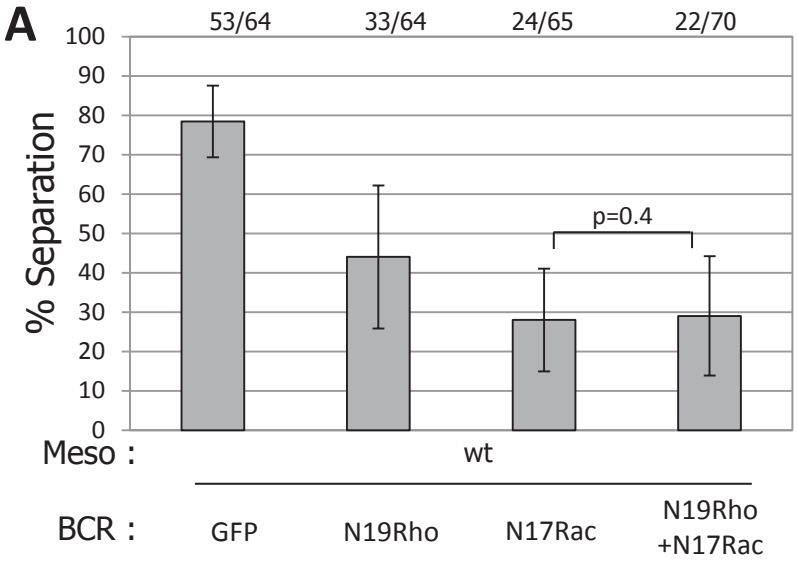
A
53/64
33/64
24/65
22/70
100
90
80
70
60
50
40
30
20
10
0
% Separation
p=0.4
Meso :
wt
BCR :
GFP
N19Rho
N17Rac
N19Rho
+N17Rac

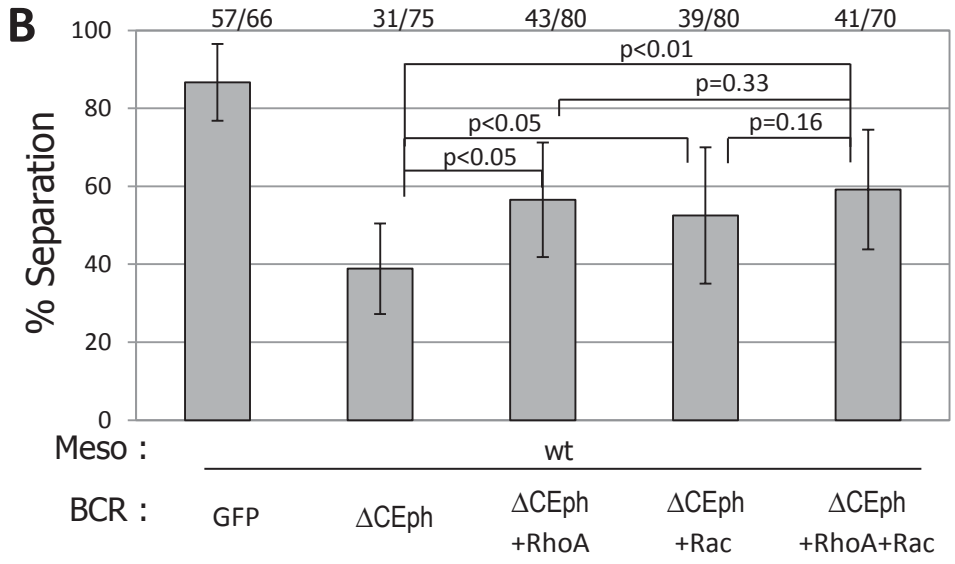
B
57/66
31/75
43/80
39/80
41/70
100
80
60
40
20
0
% Separation
p<0.01
p=0.33
p<0.05
p=0.16
p<0.05
Meso :
wt
BCR :
GFP
ΔCEph
ΔCEph
+RhoA
ΔCEph
+Rac
ΔCEph
+RhoA+Rac

Figure 2.S7

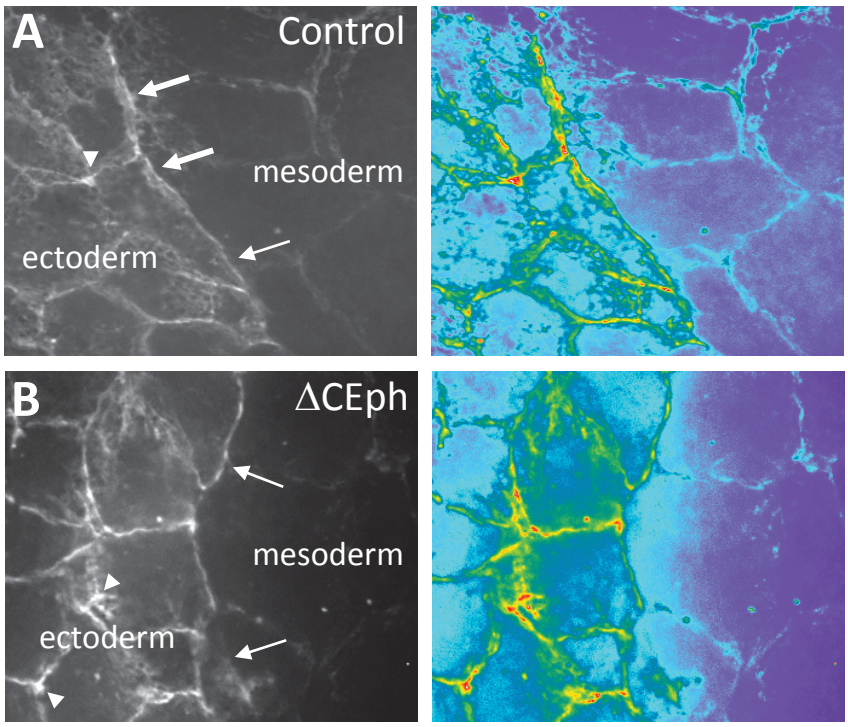
A
Control
mesoderm
ectoderm
B
ΔCEph
mesoderm
ectoderm

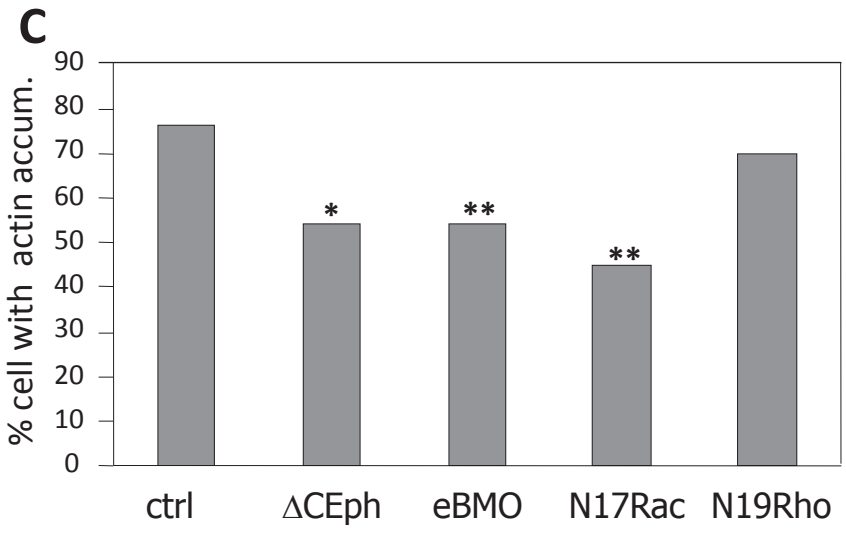
C
% cell with actin accum.
90
80
70
60
50
40
30
20
10
0
*
**
**
ctrl
ΔCEph
eBMO
N17Rac
N19Rho

Bridge to Chapter III

In the previous chapter I showed that a contact mediated signaling mechanism is involved in the separation of ectoderm from mesoderm at the Brachet's cleft. The mechanism is controlled by antiparallel signals from several Ephrin and Ephs that are expressed in both ectoderm and mesoderm. We show in this chapter that each ephrin and Eph expressed in those tissues is required for tissue separation. Different from traditional views where ligand is on one side and receptor on the other side, at the ectoderm-mesoderm boundary each cells carries an array of both ligand and receptor. This raised the question that why cell detachments only occurs at tissue interfaces and not inside tissues? In the following section I provide a simple explanation for how tissue separation by Ephrins and Ephs is confined locally. I provide functional and biochemical evidence that supports selective interactions amongst Ephrin and Ephs. Also I showed that each tissue expresses different levels of ligands and receptors. Ligands and receptors with greater affinity appear on adjacent tissues. Inside the tissues pairs with lower affinities couple thus separation is confined to the boundary. We show both experimentally and by mathematical simulation that this mechanism holds true for three boundaries that are formed during Xenopus gastrula. The following chapter is a reproduction of the manuscript below that has been reviewed at PloS Biology: Variable combinations of specific ephrin ligand/Eph receptor pairs control embryonic tissue separation. Authors: **Nazanin Rohani**, Rudolf Winklbauer and François Fagotto

Chapter III: Variable combinations of specific ephrin ligand/Eph receptor pairs control embryonic tissue separation.

Abstract

Ephrins and Eph receptors are involved in the establishment of vertebrate tissue boundaries. The complexity of the system is puzzling, however: in many instances, tissues express multiple ephrins and Ephs on both sides of the boundary, a situation that should in principle cause repulsion between cells within each tissue. Although co-expression of ephrins and Eph receptors is widespread in embryonic tissues, neurons and cancer cells, it is still unresolved how the respective signals are integrated into a coherent output. We present a simple explanation for the confinement of repulsion to the tissue interface: Using the dorsal ectoderm-mesoderm boundary of the Xenopus embryo as model, we identify selective functional interactions between ephrin- Eph pairs that are expressed in partial complementary patterns. The combined repulsive signals add up to be strongest across the boundary, where they reach sufficient intensity to trigger cell detachments. The process can be simulated using a simple model based exclusively on relative ephrin and Eph concentrations and binding affinities. We generalize these findings for the ventral ectoderm-mesoderm boundary and the notochord boundary, which both appear to function on the same principles. These results provide a paradigm for how developmental systems may integrate multiple cues to generate discrete local outcomes.

Introduction

In vertebrates, ephrins and Eph receptors have emerged as major players in the formation of cleft-like tissue boundaries. They control segmentation of rhombomeres (Cooke & Moens, 2002) and somites (Durbin et al., 1998; Kemp, Cooke, & Moens, 2009), and the separation of embryonic germ layers (Hwang et al., 2013; Park, Cho, Kim, Choi, & Han, 2011; Rohani, Canty, Luu, Fagotto, & Winklbauer, 2011). Ephrins as well as Eph receptors are divided into A and B subclasses, based on their structural and binding characteristics. They are considered to bind promiscuously within each subclass, EphrinAs with EphAs and EphrinBs with EphBs (Pasquale, 2004), with the exceptions of EphA4, which can interact with both ephrinAs and Bs, and EphB2, which can bind EphrinA5 (Himanen et al., 2004; Kullander & Klein, 2002; Murai & Pasquale, 2003). Classically, a single ephrin-Eph pair is expressed in a complementary pattern in adjacent tissues. However, this simple model can hardly account for many physiological situations, where each cell type may express multiple ephrins and Eph receptors (Astin et al., 2010; Hruska & Dalva, 2012) One must assume that these molecules interact in more selective ways. Consistently, in vitro studies have yielded a wide range of binding affinities between various ephrins and Eph receptors, suggesting a substantial degree of specificity, but the biological significance of these differences has not been clearly established (Astin et al., 2010; Blits-Huizinga, Nelersa, Malhotra, & Liebl, 2004; Flanagan & Vanderhaeghen, 2003). Moreover, the presence of ephrins and Ephs in the same cell introduces a whole additional layer of complexity involving effects such as ephrin-Eph cis-interactions (Kao & Kania, 2011; Marquardt et al., 2005) as well as potential crosstalks between the downstream signaling events (Murai & Pasquale, 2003; Poliakov, Cotrina, Pasini, & Wilkinson, 2008). Understanding how the global output is determined under in vivo conditions has thus remained a daunting challenge. An example where the integration of multiple co-expressed Eph receptors and ephrins can be tested is the ectoderm/mesoderm boundary in the early Xenopus embryo. We have demonstrated that ephrins and Ephs act

directly at the tissue interface, where they generate cycles of attachments and detachments through transient activation of Rho GTPases (Rohani et al., 2011). This mechanism based on cell contact-mediated repulsion is highly reminiscent of neuronal contact guidance, and utilizes the same molecular cues (Harbott, Marston, & Nobes, 2004). We showed that full separation required anti-parallel forward signaling across the boundary such that ephrins in the mesoderm stimulate Ephs in the ectoderm and vice versa (Rohani et al., 2011). This observation was quite puzzling, since ephrin and Eph should in principle interact equally between cells within each tissue, which should cause repulsion and eventually lead to tissue dissociation. We ask here how cell repulsion is restricted to sites of contacts between the two tissues.

Results

Dorsal ectoderm-mesoderm boundary: complementarily expressed ephrins and Ephs are specifically required and not replaceable.

To address this issue, we conducted a comprehensive characterization of the ephrin-Eph system in the early gastrula. We first compared quantitatively the transcripts of all ephrins and Ephs expressed in the dorsal ectoderm and in the mesoderm. Both tissues expressed multiple ephrins and Eph receptors. Although both A and B types are involved at the ectoderm-mesoderm boundary ((Park et al., 2011) and not shown), the contribution of the A type appears less important, as they are not sufficient on their own to induce separation ((Rohani et al., 2011) and not shown). We thus focused on the ephrin B subfamily and their receptors, which showed particularly prominent asymmetric patterns (Supplementary Fig.3.S1A). Thus, ephrinB2 and EphA4 were strongly enriched in the mesoderm, while the ectoderm accumulated ephrinB3 and EphB2-4. These expression patterns suggested that the subtypes may form selective pairs expressed in a complementary manner. Interestingly, ephrinB2, ephrinB3 and EphA4 start to be expressed just at the onset of gastrulation (Supplementary Fig.3.S1B), coinciding with the appearance of the ectoderm-mesoderm boundary. We thus focused on ephrinB2, ephrinB3, EphA4, EphB2 and EphB4, all strongly asymmetrically

distributed molecules, and also included in our analysis ephrinB1 as an example of an evenly expressed ligand (Fig.3.1C).

While ephrin/Eph depletion severely disrupts the endogenous ectoderm-mesoderm boundary ((Rohani et al., 2011)and Fig.3.1A), the embryonic phenotype is difficult to interpret, due to multiple functions of ephrins and Ephs in various aspects of gastrulation (Bisson, Poitras, Mikryukov, Tremblay, & Moss, 2007; Jones et al., 1998; Park et al., 2011; Tanaka, Kamo, Ota, & Sugimura, 2003;Winklbauer unpublished). We thus performed most of our study on a reconstituted boundary produced by apposition of ectoderm and mesoderm explants (Fig.3.1B,B'), an assay that allows an in depth dissection of tissue separation (Rohani et al., 2011; Wacker, Grimm, Joos, & Winklbauer, 2000; Winklbauer & Keller, 1996). By systematic depletions using antisense morpholino oligonucleotides (MO) (Supplementary Fig.3.S2A, D), we established that each ephrin and Eph is required, either in the ectoderm, in the mesoderm, or in both. Their depletion partially inhibited tissue separation to a degree that generally correlated with their relative tissue enrichment (Supplementary Figs. 3.S1A and S2A). Interference with ephrins or with Ephs on one side of the boundary, by single or multiple depletions (Supplementary Fig.3.S2A) or dominant negative constructs (Rohani et al., 2011), led to a maximal reduction of separation to 30-40%, while simultaneous interference on both sides of the boundary led to a significantly stronger inhibition (Supplementary Fig.3.S2A), consistent with a requirement for two anti-parallel forward signals (Rohani et al., 2011).

After having established that each ephrin and Eph subtype is required, we asked next whether a given subtype could be replaced by another member of the family. An ephrin or Eph was depleted, and rescue was attempted by mRNA injection (Suppl. Fig.3.S2B), or by direct activation at the boundary through incubation with soluble pre-clustered ephrin or Eph extracellular domains (Fig.3.1D). Results from both types of rescues were in perfect agreement: separation could only be efficiently rescued by restoring expression of the missing subtype. Other ephrins

or Ephs gave little or no rescue even when expressed at high levels (Supplementary Fig.3.S2B, C).

These results demonstrated that each ephrin and Eph is specifically required for dorsal ectoderm mesoderm separation. The ability of EphA4-Fc fragment to rescue loss of EphA4 also uncovered a contribution from reverse signaling to tissue separation.

The specificity of Eph receptors resides in their extracellular domain.

Our results suggested a specific requirement for all ephrinB subtypes and their receptors. This could be due to specific differences in downstream signaling and hence to different roles during tissue separation. Alternatively, signaling could be uniform and additive, but depend on specific receptor-ligand interactions. To determine whether Eph receptor specificity resided in their cytoplasmic tail or in their extracellular domains, we constructed EphA4/B4 chimeras, where the respective cytoplasmic domains were swapped, and tested their ability to rescue loss of EphA4 or EphB4. In each case, rescue was obtained only with the chimeric receptor that contained the corresponding extracellular domain. The cytoplasmic domains were fully interchangeable (Fig.3.1E), suggesting that the requirement for each of these Eph receptors was probably not due to differences in signaling but rather reflected the ability to bind selected ligands. Thus, specific combinations of receptor-ligand pairs which can form at the boundary, but not or to a lesser degree, within tissues could underlie the restriction of repulsion to the boundary.

Complementarily expressed ephrins and Ephs form selective functional pairs

If indeed specific ephrin-Eph pairs formed preferentially at the boundary, we predicted that ectopic addition of ephrins normally enriched in the mesoderm may induce artificial separation of two ectoderm explants. This prediction was fully verified: ectoderm explants could be induced to repel each other by treatment with soluble Fc fragments for mesoderm-enriched ephrinB2, but not ephrinB1 (Fig.3.2A). Similarly, the separation of two mesoderm explants was efficiently

induced by incubation with ephrinB3, which is normally expressed only in the ectoderm, but not by ephrinB2 (Fig.3.2A'). As for Eph receptors, we observed that ectoderm-ectoderm separation could be induced by "mesodermal" EphA4-Fc, but not by EphB4-Fc (Fig.3.2A" and A"'). This capacity of Fc fragments to induce ectopic separation provided us with a functional assay to identify the endogenous ephrins/Ephs responding to these exogenous Fc fragments. Among potential candidate receptors for ephrinB2 in the ectoderm, EphB4 depletion strongly inhibited ephrinB2-Fc induced separation, while EphB2 depletion had a weaker effect (Fig.3.2A). The ability of ephrinB3 to induce mesoderm separation was entirely dependent on the presence of EphA4 (Fig.3.2A'). Finally, of all the three ephrin ligands expressed in the ectoderm, ephrinB3 was clearly the one responsible for EphA4-Fc-induced separation (Fig.3.2A"). Although some of these results were consistent with the relative mRNA enrichments of the various ligands/receptors (Supplementary Fig.3.S1A), others clearly implied functional selectivity. For instance, in EphA4- induced ectoderm-ectoderm separation, an explanation based only on relative levels, with promiscuous binding, predicted indeed a minimal role of ephrinB2 compared to ephrinB3, but could not predict the ineffectiveness of ephrinB1 depletion.

Differential Eph activation by specific ephrins

We directly assessed functional selectivity at the level of Eph activation (Fig.3.2B): after treatment of ectoderm explants with equal concentrations of ephrinB1, B2 or B3 Fc fragments, each Eph receptor was immunoprecipitated, and the levels of phosphorylation were monitored by Western Blot using an anti-phospho-tyrosine antibody (Astin et al., 2010). Because of poor immunoprecipitation of the endogenous EphA4 protein with available antibodies, EphA4-YFP was ectopically expressed and fished with an anti-GFP antibody, that recognizesYFP. EphA4 was highly phosphorylated in response to both ephrinB2 and ephrinB3, but not ephrinB1. EphB2 responded strongly to ephrinB2 and weakly to ephrinB1. EphB4 was activated by ephrinB2 but neither ephrinB1 nor ephrinB3. These results correlate well with ephrin-Eph affinities measured in

vitro (Blits-Huizinga et al., 2004), with the notable exceptions of the ephrinB1-EphB2 and ephrinB3-EphA4 pairs: EphB2 was reported to bind both ephrinB1 and ephrin B2 with similar affinities (Gale et al., 1996), while, on the contrary, the reported affinity of ephrinB3 for EphA4 was very low compared to ephrinB2-EphA4 (Gale et al., 1996; Qin et al., 2010). Taken together, our results show that each Eph receptor is selective for one, or at most two ephrins.

These results support the hypothesis that tissue separation is driven by asymmetric expression of specific receptor-ligand pairs. Most of the ephrin/Eph pairs identified show indeed partially complementary expression (Fig.3.2B and supplementary Fig.3.S1A). This is clearly the case for ectodermal ephrinB3 and mesodermally enriched EphA4. Likewise, ectodermally enriched EphB2 and EphB4, interact best with mesodermally enriched ephrinB2.

However, not all factors are expressed in simple complementary patterns. In particular, EphA4 does not only interact with ectodermal ephrinB3, but equally well with ephrinB2, which is abundant in the mesoderm. On the contrary, ephrinB1, evenly expressed in both tissues, can only weakly activate EphB2, which is enriched in the ectoderm.

Complementary expression of selective ephrin-Eph pairs is sufficient to account for tissue separation

Our results suggested that despite the complexity of the system, tissue separation may be simply explained by the complementary expression of specific ephrin/Eph pairs, which would generate an excess of repulsive signal at the boundary (Fig.3.3A). Nevertheless, the complicated patterns of ephrin and Eph expression could reflect a more specific need for particular ephrins and Ephs within each tissue. We examined this possibility for the ephrinB3-EphA4 pair, which is closest to a fully complementary expression pattern. We depleted ephrinB3 in the ectoderm and EphA4 in the mesoderm and asked whether separation could be rescued by ectopic re-expression of these two molecules in the opposite tissues. The results were unambiguous: swapping ephrinB3 and EphA4 efficiently restored separation (Fig.3.3B). The rescue was specific for the ephrinB3-EphA4

pair, since EphB4, which cannot function as ephrinB3 receptor, could not substitute for EphA4. This result indicates that any form of complementary expression of ephrinB3 and EphA4 is sufficient, and that tissue specific expression is not required.

Enhanced Eph signaling and myosin activation at the ectoderm-mesoderm boundary

Immunostaining of sections from wild type gastrulae with an antibody recognizing a conserved phosphorylated tyrosine site present in all EphBs demonstrated that Eph signaling was indeed activated in both ectoderm and mesoderm, but was significantly stronger at the boundary (Fig.3.4A,A'). We confirmed biochemically the existence of basal signaling in the tissues and enhanced activity at ectoderm-mesoderm contacts. Such contacts were maximized by mixing dissociated ectoderm and mesoderm cells to produce heterogeneous aggregates (Fig.3.4B). The levels of phosphorylated EphAs and EphBs in extracts of mixed aggregates were compared with those of pure ectoderm and mesoderm aggregates. Mixed aggregates showed higher p-EphA and p-EphB signals than combined homogenous ectoderm and mesoderm aggregates. We further showed that EphA phosphorylation in these ectoderm-mesoderm aggregates required ephrinB3, but not ephrinB1, further confirming the specificity of EphA4 (Supplementary Fig.3.2D'). Thus, high local Eph activation seems to restrict cell repulsion to the boundary, consistent with the preferential interactions between complementary pairs of ephrins and Ephs enriched on opposite sides of the boundary.

The typical mechanical output of Ephrin/Eph signaling in repulsive behavior involves myosin-based contraction (Gallo, Yee, & Letourneau, 2002; Groeger & Nobes, 2007). We determined the distribution of phosphorylated myosin light chain (p-MLC) in the ectoderm and mesoderm tissues and at their interface (Fig.3.4C). We observed p-MLC at cell-cell contacts within each tissue (arrowheads). The signal was significantly stronger in the ectoderm than in the mesoderm, but by far the most intense signal was consistently found in patches

along the boundary (arrows), as expected from strong bursts of ephrin/Eph signaling at this interface. EphA4/EphB4 depletion abolished specifically the boundary p-MLC staining (Fig.3.4C', C"). These results confirm that the boundary is a site of significantly stronger Eph signaling and resulting contractile activity. Note that Eph depletion had little effect on the p-MLC signal within the tissues, suggesting that the contribution of ephrin/Eph to myosin regulation in the tissues is small relative to other inputs.

Loss of Eph signaling was however sufficient to erase the boundary, causing ectoderm and mesoderm to fuse in a continuous cell mass despite the fact that there were still large differences in p-MLC levels between these two tissues. We thus proposed that separation results from a balance between cadherin adhesion and Eph signaling-dependent repulsion: Eph signaling would occur both within tissues and at the tissue interface, but only in the latter case the signal would be sufficiently intense to overcome cadherin-mediated cell-cell adhesion, thus causing cell detachment.

Separation is controlled by the balance between ephrin-Eph-dependent repulsion and the strength of cadherin-mediated adhesion

We predicted that increasing cadherin levels or decreasing contractility should inhibit detachments between ectoderm and mesoderm cells, while on the contrary decreasing cell-adhesion or increasing Eph signaling should lead to visible detachments between mesoderm cells. To verify these predictions, we examined the formation of contacts between single cells obtained by dissociation of early gastrula tissues (Fig.3.5A-I and supplementary movies S1-S6). Our dissociation conditions fully preserved both the capacity of cells of the same tissue to rapidly re-establish stable adhesions (Fig.3.5D-G) and the ability for contacts between ectoderm and mesoderm cells to reproduce the alternating cycles of attachment/detachment characteristic of the separation behavior (Fig.3.5A-B and supplementary movie S1). We first tested the effect of increasing cadherin levels or inhibiting myosin on the normal repulsion between ectoderm and mesoderm cells. Both conditions severely reduced the frequency of detachments (Fig.3.5B,

C, H and supplementary movie S2). These effects were perfectly matched in the tissue explant assay, where both conditions strongly decreased separation (Supplementary Fig.3.3,3A). Separation could be rescued between cadherin-overexpressing tissues by addition of soluble ephrinB2-Fc (Supplementary Fig.3.3A), again consistent with separation purely resulting from a balance between repulsion and adhesion.

Since we expected mild repulsion between mesoderm cells, we predicted that detachments should become visible if adhesion would be experimentally decreased. We subjected mesoderm cells to a mild cadherin-depletion (~30%, not shown), and observed that contacts were now much less stable and cells displayed the typical repulsive behavior normally observed at contacts with ectoderm cells (Fig.3.5E,H and supplementary movie S4). These retractions were entirely dependent on intact ephrin/ Eph signaling (Fig.3.5F,H and supplementary movie S5). We also predicted that mesoderm cells could become repellent even with normal cadherin levels if repulsive signals would be increased. We chose to express ephrinB3 and EphB4, because they are normally enriched in the ectoderm, and are the respective specific partners for mesoderm-enriched EphA4 and ephrinB2 (Fig.3.3A). EphrinB3/EphB4-expressing mesoderm cells readily showed strong repulsion (Fig.3.5G,H and supplementary movie S6). This balance between repulsion forces and cell-cell adhesion was also observed at the tissue level in re-aggregation assays (Supplementary Fig.3.S3B-D): diminished cohesion induced by cadherin depletion was rescued by co-depletion of EphB4, while ectopic expression of ephrinB3 and EphB4 decreased cohesion of cells with wild type cadherin levels.

Modeling the ephrin/Eph network

Our results suggested that ectoderm-mesoderm separation mainly relied on selective interaction between ephrin-Eph pairs (Fig.3.6A). Although the concept is intuitively coherent, we wanted to verify that the process could indeed be quantitatively accounted for based purely on this assumption. We considered a model built on two simple parameters: (1) the affinities between the extracellular

domains of ephrins and Ephs; and (2) their relative expression in the different tissues (Suppl. Materials). Affinities have been measured in vitro for most of the ephrin-Eph pairs (Blits-Huizinga et al., 2004). Whether these measurements faithfully reflect the strength of the in vivo interactions, and how the actual signal outputs are mechanistically related to binding affinities remains to be determined. However, the relative values correlate in most cases well with the functional selectivity observed in our experiments, indicating that they provided an acceptable approximation. We had to adjust only three values, for ephrinB1-EphB2 (increased), ephrinB2-EphA4 and ephinB3-EphA4 (decreased), which were inconsistent with the relative receptor activations apparent in our biochemical data. Actual levels of endogenous ephrin and Eph receptor proteins present at the cell surface cannot be determined at the moment, due to the lack of adequate antibodies. However, mRNA levels can be quantitatively compared by real-time PCR (Supplementary Fig.3.S1). Being aware of the obvious caveats (differential translation, stability at the surface, endocytosis), we made the simple assumption that protein levels at the cell membrane are proportional to mRNA levels. We computed a theoretical signal output for each ephrin-Eph pair, in each tissue and at tissue interfaces (see supplementary material and supplementary Fig.3.S4 for details).

We included in the simulation ephrinB1, B2, and B3 and EphA4, B2 and B4, which we had all thoroughly characterized functionally. The obtained signal outputs reproduced well the relative strengths of repulsion predicted by our experiments (Fig.3.6D): repulsion was lowest in the ectoderm, moderate in the mesoderm and strongest at the tissue interface. For the notochord-somite boundary, repulsion was similar in both tissues, and higher at the boundary. Moreover, the model reproduced the phenotypes observed upon manipulation of ephrin/Eph levels and function without the need for any further assumptions. We simulated some of the main experimental conditions, including gain of separation between ectoderm explants upon ectopic activation by “mesoderm-specific” ephrins (Fig.3.6G), the correlation between relative expression and strength of inhibition upon depletion of single ephrins (Fig.3.6H), stronger inhibition upon

interference with signals on both sides of the boundary (Fig.3.6I), and finally the swapping experiment where ephrinB3 and its specific receptor EphA4 were depleted and re-expressed on the opposite tissue (Fig.3.6J). The predicted changes in simulated signals fitted extremely well with the experimental results (Fig.3.2A, supplementary Fig.3.2A, Fig.3.3B). Thus, although additional parameters are likely to contribute to fine tuning of separation, this basic model is sufficient to explain the process.

The system appeared quite robust, particularly for both ectoderm-mesoderm boundaries, where similar outcomes were observed for a wide range of ephrin and Eph concentrations, and could even accommodate some flexibility in the Kd values. The robustness of the system controlling the dorsal boundary appeared to be largely due to the two antiparallel complementary ephrinB3-EphA4 and ephrinB2-EphB2 pairs, which operated as mutual backups and together dominated over other signals, including the strong intratissue ephrinB2-EphA4 interactions. Our characterization of the three ephrinBs and of three out of their five receptors showed that they were sufficient to account for early tissue separation. Yet, several other ephrins and Eph receptors are expressed in the gastrula embryo. We also determined the relative mRNA levels for ephrinA1,A3,A5 and EphB1,B3, A2 and A5 in the dorsal ectoderm and mesoderm tissues, and evaluated their potential impact. Addition of these molecules in the simulation using the published affinities increased the basal signal in all tissues, but the general pattern of signaling differentials remained very similar (data not shown).

Selective ephrin-Eph pairs at the ventral ectoderm-mesoderm and at the notochord boundaries

We decided to examine ephrin/Eph expression in two other regions of the gastrula embryo where important boundaries form the ventral ectoderm-mesoderm boundary (Fig.3.6B) and the notochord boundary (Fig.3.6C). The former appears at midgastrula and involves a mesoderm known to have different properties than dorsal axial mesoderm. The notochord boundary appears at the end of gastrulation to partition the dorsal mesoderm into the axial notochord and lateral paraxial

mesoderm (prospective somitic mesoderm). We found that the same set of ephrin/Ephs was expressed in those regions. The expression patterns revealed common themes as well as some significant differences: In the case of the ventral boundary, the ephrinB3-EphA4 complementarity was preserved, as well as the mesoderm enrichment of ephrinB2 (Fig.3.6B and supplementary Fig.3.S1A). However, EphB4, which was enriched in the ectoderm on the dorsal side, was now homogenously expressed, while on the contrary ephrinB1, equal on both sides of the dorsal boundary, was here strongly asymmetric, now fully complementary to its receptor EphB2. In the case of the notochord boundary, late gastrula dorsal mesoderm showed very interesting expression patterns: the notochord had preserved strong EphA4 and ephrinB2 expression, which were the major characteristics of the early mesoderm. The paraxial mesoderm, however, had dramatically modified its ephrin/Eph expression, acquiring typical features of ectoderm, i.e. low EphA4 and high EphB4 (Fig.3.6C and supplementary Fig.3.S1A). As for ephrins, differences were much milder, although highly reproducible: the notochord remained more "mesoderm-like" (higher ephrinB2, lower ephinB3), the paraxial mesoderm was now more "ectoderm-like".

These observations suggested that tissues that became separated by boundaries expressed some sort of "modules" characterized in particular in all cases by complementary ephrinB3-EphA4 expression, but had some flexibility for other components. We verified that these configurations could also lead to stronger signaling across the boundary in our simulations (Fig.3.6E,F and supplementary Fig.3.S4).

We then tested experimentally the role of key players, at both boundaries. In the case of the ventral boundary, we used the classical separation assay, attempting both loss- and gain-of-function experiments. All the results were in perfect agreement with the expression patterns and with our model: Both mesoderm-enriched ephrinB1 and B2 could induce robust separation between two ectoderm explants when added as soluble Fc fragments (supplementary Fig.3.S5B), an effect that could not be obtained with ephrinB1 on the dorsal side (Fig.3.2A). We could now use the assay to identify the functional partner of ephrinB1 on the

ectoderm surface: we found that EphB2, but not EphB4, depletion, significantly inhibited separation, functionally validating our biochemical results (Fig.3.2B). Fully consistently, ephrinB1 depletion in the mesoderm, which had only a weak effect on the dorsal side, affected here separation much more drastically (supplementary Fig.3.S5C). Depletion in the ectoderm of its receptor EphB2 similarly inhibited separation.

We studied the role of ephrins and Ephs on the notochord boundary by targeted depletion in a restricted region of the embryo. The effect on the integrity of the boundary was examined on sections of whole embryos (Fig.3.7). We observed strong disruption of the boundary by ephrin/Eph MO injection. Each ephrin/Eph MO disrupted the boundary only when targeted to the expressing tissue: ephrinB3 MO and EphB4 MO in the paraxial mesoderm, EphA4 MO in the notochord. EphrinB2 MO was the only one which had an effect on both sides. The observed phenotypes were perfectly consistent with the prediction from the model (Fig.3.6C,7L): for instance the only receptor for ephrinB3 is EphA4, enriched in the notochord, thus ephrinB3 depletion may only impair separation when targeted to the opposite tissue. EphrinB2, however, can stimulate both EphA4 and EphB4, explaining the widespread effect of its depletion.

We further verified that this functional selectivity was purely due to extracellular interactions: we used the EphA4 and B4 chimeras to rescue disruption of the notochord boundary upon EphA4 or EphB4 depletion. In both cases, rescue was only achieved by expression of the chimeric construct that harboured the right extracellular domain (Fig.3.7F-K,M).

Discussion

This study reconciles several previous puzzling observations and provides a coherent description of boundary formation based on selective repulsion between two cell populations. In particular, it explains how in tissues with widespread co-expression of ephrin ligands and Eph receptors, cell-cell repulsion due to receptor-ligand interaction can be restricted to tissue boundaries. Situations where ephrins and Ephs are co-expressed were expected to be dauntingly complex,

considering the many possible cross-regulations proposed to occur and the potentially distinct pathways that each member of these families may stimulate. However, we found that the essence of the early boundaries can be represented by a surprisingly simple model where the final output can be fully predicted based on the relative selectivity of the extracellular interactions and the abundance of the various components.

By analyzing the ectoderm-mesoderm boundary of the Xenopus gastrula in detail, we found surprisingly clear cut responses, which argued that the ephrin-Eph receptor interactions are more specific than promiscuous. Yet, our simulations showed that nothing must be invoked to explain these contrasted outputs but known differences for the binding affinities of different ephrin-Eph combinations. Our functional and biochemical results were generally well correlated with the relative affinity values, with the exceptions of ephrinB1-EphB2, ephrinB2-EphA4 and ephrinB3-EphA4. These discrepancies may be due to context-dependent differences, but may also reflect the intrinsic imprecision of in vitro affinity measurements. Indeed, values differing by as much as tenfold were reported for some ephrin-Eph pairs (Blits-Huizinga et al., 2004; Flanagan & Vanderhaeghen, 2003). Note that our model still predicts a decisive role of the ephrinB3-EphA4 pair, even when taking the high published Kd values. Its consistent complementary expression indeed compensates for the lower affinity.

The complementary expression of the ephrinB3-EphA4 pair is one of the general rules that emerged from our study: The comparison of three morphologically similar, cleft-like boundaries which form during Xenopus gastrulation and depend on Eph-ephrin signaling allowed us to extract recurrent regulatory motives in the form of complementary receptor-ligand pairs: ephrinB3-EphA4, ephrinB1-EphB2, and ephrinB2-EphB4 (Fig.3.6). For each boundary, at least two of these three pairs show complementary expression patterns. Moreover, we had shown previously that complete ectoderm-mesoderm boundary formation requires forward signaling into both adjacent tissues. We observed now that at all three boundaries studied here, the respective complementary pairs were arranged in an antiparallel pattern (e.g. ephrinB3-EphA4 from ectoderm to mesoderm, ephrinB2-

EphB2 from mesoderm to ectoderm). Of the complementary pairs, ephrinB3-EphA4 is most systematically exploited in the different contexts, suggesting that it may be specialized in tissue separation.

Altogether, the logic of ephrin/Eph dependent repulsion regulation at tissue interfaces can be reconstructed as follows. For the complete cleft-like separation, a minimum of two antiparallel receptor-ligand pairs is required. If both receptors and both ligands were completely specific, signaling would be completely restricted to the boundary, since the ligands and receptors co-expressed in each tissue would interact only with partners in the adjacent tissue. If interactions were completely promiscuous, signaling intensity within each tissue were similar to that across the boundary, leading to the disintegration of the whole array. If interactions were relatively specific, favoring signaling between complementarily expressed pairs, repulsion could be restricted to the boundary by a threshold mechanism where full cell-cell detachment occurs only above a certain level of signaling intensity. In this situation, additional expression of receptors and ligands, with additional strong or weak interactions, would be compatible with proper boundary formation as long as signaling remained below the threshold within each tissue, and exceeded it at the tissue interface. This third scenario is the one that we encountered in the embryo. Such dynamic yet robust system appears perfectly suited for the complex morphogenesis of vertebrate embryos. For example, they allow combining multiple functions of ephrin/Eph signaling, in the same tissues (Poliakov, Cotrina, & Wilkinson, 2004;Smith, Robinson, Patel, & Wilkinson, 1997; Winklbauer unpublished). Further more ephrin-Eph signaling intensities within tissues reflect very well their properties: outputs are predicted to be significantly higher in both dorsal and ventral mesoderm compared to ectoderm (Fig.3.6D-E), but relatively homogenous in the notochord and paraxial mesoderm, which have largely similar morphogenetic properties during this early phase of convergence-extension (Fig.3.6F).

The rules identified in this study provide a coherent logic to tissue separation. For instance, one now understands how separation between dorsal ectoderm and

mesoderm is established at the onset of gastrulation (Wacker et al., 2000). The system builds on the EphB receptors, which are already expressed before gastrulation (Supplementary Fig.3.S1B). Their enrichment in the prospective ectoderm is the typical default distribution for maternal components. This intrinsic bias in expression becomes functionally relevant once the mesoderm starts expressing ephrinB2, the strongest ligand for EphB receptors, initiating a forward signal into the ectoderm. The simultaneous expression of ephrin B3 in the ectoderm and its receptor EphA4 in the mesoderm provides the antiparallel forward signal into the mesoderm, completing the requirement for full tissue separation at this boundary. In subsequent stages this pattern is progressively modified. Complementary expression of ephrinB3 and EphA4 is still involved in all cases, but other components, including those which were maternally expressed, are now tightly regulated and change their expression pattern. This is the case for ephrinB1, which while ubiquitously expressed and hence neutral during dorsal ectoderm-mesoderm boundary formation, becomes mesoderm-enriched to play a prominent role on the ventral side. Other pairs, such as ephrinB2-EphA4, should interact extensively within a tissue, presumably providing tissue-specific functions.

Are other boundaries controlled by a similar integrated network? Information of ephrin/Eph expression patterns in other systems is incomplete and not quantitative, but somites and most rhombomeres express more than one ephrin and/or Eph (Cooke & Moens, 2002; Kemp et al., 2009), in patterns that are consistent with the basic principles described in our study: For instance, ephrinB3 and EphA4 are expressed in complementary patterns in several rhombomeres, and are never enriched on the same side of the boundary. EphrinB2, on the contrary, is found both opposite to AND on the same side as its receptors (Cooke, Kemp, & Moens, 2005; Flanagan & Vanderhaeghen, 2003; Kemp et al., 2009).

These findings reveal that the surface of embryonic cells is endowed with a rich array of receptors that upon direct contact with neighboring cells can establish

very specific interactions. We show how such systems, by integrating the signals generated by all the combinations of high and low affinities interactions, can produce clear cut decisions at tissue interfaces and at the same time tolerate a good degree of within-tissue signaling. The key to this behavior of the ephrin/Eph system is the balance of adhesion and repulsion and its regulated breakdown at a preset threshold for repulsion. While this model can largely explain tissue separation, our results do not exclude that particular ephrins or Ephs may play important additional roles. They may allow for the fine-tuning of the various signals, both at the boundary and within the tissues. EphrinB2-EphA4 constitutes an example of a pair that, at all stages, interacts extensively within a tissue and may provide tissue-specific functions. One such additional layer of regulation that remains to be investigated is suggested by our re-aggregation assays, which showed that ephrinB2 or EphB4 depletion decreased cohesion of the ectoderm (Rohani et al., 2011), indicating that at least under some circumstances these molecules behave as "pro-adhesive" in the ectoderm, while they are repulsive in the mesoderm and across the boundary.

We also provide here an important distinction between activities that are intrinsic to each tissue and reactions that occur specifically at the boundary. Our observation that global levels of myosin activation are much higher in the ectoderm is fully consistent with its well-known stiffness and much lower capacity for spreading on adhesive substrates and for migration (Krens, Möllmert, & Heisenberg, 2011; Krieg et al., 2008; Luu, David, Ninomiya, & Winklbauer, 2011; Wacker et al., 2000; Winklbauer & Kwang, 2009). However, we also detect a second p-MLC pool, which, unlike the former, is Eph-dependent, and highly concentrated at the boundary interface (Fig.3.3C). Despite a large difference in "basal" myosin activity, the two tissues cannot remain separated in the absence of Eph signaling. Previous hypotheses based on differential adhesion/tension fail to accurately describe this situation. Our observations are however in full agreement with our model of "selective repulsion" controlled by potent and highly localized ephrin-Eph reactions, dominating at specific cell-cell contacts over the adhesive

and tensile tissue properties. To explain his original discovery of cell sorting, Holtfreter had hypothesized that various cell types harbour different surface cues that he called “affinities” (Holtfreter, 1939). The combinatorial network of ephrins and Ephs here unravelled provides a molecular basis to this concept. Ephrins and Ephs and other similar cell-cell contact-dependent cues are expressed in a wide variety of tissues, both in the embryo and in the adult, and we predict that the principles uncovered in the Xenopus gastrula may apply to a vast spectrum of cellular processes and account for the ability of cell types to distinguish between “self” and “non-self” and thus organize into multicellular structures.

Experimental Procedures

In vitro separation assay

The assay was performed as previously described (Winklbauer & Kwang, 2009). For in vitro activation of Eph receptors, explants were either pre-incubated with pre-clustered ephrinB/Eph-Fc fragments (40nM in MBSH) for 15 min at room temperature (experiment of Figure1D) or the entire assay was performed in the presence of Fc fragments (Figure 3.2A). Induced mesoderm was produced as described before (Chen et al., 2004; McCrea, Brieher, & Gumbiner, 1993). For the statistical analysis, results were compared using the two-tailed paired-sample Student’s t-test.

Live imaging

Tissues expressing membrane-targeted Cherry or GFP, as well as various mRNAs/MOs were dissociated and cells were transferred to glass bottom petri dish (Fluoro dish, World Precision Instruments) coated with 0.01 mg/ml Fibronectin, cell behaviour was filmed for 2hours by a WaveFX spinning disc confocal (Quorum technologies) mounted on an automated DMI6000B Leica microscope, controlled with Volocity 3DM software (Improvision). Image

processing consisted of merging 2 to 3 planes from z stacks, assigning pseudocolors, and adjusting image contrast using Metamorph software.

Analysis of Eph and p-Eph levels by Western Blot

Cells from 14 ectoderm and mesoderm dissected explants were dissociated and an equal amount of cells were re-aggregated either as mixed ectoderm/mesoderm aggregates, or as separate ectoderm and mesoderm aggregates for 1hr on agarose-coated plates in 1X MBSH. Mixed aggregates formed both homotypic ectoderm-ectoderm and mesoderm-mesoderm contacts as well heterotypic ectoderm-mesoderm contacts, which mimicked the contacts at the boundary.

The re-aggregation time was set to maximize heterotypic contacts. Separate homotypic aggregates were combined for extraction, thus yielding the same amount of material as the mixed aggregates, and served as control. Extracts were probed by Western blot for EphA, EphB, p-EphA and p-EphB.

Plasmids and constructs:

Membrane-targeted GFP and Cherry, Xenopus ephrinB1 and ephrinB2 were described previously (Rohani et al., 2011). Xenopus EphB4 and ephrinB3 in pCS2+ were gifts from Dr. A. Brändli (Helbling et al., 1999). Xenopus EphA4 (Pagliaccio) in pBluescript KS by DR Bob Winning (Winning & Sargent, 1994) was a gift from DR T. Sargent. Chicken EphA4-GFP in peGFPN2 was a gift from Dr. A. Kania (Kania, Johnson, & Jessell, 2000). EphA4 was subcloned into the pCS2+and C-terminally fused to eYFP. Alk4*, a constitutively active Activin receptor, was a gift from Dr. J. Smith (Armes & Smith, 1997). β-catenin in pSP36T was a gift from Drs. P. McCrea and B.M. Gumbiner (McCrea et al., 1993).

To construct Eph chimeras with swapped cytoplasmic domains a restriction site was introduced at the end of transmembrane domain in each original receptor (Nhe1 for EphB4 and Spe1 for EphA4) by site-directed mutagenesis (Quick Change XII, Stratagene). The two resulting mutants, called EphA4* and EphB4*, had respectively a change from bp1926 tgtcat to actagt and from bp 1763 ggtggt

to gctagc corresponding to a V to L and V to A substitution corresponding to the last hydrophobic amino acid of the trans memberane domain amino acid 558-559 of Xenopus EphB4 and EphA4 .EphA4* was subcloned into pCS2+ for consistency with EphB4. EphA4* and EphB4* in pCS2+ rescued loss of the corresponding endogenous Ephs with the same efficiency as the original A4 and B4 constructs (Fig.3.1E). The newly introduced Spe1 and Nhe1 sites were used to cut and exchange the fragments corresponding to the sequences of the cytoplasmic tails, yielding EphA4B4 (extracellular and transmembrane domains of A4 and cytoplasmic tail of B4) and EphB4A4 (extracellular and transmembrane domains of B4 and cytoplasmic tail of A4).

RT-PCR and qPCR

RT-PCR was performed using mRNA extracted from whole stage 9-12 embryos (Rohani et al., 2011). Loading was equalized by comparing levels of FGFR. Two independent experiments showed identical temporal patterns of expression. RT-qPCR was performed using mRNA extracted from ectoderm and dorsal mesoderm at stage 10.5. qPCR was carried out using CFX 96 Thermo cycler (Biorad). The PCR reactions were set up using 5 µl of RT (20 to 50 times diluted) with 5 µl of SYBR green (Biorad) ½ dilution , 5 µl of 3X PCR-MgCl2 buffer (Invitrogen) , 5µl of 6% dilution of primers (6 pM). The primers are listed below. Cycling conditions were: 94°C for 15 sec, and 58°C for 30 sec, 72.0°C for 1 min. Quantification was based on a dilution series (5 fold steps) of the whole embryo RT. Relative expression levels were normalized as ratio to ODC, a ubiquitous gene with homogenous distribution in Xenopus embryos(Tannahill, Isaacs, Close, Peters, & Slack, 1992). Reaction efficiencies determined from calibration curves for each primer were between 85 and 120%.

Simulation of ephrin-Eph signal outputs

Principle and assumptions

We used a semi-quantitative model to estimate ephrin-Eph signaling outputs under conditions of complex receptor-ligand expression. While actual ephrin/Eph

binding must follow complex rules, due in particular to restricted diffusion in the two dimensions of the cell membrane, cooperative binding and multimerisation, we based our model on simple mass action (supplementary Fig.3.S4).

We applied the mass action law to write

$$Kd = [ephrinfree][Ephfree]/[ephrin\text{-}Eph] \quad (1)$$

with [ephrinfree] and [Ephfree] the membrane densities of free ephrin ligands and Eph receptors, respectively, and [ephrin-Eph] the density of bound receptors. Further, the total density of ephrins [ephrintot] = [ephrinfree] + [ephrin-Eph] and that of receptors [Ephtot] = [Ephfree] + [ephrin-Eph]. Inserting this into Eq. (1) yields

$$[ephrin\text{-}Eph] = [ephrintot][Ephtot]/ Kd + [ephrintot] + [Ephtot] - [ephrin\text{-}Eph] \quad (2).$$

We approximated the denominator by

$$Kd + f([ephrintot] + [Ephtot]) \quad (3),$$

introducing $f<1$ as a dimensionless correction factor which reduces the value of the denominator instead of the subtraction of [ephrin-Eph]. Varying f between 0 and 0.8 changed the output strengths but had little effect on their relative order (boundary > mesoderm > ectoderm).

Forward signal intensity Sf for a particular ephrin-Eph pair was thus calculated as

$$Sf = [ephrin\text{-}Eph] = [ephrintot]*[Ephtot]/(Kd + f* ([ephrintot]+[Ephtot])) \quad (4).$$

Equation (4) was used to calculate forward signal output for each ephrin-Eph pair, within each tissue and at tissue interfaces. We estimated the contribution of reverse signals by expressing them as a fraction r of the forward signal, Sr = Sf * r. For ephrinB3, which transmitted a strong reverse signal in both ectoderm and mesoderm, we set r = 1; for ephrinB2, based on its mild reverse activity in functional assays (not shown), r = 0.3. Reverse ephrinB2 signal was exclusively found in the mesoderm. EphrinB1 showed no detectable reverse activity (data not

shown). Reverse signaling only provided a minor contribution to the global outputs in our simulations.

Parameter values

Apparent concentrations

We assumed that membrane densities were proportional to the relative mRNA levels for all ephrins and Ephs. We set the highest mRNA level encountered as unity, and expressed all others as fractions thereof. We then converted these values to nM units by multiplication with a factor which gave realistic protein concentrations to be used with published kD values. This conversion factor was varied to obtain different ranges of nominal concentrations to be compared in our model. We found that, for both dorsal and ventral boundaries, very similar global output patterns were obtained over a wide range of apparent concentrations, with an upper limit close to 50nM for the most abundant ephrinB3, to the lowest tested range (fM). The range that yielded the expected behavior at the notochord boundary was narrower.

Apparent affinities

Apparet affinities were directly taken from in vitro biochemical affinity values (Blits-Huizinga et al., 2004; Flanagan & Vanderhaeghen, 2003). Some were however adapted to take into account the results of our functional and biochemical experiments: for ephrinB1-EphB2 interaction, which was found to be much less effective than ephrinB2-EphB2, the value was decreased to 10nM, which corresponded to the category of intermediate-range ephrin-Eph interactions, between high (0.5-2nM) and the low "non-specific" (<100nM) affinities(Blits-Huizinga et al., 2004; Flanagan & Vanderhaeghen, 2003). EphrinB2-EphA4 and ephrin B3-EphA4, which reacted much more intensively than predicted from the published values, had their affinity increased to the range of the other strong interactions (~1nM as for ephrinB2-EphB2 and ephrinB2-EphB4). Note however that the model still correctly simulated the increased signal at the boundaries even when using the weaker published affinities.

Acknowledgements

We thank Dr. Keith Murai for enlightening discussions and critical reading of the manuscript. We thank the various researchers who provided us with reagents, in particular Drs. Pasquale and Greenberg for the generous gift of antibodies. We thank the CIAN for support with confocal imaging. This work was supported by CCSRI grants # 017162/ 700915 to FF and by CIHR grant # MOP-53075 to RW.

References

Armes, N.A., & Smith, J.C. (1997). The ALK-2 and ALK-4 activin receptors transduce distinct mesoderm-inducing signals during early Xenopus development but do not co-operate to establish thresholds. *Development, 124*(19), 3797-3804.

Astin, Jonathan W., Batson, Jennifer, Kadir, Shereen, Charlet, Jessica, Persad, Raj A., Gillatt, David, . . . Nobes, Catherine D. (2010). Competition amongst Eph receptors regulates contact inhibition of locomotion and invasiveness in prostate cancer cells. *Nat Cell Biol, 12*(12), 1194-1204. doi: http://www.nature.com/ncb/journal/v12/n12/abs/ncb2122.html#supplementary-information

Bisson, Nicolas, Poitras, Luc, Mikryukov, Alexander, Tremblay, Michel, & Moss, Tom. (2007). EphA4 Signaling Regulates Blastomere Adhesion in the Xenopus Embryo by Recruiting Pak1 to Suppress Cdc42 Function. *Mol. Biol. Cell, 18*(3), 1030-1043. doi: 10.1091/mbc.E06-04-0294

Blits-Huizinga, Carla T., Nelersa, Claudiu M., Malhotra, Arun, & Liebl, Daniel J. (2004). Ephrins and their Receptors: Binding versus Biology. *IUBMB Life, 56*(5), 257-265. doi: 10.1080/15216540412331270076

Chen, Yumei, Mironova, Ekaterina, Whitaker, Lisha L., Edwards, Laura, Yost, H. Joseph, & Ramsdell, Ann F. (2004). ALK4 functions as a receptor for multiple TGFβ-related ligands to regulate left–right axis determination and mesoderm induction in Xenopus. *Developmental Biology, 268*(2), 280-294. doi: 10.1016/j.ydbio.2003.12.035

Cooke, Julie E., Kemp, Hilary A., & Moens, Cecilia B. (2005). EphA4 Is Required for Cell Adhesion and Rhombomere-Boundary Formation in the Zebrafish. *Current Biology, 15*(6), 536-542. doi: http://dx.doi.org/10.1016/j.cub.2005.02.019

Cooke, Julie E., & Moens, Cecilia B. (2002). Boundary formation in the hindbrain: Eph only it were simple&. *Trends in neurosciences, 25*(5), 260-267.

Durbin, Lindsey, Brennan, Caroline, Shiomi, Kensuke, Cooke, Julie, Barrios, Arantza, Shanmugalingam, Shantha, . . . Holder, Nigel. (1998). Eph signaling is required for segmentation and differentiation of the somites. *Genes & Development, 12*(19), 3096-3109. doi: 10.1101/gad.12.19.3096

Flanagan, John G., & Vanderhaeghen, Pierre. (2003). THE EPHRINS AND EPH RECEPTORS IN NEURAL DEVELOPMENT. *Annual Review of Neuroscience, 21*(1), 309-345. doi: 10.1146/annurev.neuro.21.1.309

Gale, Nicholas W., Holland, Sacha J., Valenzuela, David M., Flenniken, Ann, Pan, Li, Ryan, Terrence E., . . . Yancopoulos, George D. (1996). Eph Receptors and Ligands Comprise Two Major Specificity Subclasses and Are Reciprocally Compartmentalized during Embryogenesis. *Neuron, 17*(1), 9-19. doi: 10.1016/s0896-6273(00)80276-7

Gallo, Gianluca, Yee, Hal F., & Letourneau, Paul C. (2002). Actin turnover is required to prevent axon retraction driven by endogenous actomyosin contractility. *The Journal of Cell Biology, 158*(7), 1219-1228. doi: 10.1083/jcb.200204140

Groeger, Gillian, & Nobes, Catherine D. (2007). Co-operative Cdc42 and Rho signaling mediates ephrinB-triggered endothelial cell retraction. *Biochem J, 404*(1), 23-29. doi: 10.1042/bj20070146

Harbott, Lene K., Marston, Daniel J., & Nobes, Catherine D. (2004). Ephrin-Regulated Contact Repulsion of Growth Cones. In M. P. P. C. Anne Ridley (Ed.), *Cell Motility* (pp. 61-74).

Helbling, Paul M., Saulnier, Didier M.E., Robinson, Vicky, Christiansen, Jeff H., Wilkinson, David G., & Brändli, André W. (1999). Comparative analysis of embryonic gene expression defines potential interaction sites for *Xenopus* EphB4 receptors with ephrin-B ligands. *Developmental Dynamics, 216*(4/5), 361-373.

Himanen, Juha-Pekka, Chumley, Michael J., Lackmann, Martin, Li, Chen, Barton, William A., Jeffrey, Phillip D., . . . Nikolov, Dimitar B. (2004). Repelling class discrimination: ephrin-A5 binds to and activates EphB2 receptor signaling. *Nat Neurosci, 7*(5), 501-509. doi: http://www.nature.com/neuro/journal/v7/n5/suppinfo/nn1237_S1.html

Hruska, Martin, & Dalva, Matthew B. (2012). Ephrin regulation of synapse formation, function and plasticity. *Molecular and Cellular Neuroscience, 50*(1), 35-44. doi: 10.1016/j.mcn.2012.03.004

Hwang, Yoo-Seok, Lee, Hyun-Shik, Kamata, Teddy, Mood, Kathleen, Cho, Hee Jun, Winterbottom, Emily, . . . Daar, Ira O. (2013). The Smurf ubiquitin ligases regulate tissue separation via antagonistic interactions with ephrinB1. *Genes & Development, 27*(5), 491-503. doi: 10.1101/gad.208355.112

Jones, Teri L., Chong, Lisa D., Kim, Jaebong, Xu, Ren-He, Kung, Hsiang-Fu, & Daar, Ira O. (1998). Loss of cell adhesion in Xenopus laevis embryos mediated by the cytoplasmic domain of XLerk, an erythropoietin-producing hepatocellular ligand. *Proceedings of the National Academy of Sciences of the United States of America, 95*(2), 576-581.

Kania, Artur, Johnson, Randy L., & Jessell, Thomas M. (2000). Coordinate Roles for LIM Homeobox Genes in Directing the Dorsoventral Trajectory of Motor Axons in the Vertebrate Limb. *Cell, 102*(2), 161-173. doi: 10.1016/s0092-8674(00)00022-2

Kao, Tzu-Jen, & Kania, Artur. (2011). Ephrin-Mediated cis-Attenuation of Eph Receptor Signaling Is Essential for Spinal Motor Axon Guidance. *Neuron, 71*(1), 76-91.

Kemp, Hilary A., Cooke, Julie E., & Moens, Cecilia B. (2009). EphA4 and EfnB2a maintain rhombomere coherence by independently regulating intercalation of progenitor cells in the zebrafish neural keel. *Developmental Biology, 327*(2), 313-326.

Krens, S. F. Gabby, Möllmert, Stephanie, & Heisenberg, Carl-Philipp. (2011). Enveloping cell-layer differentiation at the surface of zebrafish germ-layer tissue explants. *Proceedings of the National Academy of Sciences, 108*(3), E9-E10. doi: 10.1073/pnas.1010767108

Krieg, M., Arboleda-Estudillo, Y., Puech, P. H., Kafer, J., Graner, F., Muller, D. J., & Heisenberg, C. P. (2008). Tensile forces govern germ-layer organization in zebrafish. *Nat Cell Biol, 10*(4), 429-436.

Kullander, K., & Klein, R. (2002). Mechanisms and functions of Eph and ephrin signaling. *Nature reviews, 3*, 475-485.

Luu, Olivia, David, Robert, Ninomiya, Hiromasa, & Winklbauer, Rudolf. (2011). Large-scale mechanical properties of Xenopus embryonic epithelium. *Proceedings of the National Academy of Sciences, 108*(10), 4000-4005. doi: 10.1073/pnas.1010331108

Marquardt, Till, Shirasaki, Ryuichi, Ghosh, Sourav, Andrews, Shane E., Carter, Nigel, Hunter, Tony, & Pfaff, Samuel L. (2005). Coexpressed EphA Receptors and Ephrin-A Ligands Mediate Opposing Actions on Growth Cone Navigation from Distinct Membrane Domains. *Cell, 121*(1), 127-139. doi: 10.1016/j.cell.2005.01.020

McCrea, P D, Brieher, W M, & Gumbiner, B M. (1993). Induction of a secondary body axis in Xenopus by antibodies to beta-catenin. *The Journal of Cell Biology, 123*(2), 477-484. doi: 10.1083/jcb.123.2.477

Murai, Keith K., & Pasquale, Elena B. (2003). Eph'ective signaling: forward, reverse and crosstalk. *Journal of Cell Science, 116*(14), 2823-2832.

Park, Edmond Changkyun, Cho, Gun-Sik, Kim, Gun-Hwa, Choi, Sun-Cheol, & Han, Jin-Kwan. (2011). The involvement of Eph–Ephrin signaling in tissue separation and convergence during Xenopus gastrulation movements. *Developmental Biology, 350*(2), 441-450. doi: 10.1016/j.ydbio.2010.12.012

Pasquale, Elena B. (2004). Eph-ephrin promiscuity is now crystal clear. *Nat Neurosci, 7*(5), 417-418.

Poliakov, Alexei, Cotrina, Maria L., Pasini, Andrea, & Wilkinson, David G. (2008). Regulation of EphB2 activation and cell repulsion by feedback control of the MAPK pathway. *The Journal of Cell Biology, 183*(5), 933-947. doi: 10.1083/jcb.200807151

Poliakov, Alexei, Cotrina, Marisa, & Wilkinson, David G. (2004). Diverse Roles of Eph Receptors and Ephrins in the Regulation of Cell Migration and Tissue Assembly. *Developmental Cell, 7*(4), 465-480.

Qin, Haina, Noberini, Roberta, Huan, Xuelu, Shi, Jiahai, Pasquale, Elena B., & Song, Jianxing. (2010). Structural Characterization of the EphA4-Ephrin-B2 Complex Reveals New Features Enabling Eph-Ephrin Binding Promiscuity. *Journal of Biological Chemistry, 285*(1), 644-654. doi: 10.1074/jbc.M109.064824

Rohani, Nazanin, Canty, Laura, Luu, Olivia, Fagotto, François, & Winklbauer, Rudolf. (2011). EphrinB/EphB Signaling Controls Embryonic Germ Layer Separation by Contact-Induced Cell Detachment. *PLoS Biol, 9*(3), e1000597. doi: 10.1371/journal.pbio.1000597

Smith, Alexa, Robinson, Vicky, Patel, Ketan, & Wilkinson, David G. (1997). The EphA4 and EphB1 receptor tyrosine kinases and ephrin-B2 ligand regulate targeted migration of branchial neural crest cells. *Current biology : CB, 7*(8), 561-570.

Tanaka, Masamitsu, Kamo, Takaharu, Ota, Satoshi, & Sugimura, Haruhiko. (2003). Association of Dishevelled with Eph tyrosine kinase receptor and ephrin mediates cell repulsion. *EMBO J, 22*(4), 847-858.

Tannahill, D., Isaacs, H.V., Close, M.J., Peters, G., & Slack, J.M. (1992). Developmental expression of the Xenopus int-2 (FGF-3) gene: activation by mesodermal and neural induction. *Development, 115*(3), 695-702.

Wacker, Stephan, Grimm, Kristina, Joos, Thomas, & Winklbauer, Rudolf. (2000). Development and Control of Tissue Separation at Gastrulation in Xenopus. *Developmental Biology, 224*(2), 428-439.

Winklbauer, Rudolf, & Keller, Ray E. (1996). Fibronectin, Mesoderm Migration, and Gastrulation in Xenopus. *Developmental Biology, 177*(2), 413-426.

Winklbauer, Rudolf, & Kwang, W. Jeon. (2009). Chapter 5 Cell Adhesion in Amphibian Gastrulation *International Review of Cell and Molecular Biology* (Vol. Volume 278, pp. 215-275): Academic Press.

Winning, Robert S., & Sargent, Thomas D. (1994). Pagliaccio, a member of the Eph family of receptor tyrosine kinase genes, has localized expression in a subset of neural crest and neural tissues in Xenopus laevis embryos. *Mechanisms of Development, 46*(3), 219-229. doi: 10.1016/0925-4773(94)90072-8

Figure Legends

Figure 3.1:

(A) Ephrin-Eph signaling is required for ectoderm-mesoderm separation. COMO: Control morpholino. The boundary separating ectoderm (E) from mesoderm (M) is marked by arrowheads. EphrinB3 MO: Depletion of ephrins or Ephs (here ephrinB3) by injection of antisense morpholino oligonucleotides (MO) causes loss of ectoderm-mesoderm boundary. Arrowheads point to a fuzzy remnant of ectoderm-mesoderm interface. (B) Diagram of the early Xenopus gastrula and of the tissue separation assay. (B') Ectoderm injected with ephrinB3 MO fail to maintain separation and incorporate mesoderm explants (arrows). Arrowheads: explants remaining separated.(C) Asymmetric expression of multiple ephrins and Ephs across the ectoderm-mesoderm boundary. Schematic representation of the relative expression of ephrins and Eph receptors analyzed in this study, based on RT-qPCR (Supplementary Fig.3.S1A).(D) Each ephrin/Eph is specifically required and not replaceable. EphrinB1 and ephrinB3 were depleted in the ectoderm (eB1MO, eB3MO), and EphA4 in the mesoderm (A4MO). Separation could be restored by treating directly the surface of the other tissue explant for 15 min with soluble Fc fragments of the corresponding ephrin/Eph molecule, but not with other ephrins/Ephs. cFc: control anti-human Fc antibody. * and ** = $p<0.05$ and $p<0.01$ (Student's Ttest). (E) The specific role of Eph receptors requires their extracellular domain but the cytoplasmic tails are interchangeable. Chimeras were designed in which cytoplasmic domains of EphA4 and EphB4 were swapped (AB and BA). Each chimera was tested for the ability to rescue depletion of endogenous EphA4 in the mesoderm or EphB4 in the ectoderm. Separation could be rescued by the constructs that contained the corresponding extracellular domain (AB for EphA4, BA for EphB4), but not by the constructs that contained the cytoplasmic domain. A* and B* were control constructs which were wild type except for two amino acids within the end of the transmembrane domain, which had to be substituted in AB and BA to produce the chimeric constructs (see Supplementary Materials and Methods).

Figure 3.1

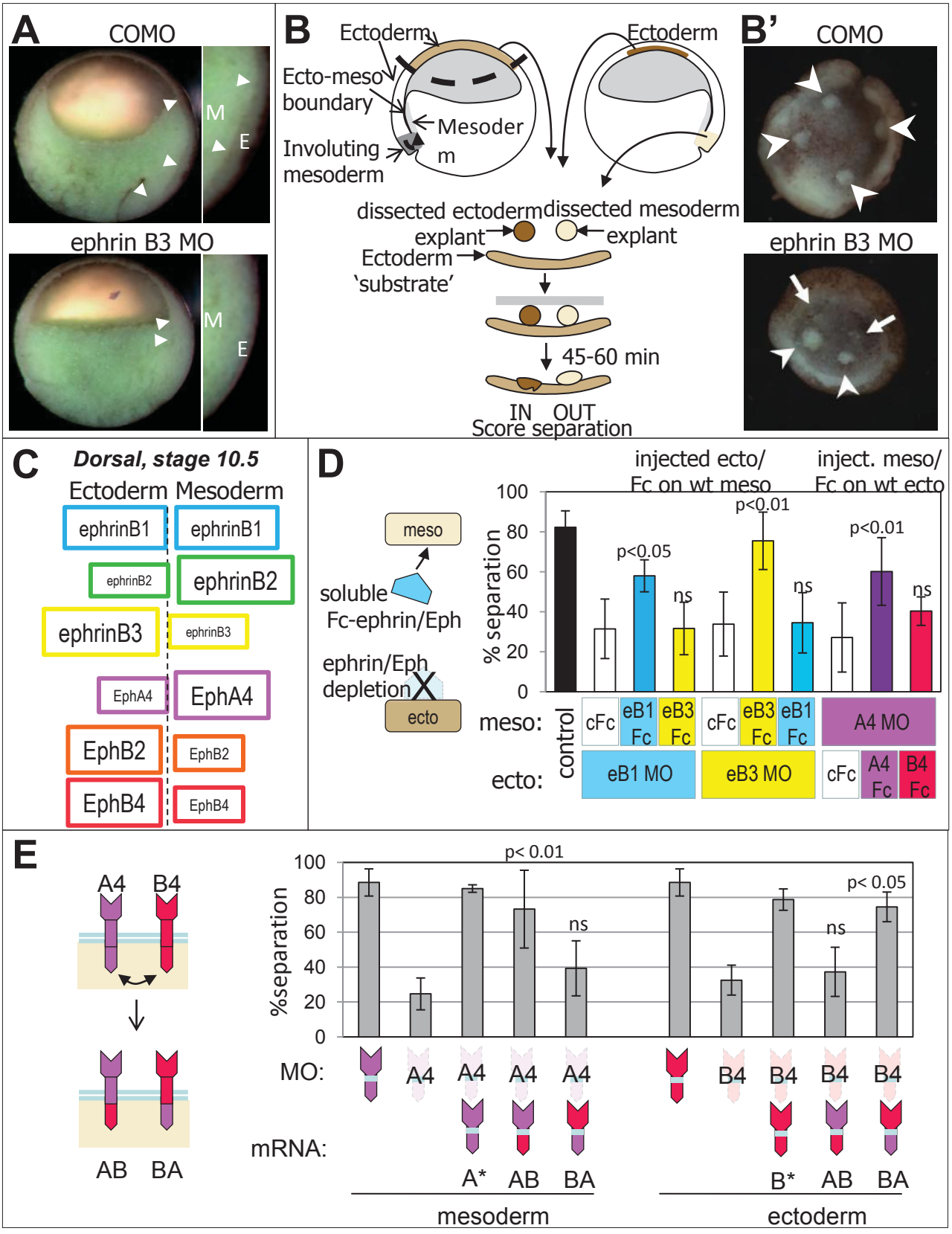
A
COMO
M
E
ephrin B3 MO
M
E
B
Ectoderm
Ecto-meso boundary
Involuting mesoderm
Mesoderm
Ectoderm
dissected ectoderm explant
dissected mesoderm explant
Ectoderm 'substrate'
45-60 min
IN OUT
Score separation
B'
COMO
ephrin B3 MO
C
Dorsal, stage 10.5
Ectoderm Mesoderm
ephrinB1
ephrinB2
ephrinB3
EphA4
EphB2
EphB4
D
meso
soluble Fc-ephrin/Eph
ephrin/Eph depletion
ecto
injected ecto/ Fc on wt meso
inject. meso/ Fc on wt ecto
% separation
p<0.05
p<0.01
ns
meso:
ecto:
control
cFc
eB1 Fc
eB3 Fc
A4 MO
eB1 MO
eB3 MO
A4 Fc
B4 Fc
E
A4
B4
AB
BA
%separation
p< 0.01
p< 0.05
ns
MO:
mRNA:
A*
AB
BA
B*
mesoderm
ectoderm

Figure 3.2:

(A) Characterization of functional ephrin-Eph specificity and identification of functional cognate receptors. Separation was induced ectopically between two explants from the same tissue (ectoderm-ectoderm or mesoderm-mesoderm) by direct stimulation with ephrins/Ephs normally enriched in the other tissue (see Fig.3.1C), thus mimicking the endogenous asymmetric ephrin/Eph expression. The endogenous functional partners where then identified by depleting of single candidates and determining which of them was required for ectopic separation. (A) Control ectoderm explants mixed completely. Separation of ectoderm explants was induced by soluble Fc fragments corresponding to "mesoderm-specific" ephrinB2, but not ephrinB1, already endogenously enriched in the ectoderm. EphrinB2-Fc-induced separation was strongly inhibited by EphB4MO (red arrow), but only weakly by EphB2MO, indicating that EphB4 is the main receptor for ephrinB2. (A') Mesoderm aggregates were tested on large mesoderm layers artificially produced in the animal pole of the embryo (see Supplementary Materials and Methods). Separation was induced by Fc fragments of "ectoderm-specific" ephrinB3, but not ephrinB2. Ephrin3-induced separation was reversed by EphA4MO but not by EphB4MO (red arrow). (A") Ectopic separation between ectoderm explants was induced specifically by "mesodermal" EphA4 but not by "ectodermal" EphB4. Separation was inhibited only by ephrinB3MO (red arrow). (A"') Examples of mixing of ectoderm explants incubated with control Fc (arrows) and of separation of ectoderm explants treated with EphA4-Fc (arrowheads). (B) Biochemical analysis of differential activation of Eph receptors by ephrin ligands. Ectoderm explants were treated with 20mM ephrinB1, B2, B3 Fc fragments or with control anti-Fc antibodies for 1 hour, and then lysed. Endogenous EphB2 and EphB4, and EphA4-YFP were immunoprecipitated and analyzed by immunoblots for phospho-tyrosine and for total Eph levels. EphA4 was strongly phosphorylated in response to both ephrinB2 and ephrinB3, but not ephrinB1, which gave levels similar to negative controls. EphB2 responded strongly to ephrinB2, and only weakly to ephrinB1. EphB4 was highly phosphorylated in response to ephrinB2, while activation by ephrinB1 or

ephrinB3 was negligible. IgG: control immunoprecipitation with non-immune IgGs.

Figure 3.2

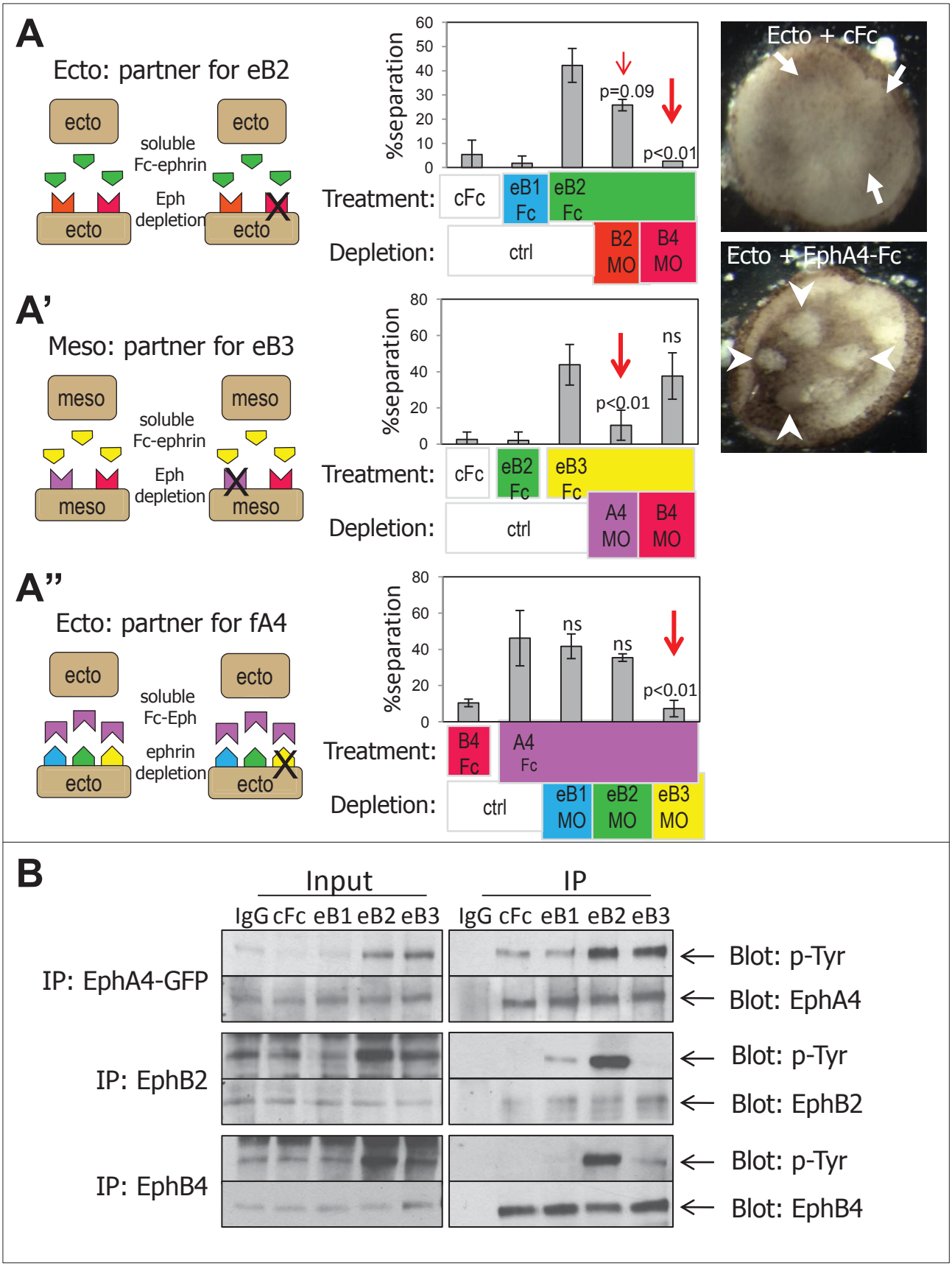
A
Ecto: partner for eB2
ecto
ecto
soluble
Fc-ephrin
Eph
depletion
ecto
ecto
%separation
p=0.09
p<0.01
Treatment:
cFc
eB1 Fc
eB2 Fc
Depletion:
ctrl
B2 MO
B4 MO
Ecto + cFc
A'
Meso: partner for eB3
meso
meso
soluble
Fc-ephrin
Eph
depletion
meso
meso
%separation
ns
p<0.01
Treatment:
cFc
eB2 Fc
eB3 Fc
Depletion:
ctrl
A4 MO
B4 MO
Ecto + EphA4-Fc
A''
Ecto: partner for fA4
ecto
ecto
soluble
Fc-Eph
ephrin
depletion
ecto
ecto
%separation
ns
ns
p<0.01
Treatment:
B4 Fc
A4 Fc
Depletion:
ctrl
eB1 MO
eB2 MO
eB3 MO
B
Input
IP
IgG cFc eB1 eB2 eB3
IgG cFc eB1 eB2 eB3
IP: EphA4-GFP
Blot: p-Tyr
Blot: EphA4
IP: EphB2
Blot: p-Tyr
Blot: EphB2
IP: EphB4
Blot: p-Tyr
Blot: EphB4

Figure 3.3:

Ectoderm-mesoderm separation relies purely on asymmetric expression of specific ephrin/Eph pairs across the boundary, irrespective of the direction of the asymmetry. (A) Summary of the main ectoderm and mesoderm-enriched ephrins/Ephs and of the preferred functional interactions. (B) EphrinB3 was depleted in the ectoderm and EphA4 in the mesoderm. The resulting loss of separation was rescued by their re-expression in the opposite tissue (i.e. ephrinB3 in the mesoderm and EphA4 in the ectoderm, red arrow). Separation required the appropriate specific pair of ephrin/Eph, as expression of EphB4, which cannot function as receptor for ephrinB3 was unable to rescue.

Figure 3.3

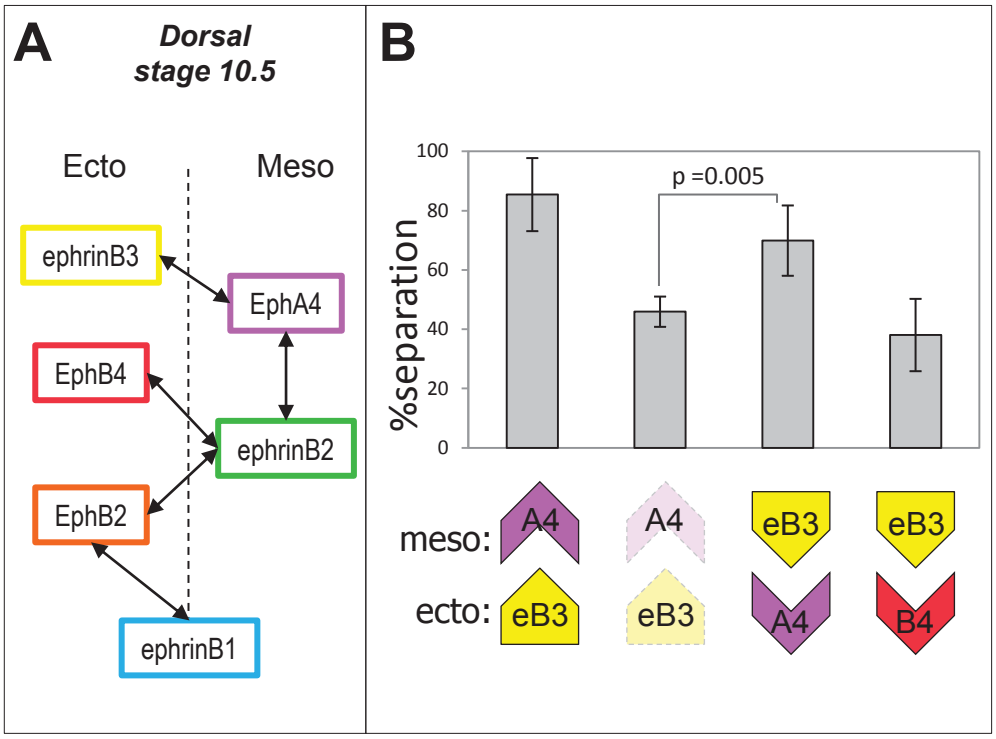
A
Dorsal
stage 10.5
Ecto
Meso
ephrinB3
EphA4
EphB4
ephrinB2
EphB2
ephrinB1
B
100
80
60
40
20
0
%separation
p =0.005
meso:
ecto:
A4
A4
eB3
eB3
eB3
eB3
A4
B4

Figure 3.4:

Increased Eph receptor and myosin activation at the ectoderm-mesoderm contacts (A) Detection of phospho-EphB by immunofluorescence of a sagittal section from wild type early gastrula embryo. The upper panel shows a general view of the dorsal region, the lower panel an enlarged view of the ectoderm-mesoderm boundary. (A') Quantification of signal intensity measured for phospho-EphB and phospho-EphA at cell-cell contacts along the boundary and inside each tissue. (B, B') Biochemical comparison of Eph phosphorylation levels between homogenous tissue aggregates and mixed ectoderm mesoderm aggregates. (B) Schematic description of the experiment: Dissociated ectoderm and mesoderm cells were mixed and left to re-aggregate for 30 min, which produced a maximal number of "heterotypic" ectoderm-mesoderm contacts mimicking contacts at the boundary. Homogenates from these mixed aggregates (E/M mix) were compared to the same amount of cells assembled into separate ectoderm and mesoderm aggregates, thus forming only "homotypic" contacts, and combined during homogeneization (E+M ctrl). (B') Western blots were probed for total and phospho-EphA, phospho-EphB, total EphA and EphB. Mixed aggregates showed reproducibly higher level of p-Eph signals (arrows), which indicate stronger activation at boundary contacts. Arrowheads: non-specific bands. GAPDH was used as loading control. (C,C',C") Selective accumulation of phospho-myosin light chain (p-MLC) along the ectoderm- mesoderm boundary and its dependence on ephrin/Eph signaling: Ectoderm and mesoderm explants were combined, incubated for 1hr, and fixed. Cryosections were immunostained for phospho-myosin light chain (p-MLC). (C) Normal boundary (underlined by a dashed line) between wild type tissues. p-MLC levels are higher in the ectoderm than the mesoderm, but highest along the boundary (arrows). Arrowheads point to p-MLC signal along membranes within each tissue. (C') Loss of p-MLC staining at the tissue interface upon Eph depletion: EphB4-depleted ectoderm and EphA4-depleted mesoderm showed largely unchanged tissue staining, but p-MLC was prominently missing from the fused interface, delineated by the dashed line. (C") Quantification of p-MLC signal intensity at the boundary and inside the tissues .

Figure 3.4

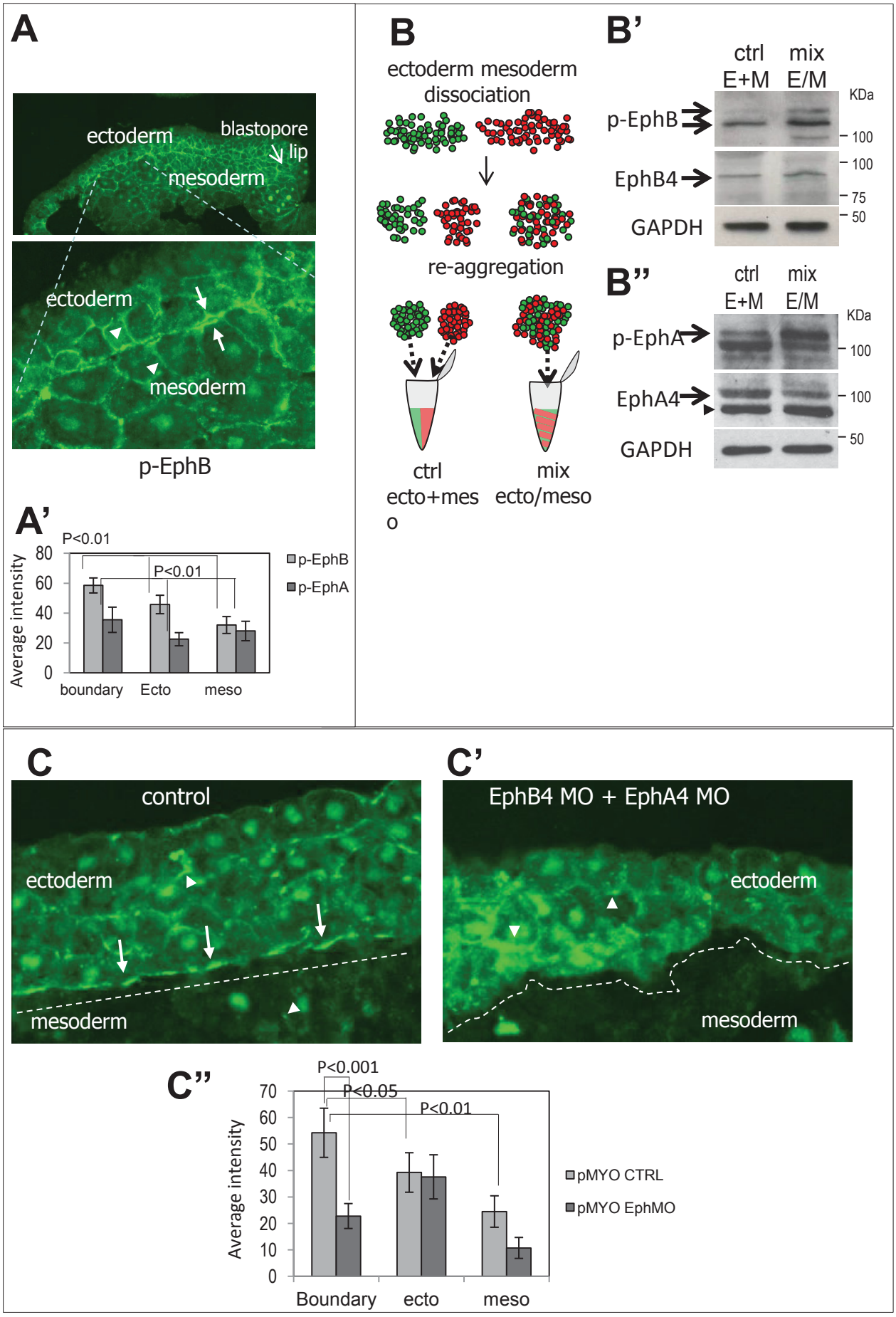
A
ectoderm
blastopore lip
mesoderm
ectoderm
mesoderm
p-EphB
A'
P<0.01
P<0.01
Average intensity
80
60
40
20
0
boundary
Ecto
meso
p-EphB
p-EphA
B
ectoderm mesoderm dissociation
re-aggregation
ctrl ecto+meso
mix ecto/meso
B'
ctrl E+M
mix E/M
KDa
p-EphB
EphB4
GAPDH
100
100
75
50
B''
ctrl E+M
mix E/M
KDa
p-EphA
EphA4
GAPDH
100
100
50
C
control
ectoderm
mesoderm
C'
EphB4 MO + EphA4 MO
ectoderm
mesoderm
C''
P<0.001
P<0.05
P<0.01
Average intensity
70
60
50
40
30
20
10
0
Boundary
ecto
meso
pMYO CTRL
pMYO EphMO

Figure 3.5:

Tissue separation is controlled by a balance between ephrin/Eph-mediated repulsion and cadherin adhesion.

(A-C). Ectoderm-mesoderm repulsion requires myosin activity and is antagonized by cadherin adhesion. Selected frames from time lapse confocal movies (Supplemental Material) showing dynamics of cell-cell contacts between single embryonic cells. Cells dissociated from ectoderm and mesoderm tissues were plated on glass coated with low amounts of fibronectin (see Materials and Methods). Ectoderm cells expressed membrane-GFP and mesoderm cells membrane-Cherry. (A) Wild type ectoderm and mesoderm cells stably attached to cells from the same tissue, but contacts between ectoderm and mesoderm cells exhibited cycles of attachments (arrowheads) and detachments (arrows) recapitulating the separation behavior observed at the boundary between the two tissues. (B) After treatment with 100μM blebbistatin, most ectoderm mesoderm contacts remained stable. (C) C-cadherin overexpression in both ectoderm and mesoderm strongly decreased detachments. Note that mesoderm cells tended to surround ectoderm cells. (D-G) Evidence for sub-threshold levels of Ephrin/Eph-mediated repulsive signals between mesoderm cells. (D) Mesoderm cells (here control MO-injected) established stable contacts (arrowheads) that were maintained (concave arrowheads) throughout the duration of the recording (1 hr). (E) Cadherin-depleted mesoderm cells (cadherin MO) showed frequent figures of re-detachments (arrows), indicating the existence of repulsive signals. (F) Stable contacts between cadherin-depleted mesoderm cells were rescued by simultaneous Eph depletion, demonstrating that the repulsion observed between mesoderm cells was due to ephrin- Eph signaling. (G) Detachment between mesoderm cells could be induced by increased ephrin-Eph-mediated repulsion through ectopic expression of ephrinB3 and EphB4, the “preferred” ectoderm partners for “mesodermal” EphA4 and ephrinB2. Corresponding frame numbers of supplementary movies are indicated. (H) Quantification of the rate of attachment detachment per cell per hour.

Figure 3.5

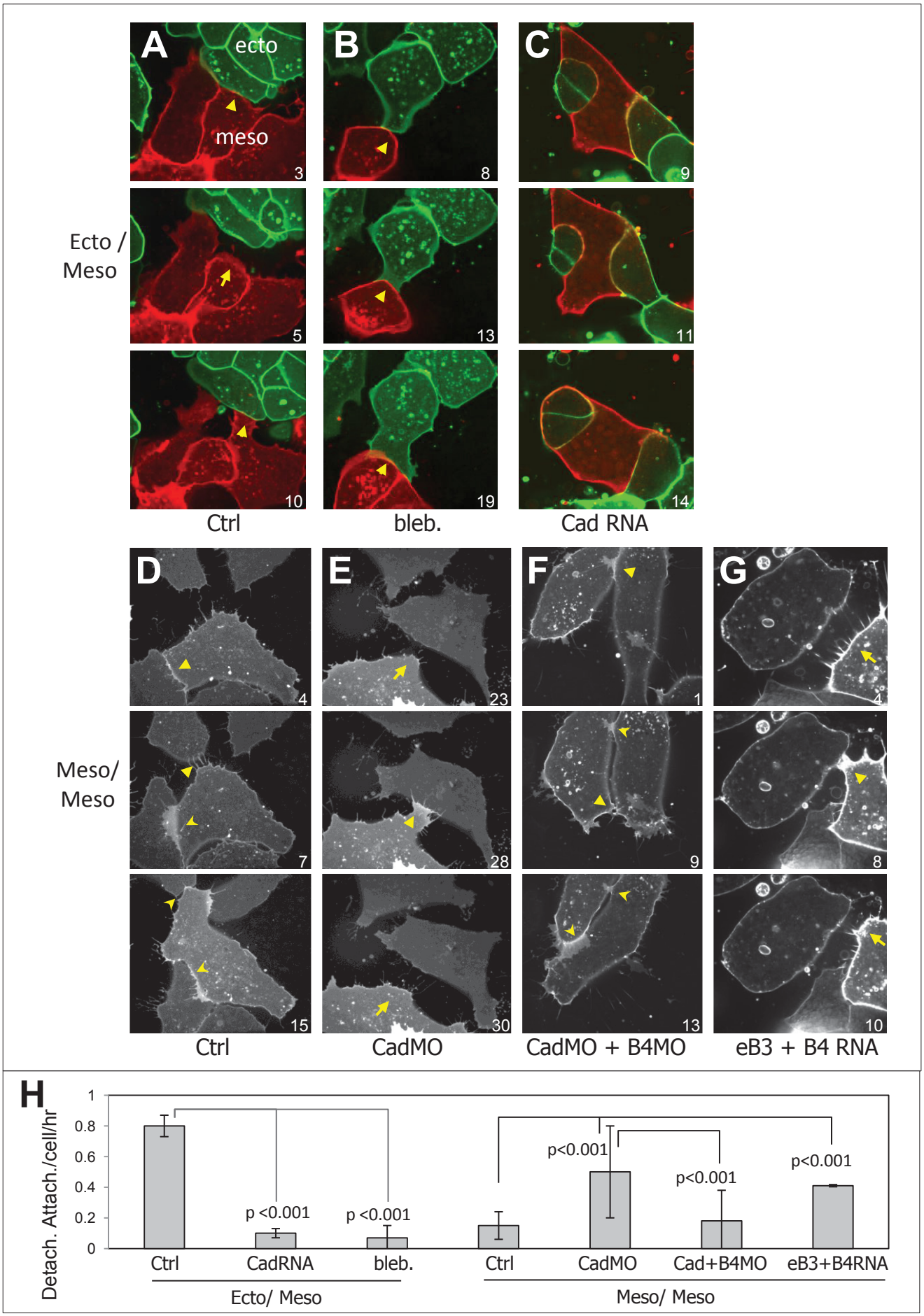
A
ecto
meso
B
C
3
8
9
Ecto / Meso
5
13
11
10
19
14
Ctrl
bleb.
Cad RNA
D
E
F
G
4
23
1
4
Meso/ Meso
7
28
9
8
15
30
13
10
Ctrl
CadMO
CadMO + B4MO
eB3 + B4 RNA
H
Detach./cell/hr
1
0.8
0.6
0.4
0.2
0
p <0.001
p <0.001
p<0.001
p<0.001
p<0.001
Ctrl
CadRNA
bleb.
Ctrl
CadMO
Cad+B4MO
eB3+B4RNA
Ecto/ Meso
Meso/ Meso

Figure 3.6:

Model and simulation of tissue separation. (A-C) Schematic representation of the three boundaries forming during Xenopus gastrulation, and simplified diagrams of the preferential ephrin-Eph pairs. The position of the boxes representing each molecule reflects its general distribution: one side of the boundary corresponds to strong asymmetric distribution. Weakly asymmetric or homogenous distributed molecules are drawn overlapping the boundary. The patterns at the dorsal and the ventral boundaries are similar, with two prominent differences for ephrinB1 and EphB4. At the end of gastrulation, the dorsal mesoderm experiences significant changes, with appearance of "ectoderm-type" ephrinB3, mostly enriched in the paraxial mesoderm (pm), which also accumulated EphB4 but excludes EphA4, now restricted to the axial mesoderm, future notochord (no). (D-E) Simulations of ephrin-Eph signaling predict enhanced activity across boundaries. Ephrin-Eph signals were computed based on the relative levels of each ephrin and Eph in each tissue and on published affinities between their extracellular domains. The resulting output were calculated by combining all signals in both directions, taking also into account all intra- and inter-tissular interactions. For the boundary, the dark blue column represents the total signal output, while the lighter columns show the ectoderm to mesoderm and mesoderm to ectoderm contributions. The values, given as arbitrary units, were kept consistent for all three boundaries. In all cases, the total signal resulted to be stronger at the boundary than in the tissues. Signal in the mesoderm was always higher than ectoderm. Parameters and individual signals are presented in supplementary Fig.3.S4.

(G-J) Simulations of gain and loss-of-function experiments. The values (arbitrary units) correspond to the total outputs across the dorsal ectoderm boundary. (G) Stimulation of repulsion between two ectoderm explants, mimicking the addition of soluble fragments (Fig.3.2). (H) Effect of ephrinB1 and B2 depletion in the mesoderm on ectoderm-mesoderm separation. (I) Effect of multiple Eph depletions in one or both tissues. (J) Reproduction of the ephrinB3-EphA4 swapping experiment of Fig.3.3.

Figure 3.6

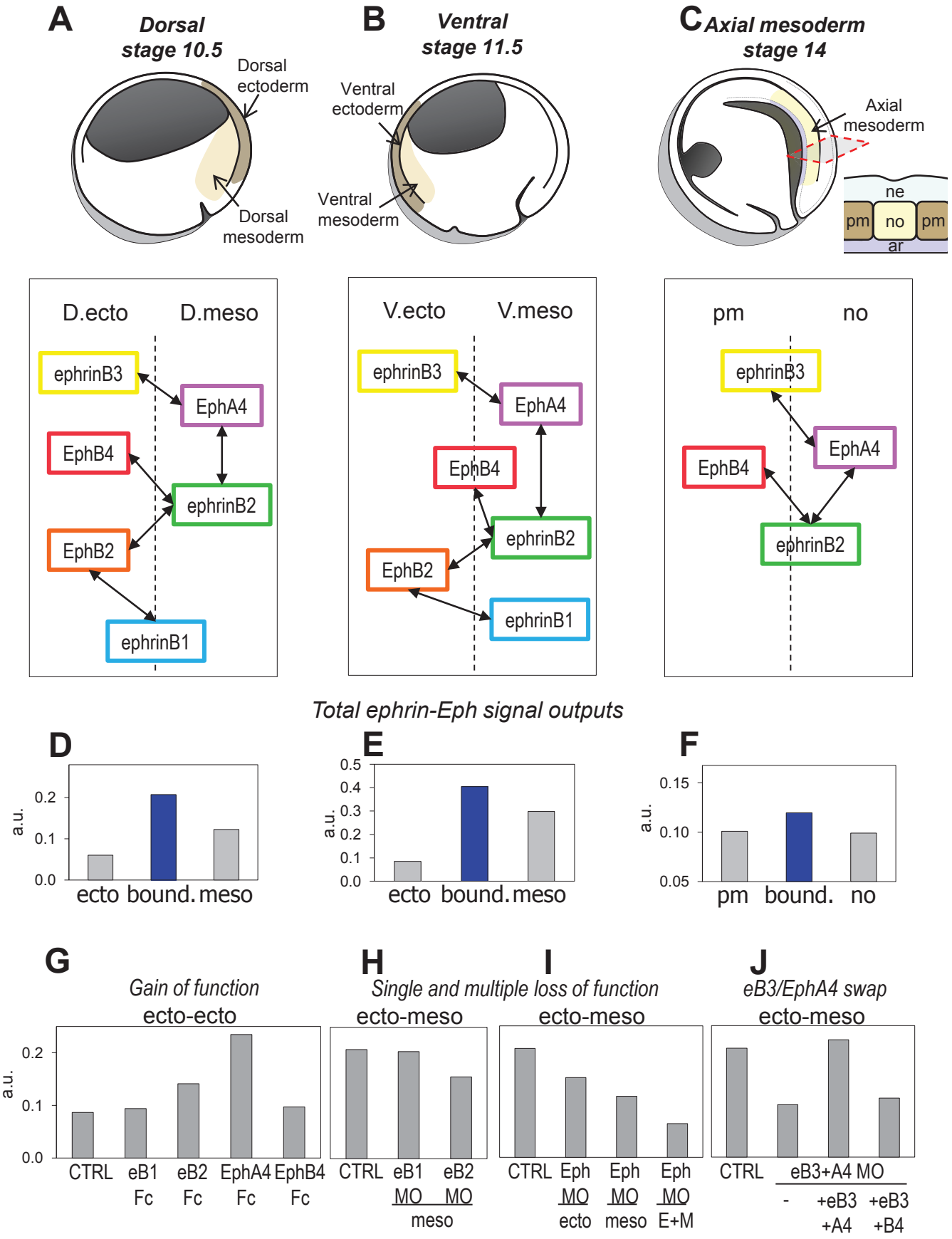
A
Dorsal
stage 10.5
Dorsal ectoderm
Dorsal mesoderm
B
Ventral
stage 11.5
Ventral ectoderm
Ventral mesoderm
C
Axial mesoderm
stage 14
Axial mesoderm
ne
pm
no
pm
ar
D.ecto
D.meso
ephrinB3
EphA4
EphB4
ephrinB2
EphB2
ephrinB1
V.ecto
V.meso
ephrinB3
EphA4
EphB4
ephrinB2
EphB2
ephrinB1
pm
no
ephrinB3
EphA4
EphB4
ephrinB2
Total ephrin-Eph signal outputs
D
a.u.
0.0
0.1
0.2
ecto bound. meso
E
a.u.
0.0
0.1
0.2
0.3
0.4
0.5
ecto bound. meso
F
a.u.
0.05
0.10
0.15
pm bound. no
G
Gain of function
ecto-ecto
a.u.
0.0
0.1
0.2
CTRL
eB1 Fc
eB2 Fc
EphA4 Fc
EphB4 Fc
H
Single and multiple loss of function
ecto-meso
CTRL
eB1 MO
eB2 MO
meso
I
ecto-meso
CTRL
Eph MO
ecto
Eph MO
meso
Eph MO
E+M
J
eB3/EphA4 swap
ecto-meso
CTRL
eB3+A4 MO
-
+eB3 +A4
+eB3 +B4

Figure 3.7:

Partially complementarily-expressed ephrins and Ephs control notochord-paraxial mesoderm separation. Manipulations were targeted to a restricted region of the dorsal mesoderm. The presence of a normal boundary was scored on sections from late gastrula embryos. Injected cells were detected by the tracer Myc-GFP (red). Only the strongest signal is visible on these images, but is sufficient to indicate the position of the injected area. Membranes were labelled with an anti-cadherin antibody (green). In D and E, FoxA4-positive nuclei appear green-cyan. FoxA4 is used as notochord marker. (B) Control notochord boundaries (arrowheads). (C) Strong disruption of both right and left boundaries (arrows) by ephrinB2 depletion. (D-E) The boundary is most effectively disrupted by ephrinB3 MO targeted to the paraxial mesoderm (D) than to the notochord (E). (F-H) EphA4 depletion in the notochord disrupts the boundary (F), which can be rescued by the AB (G) but not BA chimera (H). Thus the extracellular domain of EphA4 is necessary and sufficient for its function in the notochord. (I-K) Disruption of the boundary by EphB4 depletion in the paraxial mesoderm (I) is rescued by the BA (J) but not the AB chimera (K). (L) Quantification of boundary disruption by ephrin/Eph depletion. Disruption was scored for total embryos (t), as well as for embryos where injection was mainly targeted to the notochord (no) or to the paraxial mesoderm (pm). EphrinB2, which can interact with both EphA in the notochord and EphB4 in the paraxial mesoderm, was required in both tissues. EphrinB3 and EphB4 depletion strongly disturbed the boundary when targeted to the paraxial mesoderm, but had no effect in the notochord. The opposite was observed for EphA4, consistent with the expression patterns and the selective interactions. (M) Quantification of rescues by wild type and chimera forms of EphA4 and EphB4. In all cases, complete rescue was obtained with the corresponding wild type proteins and with the chimera containing the correct extracellular domain. The nature of intracellular domain was indifferent.

Figure 3.7

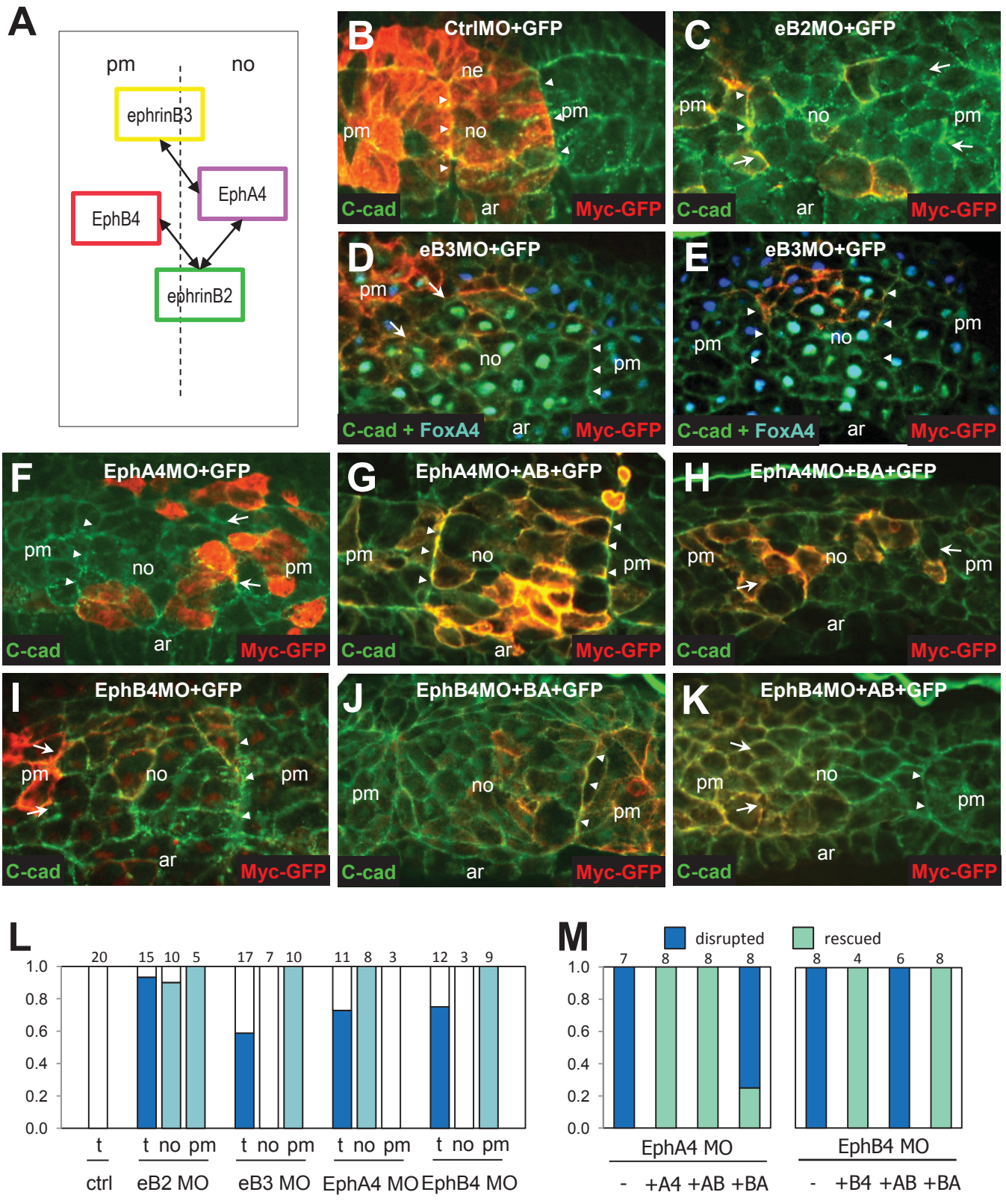
A
pm
no
ephrinB3
EphA4
EphB4
ephrinB2
B
CtrlMO+GFP
ne
pm
no
pm
C-cad
ar
Myc-GFP
C
eB2MO+GFP
pm
no
pm
C-cad
ar
Myc-GFP
D
eB3MO+GFP
pm
no
pm
C-cad + FoxA4
ar
Myc-GFP
E
eB3MO+GFP
pm
no
pm
C-cad + FoxA4
ar
Myc-GFP
F
EphA4MO+GFP
pm
no
pm
C-cad
ar
Myc-GFP
G
EphA4MO+AB+GFP
pm
no
pm
C-cad
ar
Myc-GFP
H
EphA4MO+BA+GFP
pm
no
pm
ar
C-cad
Myc-GFP
I
EphB4MO+GFP
pm
no
pm
C-cad
ar
Myc-GFP
J
EphB4MO+BA+GFP
pm
no
pm
C-cad
ar
Myc-GFP
K
EphB4MO+AB+GFP
pm
no
pm
ar
C-cad
Myc-GFP
L
20
15 10 5
17 7 10
11 8 3
12 3 9
1.0
0.8
0.6
0.4
0.2
0.0
t
t no pm
t no pm
t no pm
t no pm
ctrl
eB2 MO
eB3 MO
EphA4 MO
EphB4 MO
M
disrupted
rescued
7
8
8
8
8
4
6
8
1.0
0.8
0.6
0.4
0.2
0.0
EphA4 MO
EphB4 MO
-
+A4
+AB
+BA
-
+B4
+AB
+BA

Supplementary figure legends

Figure 3.S1:

EphrinB1-3, EphA4 and EphB1-4 temporal expression during early Xenopus development and their relative distribution in ectoderm and mesoderm of early gastrula stage

(A) RT-qPCR: Stage 10.5 ectoderm (E) and dorsal mesoderm (M). Data are compiled from two independent experiments, expressed as relative amounts. Error bars correspond to standard deviations between the two embryo batches.

(B) RT-PCR was performed for Ephrin/EphBs using mRNA extracted from whole embryos dissected at indicated stages. EphrinB1 and EphB1-4 are maternally expressed. EphrinB2, ephrinB3 and EphA4 are exclusively zygotic, starting at the onset of gastrulation (arrow).

Figure 3.S2:

Multiple Ephrin/Eph play additive role in tissue separation across the boundary.

(A) Individual and multiple knock downs. Single MO injections for each ephrin or Eph yielded a mixing phenotype, the penetrance of which related to the relative enrichment in each tissue (Supplementary Fig.3.S1B). For instance, depletion of ephrinB3 in ectoderm strongly inhibits separation, while depletion of ephrinB2 has a mild effect, while ephrinB2 depletion has a strong effect in the mesoderm. Depletion of ephrinB1 gives intermediate inhibition in both tissues. Separation remaining after multiple ephrin or Eph depletions in one tissue is ~ 30-40%. Maximal inhibition can be reached in some cases by depletion of single molecules (e.g. ephrinB3 or EphB2 in the ectoderm). Depletion of Ephs on both sides leads to almost complete inhibition of separation. Thus ephrins/Ephs play additive roles on both sides of the boundary. * and ** = $p<0.05$ and $p<0.01$ (Student's T-test) compared to controls (grey columns).

(B) Each ephrin/Eph is specifically required and not replaceable. Individual ephrins and Eph receptors were depleted in the ectoderm or in the mesoderm, which induced inhibition of separation (white columns). Separation could be fully rescued by co-injection of mRNA (amounts indicated as pg/injection) coding for the corresponding ephrin/Eph (same colors). Only partial rescue was observed

after heterotypical expression of other forms, even when expressed at high levels. * and ** indicate respectively $p<0.05$ and $p<0.01$ (Student's T-test) compared to corresponding controls (white columns). "ns" = non- significant.
(C, D) Comparison by Western blot of ephrin levels in wild type and manipulated ectoderm. C. Conditions corresponding to experiment presented in panel B. Arrow points at specific ephrin band, decreasing in eB1MO. Both bands increase in ephrinB1/3 mRNA-injected embryos. Tubulin, loading control. This blot is representative of 3 independent experiments. (D) Single and multiple ephrin depletion. Conditions are as in Figures.3.1D and S2A. In this blot, ephrinBs appear as multiple bands (arrows). (D') Conditions corresponding to experiment presented in Figure 3.3B. p-EphA4 (arrow) is increased in mixed aggregates (mix E/M) compared to ectoderm +mesoderm aggregates (E+M). This increase is abolished by depletion of ephrinB3 (eB3MO) but not ephrinB1 (eB1MO). Arrowheads: non-specific bands.

Figure 3.S3:
A) Effect of increased cadherin and of myosin inhibition on ectoderm-mesoderm separation. C-cadherin (500pg mRNA) was overexpressed in both tissues. Ephrin Fc fragments or 100μM blebbistatin were added just before recombination of the explants. Separation was significantly inhibited by cadherin overexpression or blebbistatin treatment. It was rescued by addition of soluble ephrinB2 Fc.
B-D) Tissue cohesion is compromised when cadherin is depleted or by ectopic expression of ephrin/Eph.
Dissociated ectoderm and mesoderm cells were left to re-aggregate under mild rotation. Images were taken after one hour re-aggregation. (B) Effect of cadherin and/or EphB4 depletion on mesoderm re-aggregation. (C) Effect of ephrin/Eph ectopic expression on mesoderm or ectoderm re-aggregation. Ectoderm-specific ephrinB3 and EphB4 were expressed in the mesoderm, and mesoderm-specific ephrinB2 and EphA4 in the ectoderm. (D) Aggregate quantification. Two criteria were used, which gave similar results: the average area, which reflects the extent of aggregation, and area/perimeter ratio, which integrates both the size of the

aggregates and their degree of compaction. Results from individual experiments were normalized using wild type ectoderm /mesoderm as reference (1.0) to account for batch-to-batch variation.

Figure 3.S4:

Simulation of ephrin/Eph signaling in embryonic tissues and tissue intefaces. A) Formulas and parameters used for the simulation. (B-D) Calculated signals generated by each ephrin-Eph pair for the three stages and tissue combinations (arbitrary units). (B'-D') Graphic representation of the major single ephrin-Eph interactions in the tissues and across the boundaries. The font size and the thickness of each line represents respectively the relative ephrin/Eph concentrations and the strength of the signal.

Figure 3.S5:

Ephrin/Eph gain- and loss-of-function for ventral ectoderm-mesoderm separation.
A) Summary of ephrin/Eph expression in stage 11 ventral tissues. The major differences compared to the dorsal side were the mesoderm enrichment of ephrinB1 and the even distribution of EphB4.
B) Induction of separation. Separation could be induced between two ectoderm explants by treatment with Fc fragments for mesoderm-enriched ephrinB1 and B2, but not ephrinB3. Depletion of EphB2 inhibited ephrinB1-Fc-induced separation, while EphB4 depletion had no significant effect. We conclude that EphB2 acted as preferred receptor for ephrinB1.
C) Inhibition of separation. Depletion experiments demonstrated the requirement for ephrinB3 and EphB2 on the ectoderm side, and for their corresponding partners EphA4 and ephrinB1 on the mesoderm side of the boundary. Note the stronger phenotype for ephrinB1 depletion compared to the results on the dorsal side (supplementary Fig.3.S2A), consistent with the different distributions.

Figure 3.S1

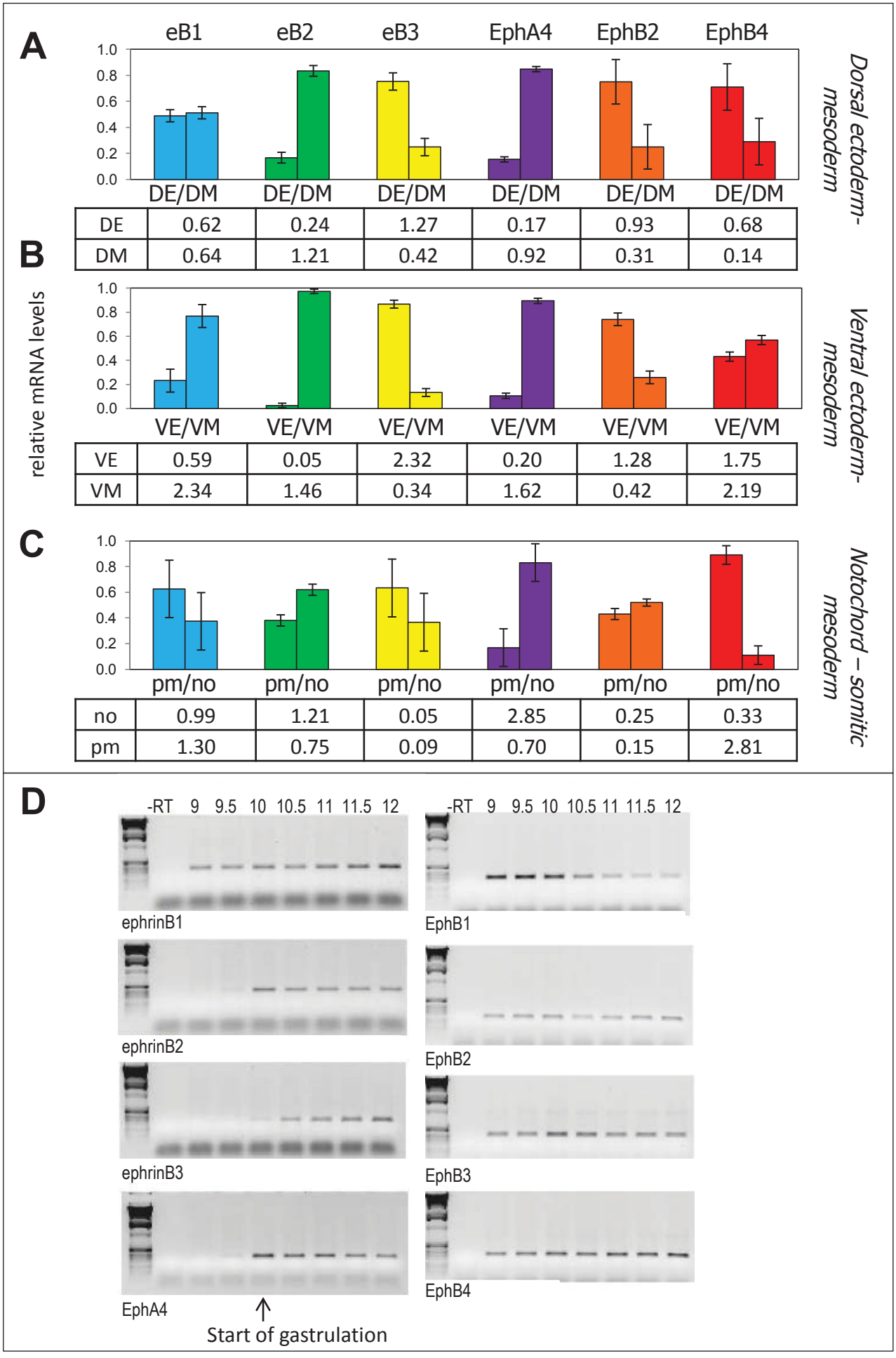
A
eB1
eB2
eB3
EphA4
EphB2
EphB4
1.0
0.8
0.6
0.4
0.2
0.0
DE/DM
DE/DM
DE/DM
DE/DM
DE/DM
DE/DM
Dorsal ectoderm-mesoderm
DE 0.62 0.24 1.27 0.17 0.93 0.68
DM 0.64 1.21 0.42 0.92 0.31 0.14
B
relative mRNA levels
VE/VM
VE/VM
VE/VM
VE/VM
VE/VM
VE/VM
Ventral ectoderm-mesoderm
VE 0.59 0.05 2.32 0.20 1.28 1.75
VM 2.34 1.46 0.34 1.62 0.42 2.19
C
pm/no
pm/no
pm/no
pm/no
pm/no
pm/no
Notochord – somitic mesoderm
no 0.99 1.21 0.05 2.85 0.25 0.33
pm 1.30 0.75 0.09 0.70 0.15 2.81
D
-RT 9 9.5 10 10.5 11 11.5 12
ephrinB1
EphB1
ephrinB2
EphB2
ephrinB3
EphB3
EphA4
EphB4
Start of gastrulation

Figure 3.S2

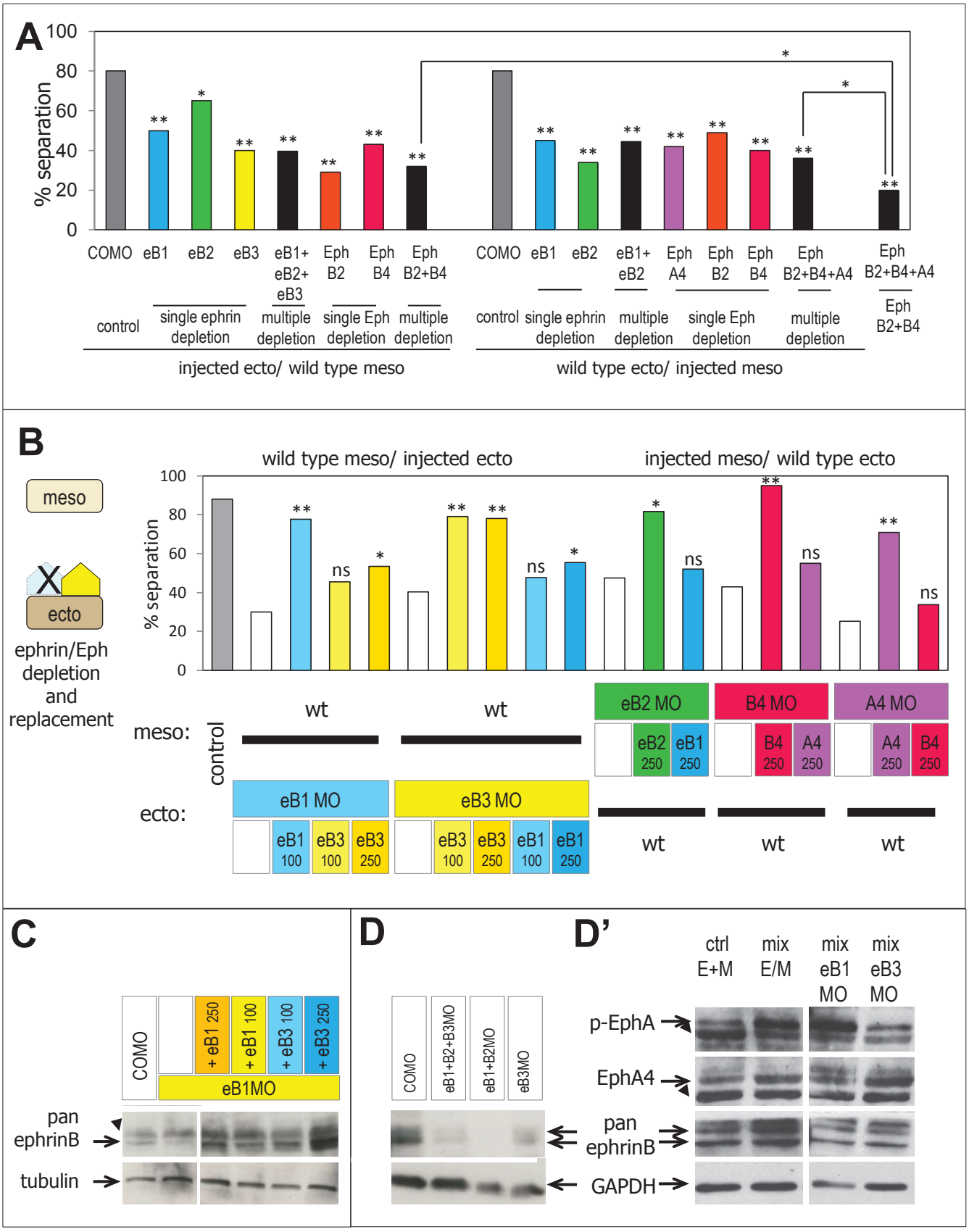
A
% separation
COMO
eB1
eB2
eB3
eB1+ eB2+ eB3
Eph B2
Eph B4
Eph B2+B4
control
single ephrin depletion
multiple depletion
single Eph depletion
multiple depletion
injected ecto/ wild type meso
eB1+ eB2
Eph A4
Eph B2
Eph B4
Eph B2+B4+A4
Eph B2+B4
wild type ecto/ injected meso
B
meso
ecto
ephrin/Eph depletion and replacement
wild type meso/ injected ecto
injected meso/ wild type ecto
meso:
ecto:
control
wt
eB1 MO
eB3 MO
eB2 MO
B4 MO
A4 MO
C
COMO
+ eB1 250
+ eB1 100
+ eB3 100
+ eB3 250
eB1MO
pan ephrinB
tubulin
D
COMO
eB1+B2+B3MO
eB1+B2MO
eB3MO
D'
ctrl E+M
mix E/M
mix eB1 MO
mix eB3 MO
p-EphA
EphA4
pan ephrinB
GAPDH

Figure 3.S3

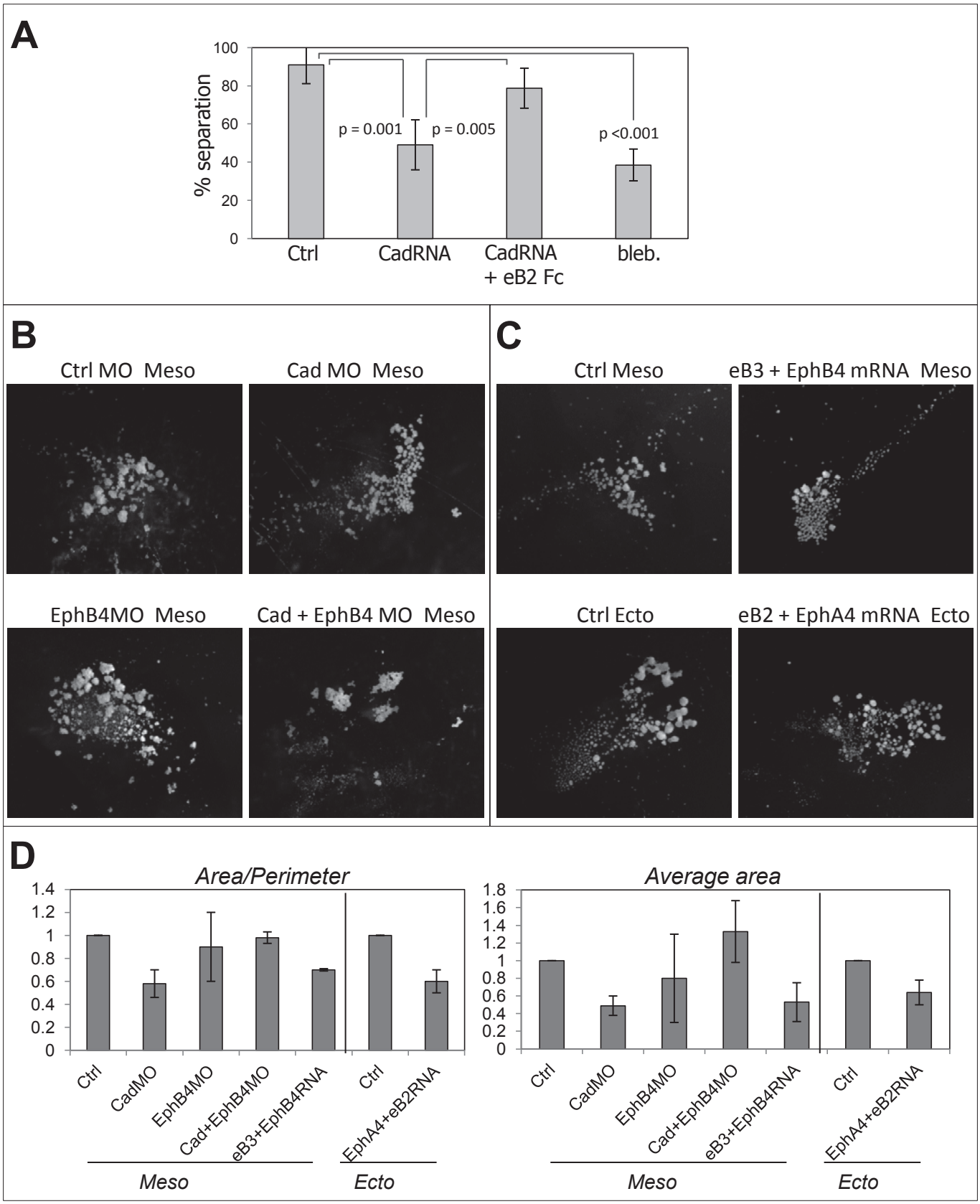
A
% separation
100
80
60
40
20
0
p = 0.001
p = 0.005
p <0.001
Ctrl
CadRNA
CadRNA + eB2 Fc
bleb.
B
Ctrl MO Meso
Cad MO Meso
EphB4MO Meso
Cad + EphB4 MO Meso
C
Ctrl Meso
eB3 + EphB4 mRNA Meso
Ctrl Ecto
eB2 + EphA4 mRNA Ecto
D
Area/Perimeter
1.4
1.2
1
0.8
0.6
0.4
0.2
0
Ctrl
CadMO
EphB4MO
Cad+EphB4MO
eB3+EphB4RNA
Ctrl
EphA4+eB2RNA
Meso
Ecto
Average area
1.8
1.6
1.4
1.2
1
0.8
0.6
0.4
0.2
0
Ctrl
CadMO
EphB4MO
Cad+EphB4MO
eB3+EphB4RNA
Ctrl
EphA4+eB2RNA
Meso
Ecto

Figure 3.S4

A

Single unidirectional signals:
Forward signal Sf = ([ephrin] x [Eph]) x 1/(Kd + *f* x ([ephrin]+[Eph]))
Reverse signal Sr = Sf x r

f, saturation factor, >1 (0.5)
r, reverse factor (eb1=0, eB2 = 0.3, eB3 = 1)

"conc" (nM)	Dorsal ecto-meso		Ventral ecto-meso		Notochord	
	ecto	meso	ecto	meso	pm	so
eB1	0.10	0.10	0.09	0.35	0.05	0.19
eB2	0.03	0.19	0.01	0.22	0.20	0.11
eB3	0.57	0.06	1.06	0.05	0.01	0.01
fA4	0.02	0.14	0.03	0.24	0.43	0.03
fB2	0.42	0.05	0.57	0.06	0.04	0.02
fB4	0.05	0.02	0.13	0.33	0.05	0.41

Ephrin	Eph	Kd (nM)
eB1	fA4	>100
eB2	fA4	1
eB3	fA4	0.5
eB1	fB2	10
eB2	fB2	1
eB3	fB2	>100
eB1	fB4	>100
eB2	fB4	0.5
eB3	fB4	>100

B *Dorsal ectoderm-mesoderm*

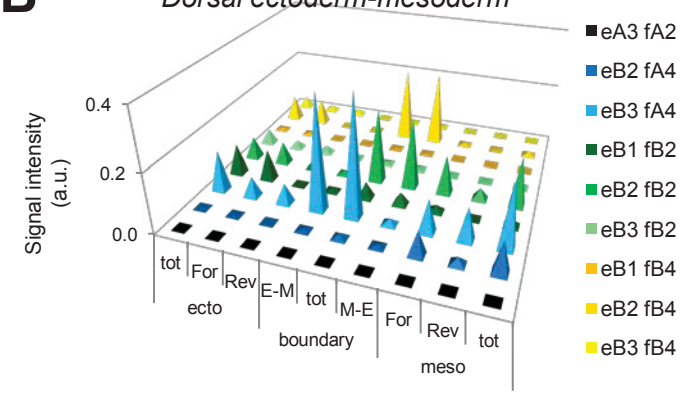

B' *D ecto* *D meso*

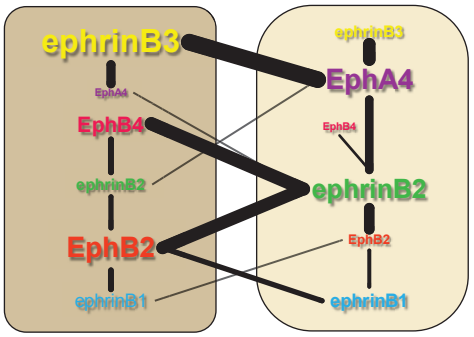

C *Ventral ectoderm-mesoderm*

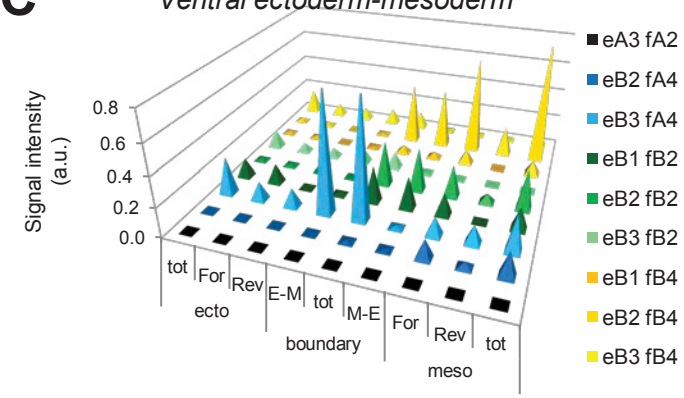

C' *V ecto* *V meso*

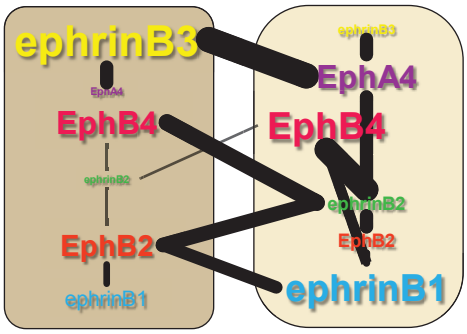

D *Notochord – somitic mesoderm*

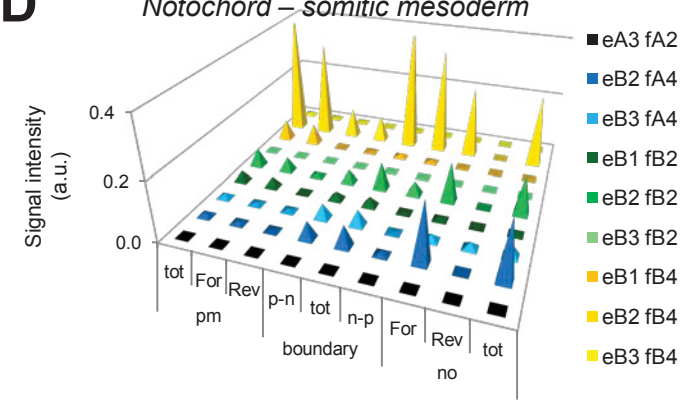

D' *pm* *no*

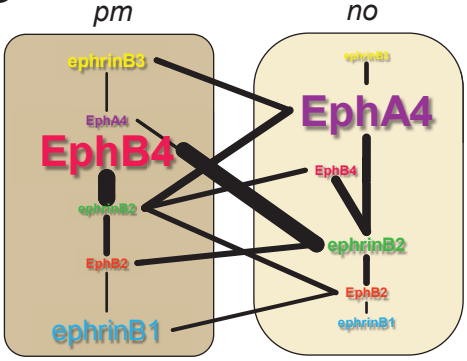

Figure 3.S5

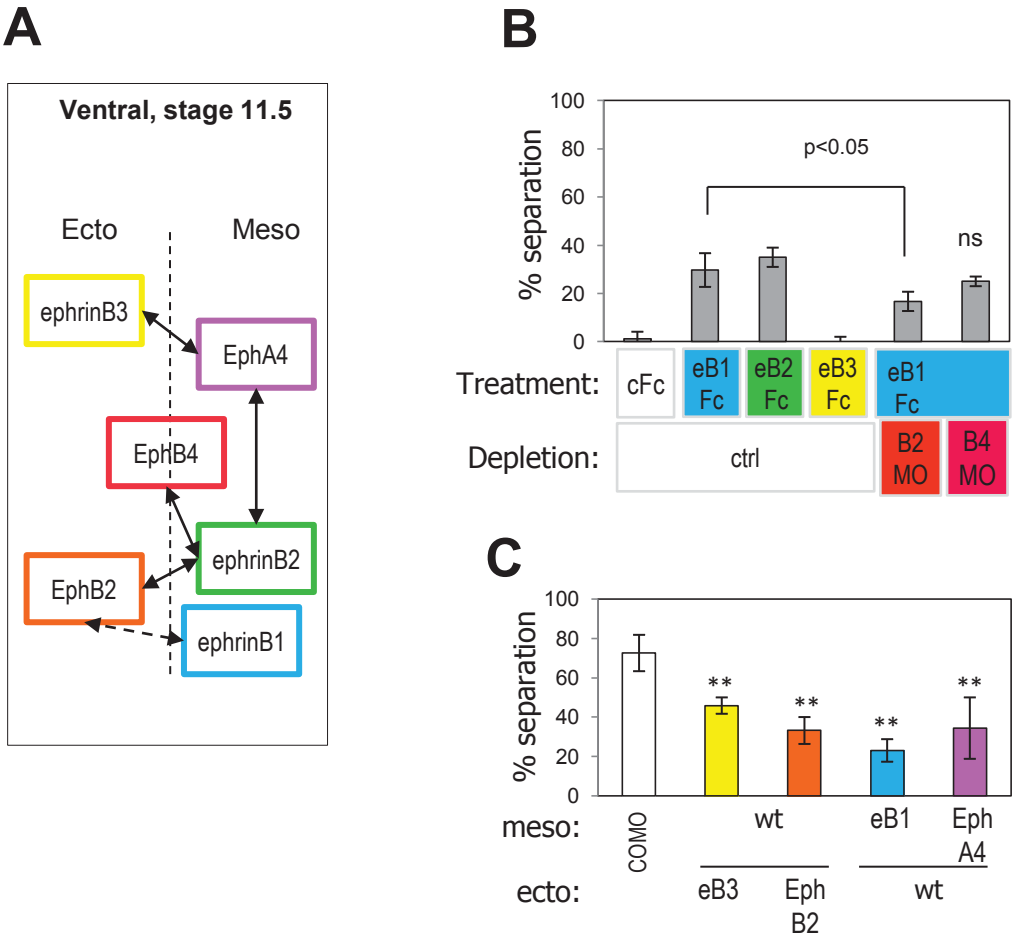
A
Ventral, stage 11.5
Ecto
Meso
ephrinB3
EphA4
EphB4
ephrinB2
EphB2
ephrinB1
B
% separation
100
80
60
40
20
0
p<0.05
ns
Treatment:
cFc
eB1 Fc
eB2 Fc
eB3 Fc
eB1 Fc
Depletion:
ctrl
B2 MO
B4 MO
C
% separation
100
80
60
40
20
0
**
**
**
**
meso:
COMO
wt
eB1
Eph A4
ecto:
eB3
Eph B2
wt

Bridge to chapter IV

We showed in the previous chapter that the formation of the three morphologically similar boundaries relies on a general rule that is dictated by the combinatorial expression of ephrins and Ephs on the cell surface. We showed by functional and biochemical approaches that the interaction of ephrins and Ephs is more selective than thought before. Indeed the asymmetric expression of the relevant ligands and receptors favor enhanced signaling across the boundary versus inside the tissues. We indeed observed higher phosphorylated Ephs at the ectoderm-mesoderm boundary. We also observed increased ephrin-Eph dependant phosphorylated myosin at the boundary. While our data from chapter II and III revealed some evidence on the mechanism that modulates actin- myosin network downstream ephrin-Eph signaling, it is not known how this affects adhesive contacts at the boundary. In the following chapter we address how cells at the presomitic-notochord boundary locally modulate cadherin mediated adhesion. We describe a cellular mechanism that relies on the contact mediated ephrin-Eph repulsive signal. Increased membrane contractility leads to local inhibition of cadherin mediated adhesion and formation of sharp boundaries. This chapter is a reproduction of the following published article in Developmental Cell as a result of equal contribution with Dr. Francois Fagotto:

A Molecular Base for Cell Sorting at Embryonic Boundaries: Contact Inhibition of Cadherin Adhesion by Ephrin/Eph-Dependent Contractility. Authors: François Fagotto*, **Nazanin Rohani***, Anne-Sophie Touret and Rui Li

Developmental Cell, Volume 27, Issue 1, 72-87, 03 October 2013
doi:10.1016/j.devcel.2013.09.004

Chapter IV: A molecular base for cell sorting at embryonic boundaries: Contact inhibition of cadherin adhesion by Ephrin/Eph-dependent contractility.

Abstract

The mechanism responsible for subdividing the embryo into individual tissues is a fundamental question in developmental biology. Various general hypotheses have been proposed, involving either differences in cell adhesion, contractility, or contact-mediated repulsion. However, the key parameter in tissue separation, i.e. the regulation of cadherin-based adhesion at the boundary, has not yet been investigated. We show that cadherin clustering is specifically inhibited at the vertebrate notochord-presomitic mesoderm boundary, preventing formation of adhesive bonds between cells of the two different types. This local regulation depends on differentially expressed ephrins and Eph receptors, which increase cell contractility and generate a membrane blebbing-like behavior along the boundary. Inhibiting myosin activity is sufficient to induce cadherin clustering and formation of stable contacts across the boundary, causing notochord and presomitic tissues to fuse. Local inhibition of cadherin adhesion explains how sharp separation can be achieved in response to cell-cell contact signals.

Introduction

Development proceeds by successive subdivisions of the embryo into various regions / compartments, and eventually tissues and organs. Each region becomes physically delimited by a boundary that prevents further cell mixing with the adjacent cell populations. In vertebrates, most boundaries will eventually evolve into strong permanent barriers made of secreted extracellular matrix. In the early stages of separation, however, tissue boundaries are highly permeable, since cells or even whole groups of cells can freely cross them under various experimental conditions (Maghzal et al., 2010; Medina, Swain, Kuerner, & Steinbeisser, 2004; Reintsch, Habring-Mueller, Wang, Schohl, & Fagotto, 2005; Rohani, Canty, Luu, Fagotto, & Winklbauer, 2011; Wacker, Grimm, Joos, & Winklbauer, 2000). Different schools of thought have tried to explain the nature of these boundaries: differential expression of homophilic adhesion molecules (Takeichi & Takeichi, 1995), quantitative differences in adhesive strength (Foty & Steinberg, 2005; Manning, Foty, Steinberg, & Schoetz, 2010; Steinberg, 1970; Steinberg & McNutt, 1999) or in cortical tension (Harris, 1976; Krieg et al., 2008; Maître et al., 2012), or ephrin/Eph-mediated cell repulsion (Cooke, Kemp, & Moens, 2005; Durbin et al., 1998; Kemp, Cooke, & Moens, 2009). The first mechanism is unlikely to act in the early embryonic stages, where adhesion generally relies on one single cadherin (J. Heasman et al., 1994; Janet Heasman et al., 1994; Tepass, 1999). As for the models based on quantitative differences in adhesion or tension, they both predict that the type and strength of interactions occurring at the tissue interface should represent an intermediate value between the properties of each tissue taken separately (Krieg et al., 2008; Maître et al., 2012; Manning, Foty, Steinberg, & Schoetz, 2010). Yet, when boundary interfaces are observed in more detail, they reveal unique characteristics that are not observed within the tissues: For instance in Drosophila, prominent acto-myosin cables run along the parasegmental boundaries and appear to be required to maintain separation of these compartments (Monier, Pélissier-Monier, & Sanson, 2011). In Xenopus, the ectoderm-mesoderm boundary is characterized by local cycles of attachments-detachments (Rohani et al., 2011). Whether these two examples may be related to

some common principle or reflect different modes of tissue separation remains unknown, but both clearly indicate that what happens at the contact between two cell types cannot necessarily be predicted by the properties of the individual cell populations.

We have thus set to study early tissue interfaces directly, using two models in Xenopus: the boundary between ectoderm-mesoderm (Rohani et al., 2011), and the subsequent partition of dorsal mesoderm into notochord and the presomitic - also called paraxial- mesoderm (Reintsch et al., 2005). Using independent approaches, both studies demonstrate that cells can sense the identity of the neighbouring cells: they discriminate between "homotypic contacts" with cells of the same tissue and "heterotypic contacts" with cells of another tissue, since stable adhesive bonds can only be formed at the former contacts. In the case of ectoderm-mesoderm separation, we have identified the molecular nature of the "heterotypic contact cues", which is due to ephrin-Eph signals generating Rho/Rac-dependent cycles of attachments-detachments (Rohani et al., 2011); Rohani et al., unpublished results).

An important unresolved question was the downstream mechanism mediating the actual separation of the two tissues. What is the status of cadherins at heterotypic contacts and how are they regulated? The study of the notochord boundary seemed particularly promising to elucidate this question: while cohesion increases in both notochord and presomitic mesoderm tissues as they enter the phase of convergence-extension (Moore, Keller, & Koehl, 1995), adhesion between them seems to drop instantaneously as the boundary appears. To understand this phenomenon, we have directly investigated the status of cadherins within the tissues and at the boundary. Cadherins are known to form large multimeric clusters, which, similarly to focal contacts for integrins, are considered to be required to produce substantial adhesive force. These clusters are further connected to the actin cytoskeleton through yet not fully elucidated protein complexes that include catenins as core components (Ratheesh & Yap, 2012). In early embryonic cells, these cadherin clusters distribute along the membranes as discrete spots, called "puncta" or "spot junctions" (Tepass & Hartenstein, 1994;

Winklbauer & Kwang, 2009), that can be used to monitor sites of cell-cell adhesion (Cavey, Rauzi, Lenne, & Lecuit, 2008). Here we show that loss of adhesion at the notochord boundary is not due to the exclusion of cadherins from this interface, but rather to local acto-myosin contractility that inhibits cadherin clustering. We further demonstrate that increased acto-myosin contractility and inhibition of cadherin clustering along the boundary are a consequence of ephrin-Eph signaling, supporting a general role of these repulsive cues in vertebrate tissue separation.

Results

Cadherin clustering is inhibited at the boundary interface

In late gastrula embryos (stage 12.5), the notochord boundary is already well established, but while it will later be "sealed" by extracellular matrix, it is still completely "permeable", as demonstrated by the ability of single cells to rapidly sort from one tissue to the other (Reintsch et al., 2005). Macroscopically, the newly formed notochord shows little to no adhesion to the adjacent somatic mesoderm, since these two tissues freely separate from each other during microdissection. We asked whether this property corresponded to differences in adhesive structures by examining the distribution of C-cadherin, which is the only cadherin expressed at significant levels at this stage. Both endogenous and exogenously expressed C-cadherin-GFP showed essentially the same general pattern (Fig.4.1B,C). At homotypic contacts within each tissue, C-cadherin was concentrated in numerous dense spots decorating the plasma membranes (arrows), which typically correspond to discrete adhesive contacts, also called cadherin "puncta" (Adams & Adams, 1998; Cavey et al., 2008; Tepass & Hartenstein, 1994; Vasioukhin, Bauer, Yin, & Fuchs, 2000) (Fig.4.1B,C). The boundary interface appeared however quite different: fewer puncta were observed (Fig.4.1B,C) and a prominent diffuse signal gave to the boundary interface the appearance of a "curtain" (arrowheads). Note that groups of puncta were often found along the boundary at corners between two notochord or two presomitic cells (Fig.4.1C,D', yellow arrows). These structures could be well resolved by

live confocal microscopy, which unambiguously demonstrated that they did not involve heterotypic contacts across the boundary but represented lateral homotypic "junctions" (Fig.4.1D,D' yellow arrows). Quantification of C-cadherin-GFP in live explants showed that the puncta density was ten times lower at the boundary (Fig.4.1B',B",C' and S1C). The proportion of cadherin included in the clusters was also much smaller (Fig.4.1B"'). The difference was smaller in fixed samples, which can be explained by the fact that the identity of many contacts could not be established with certainty, due to imperfect membrane preservation and lower resolution, which led us to conservatively overestimate heterotypic puncta (see legends) (Fig.4.1C'). The average signal intensity for endogenous cadherin was also higher at the boundary (Fig.4.1C'), probably due to better epitope accessibility compared to homotypic clusters in fixed samples. These potential caveats made us favor live explants, and we used the former for most of our study. C-cadherin-GFP-expressing embryos developed normally despite the known sensitivity of early development (Lee & Gumbiner, 1995) indicating that this construct did not significantly alter adhesive and migratory properties under our experimental conditions. The "smooth undulating curtain" could be considered as a hallmark of the boundary, sufficient on its own to unambiguously identify this structure. While we cannot exclude the existence of other smaller scale organization/clustering outside of these puncta, our results were strongly indicative of a much more diffuse cadherin distribution at the boundary interface.

The most obvious reasons for the deficit in cadherin clusters could be readily discarded: a) It could not be explained by the total cadherin levels, which were only marginally lower at the boundary of live explants (Fig.4.1B"'); b) Cells were constantly in close apposition, as the two membranes could not be resolved (Fig.4.1F) and cells appeared to press against each other across the boundary (Fig.4.2A and movie S1); c) Mesoderm cells did not show signs of apical-basolateral polarity at this stage (Fig.4.S1F,F'). d) The distribution of the basic components of the adhesion complexes, β-catenin, α-catenin, p120catenin,

appeared identical to cadherin (Fig.4.1D,E and 4.S1G). The intensity ratio between α-catenin and cadherin signals was similar at homotypic contacts in the tissues and at heterotypic non-adhesive contacts along the boundary (Fig.1D"and 4.S1G"'), indicating that puncta and smooth membranes have a similar composition in terms of the core of the cadherin-associated complex. In conclusion, the scarcity of cadherin clusters at the boundary did not appear to be due to a physical gap that would prevent cadherin interactions, nor to an exclusion of cadherins from this interface, but rather a specific "instructive" mechanism inhibiting cadherin clustering across the boundary. This mechanism did not seem to involve disruption of the basic cadherin-catenin complex.

Inhibition of clustering is independent of cadherin levels and subtype

The smooth distribution of C-cadherin at the boundary appeared to be an extremely robust trait. Quantifitative comparison of cadherin-GFP distribution between weakly and strongly expressing cells demonstrated that although puncta density tended to increase with cadherin levels both at homotypic and heterotypic contacts, heterophilic contacts showed in all cases the same strong deficit in puncta density (Fig.4.S1A-C). The rule applied to all of our images: compared to homotypic contacts with similar cadherin levels, heterotypic contacts always displayed a much lower number of puncta. The robustness of the process is further illustrated by the extreme example shown in Fig.4.S1D: expression of a dominant negative mutant of cadherin lacking the extracellular domain (ΔEcad) induces a dramatic destabilization of endogenous cadherins (Reintsch et al., 2005). We found that these cells were still able to distinguish between the different contacts, recruiting most of the remaining cadherins to form homotypic puncta (Fig.4.S1D, yellow arrows). Taken together, our data show that the smooth pattern observed at the boundary was independent of cadherin levels, implying that clustering was locally inhibited by a specific mechanism.

The lack of clusters along the boundary was not a phenomenon specific to C-cadherin: E-cadherin normally starts to be expressed only at the end of

gastrulation in the non-neural ectoderm (data not shown). When ectopically-expressed in the dorsal mesoderm, its distribution closely followed the normal C-cadherin pattern (Fig.4.1SE,E'): it formed dense spots at contacts within the tissues(arrows), while segments of smooth membrane were visible along the boundary (arrowheads). Note that two non-classical cadherins, PAPC and AxPC, are expressed complementarily in the trunk mesoderm during gastrulation - in the paraxial mesoderm and in the notochord, respectively. However, protocadherins do not appear to function as adhesion molecules but rather as regulators of C-cadherin adhesion (Chen & Gumbiner, 2006), and ectopic PAPC expression in notochord cells was not sufficient to sort them to the presomitic mesoderm (data not shown). We conclude that cluster formation at homotypic contacts is largely independent of cadherin levels or cadherin type, and that inhibition of clustering along the boundary appears to be dictated by a different and strongly dominant mechanism.

Dynamics of boundary behavior

In contrast to the stability of the homotypic contacts within each of the two tissues, the boundary appeared to be a remarkably dynamic region (Fig.4.2A and 4.S2A). We identified two types of behavior at the boundary: a rapid undulation, resembling the flapping of a flag (Fig.4.2A" and movie S1) and an equally rapid formation of transient protrusions or digitations that emanated from both tissues and intermingled (Fig.4.2A' and movie S1). This behavior was quite reminiscent of classical blebbing. Time lapse images of mosaic embryos containing single cells expressing membrane-targeted Cherry fluorescent protein (Fig.4.S2A,A') showed protrusions freely exploring the boundary interface. Cells remained almost permanently in intimate contact: as one cell would retract, the abutting cell would instantaneously fill the gap (Fig.4.2A). The membrane behavior could switch between undulations and emission of protrusions (movie S1), and we hypothesized that these were manifestations of a single underlying mechanism (see below).

Induction of a "smooth boundary" at ectopic heterotypic contacts

Expression of a LEF-VP16 fusion construct, which constitutively activates β-catenin/TCF signaling, dominantly confers somitic fate, even to cells located in the notochord (Reintsch et al., 2005). This allowed us to study single presomitic cells surrounded by notochord cells. These cells move randomly within the notochord until they contact the paraxial mesoderm, in which case they rapidly cross the boundary and irreversibly integrate into the paraxial mesoderm (Reintsch et al., 2005). To investigate the behavior of these cells at high resolution, we injected a DNA plasmid coding for both nuclear LEF-VP16 and membrane-targeted Cherry fluorescence protein (see Materials and Methods). At stage 12.5, most LEF-VP16-expressing cells had already sorted to the presomitic mesoderm (Reintsch et al., 2005). We confirmed that they were well integrated in the tissue, establishing numerous cadherin puncta with their neighbours (Fig.4.S2B, arrows), and that control cells expressing membrane-Cherry alone had a normal cadherin distribution, in the tissues and at the boundary (Fig.4.S2C). We searched for LEF-VP16-expressing cells still located in the notochord, and found that their contacts with the surrounding notochord cells mimicked the properties of the endogenous boundary, displaying a smooth cadherin pattern (Fig.4.2B, white arrowheads) and undulations (Fig.4.2B, yellow arrowhead) or blebbing (Fig.4.2A and movie S2). These mislocalized cells were fully able to distinguish between homotypic and heterotypic contacts: We found configurations where two LEF-VP16-expressing cells formed a pair in the notochord (Fig.4.2C). While heterotypic contacts with the surrounding notochord cells were much smoother than normal homotypic contacts (Fig.4.2C, arrowheads), bright cadherin clusters formed specifically at contacts between the LEF-VP16-positive cells (Fig.4.2C, yellow arrows). These patterns were quantified: Heterotypic contacts had slightly decreased total cadherin levels, but four times less puncta than normal homotypic contacts (Fig.4.2E,E'). The fraction of cadherin concentrated in puncta was proportionally decreased too (Fig.4.2E). Homotypic contacts

between two LEF-VP16 cells, on the contrary, gave for all three parameters values comparable to those of notochord homotypic contacts. We conclude that the "boundary-like" smooth cadherin pattern of LEF-VP16 cells in the notochord was not due to a general loss of cell-cell adhesion, but resulted specifically from the heterotypic nature of their contacts with notochord cells. Note that some LEF-VP16-expressing cells may not have yet fully developed presomitic properties, which may explain the slightly higher average puncta density of puncta measured at ectopic heterotypic contacts compared to the endogenous boundary.

Consistent with their failure to establish adhesive cadherin contacts with adjacent notochord cells, LEF-VP16-expressing cells showed slug-like movements, and seemed to be squished by the notochord cells (Fig.4.S2D), which accounts for their random migration (Reintsch et al., 2005). Their actual sorting from the notochord to the presomitic mesoderm was very difficult to image at high resolution, due to its unpredictability and rapidity (Reintsch et al., 2005). In the very few cases (only three cells) where we were able to record the early contact with the presomitic tissue, the intensity of the cadherin signal increased instantaneously, indicating the immediate formation of dense clusters (Fig.4.S2E, arrows). Thus, the ability or inability to form these puncta according to the identities of the contacting cells appears to fully explain their sorting behavior.

Evidence for tensile structures and for blebbing-like behavior at the boundary

The fact that yolk platelets were completely excluded from the boundary area (Fig.4.1B,D) was indicative of the presence of a particularly thick layer of cortical cytoskeleton, which could be responsible for the peculiar membrane behavior. Indeed, a prominent accumulation of filamentous actin marked the position of the boundary as reproducibly as the smooth cadherin pattern (Fig.4.3A, quantification in Fig.4.S4). This enrichment was confirmed in fixed, non-manipulated whole embryos (Fig.4.S3A). Single LEF-VP16-expressing cells in the notochord

exhibited massive accumulation of filamentous actin into extensive stress fiber-like structures (Fig.4.2D,E'), consistent with the fact that these cells were completely surrounded by heterotypic contacts.

Live analysis revealed the existence of two types of actin structures, which differed with regards to their relationship with the plasma membrane and could be clearly distinguished during outward bulging of the membrane (Fig.4.3A and movie S2): The first one consisted of a continuous layer closely lining the membranes on both sides of the boundary, and following all their undulating and protrusive movements (red arrowheads). The second corresponded to a network of actin fibers (red arrows), which maintained a stationary position, oriented roughly parallel to the boundary (highlighted in diagrams of Fig.4.3A). The two structures remained connected by sparse links, prominently at both sides of the forming bulges or protrusions (arrowheads). At these anchoring points, the membranes showed steep bends, whose orientation seemed dictated by that of the actin filaments. Numerous membrane invaginations were constantly pulled inside the cell (white concave arrowheads). These images clearly reflected tensile actin-based structures connected intermittently to the plasma membrane. We confirmed the existence of prominent contractile structures along the boundary by detecting accumulation of phosphorylated myosin light chain in fixed samples (Fig.4.S3B). Live imaging of myosin light chain revealed that this structure was made of discontinuous fibers (Fig.4.3B,C) formed by local transient bursts (data not shown).

The actin and myosin pattern and the membrane dynamics were strikingly reminiscent of the classical blebbing behavior observed in some cell types (Charras & Paluch, 2008). The protrusions formed a continuum with blebs that filled the gap of the boundary (Fig.4.3C', asterisks) created on the most ventral side of the explants by the removal of the archenteron roof (Fig.4.1A", thin dotted red line equivalent to superficial focal planes). The high similarity to classical blebs was further confirmed by high levels of Dia1, but not Arp3 nor Ena, colocalizing with the membrane-associated pool of actin at the boundary interface

and in the protrusions (Fig.4.3E,E' and 4.S3, quantifications in Fig.4.S4). Dia1 is thought to participate in the assembly of a new cortex that is responsible for bleb retraction (Charras & Paluch, 2008). Note however that Dia1 was also found along homotypic contacts, and thus was not a unique feature of the boundary. All forms of blebs and protrusions observed along the boundary showed identical characteristics, indicating that they corresponded to different morphological manifestations of the same phenomenon. We conclude that the boundary is characterized by contractile structures that exert high tension oriented roughly parallel to the tissue interface and provide the plasma membrane with bleb-like properties. We hypothesized that this phenomenon could be the actual cause of cadherin cluster inhibition and ultimately of tissue separation.

Early events during establishment of the notochord boundary

Boundary formation is a continuous process that takes place in the region of the dorsal mesoderm that has just involuted (Fig.4.1A"'). By imaging the cells immediately posterior to the end of the visible boundary, we were able to follow the changes that preceded the appearance of the mature boundary (Fig.4.4A,B and movie S3). Compared to the cells in the more anterior region where notochord and presomitic mesoderm have separated (Fig.4.4A, frame #33), the cells of the newly involuted mesoderm appeared rounder and exhibited less prominent C-cadherin clustering (Fig.4.4A, frame #2), probably reflecting the fact that they were not yet under the strong tension exerted by convergence-extension movements. The process leading to boundary formation occurred within a 3-5 cells wide region. It did not appear to be strictly coordinated, since the onset and the duration varied between neighboring cells (Fig.4.4A,B). Each individual cell, however, followed a stereotypical sequence, described in detail in the legend of Figure 4 and summarized in Table 4.1. The process can be described as follows: The position of the future boundary was first marked by a faint signal for filamentous actin (Fig.4.4A', #2, and B', #3). Actin then started to massively accumulate, first near the cell edges, and then all along the interface (Fig.4.4A',

frames #6-19). Cadherin distribution changed relatively early on, with accumulation at lateral junctions (Fig.4.4A", yellow arrowheads). Along the heterotypic interface, it sometimes became rapidly smooth, but often went first through a phase of strong but unstable clustering (Fig.4.4A'', white arrows). Remarkable oscillations in the length of heterotypic contacts clearly reflected contractions directed parallel to the boundary interface (Fig.4.4A''', B', dotted double arrows). The boundary straightened during this phase. The final smooth cadherin pattern of the mature boundary was invariably reached simultaneously with the start of blebbing (Fig.4.4A",B", white arrowheads). Collectively, these observations indicate that increased contractility at heterotypic contacts is an early and quite dramatic event, which may control other aspects of boundary formation, including changes in cadherin distribution, and ultimately tissue separation.

Myosin activity is required for cell sorting and tissue separation

To assess the role of contractile structures, we first tested the effect of interfering with myosin activation on cell sorting between the notochord and the presomitic mesoderm. We used our mosaic assay, where a small number of cells of the presumptive dorsal mesoderm are manipulated by plasmid DNA injection, and the percentage of these cells located in the notochord is scored at the end of gastrulation (Reintsch et al., 2005). Control cells (e.g. expressing GFP, Fig.4.5B) tend to distribute relatively evenly between both tissues, but cells expressing the Lef-VP16 fusion construct are efficiently excluded from the notochord and accumulate in the adjacent presomitic mesoderm (<5% miss-sorting, Figure 5A,B). Interference with the Rho pathway by expression of either a dominant negative RhoA variant or of the Rho-binding domain of Rhotekin significantly impaired cell sorting of Lef-VP16-expressing cells (Fig.4.5A',B). Sorting was also inhibited by incubation of whole embryos in the presence of the ROK inhibitor Y26732 or the MLCK inhibitor ML7 (Fig.4.5C). The weaker effect of these soluble inhibitors was expected due to limited diffusion through the large embryo. Note that an effect of myosin inhibition on cell migration could not

explain our results, because even in the absence of migration LEF-VP16 expressing cells would have been expected to cluster with other abutting cells of the same presomitic fate, and those clusters should have formed boundaries with notochord cells. On the contrary, all manipulated cells appeared well integrated in the notochord (Fig.4.5A", asterisk, and 4.S2B). Thus, inhibition of the Rho-ROK and MLCK pathways appeared to affect the actual ability to discriminate between homotypic and heterotypic contacts. We directly tested the role of myosin on the endogenous boundary by treating dorsal mesoderm explants, in which cells had free access to soluble molecules, with the myosin ATPase inhibitor blebbistatin. Blebbistatin caused rapid fusion of the notochord boundary (Fig.4.5D, arrows, and 4.5E). We then asked if myosin activity was responsible for preventing cadherin clusters at the boundary. After blebbistatin treatment, we observed massive formation of cadherin clusters at heterotypic contacts along the notochord-presomitic mesoderm interface (Fig4.5F', arrows). These contacts were stable (Fig.4.5F", arrow), demonstrating that myosin inhibition was indeed sufficient to reverse inhibition of adhesion between these two tissues. This cellular phenotype was robust and highly reproducible (Fig.4.5G). We conclude that myosin activity acts upstream of cadherin-mediated adhesion in notochord separation, and that it is required for both proper cell sorting and boundary behavior. Note that, consistent with the boundary remnants observed at low magnification (Fig.4.5D), the areas of intimate cadherin contacts (Fig.4.5F', arrows) were interspersed with residual blebs (arrowheads). These blebs tended to be much more static (Fig.4.5F" and movie S4), which is the characteristic effect of blebbistatin and is consistent with myosin being required for bleb retraction and restoration of "normal" cortical properties (Charras & Paluch, 2008). Importantly, cadherin clusters still failed to appear at the blebs (Fig.4.5F", arrowheads).

Ephrin/Eph signaling is required for cell sorting, myosin activation and cadherin regulation at the boundary

We then investigated the source of the signal that triggers myosin activation at heterotypic contacts. We considered ephrins and Eph receptors as the first candidates and screened their expression pattern in notochord and presomitic tissues by RT-qPCR (Fig.4.S5A). We found that EphB4 and ephrinB2, its mosteffective ligand in the Xenopus system (Rohani et al., unpublished), were expressed in complementary patterns, with EphB4 being highly enriched in the presomitic mesoderm and ephrinB2 more abundant in the notochord (Fig.4.6A and 4.S5A). Thus, the ephrinB2-EphB4 pair looked like a good candidate to mediate repulsion at heterotypic contacts between the two tissues. We also found a high enrichment of EphA4 in the notochord. Although the selectivity of EphA4 is still not well defined, we also included it in our functional analysis because it appears to be systematically expressed in asymmetric patterns and functionally involved at other embryonic boundaries (Cooke et al., 2005; Watanabe, Sato, Saito, Tadokoro, & Takahashi, 2009) Rohani et al., unpublished)

In the mosaic assay, LefVP16-expressing cells completely failed to sort in embryos injected with antisense morpholino oligonucleotides (MO) targeting ephrinB2, EphB4 or EphA4 (Fig.4.6B',C).EphrinB2, EphA4 or EphB4 MOs, and dominant negative EphB4 (EphB4ΔC), also severely disrupted the endogenous boundary (Fig.4.6D,E') without affecting cell fate (Fig.4.6G'). The effect of EphA4 and B4 MOs was specifically observed when they were targeted to the tissue expressing high levels of the corresponding receptor (Fig.4.6D).

Interference with ephrin/Eph signaling drastically decreased and often completely erased p-MLC accumulation along the boundary (Fig.4.6F' and 4.S5B) . p-MLC levels inversely correlated with the levels of MOs (reflected by the co-injected GFP marker) and with the severity of the boundary phenotype. Note that the p-MLC signal at contacts within the tissue was similar in the notochord and the presomitic mesoderm and seemed insensitive to ephrin/Eph interference (Fig.4.S5B). We conclude that increased p-MLC at the notochord boundary is specifically and entirely dependent on ephrin/Eph signaling. The perfect correlation between acute myosin activation and the presence of an organized boundary (e.g. arrowheads in Fig.4.6F') further supports our hypothesis that

myosin activation downstream of ephrins/Ephs is responsible for notochord separation.

We also examined the effect of ephrin/Eph loss-of-function on cadherin at the boundary by live confocal microscopy (Fig.4.6H and movie S5). EphA4 MO, EphB4 MO and EphB4ΔC, all efficiently caused extensive overlap of notochord and presomitic cells. Bleb-like structures were largely but not completely absent (Fig.4.6H,H', flat arrowheads, J) and numerous cadherin clusters appeared at heterotypic contacts (Fig.4.6H,H', concave arrowheads, I). We conclude that ephrins and Ephs are the contact cues that control separation at the notochord boundary.

Discussion

The notochord boundary is the product of local reactions

Previous models for tissue separation have opposed three major mechanisms, cell-cell adhesion, cortical tension, and contact inhibition. Our findings bring these three parameters into a single coherent description of tissue separation. The key feature of the system resides in the local control at sites of heterotypic contact. The traditional models of differential adhesion or tension, sensus stricto, assumed that the characteristics of the system could be inferred from the global properties of the two tissues, and that adhesion and tension at the boundary should represent some middle point between those of each separate population (Harris, 1976; Krieg et al., 2008; Maître et al., 2012; Manning et al., 2010; Steinberg, 1970). Based on our observations, the central role of the balance between tension and adhesion enunciated in the classical biophysical models of cell sorting (Harris, 1976; Steinberg, 1970) still holds true, but these two parameters are now subordinated to spatially-restricted signals instructed by ephrins and Ephs (Fig.4.7A). This repulsion-based mechanism enables cells to switch rapidly and reversibly from full adhesion at homotypic contacts to low or even no adhesion at heterotypic

contacts, which explains the efficiency and speed of sorting of notochord and presomitic cells (Reintsch et al., 2005) and the sharpness and straightness of the boundary.

Inhibition of adhesion is under the control of myosin contractility

The deficit in cadherin clusters provides a molecular explanation for the low adhesiveness of the tissue boundary interface. This property could not have been predicted based on the characteristics of the two tissues taken in isolation: notochord and presomitic mesoderm homotypic contacts are indeed qualitatively and quantitatively undistinguishable (Fig.4.1A,B). The strong propensity to concentrate cadherins in clusters at homotypic contacts and the equally strong resilience for clustering at heterotypic contacts also accounts for the surprising ability of cells to sort properly independently of cadherin levels (Reintsch et al., 2005).

The massive accumulation of actomyosin fibers and the visible signs of high tension along the boundary were also not predicted by the differential adhesion/tension hypotheses. We provide here direct demonstration that ephrin signaling-dependent myosin activity is responsible for the inhibition of cadherin clustering and for tissue separation (although we do not exclude the possible contribution of additional mechanisms).

Myosin activity is known to influence cell-cell adhesion both negatively, by creating cortical tension, and positively, by stimulating a mechanosensing α-catenin-vinculin link to the actin cytoskeleton (Huveneers et al., 2012; Yonemura, Wada, Watanabe, Nagafuchi, & Shibata, 2010). In Xenopus mesoderm tissues, p-MLC does colocalize with cadherin at homotypic contacts (Fig.4.S3C'), but blebbistatin did not seem to affect these contacts under our experimental conditions, while, on the contrary, it stimulated formation of new cadherin clusters across the boundary. The high contractility of this interface is presumably incompatible with adhesion. We did observe during establishment of boundary an intermediate phase where heterotypic contacts seemed to resist to the waves of

contraction by engaging more cadherins into puncta (Fig.4.7B). This phenomenon is highly reminiscent of the classical tension-dependent reinforcement of integrin focal contacts (Puklin-Faucher & Sheetz, 2009; Schwartz & DeSimone, 2008). After this phase of tug of war, however, cadherin adhesions disappeared concomitant with the appearance of blebs.

Note that the mechanism uncovered here departs from the simplest intuitive model of de-adhesion, where contractility would prevent adhesive bonds by physically pulling the two apposing membranes apart. Here, on the contrary, the membranes were pressed against each other by the outward movement due to blebbing. The fact that cadherin clustering failed despite this close physical apposition suggested that high tension created an unfavorable membrane-cytoskeleton configuration.

Actomyosin activity is also elevated at Drosophila compartment and Xenopus ectoderm-mesoderm boundaries (Aliee et al., 2012; Landsberg et al., 2009; Monier, Pelissier-Monier, Brand, & Sanson, 2010). The actomyosin structures observed in Drosophila were presented as "supracellular cables" (Aliee et al., 2012; Landsberg et al., 2009; Monier et al., 2010), but this description would be an oversimplification in the case of the notochord boundary. The actin cortical network does span the entire length of the cell contacts, but myosin positive cables are discontinuous and transient, and depend on local ephrin signals. Whether similar dynamic systems control other boundaries will be an exciting question for future studies.

Similarities and differences with the ectoderm-mesoderm boundary

We have now added the notochord boundary to the list of vertebrate boundaries that depend on ephrin-Eph signaling. The situation at the notochord boundary is particularly complex, with at least two ephrinBs and five cognate receptors as well as additional ephrinAs and EphAs (Fig.4.S5 and data not shown) expressed in the notochord and presomitic mesoderm at different levels. While we do not have yet a complete picture of the specificity of the various ephrin/Eph pairs, the strength of the loss-of-function phenotypes and their specific impact on local

myosin activation constitute compelling evidence for a key role of these molecules.

The degree of adhesion/repulsion at tissue interfaces appears well adjusted to accommodate the specific requirements of each system: The almost complete lack of adhesion at the notochord-presomitic mesoderm boundary seems to be an extreme case. These tissues must be able to slide freely relative to each other for proper convergence-extension (Keller et al., 1989). Furthermore, somitic and notochord fates remain highly labile during these stages (Domingo & Keller, 1995), and the system may not tolerate well contacts between the two cell types. Significant adhesion must be maintained at the ectoderm-mesoderm boundary, since the mesoderm uses the ectoderm surface as a substrate for migration. Blebs are less frequently observed (data not shown) and temporary adhesive contacts are frequently established (Rohani et al., 2011), probably corresponding to the intermediate situation observed during formation of the notochord boundary (Fig.4.7B). We speculate that the same inhibitory action of cortical contraction on cadherin adhesion represents a general mechanism controlling vertebrate tissue separation, which would manifest itself under different forms depending on the intensity of ephrin-Eph signaling and on other factors, such as the basal contractile and adhesive states of the tissues.

Experimental procedures

Live imaging of dorsal mesoderm explants

mRNA coding for various fluorescent fusion proteins were injected in the two cell-stage embryo to obtain widespread expression in the dorsal mesoderm. mRNA were titrated to achieve low levels of expression that would not interfere with normal development. In some experiments, single cells were labeled/manipulated by injection of plasmid DNA at the 8-cell. Dorsal explants were cut at stage 12½. The endodermal epithelium (archenteron roof) was removed to expose the axial/paraxial mesoderm, and the explants were flattened on 1μg/ml fibronectin- coated glass, secured with a silicon-supported coverglass, and cultured in MBSH at RT.

Images/time-lapse movies were obtained Quorum technologies WaveFX spinning disc confocal mounted on an automated DMI6000B Leica microscope was used, with a 40x HCX PL APO CS, NA= 1.25 oil objective. CFP, GFP, YFP and Cherry were excited with 440, 491 and 561nm diode lasers, and the emission filters were respectively 483/32, 520/35, 543/40 and 624/40. Yolk autofluorescence were excited by far red light (638nm diode laser, 692/40 emission filter). Images were collected with EM CCD 512X512 BT camera and controlled with Improvision Volocity 3DM software. z-stacks were typically collected with 1μm distance between planes. Image processing was performed with Metamorph (Universal Imaging Corporation) and Adobe Photoshop7 software.

Immunofluorescence

Cryosectioning and immunofluorescence were performed as described in (Fagotto & Brown, 2009; Schohl & Fagotto, 2002). For phalloidin staining, whole embryos were fixed in 4% formaldehyde in MBSX for 1hr, followed by permeabilization (1% formaldehyde, 0.1%TritonX100), 1 h incubation with blocking buffer (10% sheep serum), and overnight incubation with

2 U/ml Alexa488-phalloidin (Invitrogen) in 10% sheep serum. The samples were then processed for embedding, cryosectioning and immunofluorescence.
Images were obtained using either an epifluorescence microscope Axiovert TV135 (Carl Zeiss, Inc.) equipped with a 25x N.A. 0.8 water immersion objective (Carl Zeiss, Inc.) and a CCD camera (Retiga 2000R; Quantitative Imaging Corporation), or an epifluorescence microscope DM IRE2 (Leica) equipped with a 20x/0.70 IMM Corr CS oil immersion objective and an ORCA-ER camera (Hamamatsu Photonics). Images were acquired using AnalySIS (Soft Imaging System GmbH) and MetaMorph (MDS Analytical Technologies) software.

Image processing and quantification

Images were analyzed using ImageJ. Most figures display vertical projection of several z planes. For quantification, cadherin puncta were identified on longitudinal line scans of membranes in single focal planes. The width of the line was set to include the whole thickness of the cadherin signal. A threshold was set based on cadherin average intensity, and peaks above threshold were counted as puncta. Direct visual counting of spots on the original images, both on single planes and on 3D reconstitutions confirmed the values obtained. Membrane localization of cytoskeleton components was quantified on broad transversal line scans.

Acknowledgements

We are thankful to Drs. Bill Bement, André Brändli, Ken Cho, Gergana Gateva, Barry Gumbiner, Rolf Kemler, Pierre McCrea, Elena Pasquale, Naoki Watanabe, and Alpha Yap for their generous gift of plasmids and antibodies. We thank Laura Canty for her critical reading of our manuscript. This work was supported by grants from the Natural Sciences and Engineering Research Council of Canada (261679-03) and Canadian Cancer Society Research Institute (017162/700915) (to F.F.). This work is dedicated to Dr. Ray Keller, a pioneer in the field and mentor to us all.

References

Adams, C. L., & Adams. (1998). Mechanisms of Epithelial Cell-Cell Adhesion and Cell Compaction Revealed by High-resolution Tracking of E-Cadherin-Green Fluorescent Protein. *The Journal of cell biology, 142*(4), 1105-1119.

Aliee, Maryam, Röper, Jens-Christian, Landsberg, Katharina P, Pentzold, Constanze, Widmann, Thomas J, Jülicher, Frank, & Dahmann, Christian. (2012). Physical Mechanisms Shaping the Drosophila Dorsoventral Compartment Boundary. *Current biology : CB, 22*(11), 967-976.

Cavey, Matthieu, Rauzi, Matteo, Lenne, Pierre-Francois, & Lecuit, Thomas. (2008). A two-tiered mechanism for stabilization and immobilization of E-cadherin. *Nature, 453*(7196), 751-756. doi: http://www.nature.com/nature/journal/v453/n7196/suppinfo/nature06953_S1.html

Charras, Guillaume, & Paluch, Ewa. (2008). Blebs lead the way: how to migrate without lamellipodia. *Nat Rev Mol Cell Biol, 9*(9), 730-736.

Chen, Xuejun, & Gumbiner, Barry M. (2006). Paraxial protocadherin mediates cell sorting and tissue morphogenesis by regulating C-cadherin adhesion activity. *The Journal of Cell Biology, 174*(2), 301-313. doi: 10.1083/jcb.200602062

Cooke, Julie E., Kemp, Hilary A., & Moens, Cecilia B. (2005). EphA4 Is Required for Cell Adhesion and Rhombomere-Boundary Formation in the Zebrafish. *Current Biology, 15*(6), 536-542. doi: http://dx.doi.org/10.1016/j.cub.2005.02.019

Domingo, C., & Keller, R. (1995). Induction of notochord cell intercalation behavior and differentiation by progressive signals in the gastrula of Xenopus laevis. *Development, 121*(10), 3311-3321.

Durbin, L., Durbin, C., Brennan, K., Shiomi, J., Cooke, A., Barrios, S., . . . Holder. (1998). Eph signaling is required for segmentation and differentiation of the somites. *Genes & development, 12*(19), 3096-3109.

Fagotto, François, & Brown, CarolynM. (2009). Detection of Nuclear β-catenin in Xenopus Embryos. In E. Vincan (Ed.), *Wnt Signaling* (Vol. 469, pp. 363-380): Humana Press.

Foty, Ramsey A., & Steinberg, Malcolm S. (2005). The differential adhesion hypothesis: a direct evaluation. *Developmental Biology, 278*(1), 255-263. doi: http://dx.doi.org/10.1016/j.ydbio.2004.11.012

Harris, Albert K. (1976). Is cell sorting caused by differences in the work of intercellular adhesion? A critique of the steinberg hypothesis. *Journal of Theoretical Biology, 61*(2), 267-285. doi: http://dx.doi.org/10.1016/0022-5193(76)90019-9

Heasman, J., Ginsberg, D., Geiger, B., Goldstone, K., Pratt, T., Yoshida-Noro, C., & Wylie, C. (1994). A functional test for maternally inherited cadherin in Xenopus shows its importance in cell adhesion at the blastula stage. *Development, 120*(1), 49-57.

Heasman, Janet, Crawford, Aaron, Goldstone, Kim, Garner-Hamrick, Peggy, Gumbiner, Barry, McCrea, Pierre, . . . Wylie, Chris. (1994). Overexpression of cadherins and underexpression of β-catenin inhibit dorsal mesoderm induction in early Xenopus embryos. *Cell, 79*(5), 791-803. doi: http://dx.doi.org/10.1016/0092-8674(94)90069-8

Huveneers, Stephan, Oldenburg, Joppe, Spanjaard, Emma, van der Krogt, Gerard, Grigoriev, Ilya, Akhmanova, Anna, . . . de Rooij, Johan. (2012). Vinculin associates with endothelial VE-cadherin junctions to control force-dependent remodeling. *The Journal of Cell Biology, 196*(5), 641-652. doi: 10.1083/jcb.201108120

Keller, Ray, Keller, Mark, Cooper, Mike, Danilchik, Paul, Tibbetts, Paul, & Wilson. (1989). Cell intercalation during notochord development inXenopus laevis. *The journal of experimental zoology, 251*(2), 134-154.

Kemp, Hilary A., Cooke, Julie E., & Moens, Cecilia B. (2009). EphA4 and EfnB2a maintain rhombomere coherence by independently regulating intercalation of progenitor cells in the zebrafish neural keel. *Developmental Biology, 327*(2), 313-326.

Krieg, M., Arboleda-Estudillo, Y., Puech, P. H., Kafer, J., Graner, F., Muller, D. J., & Heisenberg, C. P. (2008). Tensile forces govern germ-layer organization in zebrafish. *Nat Cell Biol, 10*(4), 429-436. doi: http://www.nature.com/ncb/journal/v10/n4/suppinfo/ncb1705_S1.html

Landsberg, Katharina P., Farhadifar, Reza, Ranft, Jonas, Umetsu, Daiki, Widmann, Thomas J., Bittig, Thomas, . . . Dahmann, Christian. (2009). Increased Cell Bond Tension Governs Cell Sorting at the Drosophila Anteroposterior Compartment Boundary. *Current Biology, 19*(22), 1950-1955. doi: http://dx.doi.org/10.1016/j.cub.2009.10.021

Lee, Chung-Hyun, & Gumbiner, Barry M. (1995). Disruption of Gastrulation Movements in Xenopus by a Dominant-Negative Mutant for C-cadherin. *Developmental Biology, 171*(2), 363-373. doi: http://dx.doi.org/10.1006/dbio.1995.1288

Maghzal, N., Maghzal, E., Vogt, W., Reintsch, J. S., Fraser, F., & Fagotto. (2010). The tumor-associated EpCAM regulates morphogenetic movements through intracellular signaling. *The Journal of cell biology, 191*(3), 645-659.

Maître, Jean-Léon, Berthoumieux, Hélène, Krens, Simon Frederik Gabriel, Salbreux, Guillaume, Jülicher, Frank, Paluch, Ewa, & Heisenberg, Carl-Philipp. (2012). Adhesion Functions in Cell Sorting by Mechanically Coupling the Cortices of Adhering Cells. *Science, 338*(6104), 253-256. doi: 10.1126/science.1225399

Manning, M. Lisa, Foty, Ramsey A., Steinberg, Malcolm S., & Schoetz, Eva-Maria. (2010). Coaction of intercellular adhesion and cortical tension specifies tissue surface tension. *Proceedings of the National Academy of Sciences*. doi: 10.1073/pnas.1003743107

Medina, A., Swain, R., Kuerner, K.-M., & Steinbeisser, H. (2004). Xenopus paraxial protocadherin has signaling functions and is involved in tissue separation. *EMBO J., 23*, 3249–3258.

Monier, Bruno, Pelissier-Monier, Anne, Brand, Andrea H., & Sanson, Benedicte. (2010). An actomyosin-based barrier inhibits cell mixing at compartmental boundaries in Drosophila embryos. *Nat Cell Biol, 12*(1), 60-65. doi: http://www.nature.com/ncb/journal/v12/n1/suppinfo/ncb2005_S1.html

Monier, Bruno, Pélissier-Monier, Anne, & Sanson, Bénédicte. (2011). Establishment and maintenance of compartmental boundaries: role of contractile actomyosin barriers. *Cellular and Molecular Life Sciences, 68*(11), 1897-1910. doi: 10.1007/s00018-011-0668-8

Moore, S.W., Keller, R.E., & Koehl, M.A. (1995). The dorsal involuting marginal zone stiffens anisotropically during its convergent extension in the gastrula of Xenopus laevis. *Development, 121*(10), 3131-3140.

Puklin-Faucher, Eileen, & Sheetz, Michael P. (2009). The mechanical integrin cycle. *Journal of Cell Science, 122*(2), 179-186. doi: 10.1242/jcs.042127

Ratheesh, Aparna, & Yap, Alpha S. (2012). A bigger picture: classical cadherins and the dynamic actin cytoskeleton. *Nat Rev Mol Cell Biol, 13*(10), 673-679.

Reintsch, Wolfgang E., Habring-Mueller, Anette, Wang, Renee W., Schohl, Anne, & Fagotto, François. (2005). β-Catenin controls cell sorting at the notochord–somite boundary independently of cadherin-mediated adhesion. *The Journal of Cell Biology, 170*(4), 675-686. doi: 10.1083/jcb.200503009

Rohani, Nazanin, Canty, Laura, Luu, Olivia, Fagotto, François, & Winklbauer, Rudolf. (2011). EphrinB/EphB Signaling Controls Embryonic Germ Layer Separation by Contact-Induced Cell Detachment. *PLoS Biol, 9*(3), e1000597. doi: 10.1371/journal.pbio.1000597

Schohl, Anne, & Fagotto, François. (2002). β-catenin, MAPK and Smad signaling during early Xenopus development. *Development, 129*(1), 37-52.

Schwartz, Martin A., & DeSimone, Douglas W. (2008). Cell adhesion receptors in mechanotransduction. *Current Opinion in Cell Biology, 20*(5), 551-556. doi: http://dx.doi.org/10.1016/j.ceb.2008.05.005

Steinberg, Malcolm S. (1970). Does differential adhesion govern self-assembly processes in histogenesis? Equilibrium configurations and the emergence of a hierarchy among populations of embryonic cells. *Journal of Experimental Zoology, 173*(4), 395-433.

Steinberg, Malcolm S., & McNutt, Patrick M. (1999). Cadherins and their connections: adhesion junctions have broader functions. *Current Opinion in Cell Biology, 11*(5), 554-560. doi: http://dx.doi.org/10.1016/S0955-0674(99)00027-7

Takeichi, M., & Takeichi. (1995). Morphogenetic roles of classic cadherins. *Current opinion in cell biology, 7*(5), 619-627.

Tepass, Ulrich. (1999). Genetic analysis of cadherin function in animal morphogenesis. *Current Opinion in Cell Biology, 11*(5), 540-548. doi: http://dx.doi.org/10.1016/S0955-0674(99)00025-3

Tepass, Ulrich, & Hartenstein, Volker. (1994). The Development of Cellular Junctions in the Drosophila Embryo. *Developmental Biology, 161*(2), 563-596. doi: http://dx.doi.org/10.1006/dbio.1994.1054

Vasioukhin, Valeri, Bauer, Christoph, Yin, Mei, & Fuchs, Elaine. (2000). Directed Actin Polymerization Is the Driving Force for Epithelial Cell–Cell Adhesion. *Cell, 100*(2), 209-219. doi: http://dx.doi.org/10.1016/S0092-8674(00)81559-7

Wacker, S., Grimm, K., Joos, T., & Winklbauer, R. (2000). Development and control of tissue separation at gastrulation in Xenopus. *Dev. Biol., 224*, 428-439.

Watanabe, Tadayoshi, Sato, Yuki, Saito, Daisuke, Tadokoro, Ryosuke, & Takahashi, Yoshiko. (2009). EphrinB2 coordinates the formation of a morphological boundary and cell epithelialization during somite segmentation. *Proceedings of the National Academy of Sciences, 106*(18), 7467-7472. doi: 10.1073/pnas.0902859106

Winklbauer, Rudolf, & Kwang, W. Jeon. (2009). Chapter 5 Cell Adhesion in Amphibian Gastrulation *International Review of Cell and Molecular Biology* (Vol. Volume 278, pp. 215-275): Academic Press.

Yonemura, Shigenobu, Wada, Yuko, Watanabe, Toshiyuki, Nagafuchi, Akira, & Shibata, Mai. (2010). [alpha]-Catenin as a tension transducer that induces adherens junction development. *Nat Cell Biol, 12*(6), 533-542. doi: http://www.nature.com/ncb/journal/v12/n6/suppinfo/ncb2055_S1.html

Figure Legends

Figure 4.1:

Inhibition of cadherin clustering at the notochord boundary

(A-A”’) Experimental setting: (A) Diagram of a late gastrula embryo. (A’) Transversal section of dorsal structures. (A”) Live confocal microscopy of dorsal explants after removal of the archenteron roof. (A”’) Ventral view of explant, with examples of cells in the region where the boundary forms and along the mature boundary. am, anterior mesoderm; ar, archenteron roof; bl, blastopore lip; ne, neuroderm; no, notochord; pm, paraxial/ presomitic mesoderm.
(B) C-cadherin-GFP distribution in live explants. Vertical projection of a stack of five z-planes (1μm apart). The boundary is characterized by a smooth undulating C-cadherin-GFP signal (arrowheads) that contrast with the punctated membranes within each tissue (arrows). Far red autofluorescence of the yolk was re-colored in blue. Note the yolk-free cytoplasm along the boundary (asterisk).
(B’-B”) Quantification: (B’) Line scans from membranes marked by dotted lines in (B). Blue line: homotypic contact between presomitic mesoderm cells (s-s). Puncta appear as sharp peaks (vertical arrows). Red line: smoother notochord-presomitic mesoderm interface (n-s). (B”) Puncta density along notochord (n-n), presomitic mesoderm (s-s) and boundary (n-s) contacts. T, total contacts; L, lateral contacts perpendicular to the boundary; P, parallel to the boundary. (B”’) Relative total signal intensity (average for n-n contacts set at 1) and % of signal concentrated in puncta (green surfaces in B’). Error bars: SD. *, ***: p values < 0.05 and < 10^{-6}, Student’s t-test. 17 to 32 cell interfaces from 7 independent experiments were measured for each category.
(C) Immunolocalization of endogenous C-cadherin. Tilted 3D reconstitution of a 10μm-thick horizontal section from a whole embryo. Arrows point to cadherin puncta, arrowheads to the characteristic bright smooth pattern found at the boundary. (C’) Quantification of puncta density and relative total signal intensity for endogenous cadherin. Most puncta observed along the boundary coincided with the edge of lateral homotypic contacts (yellow arrows in C), in which case they were excluded from quantification, the resolution being insufficient to

allocate them to one type of contacts. Error bars: SD. *: p values < 0.05, Student's t-test, 12 boundaries, 6 independent experiments.
(D) Co-localization of C-cadherin, β-catenin and α-catenin. Vertical projection of five z-planes. Note that the membranes appear slanted in this projection. (D') Enlarged image showing a typical concentration of cadherin puncta (yellow arrows) forming a lateral junction at the edge of homotypic contacts. Concave arrowheads point to additional puncta decorating the homophilic contact and flat arrowheads to the smooth cadherin pattern along the boundary. (D") Line scans (dotted line in D) for Che-α-catenin and C-cadherin-YFP signals. Arrows point at the edges of two lateral junctions that flank the homotypic contact (n-s). The ratio between α-catenin and C-cadherin was similar for smooth membranes and puncta.
(E) YFP-p-120ctn also shows the typical smooth boundary pattern (arrowheads). Arrows: puncta at homotypic contacts. Vertical projection of six z-planes.
(F) Expression of membrane-targeted Cherry confirm the tight membrane apposition at the boundary (arrowheads). See also Figure 4.S1.

Figure 4.1

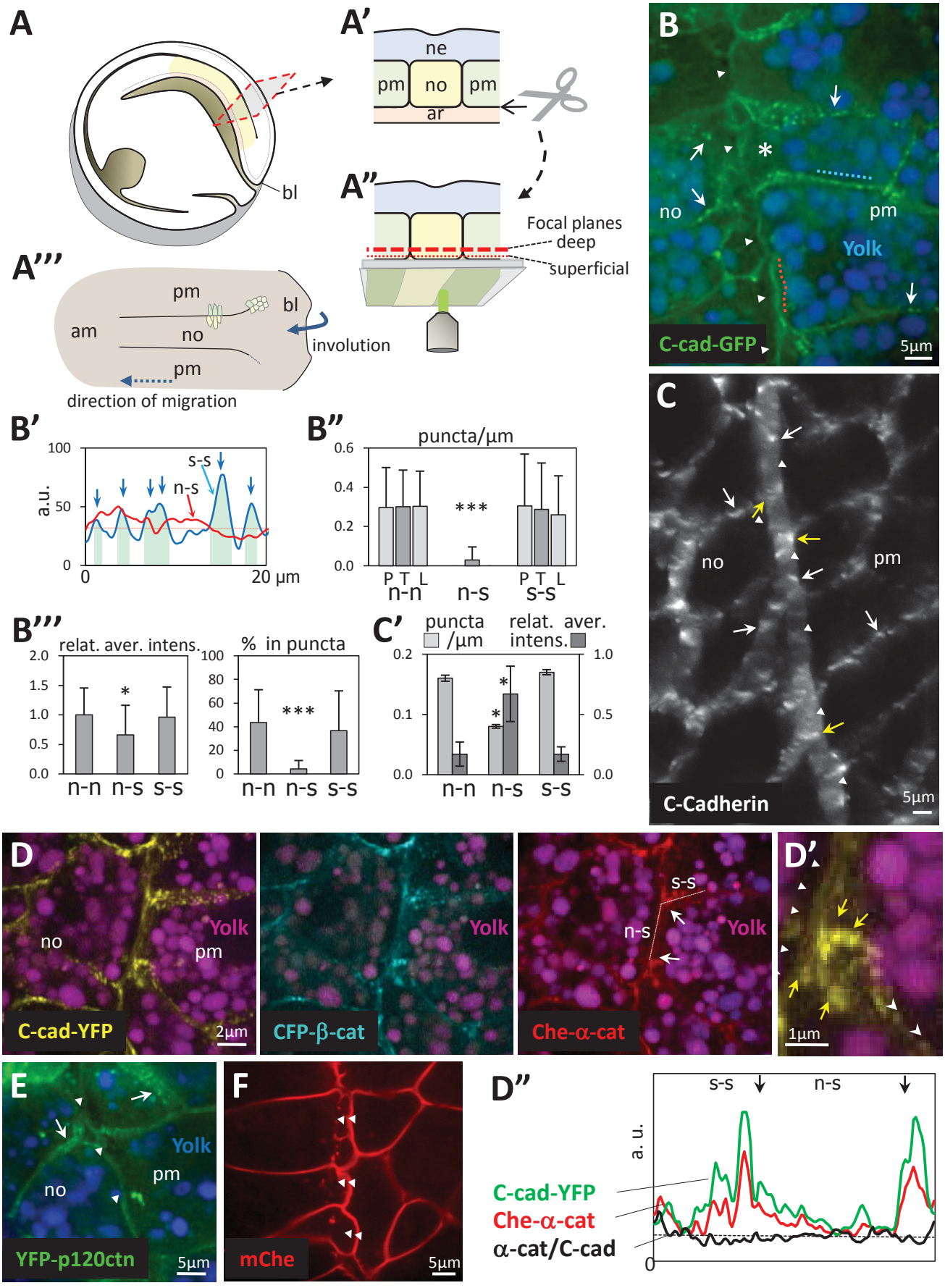
A
bl
A'
ne
pm
no
pm
ar
A''
Focal planes
deep
superficial
A'''
pm
bl
am
no
pm
involution
direction of migration
B
no
pm
Yolk
C-cad-GFP
5µm
C
no
pm
C-Cadherin
5µm
B'
100
50
0
a.u.
s-s
n-s
0
20 µm
B''
puncta/µm
0.6
0.4
0.2
0.0
***
P T L
n-n
n-s
s-s
B'''
relat. aver. intens.
2.0
1.5
1.0
0.5
0.0
*
n-n n-s s-s
% in puncta
100
80
60
40
20
0
***
n-n n-s s-s
C'
puncta /µm
relat. aver. intens.
0.2
0.1
0.0
1.0
0.5
0.0
*
*
n-n n-s s-s
D
no
Yolk
pm
C-cad-YFP
2µm
Yolk
CFP-β-cat
s-s
n-s
Yolk
Che-α-cat
D'
1µm
E
Yolk
pm
no
YFP-p120ctn
5µm
F
mChe
5µm
D''
s-s
n-s
a. u.
C-cad-YFP
Che-α-cat
α-cat/C-cad
0

Figure 4.2:

Plasma membrane dynamics at the notochord boundary

(A-A") Frames from time lapse confocal movie of explant expressing C-cadherin-GFP (movie S1). Vertical projection of 4 z-planes. (A) General view with position of the areas enlarged in A' and A". (A') Transient formation and retraction of multiple interdigitations at the boundary. Arrows: connection between cell body and protrusion. Asterisk: section of a digitation. (A") Typical "flagging" of the boundary membranes (arrowheads). Note the stable position of the lateral membranes (crosses). (B-C) Cell-autonomous inhibition of cadherin clustering at heterotypic contacts in mosaic embryos. Single presomitic cells were induced in the notochord field by injection of a plasmid coding for constitutively active LEF-VP16 (Reintsch et al, 2005). Cells were traced in live explants through membrane Cherry (red), expressed by the LEF-VP16 plasmid under the control of a separate promoter (see Materials and Methods). Each image is a vertical projection of multiple z-planes. (B) mCherry/LEF-VP16-positive cell (asterisk) surrounded by wild type notochord cells. Cadherin largely failed to cluster at heterotypic contacts (white arrowheads), while forming numerous puncta at homotypic notochord contacts (arrows). The yellow arrowhead follows the typical "flagging" behavior of a heterotypic contact. (C) Example of two mCherry/LEF-VP16-positive cells, labeled 1 and 2, showing strong cadherin puncta at homotypic contacts (yellow arrows). White arrowheads and arrows point respectively to smooth cadherin signal at heterotypic contacts and to clusters between notochord cells. (D) Massive accumulation of filamentous actin (Cherry-utrophin mRNA, red) in cells co-expressing membrane GFP/ LEF-VP16 (green). Note stress fiber-like structures spanning through the cell (arrows). Wild type notochord cells showed low utrophin signal except at corners joining three cells (arrowhead). (E,E') Quantification. (E) Cadherin puncta density at wild type notochord contacts (n-n), heterotypic contacts between LEF-VP16-expressing and wild type notochord cells (n-LEF), and homotypic contacts between LEF-VP16-expressing cells (LEF-LEF). 7 individual experiments were quantified. (E') Average cadherin and utrophin intensities relative to homotypic contacts. 12

instances from 5 individual experiments were quantified. Error bars: SD. **, p <0.01; ns, not significant. See also Figure 4.S2.

Figure 4.2

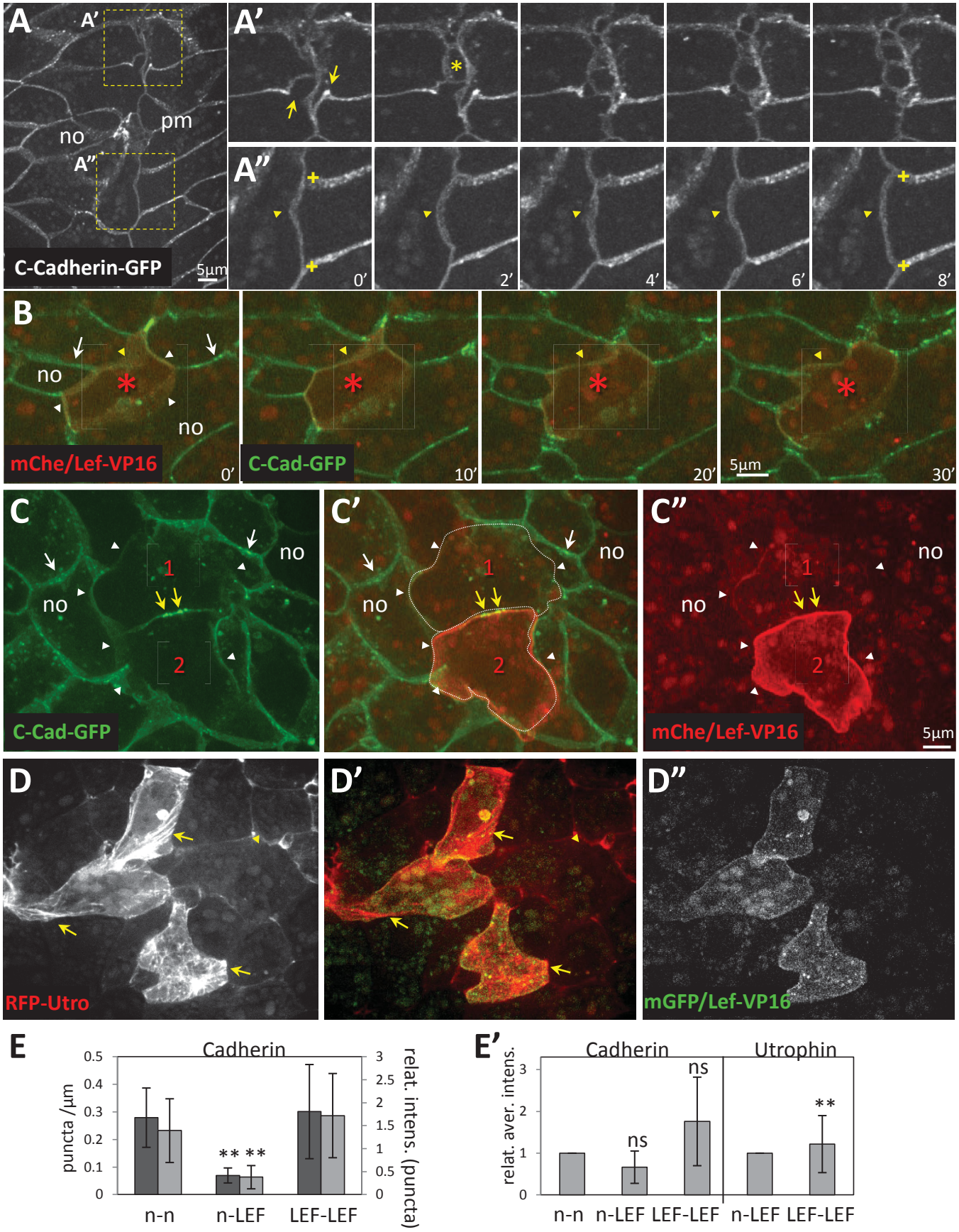
A
A'
pm
no
A''
C-Cadherin-GFP
5µm
A'
A''
0'
2'
4'
6'
8'
B
no
no
mChe/Lef-VP16
0'
C-Cad-GFP
10'
20'
5µm
30'
C
C'
C''
no
1
2
C-Cad-GFP
mChe/Lef-VP16
5µm
D
D'
D''
RFP-Utro
mGFP/Lef-VP16
E
Cadherin
puncta /µm
relat. intens. (puncta)
** **
n-n
n-LEF
LEF-LEF
E'
Cadherin
Utrophin
relat. aver. intens.
ns
ns
**
n-n
n-LEF
LEF-LEF
n-LEF
LEF-LEF

Figure 4.3:

Evidence for dynamic contractile structures and blebbing-like membrane behavior along the boundary

(A) Live imaging of the plasma membrane (mGFP) and cortical filamentous actin (Red-utrophin). Frames are taken from supplemental movie S2. Vertical projection of six z-planes. (A'-A''') Enlarged view from frame #2. Red arrowheads point to the membrane-associated pool and red arrows to the network of fibers from which the membrane separated during formation of bleb-like protrusions (asterisks). White arrowheads: Actin anchor points and corresponding membrane bends. Concave white arrowheads: deep transient membrane invaginations pulled along and/or toward the actin network. White arrows: sparse actin along homotypic contacts. The drawings below each frame highlight the approximate positions of fluctuating membrane and associated actin (dashed orange line) and of the comparably more stationary network (red lines).
(B,C) Live imaging of explants expressing MLC-Cherry (red), C-cadherin-YFP (green), and eCFP (blue), used as soluble cytoplasmic marker. Vertical projections of four z-planes. (B) Deep focal plane. MLC-positive fibers concentrated along the boundary (arrowheads). Note that the signal is inhomogeneous and discontinuous (star). (B''') Enlarged view: the strongest MLC signal (arrowheads) is separated from the boundary membranes (cadherin signal, arrows). (C) Superficial focal plane. Bleb-like structures (asterisks) protrude beyond the MLC fibers (arrowheads). (C''') Detail of MLC fibers.
(D-E) Actin - Dia1 colocalization at the boundary (arrowheads). (D) Deep focal plane. Insert: detail of Dia1 membrane accumulation (arrow) and actin fibers connecting the two basal sides of a bulge (concave arrowhead). (E) Superficial focal plane with numerous blebs (asterisks). See also Figure 4.S3 and S4.

Figure 4.3

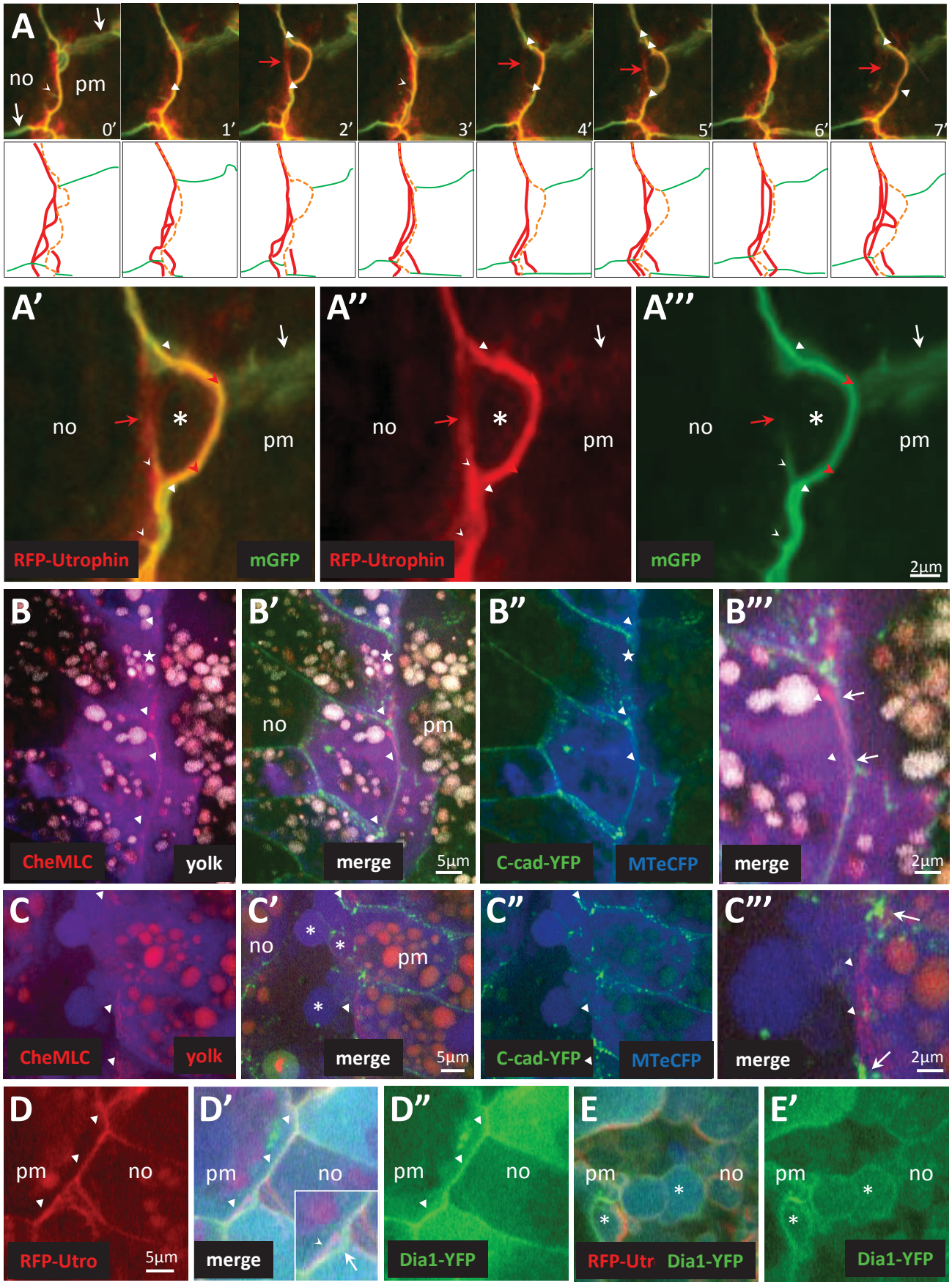
A
no
pm
0′
1′
2′
3′
4′
5′
6′
7′
A′
A″
A‴
RFP-Utrophin
mGFP
2μm
B
B′
B″
B‴
CheMLC
yolk
merge
5μm
C-cad-YFP
MTeCFP
C
C′
C″
C‴
D
D′
D″
E
E′
RFP-Utro
Dia1-YFP

Figure 4.4:

Live imaging of the establishment of the boundary

(A) General view of cells just posterior to the boundary, visible at the bottom left (blue arrow). Selected frames from supplemental movie S5, frame time interval = 5 min. Vertical projection of 3 focal planes. At the start of the sequence, the notochord cell labeled * had just initiated the characteristic development of separation behavior. Its anterior neighbor was already in contact with the mature boundary. Its posterior neighbor, labeled **, had started the process slightly ahead, but appeared delayed at the end of the sequence. (A') Actin. A faint line marked the future boundary interface in frame #2 (cell edges marked by red arrowheads). The signal increased in the following frames, starting from the edges (#6, red arrows). Blebbing appeared in #33 (round head arrows). (A") Cadherin. Yellow arrowheads: increased accumulation at lateral junctions. #15, white arrowhead: temporary smooth membrane. #19, white arrow: phase of strong but transient cadherin clusters. #33, arrowheads: final smooth cadherin pattern for cell *. (A"') Diagram of cell outlines and actin accumulation (red). Double arrows highlight the contractile oscillations and the dashed line the straightening of the boundary.

(B-B") Detail of a cell (*) undergoing transition from homotypic to heterotypic contact. Vertical projection of 3 planes. The mature boundary is outside of the field (blue arrow in #3). White concave arrowheads: edges of the two future heterotypic contacts between cell * and cells Φ and Θ. #3: The boundary (dotted jagged line) was first marked by actin accumulation, starting at one of the cell edges, then the second edge (white arrows). Cell contacts initially displayed mild cadherin clustering (yellow arrowheads). #5: The interface with cell Θ contracted (dotted double arrows). #9, contact with cell Φ: massive increase in actin, start of blebbing (bullet and curved dashed line), complete loss of puncta and dramatic decrease in cadherin signal (white arrowhead). #11: Actin accumulation spread through the whole interface and the boundary straightened (dotted line). See also Table 4.1.

Figure 4.4

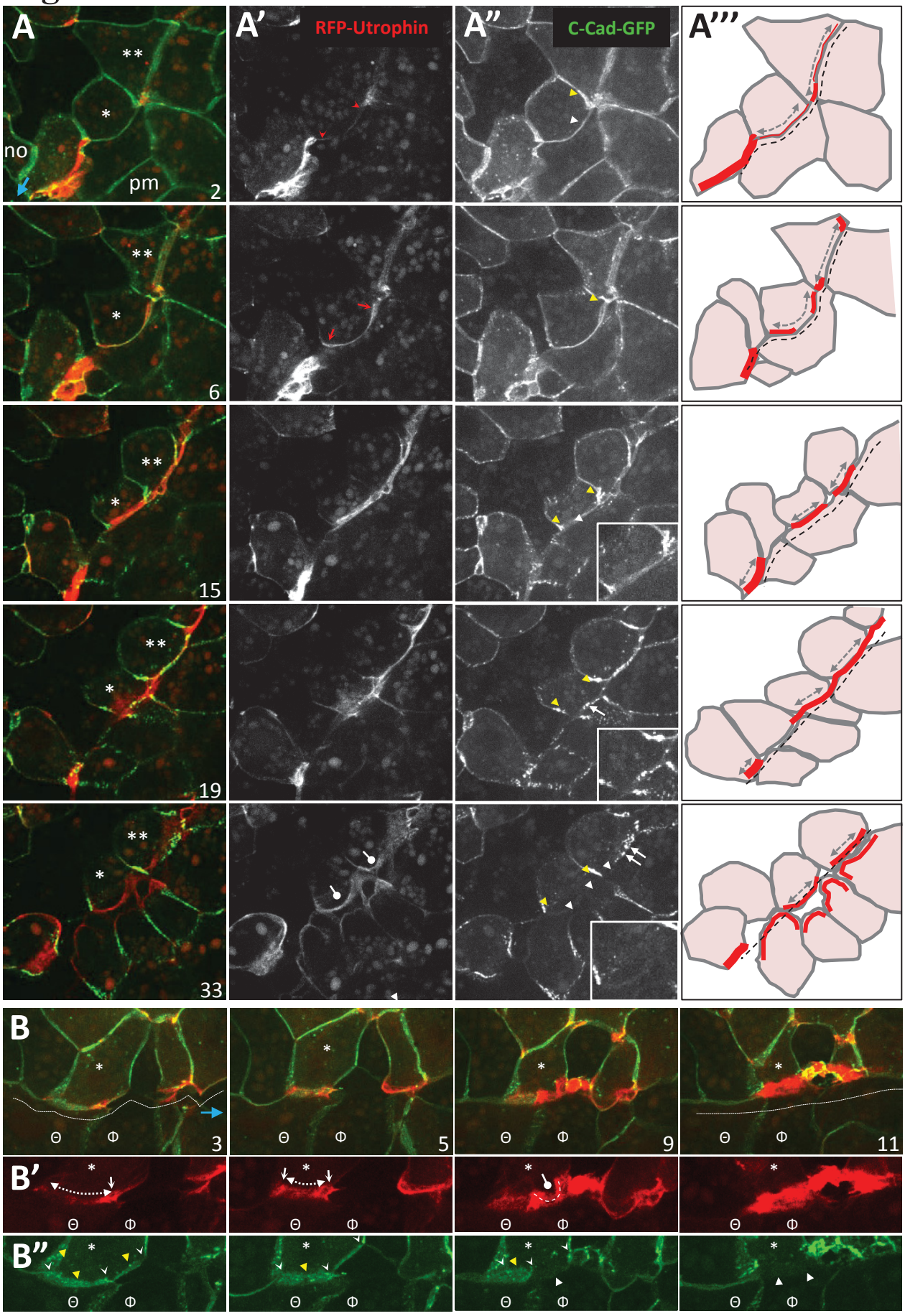

Table 1

Structures/molecules involved	Process	Frequency
Actin cytoskeleton	Initial thin line marks the future boundary[1]	78%
Actin cytoskeleton	Early accumulation at lateral edges[1]	90%
C-cadherin	Cluster concentration on lateral contacts, formation of homotypic lateral junctions[1]	81%
Actin cytoskeleton	Progressive accumulation along the boundary interface	100%
Cell morphology	Cycles of cell contraction (direction parallel to heterotypic contacts)	100%
C-cadherin	Cycles of appearance/disappearance of transient strong heterotypic puncta	61%
Cell morphology	Straightening of the boundary	100%
Actin cytoskeleton	Blebbing[1,2]	71%
C-cadherin	Permanent smooth cadherin pattern at heterotypic contacts[1,2]	71%
C-cadherin	General increase in clustered cadherin at homotypic contacts within tissues[3]	60%

Characteristic events during formation of the notochord boundary: A series of stereotypical changes were observed, which were identified by studying the distribution of filamentous actin, clustering of C-cadherin, and cell morphology. 30 explants were analyzed from 8 independent experiments, and the percentage of instances where a given event was detected is provided in the last column. Notes: 1. The start or the end of the process were missing from several recordings, which accounts for the fact that early and late events scored lower percentages. 2. The final disappearance of transient clusters precisely coincided with the appearance of blebs. 3. The first and the last frames were compared. Note that the initial degree of clustering was variable.

Figure 4.5:

Myosin activity is required for cell sorting and inhibition of cadherin clustering

(A-C) Inhibition of Rho/ROK /MLCK interferes with cell sorting in mosaic embryos. (A, A') Transversal sections showing cells expressing LEF-VP16 (detected through its myc-tag, green) alone or co-expressed with the Rho inhibitor construct GTPase Binding Domain of Rhotekin (RhtkGBD). Plasma membranes were stained for β-catenin, nuclei with Höchst. Boundaries are indicated with dotted lines. (B,C) Quantification. Control cells distributed evenly between both tissues (~40% in the notochord). LEF-VP16-induced presomitic cells were almost completely excluded from the notochord. Sorting was inhibited by co-expression of dominant negative Rho (dnRho) or RhtkGBD (B), or incubation of the whole embryo in the presence of ROK (Y27632) or MLCK (ML-7) inhibitors (C). (D-E) Inhibition of Myosin II ATPase activity by blebbistatin causes fusion of the notochord boundary in a dose-dependent manner. (D) Examples of bright field images. Arrowheads: regular boundaries; arrows: partially fused boundaries (arrows). (E) Quantification. Boundaries were scored as "normal", "partially fused" (~ half of the length intact) or "fused or absent" (less than ¼ intact). (F-G) Blebbistatin treatment induces cadherin clustering and cell mixing across the notochord boundary. Frames from confocal movies of C-cadherin-GFP-expressing dorsal explants. Vertical projection of six focal planes. (F) Control explant. Arrowheads point to the smooth cadherin pattern along the boundary. (F') Blebbistatin-treated explant (see movie S4). Arrows: cadherin puncta at contacts between notochord and presomitic cells. Arrowheads: blebs with smooth cadherin distribution. (F") Detail of selected frames from the same movie. Arrows: dense puncta at contacts. Arrowheads: blebs remain much more stable than in controls (compare with Figure 4.2A and movies S1, S2, S3). (G) Quantification. Numbers on top indicate number of scored cells and number of embryo explants (5 independent experiments). Error bars: SD.

Figure 4.5

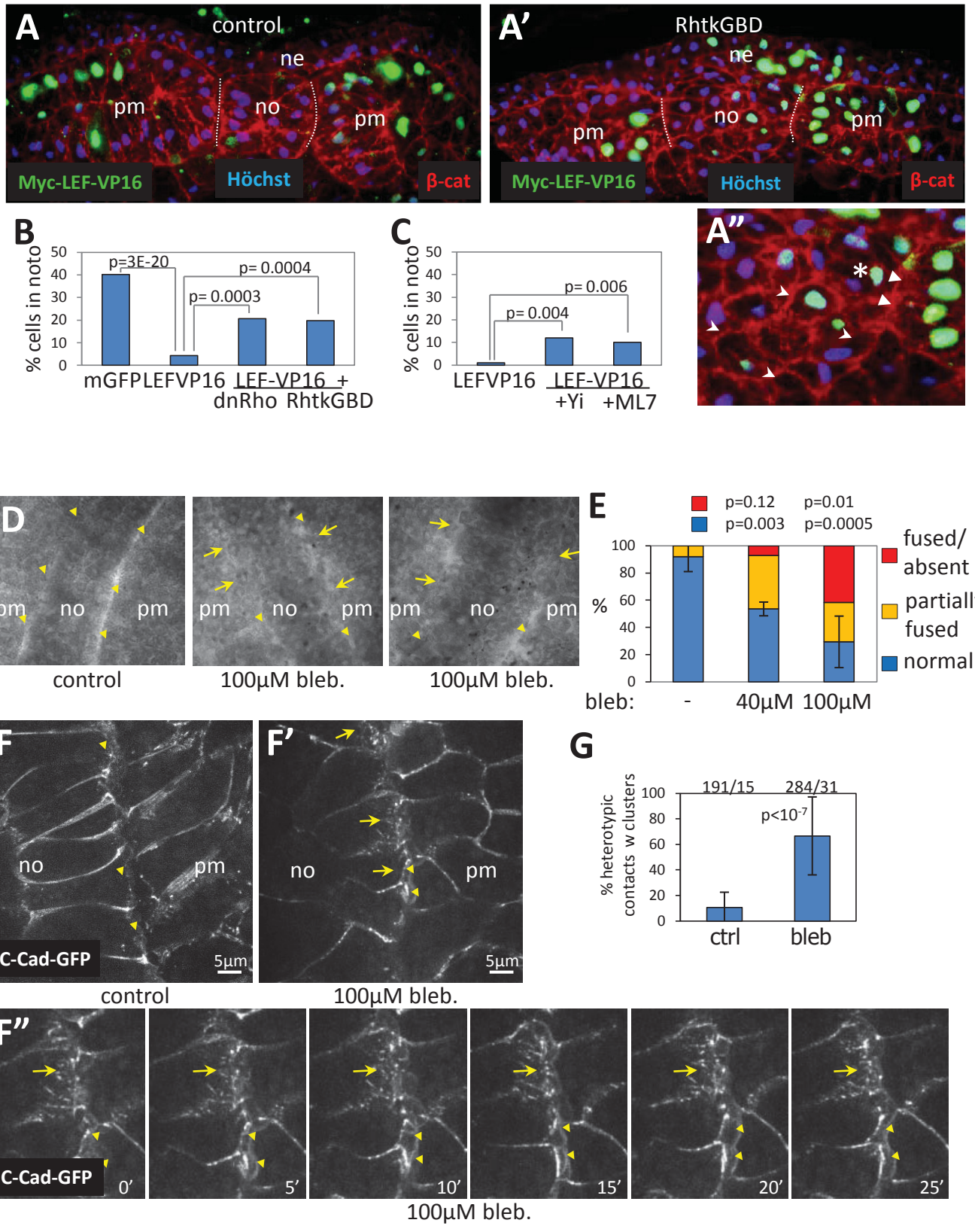
A
control
ne
pm
no
pm
Myc-LEF-VP16
Höchst
β-cat
A'
RhtkGBD
ne
pm
no
pm
Myc-LEF-VP16
Höchst
β-cat
B
% cells in noto
p=3E-20
p= 0.0004
p= 0.0003
mGFP
LEFVP16
LEF-VP16 + dnRho
LEF-VP16 RhtkGBD
C
% cells in noto
p= 0.006
p= 0.004
LEFVP16
LEF-VP16 +Yi
LEF-VP16 +ML7
A"
D
pm
no
pm
control
100µM bleb.
100µM bleb.
E
p=0.12
p=0.01
p=0.003
p=0.0005
% fused/ absent
partially fused
normal
bleb:
-
40µM
100µM
F
F'
no
pm
C-Cad-GFP
5µm
control
100µM bleb.
G
% heterotypic contacts w clusters
191/15
284/31
p<10-7
ctrl
bleb
F"
C-Cad-GFP
0'
5'
10'
15'
20'
25'
100µM bleb.

Figure 4.6:

Ephrin/Eph signaling is required for cell sorting, myosin activation, and inhibition of cadherin clustering at the notochord boundary.

(A) Scheme of differential expression of ephrinB2, EphA4 and B4 in the dorsal mesoderm (see relative values in Figure 4.S5).

(B-C) Ephrin/Eph depletion blocks sorting of LEF-VP16-expressing cells. LEF-VP16 DNA was coinjected with control (B) or Ephrin/Eph morpholino oligonucleotides (MO)(B'). Sections were stained for myc-tagged LEF-VP16 (red nuclei), C-cadherin (green membranes), FoxA4 (green nuclei), a nuclear marker for axial tissues (notochord, floor plate and archenteron roof), and Höchst (blue nuclei). Eph-depletion caused a significant number of LEF-VP16-expressing cells to remain inside the notochord (arrows). (C) Quantification from 3 independent experiments. p values correspond to comparison with LEF-VP16 alone.

(D-F) Interference with ephrin/Eph function perturbs the formation of the endogenous boundary. Embryos were injected with MOs or EphB4ΔC mRNA together with Myc-GFP mRNA as a tracer.

(D) Quantification. Each boundary was given a score of 0 (intact), 0.5 (partially disrupted) or 1 (absent). Columns represent the average score; the number of analyzed boundaries is indicated on top. Three categories of embryos were counted for Eph MO interference: total (t), notochord-targeted (no) or presomitic-targeted (pm) injection. The boundaries were strongly disrupted or absent in all cases where the injection targeted the tissue expressing high levels of the corresponding Eph (A4 in the presomitic mesoderm, B4 in the notochord). Injections targeted to the opposite tissue had no effect. *: $p<0.02$; **: $p<0.001$, 7 independent experiments.

(E, E') Examples of control and disrupted boundaries. Sections were immunostained for C-cadherin (green) and Myc-GFP, used as tracer (red). Flat arrowheads: normal boundary. Concave arrowheads: partial disruption of a boundary bordered by Myc-GFP/EphA4 MO-positive notochord cells (concave

arrowhead). Arrows: boundary absent, a group of injected cells spanning the area between notochord and presomitic mesoderm.

(F,F') MLC activation at the boundary requires ephrin/Eph signaling. (F) Strong continuous accumulation of p-MLC staining along the boundaries of control MO-injected embryos (arrowheads). (F') Partial (concave arrowheads) or complete (arrows) loss of p-MLC signal at the boundary in EphB4 MO-injected embryo. Images for other ephrin/Eph interfering conditions are presented in Figure 4.S5.

(G,G') Ephrin/Eph depletion does not affect notochord cell fate. FoxA4 positive notochord was still clearly identifiable in EphB4 MO-injected embryos, despite severely disrupted boundaries.

(H-J) Interference with ephrin/Eph function causes cadherin clustering across the boundary. (H) Frames from movie S5, EphA4 MO-injected explant expressing cadherin-GFP. Notochord cells and presomitic cells, marked respectively with orange "1" and blue "2", had extensively intercalated. Numerous cadherin puncta were observed at heterotypic contacts (concave arrowheads). Flat arrowheads: remaining blebs. (H') Detail of frame 20'. (I) Quantification: percentage of cells with clusters at the notochord-presomitic mesoderm interface. (J) Quantification of blebbing activity. Only unambiguous blebbing was quantified. Membrane undulations ("flapping"), although similarly inhibited by Eph depletion, were not easily measurable. 5 independent experiments.

Figure 4.6

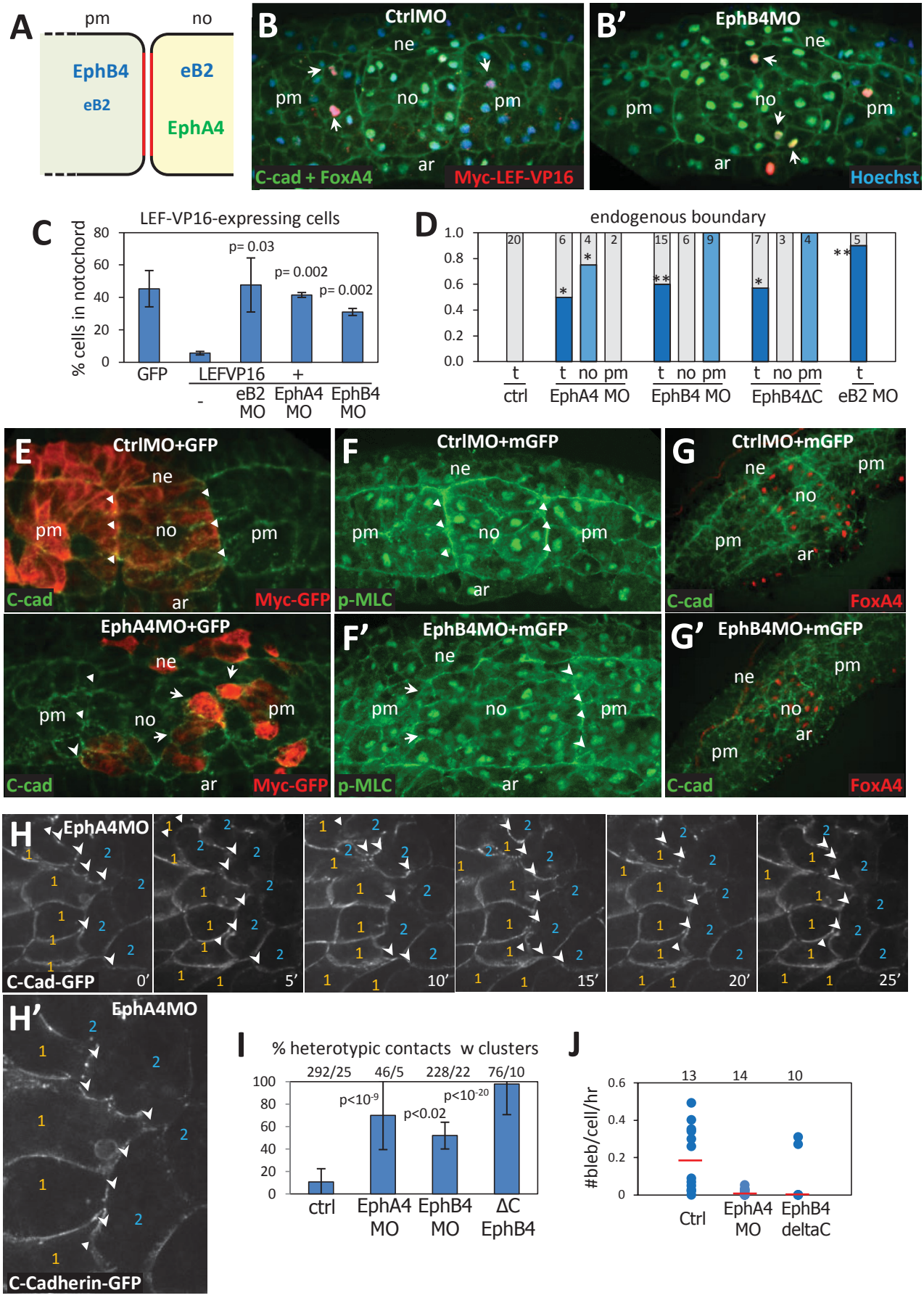
A
pm
no
EphB4
eB2
eB2
EphA4
B
CtrlMO
ne
pm
no
pm
ar
C-cad + FoxA4
Myc-LEF-VP16
B'
EphB4MO
ne
pm
no
pm
ar
Hoechst
C
LEF-VP16-expressing cells
% cells in notochord
p= 0.03
p= 0.002
p= 0.002
GFP
LEFVP16
-
+
eB2 MO
EphA4 MO
EphB4 MO
D
endogenous boundary
t
ctrl
t no pm
EphA4 MO
t no pm
EphB4 MO
t no pm
EphB4ΔC
t
eB2 MO
E
CtrlMO+GFP
ne
pm
no
pm
ar
C-cad
Myc-GFP
F
CtrlMO+mGFP
ne
pm
no
pm
ar
p-MLC
G
CtrlMO+mGFP
ne
pm
no
pm
ar
C-cad
FoxA4
EphA4MO+GFP
ne
pm
no
pm
ar
C-cad
Myc-GFP
F'
EphB4MO+mGFP
ne
pm
no
pm
ar
p-MLC
G'
EphB4MO+mGFP
ne
pm
no
ar
pm
C-cad
FoxA4
H
EphA4MO
C-Cad-GFP
0'
5'
10'
15'
20'
25'
H'
EphA4MO
C-Cadherin-GFP
I
% heterotypic contacts w clusters
292/25
46/5
228/22
76/10
p<10-9
p<0.02
p<10-20
ctrl
EphA4 MO
EphB4 MO
ΔC EphB4
J
#bleb/cell/hr
13
14
10
Ctrl
EphA4 MO
EphB4 deltaC

Figure 4.7:

Model for regulation of cell-cell adhesion at the boundary.

(A) Cell-cell contact-dependent signals generate cortical contraction, which inhibit cadherin clustering. Cadherins are represented in green, the actin cytoskeleton in red, and ephrin/Eph in yellow and orange. Low contractility along the lateral cell contacts is compatible with intimate cell-cell adhesion mediated by cadherin clusters. Ephrin-Eph signaling across the boundary triggers increased local contractility, which causes detachment of the plasma membrane from the actin cortex and prevents cadherin clustering. The resulting interface displays high membrane dynamics and very low cell-cell adhesion (dotted green line). The accumulation of filamentous actin and Dia1 along the membrane of the blebs corresponds to the rapid re-formation of a submembranous actin layer involved in bleb retraction.

(B) Summary of the events leading to the emergence of the boundary. Contractile fibers assemble along the future boundary. Progressive actin accumulation is accompanied by strong cortical contraction and by changes in cadherin localization: lateral connections are progressively reinforced, while a transient increase in clustering is observed across the boundary. Eventually, the cortical tension reaches sufficient levels to trigger membrane blebbing (or equivalent membrane undulations, not shown) and cadherin adhesions are stably inhibited. See also movie S3.

Figure 4.7

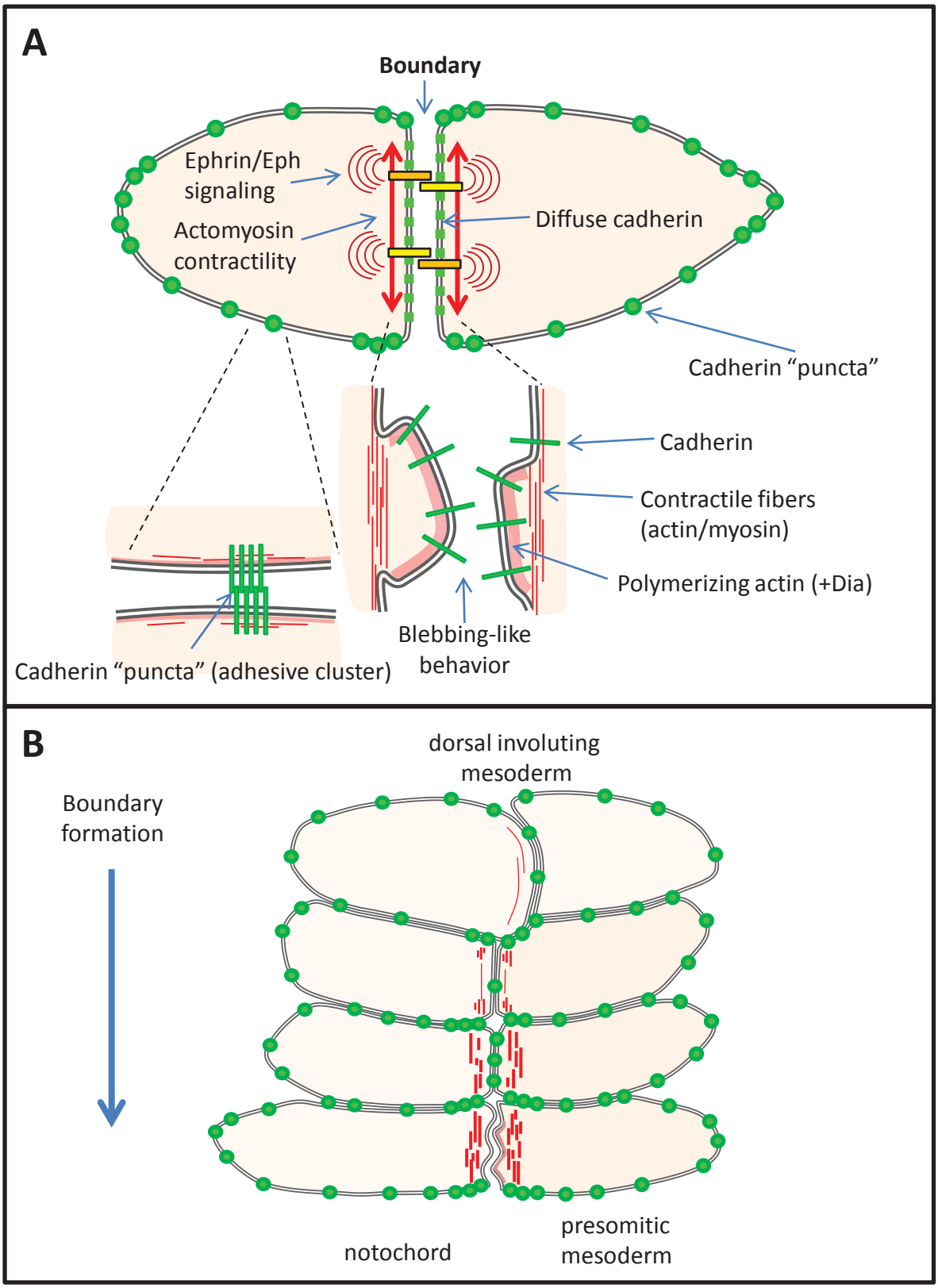
A
Boundary
Ephrin/Eph signaling
Actomyosin contractility
Diffuse cadherin
Cadherin "puncta"
Cadherin
Contractile fibers (actin/myosin)
Polymerizing actin (+Dia)
Blebbing-like behavior
Cadherin "puncta" (adhesive cluster)
B
dorsal involuting mesoderm
Boundary formation
notochord
presomitic mesoderm

Supplemental Figures and legends

Figure 4.S1:

A-E) Inhibition of cadherin clusters across the boundary is independent of cadherin levels. A-C) Quantitative analysis of contacts between cells expressing different cadherin levels in live dorsal mesoderm explants. A) Fields were selected where a single cell expressing high C-cadherin- GFP (asterisk) was surrounded by cells expressing low-medium cadherin levels. These high cadherin-expressing cells always localized on the notochord side of the boundary, due to β-catenin sequestration, which decreased Wnt signaling and induced sorting to the notochord (Reintsch et al,2005). High cadherin-expressing cell should in principle be able to establish similar contacts with all neighboring cells displaying equivalent cadherin levels. A') Diagram of the cell outlines. The membranes at the boundary are in red. Colored lines indicate examples of contacts corresponding to the profiles shown in B. The strong lateral homotypic junctions along the boundary were not included. B, B') Examples of intensity profiles. B) Comparison of a homotypic (light blue) and a heterotypic contact (orange) between the high cadherin-expressing cell and its notochord and presomitic neighbors. A horizontal homotypic contact between two low expressing cells is also included (dark blue). B') Comparison of a homotypic (medium blue) and a heterotypic contact (red) between low cadherin-expressing cells. Arrows point at typical peaks corresponding to cadherin puncta. In all cases, heterotypic contacts show fewer peaks, even when compared to homotypic contacts displaying lower signal intensities.C-C') Quantification of puncta density (C) and intensity signal in puncta (C') for homotypic (h) and boundary heterotypic contacts Puncta density and relative signal intensity showed dependence on cadherin levels: it was significantly higher for contacts between high and low cadherin-expressing cells, than for normal contacts. However, the puncta density remained very low at heterotypic contacts under all conditions. Data from ten independent experiments.

D) C-cadherin downregulation. Embryos were injected with plasmid DNA coding for ΔE-C- cadherin. The truncated cadherin was detected via its C-terminal myc-tag (red). The antibody used to detect endogenous cadherin (green) recognized the extracellular domain, absent in the ΔE construct. Dotted lines in D' mark the contours of the two cells. The global darker signal and the weaker clusters between the two injected cells reflect the

strong cadherin depletion in the two ΔE- expressing cells. Nevertheless, cadherin clusters were found at sites of contact with other notochord cells (arrows), including the neighboring cadherin-depleted cell (yellow arrows). Cadherin was almost completely absent from the boundary (arrowheads). Note that panel D was underexposed and panel D' overexposed (compare signal in wild type presomitic cells). E) Inhibition of cadherin clusters across the boundary is independent of cadherin subtype. E- cadherin was ectopically expressed by mRNA injection at the 2-cell stage and detected by immunofluorescence on transversal sections. The transcription factor FoxA4 was used as tissue marker, specific for the notochord and the endoderm, but absent from the presomitic mesoderm. Note that the general organization of the dorsal tissues is normal. E') Enlarged view of the boundary with smooth E-cadherin staining (arrowheads) and clusters at lateral membranes (arrows). ar, archenteron roof; fp, neural floor plate; ne, neuroderm; no, notochord; pm, presomitic mesoderm. F,F') Immunostaining for atypical PKC confirms the absence of apical-basolateral polarity in the early dorsal mesoderm tissues. Transversal sections were immunostained with anti-PKCζ (green) and C-cadherin (red) antibodies. Anti-PKCζ marked strongly the apical membranes of the outer layer of the neuroderm (ne) and of the archenteron roof (ar). All the other cells (inner layer of the neuroderm, notochord and paraxial mesoderm) showed a weak diffuse punctate signal without sign of polarization. G,G"') Localization of endogenous C-cadherin and colocalization with α-catenin along heterotypic and homotypic contacts.Horizontal section of the notochord-presomitic boundary immunostained for C-cadherin (green) G and α-catenin (red)G'. Cadherin-catenin clusters decorate the membranes in both tissues (white arrows), but are conspicuously rare along the boundary, which shows a thin smooth membrane pattern (arrowheads) except at the corner of the lateral junctions between adjacent cells of a same tissue (yellow arrows). G",G"')The intensity ratio between α-catenin and C- cadherin signals was measured at homotypic contacts (between notochord cells no/no) in the tissues and at heterotypic non-adhesive contacts (between notochord and presomitic cells no/pm) along the a-b line drawn in (G"). Red Arrows mark the dense spots at the margin of heterotypic contacts. The ratio was similar at homotypic and heterotypic contacts.

Figure 4.S2:

A) A single cell expressing membrane-targeted Cherry in an explant expressing cadherin-GFP globally. Embryos were injected with cadherin-GFP mRNA and with GAP-Cherry plasmid DNA. Vertical projection of multiple z-stack. Note that the cadherin signal at the boundary (flat arrowheads) is smooth independent of cadherin expression levels. Similarly, clusters are found at all homotypic contacts, also independent of cadherin levels (concave arrowheads). Arrow: protrusions extending and retracting along the boundary. A') Enlarged frame 35', highlighting the long protrusion (arrow). B) mCherry/LEF-VP16-expressing cells (asterisks) establish normal cadherin contacts with other presomitic cells (arrows). C) Control cells expressing mCherry alone Arrows: clusters at homotypic contacts, arrowheads: smooth heterotypic contacts. D-E) Sorting of LEV-VP16-expressing cells. D) Random motility in the notochord. Frames of confocal time lapse movie of a mosaic dorsal explant from a mosaic embryo injected with C-cadherin-GFP mRNA (global expression) and plasmid DNA coding for mCherry and LEF-VP16. The single mCherry/LEF-VP16-expressing cell (asterisk) is surrounded by smooth C-cadherin-GFP membranes (arrowheads). It shows dynamic but random shape changes and appears to slide between notochord cells. Lower panels: Cell outlines. E) Establishment of new adhesive contacts during sorting from the notochord to the presomitic mesoderm. Single mCherry/LEF-VP16-expressing cell (labeled "LEF", with smooth C-cadherin- GFP pattern indicated by arrowheads, Cherry not shown) contacts the notochord boundary (yellow arrowheads) in the second frame, which correlates with increased cadherin signal at the contact zone (arrows). Note that in the last frame the continuous smooth C-cadherin-GFP pattern of the boundary now including the integrating cell (yellow arrowheads). Lower panels: Cell outlines in red and boundary in black. E') Detail of frame 10', highlighting the newly formed homotypic contact between the LEF-VP16 expressing cell and a presomitic cell, and a heterotypic contact with the notochord (dotted lines). E") Line scans of these two contacts. The contact between the LEF-VP16 expressing cell and the presomitic cell (LEF-s) includes numerous bright puncta (puncta density ~0.3/μm, compared to an average of 0.07/μm along the entire

heterotypic contact between this cell and its neighboring notochord cells, red line panel E', frame 10').

Figure 4.S3:

A,A') Detection of filamentous actin in fixed embryos. Embryos were stained with Alexa-546- conjugated phalloidin (red), C-cadherin and the nuclear presomitic marker MyoD (both in green). Filamentous actin accumulated at the notochord boundary, as well as along the other tissue boundaries, i.e. neuroderm-mesoderm and endoderm (archenteron roof)-mesoderm. B,C,C') Detection of phospho-myosin light chain (p-MLC) in fixed embryos. Embryos were immunostained for p-MLC (red), C-cadherin and nuclear MyoD, a specific marker for presomitic mesoderm (both green). p-MLC accumulates along the notochord boundary (white arrowheads), as well as at the boundaries between the presomitic mesoderm and the neuroderm, and the archenteron roof (yellow arrowheads). D,E) Colocalization of Dia1 and filamentous actin. Live confocal imaging of an explant expressing Dia-1-YFP, RFP-Utrophin and eCFP, used as marker for soluble cytosolic proteins. Arrows point to lateral membranes, arrowheads to the boundary interface. Asterisks indicate bleb-like structures. D) Deep focal plane. E) Superficial focal plane, showing the gap exposed by removal of thearchenteron roof, filled with numerous blebs (asterisks). F) Absence of colocalization between filamentous actin and Arp3 at the boundary. Live confocal imaging of an explant expressing Arp3-YFP, RFP-Utrophin and eCFP. Concave arrowheads point at blebbing structure with a dense actin layer along the membrane, from which Arp3 is excluded. G-H) Live confocal imaging of an explant expressing Mena-YFP, RFP-Utrophin and eCFP. G) Deep focal plane. Ena is largely diffuse at the cell periphery. H) Superficial focal plane, showing Ena accumulation at small protrusions contacting the cover glass (arrows).

Figure 4.S4:

A) Quantification of p-MLC . Signal intensity of p-MLC and betacatenin were quantified on fixed embryos. p-MLC signal is significantly higher at heterotypic contacts(n-s) β-

catenin is used as a control. Data was collected from line scans of homo and hetero typic contacts from 6 independent experiments. B-F) Quantification of membrane enrichment for filamentous actin, myosin light chain, Dia1, Ena and Arp3. Confocal images were collected from live explants expressing RFP-Utrophin, MLC-Cherry, Dia1-YFP, Arp3-YFP and Ena-YFP. CFP was co-expressed and used as soluble cytoplasmic reference (examples in Fig.4.3 and supplementary Fig.4.S3). Intensity profiles of 1-2μm thick cross- sections of membranes were taken, both at lateral contacts in both tissues, and along the boundary. We excluded lateral "junctions" in the boundary area, as well as areas at the corners of three notochord or presomitic cells. Care was taken to collect data from contacts between cells displaying the widest range of expression, including "heterogenous" pairs (low and high expressing cells) to verify that the pattern was independent of levels. Each profile was divided by the corresponding control CFP profile. Values obtained for homotypic notochord or presomitic contacts were similar and were pooled. Each graph present the average of 10 profiles from 3 experiments. The x axis was centered at the position of the membrane, and the unit length was 0.25μm. p values correspond to ttest comparing the values between -0.25 and +0.25 μm with the average values at the sides (<-1.5 and >1.5μm). A) Actin showed enrichment at all membranes, but the levels were ~ 3 times higher along the boundary. $p<0.01$. B) MLC showed no enrichment at intratissular contacts, but a significant accumulation on both sides of the boundary ($p<0.01$). Note the broadest distribution compared to actin, consistent with contractile fibers often located at some distance from membrane. C) Dia1 was enriched to identical levels at all membranes ($p<0.01$). D) Ena showed a slight but significant increase signal at all membranes ($p<0.01$). E) Arp3 was not significantly enriched compared to CFP. Error bars are standard deviations.

Figure 4.S5:

A) Real-time PCR of ephrinBs and corresponding receptors expressed in the notochord and in the presomitic mesoderm, expressed in arbitrary units as relative mRNA concentrations. Two receptors, EphA4 and B4, are prominently expressed in asymmetric patterns, A4 in the notochord and B4 in the presomitic mesoderm. The identity of the

receptors has not been fully solved: EphrinB2, which is the only ligand for EphB4 (Rohani et al.), is partially enriched in a complementary pattern. Note that ephrinB2 is also ligand for at least EphA4 and EphB2. EphrinB1, enriched in the presomitic mesoderm, signals via EphB2, which is weakly expressed. EphrinB3, a ligand for EphA4, is also expressed at very low levels. Potential EphA4 ligands of the ephrinA type have not yet been investigated. B) Effect of ephrin/Eph interference on myosin activation. Embryos were injected with ephrinB2, EphA4 or EphB4 MO, or with ΔC EphB4 mRNA, together with membrane-GFP as tracer. p-MLC accumulation at the boundaries was strongly decreased or abolished by all interfering conditions. Conversion of the p-MLC signal to pseudocolors shows the specificity of ephrin/Eph interference with the boundary staining, with little to no effect on the signal within the tissues

Figure 4.S1

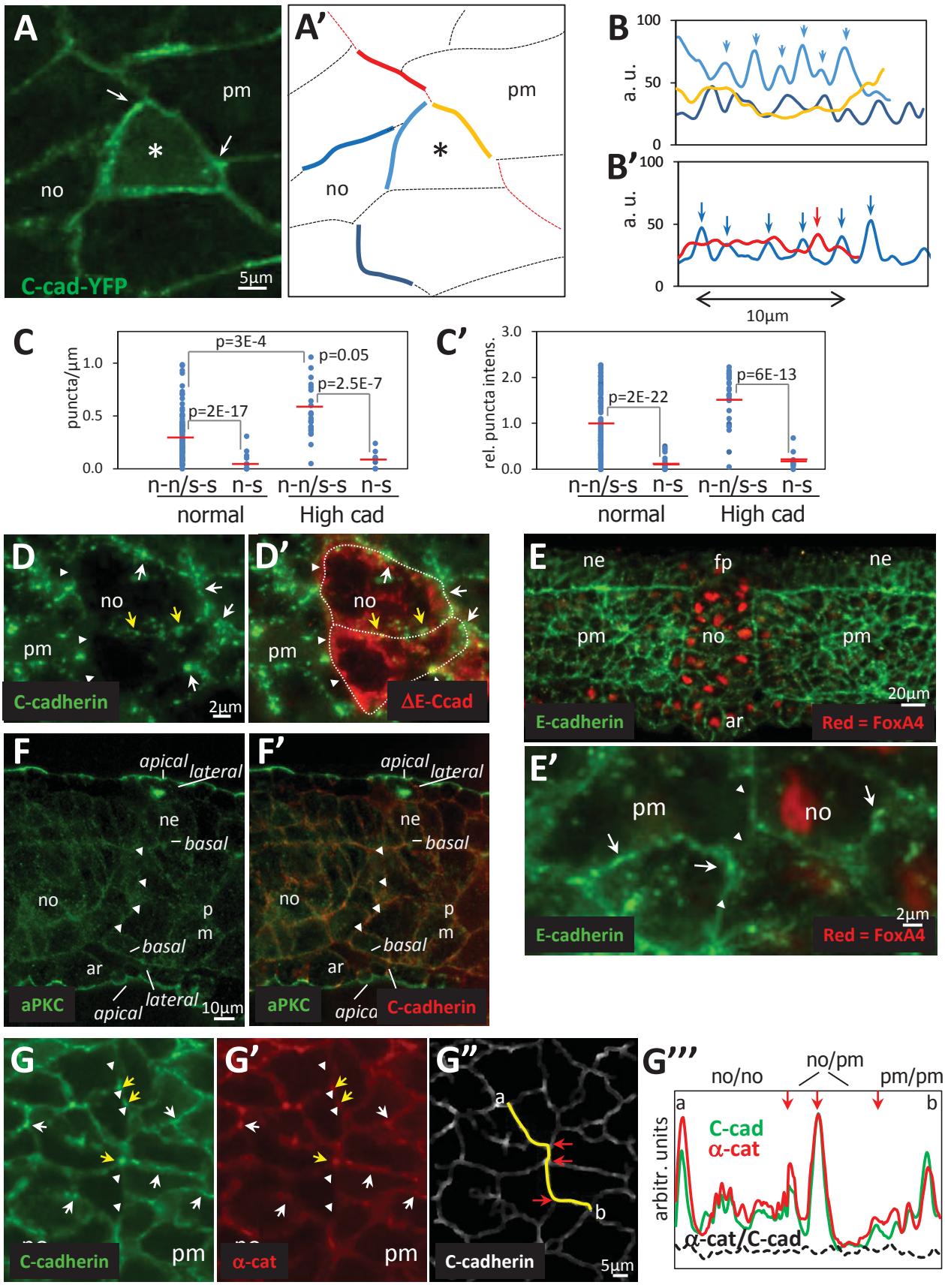
A
pm
no
C-cad-YFP
5µm
A'
pm
no
B
100
50
0
a. u.
B'
100
50
0
a. u.
10µm
C
puncta/µm
1.0
0.5
0.0
p=3E-4
p=0.05
p=2.5E-7
p=2E-17
n-n/s-s n-s n-n/s-s n-s
normal
High cad
C'
rel. puncta intens.
3.0
2.0
1.0
0.0
p=2E-22
p=6E-13
n-n/s-s n-s n-n/s-s n-s
normal
High cad
D
no
pm
C-cadherin
2µm
D'
no
pm
ΔE-Ccad
E
ne
fp
ne
pm
no
pm
20µm
E-cadherin
ar
Red = FoxA4
E'
pm
no
2µm
E-cadherin
Red = FoxA4
F
apical
lateral
ne
basal
no
p
m
basal
ar
aPKC
apical
lateral
10µm
F'
apical
lateral
ne
basal
no
p
m
basal
ar
aPKC
apica
C-cadherin
G
C-cadherin
pm
G'
α-cat
pm
G''
a
b
C-cadherin
5µm
G'''
no/no
no/pm
pm/pm
a
b
C-cad
α-cat
arbitr. units
α-cat/C-cad

Figure 4.S2

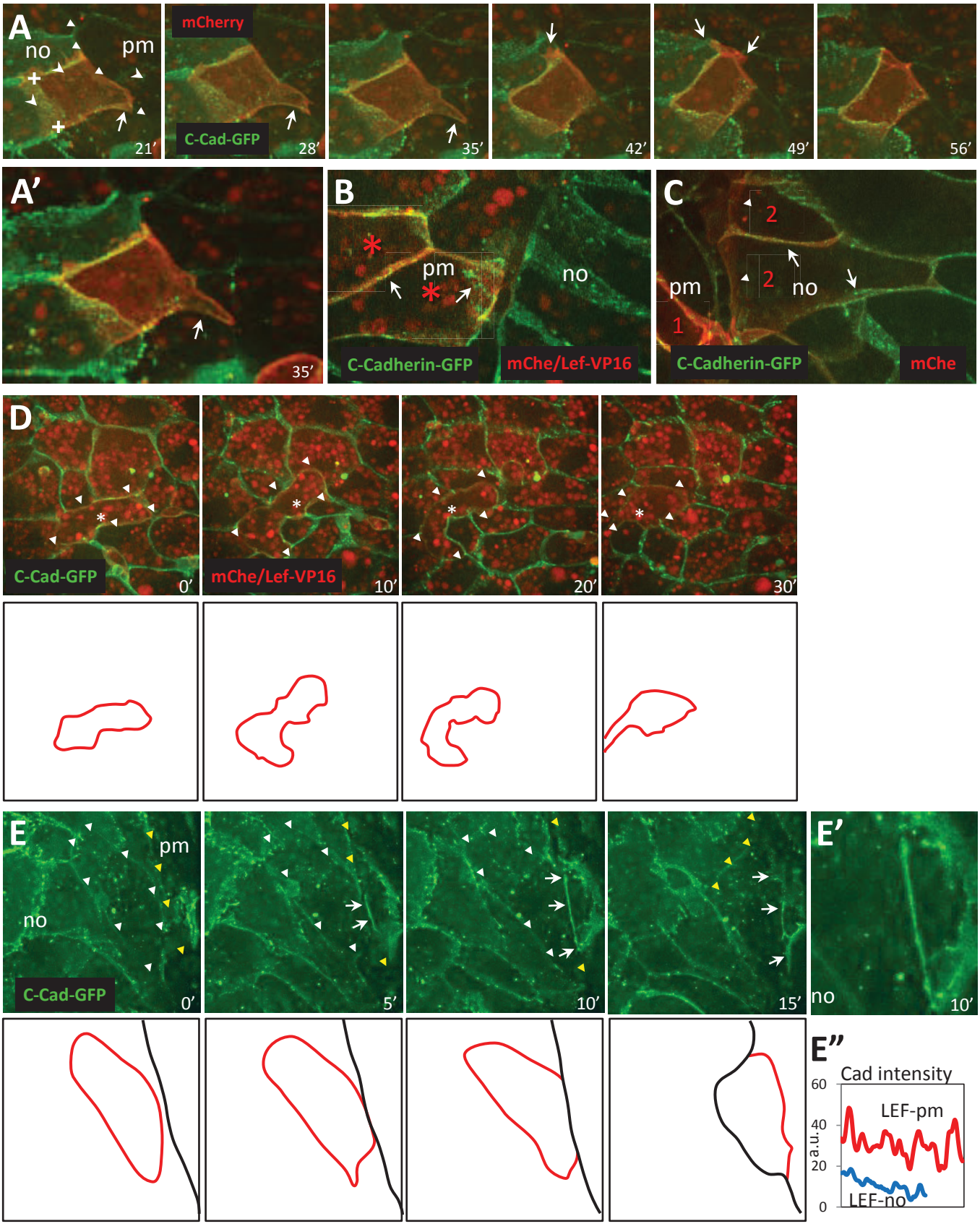
A
no
pm
21′
mCherry
C-Cad-GFP
28′
35′
42′
49′
56′
A′
35′
B
pm
no
C-Cadherin-GFP
mChe/Lef-VP16
C
2
2
pm
no
1
C-Cadherin-GFP
mChe
D
C-Cad-GFP
0′
mChe/Lef-VP16
10′
20′
30′
E
pm
no
C-Cad-GFP
0′
5′
10′
15′
E′
no
10′
E″
Cad intensity
60
40
20
0
a.u.
LEF-pm
LEF-no

Figure 4.S3

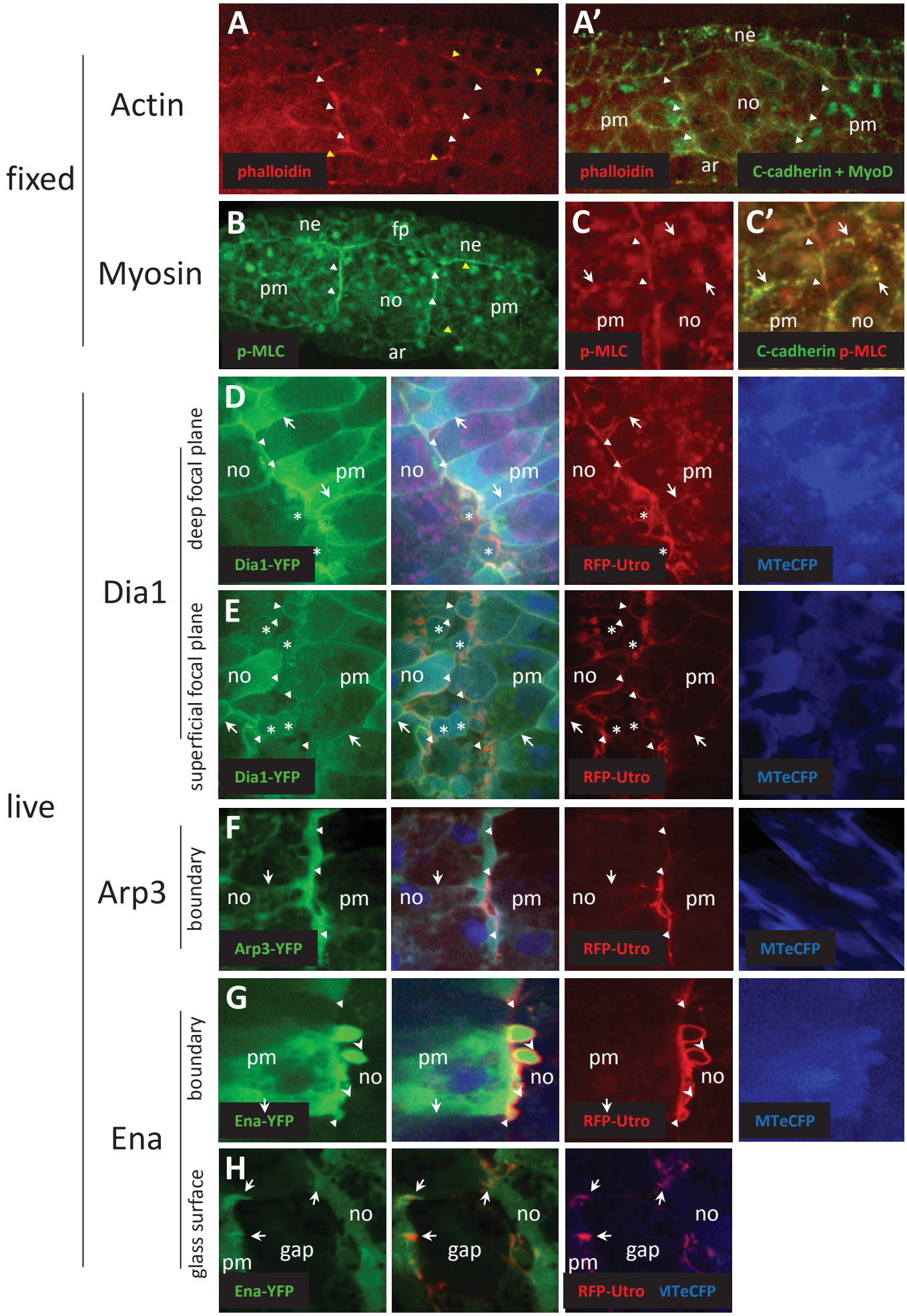
fixed
Actin
Myosin
live
Dia1
Arp3
Ena
deep focal plane
superficial focal plane
boundary
boundary
glass surface
A
phalloidin
A'
ne
no
pm
pm
phalloidin
ar
C-cadherin + MyoD
B
ne
fp
ne
pm
no
pm
p-MLC
ar
C
pm
no
p-MLC
C'
pm
no
C-cadherin p-MLC
D
no
pm
*
Dia1-YFP
*
no
pm
*
*
no
pm
*
RFP-Utro
*
MTeCFP
E
*
*
no
pm
*
*
Dia1-YFP
*
*
no
pm
*
*
no
pm
*
*
RFP-Utro
MTeCFP
F
no
pm
Arp3-YFP
no
pm
no
pm
RFP-Utro
MTeCFP
G
pm
no
Ena-YFP
pm
no
pm
no
RFP-Utro
MTeCFP
H
no
gap
pm
Ena-YFP
no
gap
no
gap
pm
RFP-Utro
MTeCFP

Figure 4.S4

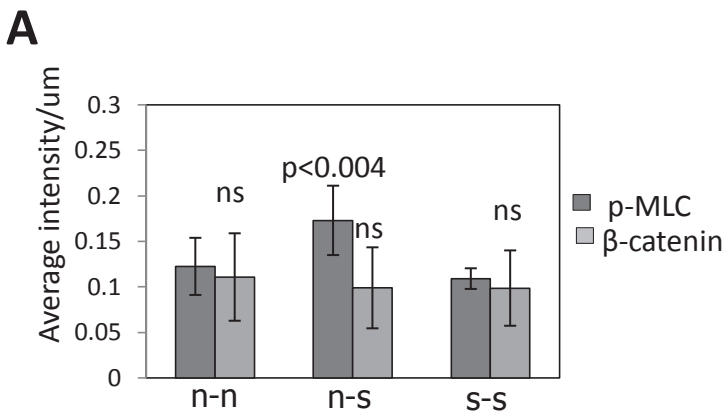
A
Average intensity/um
0.3
0.25
0.2
0.15
0.1
0.05
0
ns
p<0.004
ns
ns
n-n
n-s
s-s
p-MLC
β-catenin

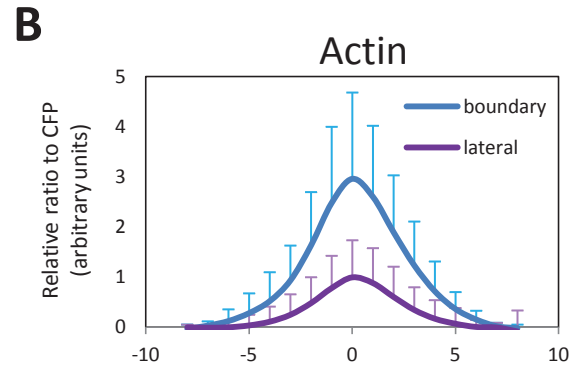
B
Actin
Relative ratio to CFP (arbitrary units)
boundary
lateral

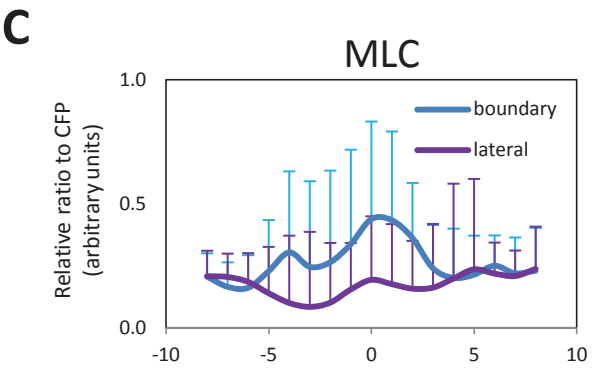
C
MLC
Relative ratio to CFP (arbitrary units)
boundary
lateral

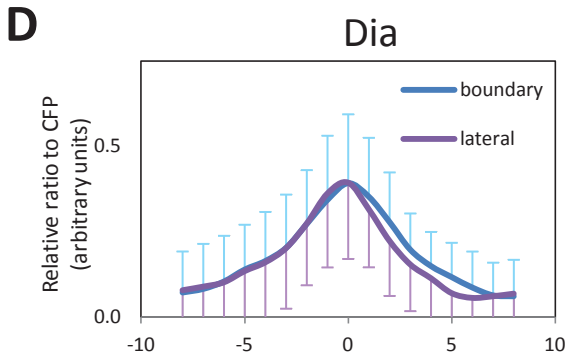
D
Dia
Relative ratio to CFP (arbitrary units)
boundary
lateral

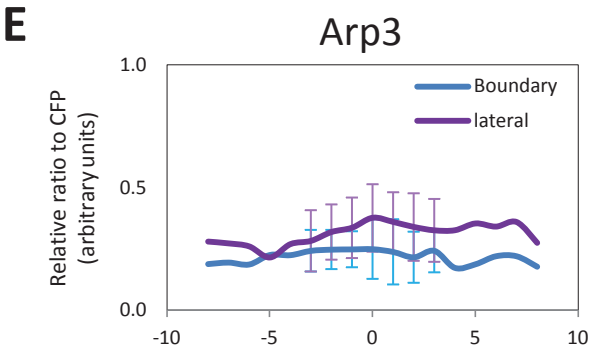
E
Arp3
Relative ratio to CFP (arbitrary units)
Boundary
lateral

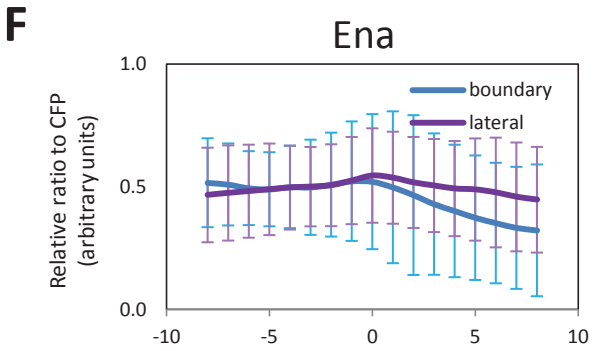
F
Ena
Relative ratio to CFP (arbitrary units)
boundary
lateral

Figure 4.S5

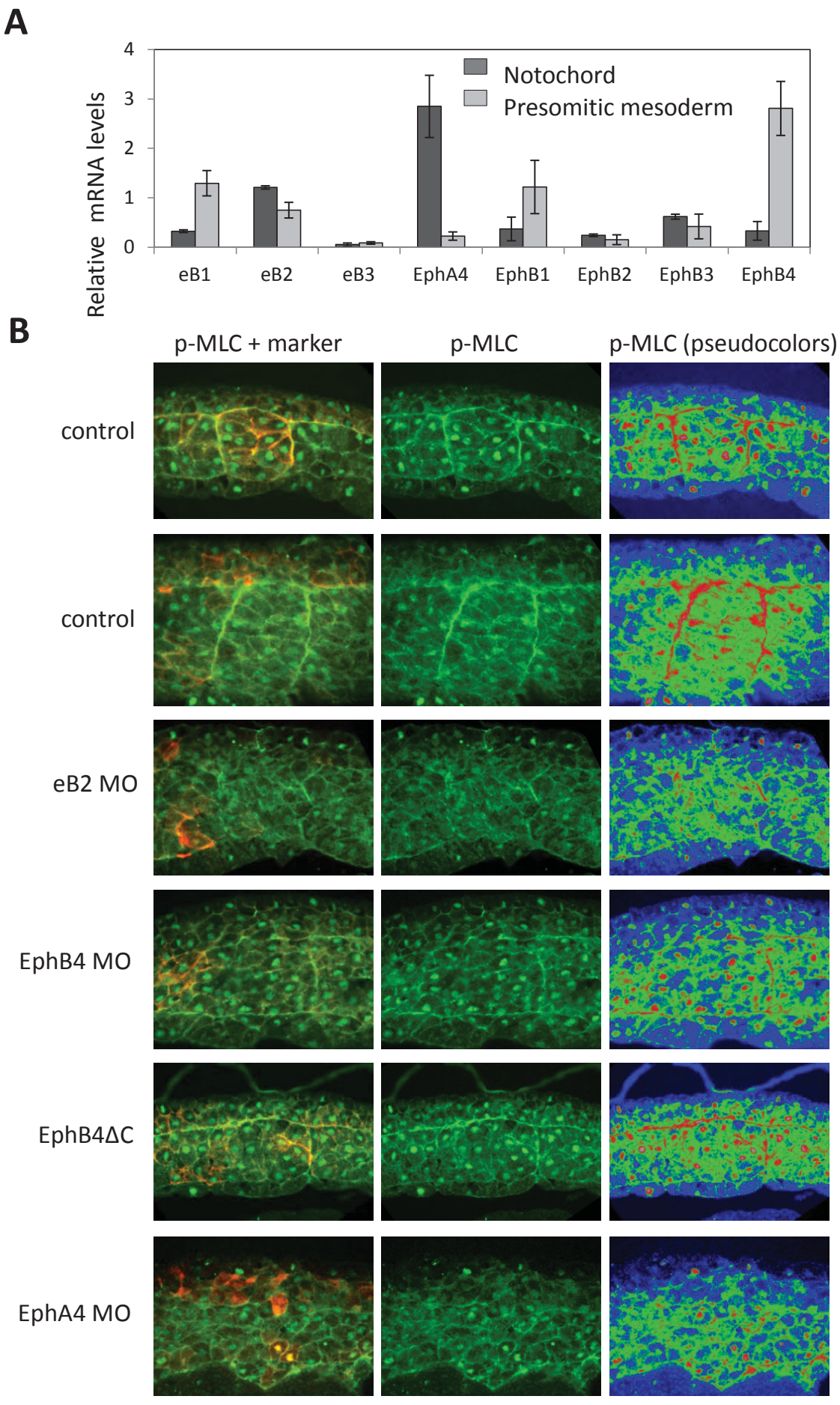
A
Relative mRNA levels
4
3
2
1
0
Notochord
Presomitic mesoderm
eB1
eB2
eB3
EphA4
EphB1
EphB2
EphB3
EphB4
B
p-MLC + marker
p-MLC
p-MLC (pseudocolors)
control
control
eB2 MO
EphB4 MO
EphB4ΔC
EphA4 MO

Chapter V: Discussion

This thesis clarifies our understanding of the mechanism by which boundaries form. It focuses on the formation of boundaries at early stages of development and for the first time provides an in depth analysis of the cellular behaviour at tissue interfaces, which until now has remained undiscovered due to the absence of high resolution cellular approaches. The core of our finding relies on the observation that cells at the boundary retract their membranes upon contact. We have shown that this behaviour is controlled by a network of ephrin and Eph molecules that interact selectively and are expressed in a partial complementary pattern in the two opposing cell types. Such specific molecular network creates a code by which cells of different tissues are distinguished. Their interaction at tissue interfaces leads to repulsion, local modulation of actin cytoskeleton, inhibition of adhesion and eventually creation of a boundary.

Comparing a model based on ephrin-Eph mediated tissue separation and the existing models:

"Contact inhibition" best describes cell behaviour at tissue boundaries

"Contact inhibition of movement" is a phenomenon which has been observed in culture cells (Abercrombie, 1970) and its role in neuronal guidance is well established (Carmona Fontaine et al., 2008; Garrod, Garrod, & Steinberg, 1973; Shih & Keller, 1992). It has been also proposed as an alternative model to DAH for cell sorting, consistent with the involvement of ephrins and Ephs at segment boundaries (Batson, Astin, & Nobes, 2013; Harbott, Marston, & Nobes, 2004; Marston, Dickinson, & Nobes, 2003; Qiling Xu, Mellitzer, & Wilkinson, 2000). However, the actual cell behaviour at the boundary has never been observed at a sufficient temporal and spatial level to demonstrate the existence of contact inhibition.

We now show that the process of boundary formation and maintenance indeed depends on direct cell to cell contact across the tissue interface. This contact induces increased contractility of the actin cytoskeleton leading to cell retraction, a reaction that is

dependent on ephrin-Eph signaling. This behavior conforms in all aspects to a bona fide case of "contact inhibition".

Revisiting DAH and DITH; a novel understanding of Holtfreter "differential affinity"

Since Holtfreter proposed the concept of "differential affinities", several studies attempted to address the nature of these "affinities". However, so far none provided a fully satisfactory molecular explanation.

The field has been strongly influenced by the differential adhesion (DAH) and the differential interfacial tension hypotheses (DITH). Note however that both models have always been subjected to criticism (Foty & Steinberg, 2005; Harris, 1976; Manning, Foty, Steinberg, & Schoetz, 2010; Malcolm S. Steinberg, 2007). It has been argued that although in vitro experiments support these models, they are not sufficient to explain tissue separation in vivo. For example, in the case of DAH, a recent study demonstrated that adhesive differences are not sufficient for the separation of ectoderm and mesoderm ((Ninomiya et al., 2012), L.Canty and F.Fagotto unpublished). Similarly the study of intrinsic biophysical properties of presomitic mesoderm suggested that a model based on DITH was not sufficient to describe somite segmentation (Grima & Schnell, 2007).

Many observations indicate that tissues separated by a boundary are not as different as thought before, in terms of adhesion and cortical tension. For instance, when one compares Xenopus ectoderm and mesoderm, cadherin levels are certainly lower in the most anterior mesoderm but not in the posterior mesoderm (Rudolf Winklbauer & Kwang, 2009), F.Fagotto unpublished), and the same is true for measures of tissue cohesion (Luu, David, Ninomiya, & Winklbauer, 2011). The case is probably most striking for the boundary that separates the notochord from the paraxial mesoderm: We found indeed that the two tissues are indistinguishable in terms of cadherins and actomyosin.

There are also doubts on physiological relevance of the tensiometric studies supporting DITH (Krens, Möllmert, & Heisenberg, 2011; Krieg et al., 2008; Maître et al., 2012; Maître & Heisenberg, 2011; Manning et al., 2010; M.S. Steinberg, 1970; Malcolm S.

Steinberg, 2007). Indeed, these measurements were performed in vitro and on single cells, and are applicable to in vivo situations only if one assumes that the mechanical properties of the tissues can be modelled based on those of individual cells (Beysens, Forgacs, & Glazier, 2000; Davis, Phillips, & Steinberg, 1997; Phillips, 1978). In particular, the model implicitly considers cortical tension as a stable parameter that remains unaffected by the nature of the local environment, including of the contacts with neighbors. However, the observation of cell behaviour at the boundary reveals that the mechanical properties of cells are constantly influenced by interaction with adjacent cells: Cells at the boundary change shape to probe the adjacent cells, make contacts, adhere, retract and de-adhere. All these parameters influence the cell's contractile energy and have never been taken into account in DITH measurements. In fact, cortical actomyosin accumulates much more at the boundary than at other contacts, an observation that is inconsistent with DITH, but fully consistent with high localized boosts in contractility due to ephrin/Eph signaling. Actomyosin "cables" also characterize the Drosophila parasegment and wing A/P boundaries (Aliee et al., 2012; Dahmann, Oates, & Brand, 2011; Landsberg et al., 2009; Monier, Pelissier-Monier, Brand, & Sanson, 2010; Monier, Pélissier-Monier, & Sanson, 2011). The mechanism controlling such local actomyosin rearrangement in Drosophila is not known. In summary, while both DAH and DITH postulate the existence of global tissue cell differences, there isn't any firm evidence that such differences are sufficient to influence in vivo tissue separation. However, we do observe dramatic differences both in terms of adhesion or contractility at the boundary, due to local ephrin-Eph signaling. In fact the observed differences between the boundary interface and contacts within tissues is much larger than any of the differences between tissues, implying that global DAH/DITH may play at most a secondary role in tissue separation.

We propose that DAH/DITH could nevertheless contribute to the process together with ephrin-Eph-mediated local changes. Such collaborative mechanism can be pictured as follows: Intrinsic differences in adhesion/tension of the two tissues may produce rough cell clusters, which may contribute to the initial sorting, of the two cell populations, but would not be sufficient to produce or maintain sharp boundaries. Local repulsive signaling would then complete the sorting process and generate the final boundary. Note

that the basic concept of "surface tension", which is at the core of DAH/DITH, remains fully valid in our model if transposed to a local scale and a dynamic model, where each individual cell-cell contact can vary in adhesion and tension and contribute to the global "energy" of the system.

Back to the initial concept of differential affinity (Holtfreter, 1939)Townes & Holtfreter, 1955), our work provides a new view, where these affinities are not directly due to the differences in adhesion or tension, but rather to cell surface cues that play the role of an identity "code". This code is complex, as it depends on an interactive network of multiple selective ephrin-Eph pairs. The readout is however quite sharp, i.e. separation or mixing. Thus, we believe that the ephrin-Eph "profiles" is a general principle that represents the "affinities" of the different embryonic tissues.

Expression of multiple ephrin and Ephs

The classical model of ephrin-Eph signaling considers systems where one cell type expresses an ephrin ligand and the other cell type the cognate Eph receptor. The overwhelming majority of studies over the past twenty years have dealt with this type of situation. In many cases, the experimental system was selected precisely because the ephrin/Eph expression patterns appeared simple, fulfilling these classical conditions. Note that a systematic search for other ligands and receptors was rarely performed: detection of a single pair expressed in a complementary pattern seemed sufficient to assume that they would alone account for the whole system. Thus, for many years, the field has almost systematically ignored the growing evidence for the generalized complexity of ephrin and Eph expression patterns. The presence of multiple ephrins and Ephs, often in the same cell types, was in fact already established in the early studies (H. Cheng, Nakamoto, Bergemann, & Flanagan, 1995; Guthrie & Lumsden, 1991; Iwamasa et al., 1999; Kury, Gale, Connor, Pasquale, & Guthrie, 2000). To date, examples have been found in all types of biological processes, including neural development, angiogenesis or cancer. Multiple expressions was also found at embryonic boundaries: Expression studies by (Baker & Antin, 2003) have reported the presence of several

ephrins and Ephs in the segments of the somites, and several ephrins and Ephs are expressed in rhombomeres (Y.-C. Cheng et al., 2004; J. Cooke et al., 2001; J. E. Cooke & Moens, 2002; Guthrie & Lumsden, 1991). We have generalized these observations, by adding to the list the ectoderm-mesoderm and the notochord boundaries. It is now beyond doubt that complex ephrin-Eph networks are present in most developing vertebrate embryonic tissues.

Systems with multiple ephrin-Eph systems have only been started to be analyzed quite recently, and only in in vitro. There were too main obstacles, one technical, i.e. the need to perform multiple knock outs/depletions and multiple rescues, the second conceptual, since it was generally believed that these molecules were redundant and would compensate for each other (D. Arvanitis & Davy, 2008; Herath et al.; Walsh & Blumenberg, 2011).

There were however some evidences for ligand-receptor specificities (Blits-Huizinga, Nelersa, Malhotra, & Liebl, 2004; J. Flanagan, Flanagan, & Vanderhaeghen, 1998; Gale et al., 1996; Wang, Chen, & Anderson, 1998), and, as discussed in the introduction, some recent seminal studies have started to dissect complex cellular systems and have uncovered sophisticated crosstalks (Astin et al., 2010; Carvalho et al., 2006; Kao & Kania, 2011).

Nothing had been done, however, to evaluate the issue in an embryonic model.

Thanks to the ease to perform large scale knockdown, in all possible combinations, the Xenopus model has allowed us to overcome at least part of the technical limitations. We could thus demonstrate that each individual ephrin and Eph receptor is required and that these molecules are not interchangeable. We could show that behind this apparent high complexity, the system may be relatively simple: The final output, tissue separation, could indeed be explained by the additive contribution of all ephrin/Eph pairs that could form at the tissue interface.

These findings have a general impact in the ephrin/Eph field, as they highlight the importance of the differential affinities. This concept had been already considered, but its implications had never been addressed in such a systematic way. It may be noteworthy to mention that knock outs in mice indicated redundancy between ephrins (Coulthard et al., 2002; Herath et al., 2012; Klein, 2004; Passante et al., 2008). It is quite possible that the

mouse embryo adapts on the long term to the loss of one of these molecules, a problem that is circumvented in our model by the short term knock down approach.

The reason for multiplicity

While we can now predict what will be the output of multiple ephrin-Eph pairs, the question remains of why so many molecules are expressed in these tissues. At first sight, a single pair of ligand and receptor should be sufficient to produce separation, and this has been indeed shown to be possible in vitro (Jørgensen et al., 2009). While very little is known about the transcriptional control of ephrin/Eph expression, their expression patterns clearly indicate that they must be under the control of the same tissue specific genes that regulate other aspects of embryonic development (Theil et al., 1998). It is thus not unreasonable to assume that these ephrins and Ephs have also functions directly associated to the fate and/or morphogenesis properties of each embryonic tissue. Studies in Zebrafish, chicken and Xenopus gastrula provide indeed some evidence for functions beyond repulsion at tissue boundaries: EphrinB2 and EphA4 seem to have an adhesive function inside rhombomeres (J. E. Cooke, Kemp, & Moens, 2005; Kemp, Cooke, & Moens, 2009). Similarly, ephrins and Ephs seem to increase cohesion of the Xenopus ectoderm (Lee et al., 2009; Lee, Nishanian, Mood, Bong, & Daar, 2008; Rohani, Canty, Luu, Fagotto, & Winklbauer, 2011). Furthermore, EphA4 in Xenopus mesoderm regulates the expression of the mesoderm specific gene (Brachyury) and affects cell migration of Xenopus mesoderm (R. Winklbauer, unpublished). Somitogenesis is an example of how ephrins and Ephs may coordinate tissue separation with other morphogenetic processes, in this case epithelialization (Barrios et al., 2003; Watanabe, Sato, Saito, Tadokoro, & Takahashi, 2009): The authors showed that ephrinB2-EphA4 bidirectional signaling is required for two different processes: on one hand, reverse signaling represses Cdc42 and thus induces epithelialization of the cells lining the posterior side of the next forming boundary. On the other hand, forward signaling maintains the posterior cell separation from anterior cell presumably through repulsion, although this has never been directly investigated. The role of ephrinB2 reverse signaling in epithelisation is an example of a specific requirement in a particular tissue. Note that in

terms of simple separation, at least in early embryos, we did not observed similar requirements, since we could swap an ephrin-Eph pair and thus perfectly rescue separation (chapter III). Thus one could imagine that the network present in embryos is the result of a compromise between requirements for particular ephrins and Ephs for tissue specific functions, and the overall need for a stronger signal at tissue interfaces, which constrains the system by the need of at least some partially complementary asymmetric pairs.

Note that an additional advantage of the multiplicity of ephrins and Ephs could be reinforcement of the process of separation: multiple parallel/antiparallel signals may ensure robust separation even though levels of single molecules may sometimes vary. It is quite conceivable that this system would have important ecological and evolutionary advantages.

The importance of differential affinity

Promiscuity of binding among different ephrin ligands and receptors is very well accepted in the field (D. Arvanitis & Davy, 2008; Blits-Huizinga et al., 2004; J. G. Flanagan & Vanderhaeghen, 2003; Haramis & Perrakis, 2006; Pasquale, 2004; Zimmer et al., 2011). It was suggested that within each class, there is almost no preference for a ligand to bind to a specific receptor. This idea was further reinforced when inter-class interactions were reported; suggesting that even inter-class promiscuity might exist. However, this concept of promiscuity did not fit with the in vitro affinity measurements, which gave very different dissociation constants for each ligand-receptor pairs. For instance, EphB2 significantly interacted with only one ephrinA (A5), and even within the B subclass, only with ephrinB1 and B2. Reciprocally, ephrinA5 bound only to a subset of EphAs and to EphB2 (Himanen et al., 2004; Wybenga-Groot et al., 2001). Similar results were obtained with virtually all tested ephrins and Ephs (Blits-Huizinga et al., 2004; J. G. Flanagan & Vanderhaeghen, 2003).

In only a very few cases the functional relevance of these differences in affinities has been addressed (Astin et al., 2010; Gerety, Wang, Chen, & Anderson, 1999; Kumar et al., 2009).

Our study is to our knowledge the first one, where different ephrins/Eph combinations have been systematically tested in vivo, and where conclusive evidence for functional selective pairing is demonstrated. It is also the first time that the multiplicity of ephrins and Ephs at tissue boundaries is taken into account to provide a global description of their role in tissue separation. Our demonstration that each ephrin and each Eph receptor is specifically required is one of the most striking demonstrations of the concept of ephrin/Eph selectivity. We further showed that the specificity of each receptor relies on its ligand binding domain. Thus, at least in first approximation, the system does not appear to rely so much on qualitative differences in intracellular signaling, but mainly on the ability of a ligand to interact specifically with a limited subset of receptors. This model is corroborated by the very good, although not perfect, correlation between the specific functional pairs identified in our study and the high affinity pairs found in the previous in vitro binding assays (Blits-Huizinga et al., 2004; J. G. Flanagan & Vanderhaeghen, 2003). Our results strongly challenge the assumption of binding promiscuity, and should stimulate reinterpretation of many previous data in other systems where multiple ephrins and Eph receptors are expressed.

The importance of ephrin-Eph asymmetric expression for tissue separation

Several studies show asymmetrical expression of ligands and receptors in adjacent cell types (Astin et al., 2010; Batlle et al., 2005; Durbin et al., 1998; Hafner et al., 2004; Herath et al., 2012; Theil et al., 1998; Q. Xu, Alldus, Holder, & Wilkinson, 1995) . However, the functional significance of these expression patterns was not directly examined. In my thesis, the distribution of several ligands and receptors was systematically analyzed for three boundary models. In all three cases, there were always at least two selective ligand-receptor pairs that showed partial asymmetry of expression. We showed that this asymmetry is crucial for tissue separation. It is required, since depletion of an ephrin or an Eph participating to any of these asymmetric pairs causes cell mixing. It is also sufficient to induce separation: Two aggregates of the same tissue can be induced to separate when an asymmetry is artificially created by ephrin or Eph overexpression.

An interesting question that remains to be addressed is the transcriptional and posttranscriptional control that achieves this highly sophisticated network of asymmetric expression. The regulation mechanisms that control ephrin/Eph levels have just recently begun to be explored. One study showed that homeobox transcription factors can regulate Eph receptor expression (D. N. Arvanitis & Davy, 2012). Another study suggested that ephrinB1protein levels in mesoderm are controlled by tissue specific ubiquitin ligases, a mechanism that seems to be required for proper ectoderm-mesoderm separation (Hwang et al., 2013). This study is consistent with our findings; in the sense that it also suggests that different ephrin levels in each tissue are important for the separation at the ectoderm-mesoderm boundary.

Ligand receptor Co-expression on the same cell: Additional level of complexity

So far, several complicated models have tried to explain the mechanisms controlling crosstalk between ligand and receptor on the same cell. One model states that ligands and receptors on the same cell can interact in cis and inhibit each other (Carvalho et al., 2006), while another model states that ephrins and Ephs on the same cell are localized on different membrane sub-domains, and are functionally independent (Marquardt et al., 2005). A recent study proposed a model that combines these two mechanisms, where cis-inhibition operates when ephrin expression is high, while otherwise ephrins and Ephs can signal independently (Kao & Kania, 2011). Experimental validation of these models is difficult, especially in the systems where, each cell expresses several ephrins and Ephs. While it is quite possible that cis-interactions participate to the overall integration of signals in embryonic tissues, it does not seem necessary to invoke this mechanism and to explain our results on tissue separation. In fact none of our data shows any sign for a significant cis-inhibition: Indeed, one would then expect that depletion/overexpression of an ephrin in one tissue should boost the repulsive activity of the Eph receptors of the same tissue. However, all our loss-of-function and gain-of function data fit with a simple "positive" contribution toward repulsion at the boundary, and they all argue that the requirement is in trans (see in particular rescue by incubation with soluble Fc-fragments). This holds true for all ephrins and all Eph receptors tested so far.

We propose that the system can be accurately explained simply based on selective ephrin-Eph trans-interactions. Although we have no experimental data about ephrin and Eph subcellular localization, we favor the idea of separate membrane concentrations for ligands and receptors, since selective trans-interactions are expected to increase ephrin/Eph local density on the membrane. The various pairs would thus act in parallel, largely independently of each other, which is exactly what our functional data suggest. This would fit with their individual contribution.
We would not exclude, however, the existence of cis-inhibitory mechanisms or other potential crosstalks that may be active in the early embryo, for example to contribute to the observed "pro-adhesive" function of ephrins within the ectoderm.

Recurrent aspects of ephrin/Eph expression patterns and possible implications for cleft like boundaries

Analyzing the expression patterns of different ligands and receptors throughout the gastrula stage of Xenopus revealed an interesting trend. Some recurrent features could be distinguished: Among those ephrin-Eph pairs that we showed to be functionally and biochemically selective, a subset appears to be systematically expressed in partial complementary patterns. These are eprhinB3- EphA4, ephrinB2-EphB4, and ephrinB2-EphB2. On the contrary, we found that another strong selective pair, ephrinB2-EphA4, was enriched within the same tissue in all three boundaries examined. The network is probably conserved: in Zebrafish, ephrinB3 is also ectodermal, while EphA4 and ephrinB2 are both expressed in the axial mesoderm (ZFIN website). Other systems seem to use the same pairs: for example, ephrinB3-EphA4 an ephrinB2-EphB2 are found in many neuronal systems, and also expressed across rhombomeric boundaries (J. E. Cooke et al., 2005; J. E. Cooke & Moens, 2002; Kemp et al., 2009). A simple logical explanation is that the pairs expressed in complementary patterns are those which are the most selective: EphA4 is the only receptor for ephrinB3, while ephrinB2 is the preferred ligand for EphB2 and EphB4. Thus this guarantees the maximal specific pairing at the interface, despite expression of other ligands and receptors.

It is also possible that particular ephrins and Ephs play specific roles in one or the other tissue, either for morphogenesis and/or for cell fate determination.
It seems that the expression of EphA4 is linked to the expression of Brachyury in mesoderm: In the early gastrula both are globally enriched in mesoderm, in the late gastrula they become restricted to its axial portion of mesoderm that becomes the notochord.

Without a complete map for the ephrin-Eph expression and a comprehensive functional analysis, it is difficult to generalize that the same pattern of expression separates cells across all boundaries. However, as discussed above and based on current available information, it seems that in several systems and boundaries the ephrin/Ephs profile follows a very common design, with two pairs of ligands and receptors (ephrinB3-EphA4 and ephirnB2-EphB4 or ephrinB2-EphB2) expressed in antiparallel complementary patterns.

Ephrin-Eph expression in cancer

Similar to cells in developing embryos, most cancer cells also exhibit a complex pattern of ephrin ligands and receptors. In fact it is suspected that the differential regulation of their levels is one of the main reasons for the emergence of tumor metastasis (Hafner et al., 2004; Herath et al., 2012). This phenomenon is not confined to a single ephrin or Eph and involves a wide array of ephrins and Ephs, which are up- or down-regulated at different steps during tumor progression. For example, in breast cancer EphA2, A7, A10, and ephrinA2 and B3 are up-regulated and are involved in tumor formation, while down-regulation of EphA1, A3, A4, A8, B3, B4, B6, and ephrinA1 and B1 are particularly important in invasion phase(Fox & Kandpal, 2004; Wu et al., 2007). This complex expression pattern and its temporal fluctuation resemble what we observe in development (D. N. Arvanitis & Davy, 2012; Brantley-Sieders, 2012; Herath & Boyd, 2010; Kumar et al., 2009).
The reason for the heterogeneity of expression profiles in cancer cells at different stages of tumor progression can be explained in light of our new findings. It seems that, in

cancer cells, a change in the ephrin-Eph "code" is associated with different outcomes (adhesion and invasion, de-adhesion and migration) depending on the particular stage of tumor development. Based on this concept of ephrin-Eph code, one would predict for instance that for a cell to become metastatic, its ephrin-Eph expression would need to be re-programmed at least twice: it would first adjust the levels of specific ligands or receptors to become adhesive to the cells of the surrounding tissues in order to remain well integrated and proliferate. At later stages of cancer progression, the metastatic cell would again adjust the ephrin-Eph codes to segregate from the tumor and intercalate in the surrounding tissue, and migrate. We thus offer a new way to interpret the several phases of asymmetric profile of the many ephrin-Eph pairs expressed in cancer. Decoding and understanding the significance of ephrin-Ephs level fluctuation at different steps of tumor progression will open up a challenging yet interesting field of study. Furthermore, combining the study of ephrins and Ephs -expressional patterns in both cancerous and benign tissues with information on their differential affinities, could help with the design of more specific therapeutic cocktails for cancer treatment(Brantley-Sieders, 2012; Hafner et al., 2004; Kumar et al., 2009).

Comparison of ephrin-Eph mediated cellular behaviour at different boundaries

This thesis provides the first detailed study of cellular behaviour on two boundaries of the Xenopus gastrula. The comparison of these two boundaries provides the opportunity to extract generalities and identify particularity that may relate to the different nature of these two interfaces.

We observed clear similarities in the mechanisms involved: 1) The cells facing the boundary are in direct contact with the cells of the adjacent tissue, and react specifically to this contact. 2) The core mechanism involves contact-mediated ephrin-Eph signaling. 3) The resulting cell contraction is a fundamental step for the subsequent events i.e. membrane retraction and de-adhesion, which effectively prevent cell mixing and create a sharp boundary. 4) In both cases, the same ephrin-Ephs are involved, and as mentioned above, they seem to be organized in networks that share common properties.

The main difference between the two boundaries seems to be about the extent to which the stable adhesion is lost: At the ectoderm-mesoderm interface the adhesion is repeatedly disrupted and re-established, while at the notochord-somite boundary it is permanently inhibited. These different behaviours may be related to various particularities of the two systems. In the case of the ectoderm-mesoderm boundary, mesoderm cells use the ectoderm as a substrate to crawl on as they involute. It is advantageous, in this type of movement, for cells at the boundary to continuously adhere to the ectoderm substrate and de-adhere. This will orient mesoderm cell migration on ectoderm more efficiently (Nagel, Tahinci, Symes, & Winklbauer, 2004; R. Winklbauer & Damm, 2012; R Winklbauer & Keller, 1996). Notochord and presomitic cells however, undergo mediolateral intercalation and convergent extension movements; cells within each tissue have to be able to pull on each other to elongate in a bipolar mode. As the boundary forms, notochord cells cease pulling across the interface and switch to monopolar elongation. This mechanism promotes converge and extension of both tissues and elongates the axial structure (Moore, Keller, & Koehl, 1995; Zhou, Kim, Wang, & Davidson, 2010; Keller et al., 2000; Keller et al., 1989; Shih & Keller, 1992). Local inhibition of adhesion that we discovered is probably the cause for the switch to monopolar configuration. Furthermore, the lack of adhesion favors independent movements of the two tissues, including intercalation of cells adding to the boundary interface (boundary capture) and the sliding of the two tissues to accommodate tissue elongation. In addition, each tissue type has distinct intrinsic contractile energy that can lead to behavioural differences at the two boundaries. For instance presomitic mesoderm and notochord seems to increase in stiffness about two to three fold after undergoing convergent extension movements (Keller et al., 2000). Thus the tissues across the two boundaries seem to differ in biomechanical energy.

We don't know yet with certainty the reason for the two different behaviors, but it could as well, be due to differences in the magnitude of ephrin-Eph signaling. Indeed, ligand and receptor expression levels are much higher at the later stage, which we assume is translated to different intensities of repulsive signals. This would be consistent with higher local contractility, detectable by the blebbing behavior along the notochord boundary.

Potential molecular mechanism for de-adhesion at the boundary

We propose that cortical contractility is the major parameter involved in tissue separation, and that it acts by reducing the ability of membranes to make stable adhesive contacts. The molecular mechanism underlying this hypothesis requires further investigation. There is however also evidence for a more direct link between ephrin-Eph signaling and de-adhesion: Solanas et al (2011) showed that EphB receptor activation and interaction with metalloproteinases and E-cadherin leads to E-cadherin cleavage (Solanas, Cortina, Sevillano, & Batlle, 2011). This process results in differential membrane localization of E-cadherin in ephrinB and EphB positive cells. Potentially a similar mechanism may be involved at the boundaries described in this thesis. Note however that we have not found clear signs of cadherin destabilization, as cadherin levels remain constant after ephrin/Eph depletion.

Ephrin-Eph signaling may also indirectly affect adhesion at the boundary by potential crosstalk with other parallel pathways. Non-canonical Wnt signaling, which seems to act in parallel to ephrin-Eph signaling for ectoderm-mesoderm separation is known to regulate adhesion and promote migration(Kida, Sato, Miyasaka, Suto, & Ogura, 2007; Kraft, Berger, Wallkamm, Steinbeisser, & Wedlich, 2012; Park, Cho, Kim, Choi, & Han, 2011; Ulrich et al., 2005; Rudolf Winklbauer & Luu, 2009). How these two pathways interact remains to be investigated.

Protocadherins are another type of regulators that are involved at the boundaries. The differential expression of PAPC and APC in presomitic and notochord tissues was reported to be involved in their sorting (Chen & Gumbiner, 2006; Lou, Li, Wang, & Ding, 2008). Also PAPC performs as a signaling molecule to down-regulate adhesion and affect sorting of ectoderm and mesoderm cells (Chen & Gumbiner, 2006; Chen, Koh, Yoder, & Gumbiner, 2009; Kim, Yamamoto, Bouwmeester, Agius, & Robertis, 1998; Lou et al., 2008). While there is not much known about the link between PAPC and ephrin-Eph signaling, one may assume that they converge at the level of GTPases activations to modulate adhesion and the cytoskeleton. PAPC, as a homophilic adhesion molecule, can also influence cell-cell adhesion. One may speculate that PAPC could be

involved in redistributing cadherin away from the boundary interface, in a mechanism similar to what has been proposed for Echinoid (Ed) in Drosophila (Laplante & Nilson, 2011; Wei et al., 2005). This would contribute to generate a cell polarity in terms of cell adhesion.

All these molecules and mechanisms may potentially be involved and a global picture of tissue separation will require integrating them with the ephrin-Eph code. One can imagine that different tissue types use several of these processes to de-adhere. But depending on the cellular and physical aspects of the cells involved, the extent of contribution from each of the above mechanisms can vary.

Conclusion

Impact on Tissue separation

Tissue separation has been studied for a long time and the role of several molecules has been studied on various boundaries. However, this is the first time that the details of the cell behaviour involved in the formation of the boundary have been studied in vivo. We also propose a mechanistic explanation for the observed behaviour that seems at least applicable to the three boundaries formed during gastrulation, and which is likely to apply to other vertebrate boundaries.

Impact on ephrin-Eph signaling

We show that the expression of multiple ephrin-Ephs on the same cell surface can lead to a predictable all-or-none output based on the simple principle of differential ligand-receptor affinity. This discovery questions the long lasting dogma in the field that assumed ligand-receptor “promiscuity” and “redundancy”, which had largely failed to explain complex situations and led to complicated alternative explanations. Thus this thesis may contribute to solve many other puzzling observations in neuronal, cancer and other systems that involve similar combinations of repulsive cues.

References

Abercrombie, M. (1970). Contact Inhibition in Tissue Culture. *In Vitro, 6*(2), 128-142.

Aliee, M., Röper, J.-C., Landsberg, Katharina P., Pentzold, C., Widmann, Thomas J., Jülicher, F., & Dahmann, C. (2012). Physical Mechanisms Shaping the Drosophila Dorsoventral Compartment Boundary. *Current biology : CB, 22*(11), 967-976.

Arvanitis, D., & Davy, A. (2008). Eph/ephrin signaling: networks. *Genes & Development, 22*(4), 416-429.

Arvanitis, D. N., & Davy, A. (2012). Regulation and misregulation of Eph/ephrin expression. *Cell Adhesion & Migration, 6*(2), 131-137.

Astin, J. W., Batson, J., Kadir, S., Charlet, J., Persad, R. A., Gillatt, D., . . . Nobes, C. D. (2010). Competition amongst Eph receptors regulates contact inhibition of locomotion and invasiveness in prostate cancer cells. *Nat Cell Biol, 12*(12), 1194-1204. doi: http://www.nature.com/ncb/journal/v12/n12/abs/ncb2122.html#supplementary-information

Baker, R. K., & Antin, P. B. (2003). Ephs and ephrins during early stages of chick embryogenesis. *Developmental Dynamics, 228*(1), 128-142. doi: 10.1002/dvdy.10354

Barrios, A., Poole, R. J., Durbin, L., Brennan, C., Holder, N., & Wilson, S. W. (2003). Eph/Ephrin Signaling Regulates the Mesenchymal-to-Epithelial Transition of the Paraxial Mesoderm during Somite Morphogenesis. *Current biology : CB, 13*(18), 1571-1582.

Batlle, E., Bacani, J., Begthel, H., Jonkeer, S., Gregorieff, A., van de Born, M., . . . Clevers, H. (2005). EphB receptor activity suppresses colorectal cancer progression. *Nature, 435*(7045), 1126-1130. doi: http://www.nature.com/nature/journal/v435/n7045/suppinfo/nature03626_S1.html

Batson, J., Astin, J. W., & Nobes, C. D. (2013). Regulation of contact inhibition of locomotion by Eph-ephrin signaling. *J Microsc, 251*(3), 232-241. doi: 10.1111/jmi.12024

Beysens, D. A., Forgacs, G., & Glazier, J. A. (2000). Cell sorting is analogous to phase ordering in fluids. *Proceedings of the National Academy of Sciences of the United States of America, 97*(17), 9467-9471.

Blits-Huizinga, C. T., Nelersa, C. M., Malhotra, A., & Liebl, D. J. (2004). Ephrins and their Receptors: Binding versus Biology. *IUBMB Life, 56*(5), 257-265. doi: 10.1080/15216540412331270076

Brantley-Sieders, D. M. (2012). Clinical relevance of Ephs and ephrins in cancer: Lessons from breast, colorectal, and lung cancer profiling. *Seminars in Cell & Developmental Biology, 23*(1), 102-108. doi: http://dx.doi.org/10.1016/j.semcdb.2011.10.014

Carmona Fontaine, C., Carmona Fontaine, H., Matthews, S., Kuriyama, M., Moreno, G., Dunn, M., . . . Mayor. (2008). Contact inhibition of locomotion in vivo controls neural crest directional migration. *Nature, 456*(7224), 957-961.

Carvalho, R. F., Beutler, M., Marler, K. J. M., Knoll, B., Becker-Barroso, E., Heintzmann, R., . . . Drescher, U. (2006). Silencing of EphA3 through a cis interaction with ephrinA5. *Nat Neurosci, 9*(3), 322-330. doi: http://www.nature.com/neuro/journal/v9/n3/suppinfo/nn1655_S1.html

Chen, X., & Gumbiner, B. M. (2006). Paraxial protocadherin mediates cell sorting and tissue morphogenesis by regulating C-cadherin adhesion activity. *The Journal of Cell Biology, 174*(2), 301-313. doi: 10.1083/jcb.200602062

Chen, X., Koh, E., Yoder, M., & Gumbiner, B. M. (2009). A Protocadherin-Cadherin-FLRT3 Complex Controls Cell Adhesion and Morphogenesis. *PLoS ONE, 4*(12), e8411. doi: 10.1371/journal.pone.0008411

Cheng, H., Nakamoto, M., Bergemann, A., & Flanagan, J. (1995). Complementary gradients in expression and binding of ELF-1 and Mek4 in development of the topographic retinotectal projection map. *Cell, 82*, 371 - 381.

Cheng, Y.-C., Amoyel, M., Qiu, X., Jiang, Y.-J., Xu, Q., & Wilkinson, D. G. (2004). Notch Activation Regulates the Segregation and Differentiation of Rhombomere Boundary Cells in the Zebrafish Hindbrain. *Developmental Cell, 6*(4), 539-550. doi: http://dx.doi.org/10.1016/S1534-5807(04)00097-8

Cooke, J., Moens, C., Roth, L., Durbin, L., Shiomi, K., Brennan, C., . . . Holder, N. (2001). Eph signaling functions downstream of Val to regulate cell sorting and boundary formation in the caudal hindbrain. *Development, 128*(4), 571-580.

Cooke, J. E., Kemp, H. A., & Moens, C. B. (2005). EphA4 Is Required for Cell Adhesion and Rhombomere-Boundary Formation in the Zebrafish. *Current Biology, 15*(6), 536-542. doi: http://dx.doi.org/10.1016/j.cub.2005.02.019

Cooke, J. E., & Moens, C. B. (2002). Boundary formation in the hindbrain: Eph only it were simple&. *Trends in neurosciences, 25*(5), 260-267.

Coulthard, M. G., Duffy, S., Down, M., Evans, B., Power, M., Kleikamp, S., . . . Lackmann, M. (2002). The role of the Eph-ephrin signaling system in the regulation of developmental patterning. *International Journal of Developmental Biology, 46*(4), 375-384.

Dahmann, C., Oates, A. C., & Brand, M. (2011). Boundary formation and maintenance in tissue development. *Nat Rev Genet, 12*(1), 43-55.

Davis, G. S., Phillips, H. M., & Steinberg, M. S. (1997). Germ-Layer Surface Tensions and "Tissue Affinities" inRana pipiensGastrulae: Quantitative Measurements. *Developmental Biology, 192*(2), 630-644.

Durbin, L., Brennan, C., Shiomi, K., Cooke, J., Barrios, A., Shanmugalingam, S., . . . Holder, N. (1998). Eph signaling is required for segmentation and differentiation of the somites. *Genes & Development, 12*(19), 3096-3109. doi: 10.1101/gad.12.19.3096

Flanagan, J., Flanagan, P., & Vanderhaeghen. (1998). THE EPHRINS AND EPH RECEPTORS IN NEURAL DEVELOPMENT. *Annual Review of Neuroscience, 21*(1), 309-345.

Flanagan, J. G., & Vanderhaeghen, P. (2003). THE EPHRINS AND EPH RECEPTORS IN NEURAL DEVELOPMENT. *Annual Review of Neuroscience, 21*(1), 309-345. doi: 10.1146/annurev.neuro.21.1.309

Foty, R. A., & Steinberg, M. S. (2005). The differential adhesion hypothesis: a direct evaluation. *Developmental Biology, 278*(1), 255-263. doi: http://dx.doi.org/10.1016/j.ydbio.2004.11.012

Fox, B. P., & Kandpal, R. P. (2004). Invasiveness of breast carcinoma cells and transcript profile: Eph receptors and ephrin ligands as molecular markers of potential diagnostic and prognostic application. *Biochem Biophys Res Commun, 318*(4), 882-892. doi: 10.1016/j.bbrc.2004.04.102

Gale, N. W., Holland, S. J., Valenzuela, D. M., Flenniken, A., Pan, L., Ryan, T. E., . . . Yancopoulos, G. D. (1996). Eph Receptors and Ligands Comprise Two Major Specificity Subclasses and Are Reciprocally Compartmentalized during Embryogenesis. *Neuron, 17*(1), 9-19. doi: 10.1016/s0896-6273(00)80276-7

Garrod, D. R., Garrod, M. S., & Steinberg. (1973). Tissue-specific Sorting-out in Two Dimensions in Relation to Contact Inhibition of Cell Movement. *Nature, 244*(5418), 568-569.

Gerety, S., Wang, H., Chen, Z., & Anderson, D. (1999). Symmmetrical mutant phenotypes of the receptor EphB4 and its specific transmembrane ligand ephrin-B2 in cardiovascular development. *Mol Cell, 4*, 403 - 414.

Grima, R., & Schnell, S. (2007). Can tissue surface tension drive somite formation? *Developmental Biology, 307*(2), 248-257. doi: http://dx.doi.org/10.1016/j.ydbio.2007.04.032

Guthrie, S., & Lumsden, A. (1991). Formation and regeneration of rhombomere boundaries in the developing chick hindbrain. *Development, 112*(1), 221-229.

Hafner, C., Schmitz, G., Meyer, S., Bataille, F., Hau, P., Langmann, T., . . . Vogt, T. (2004). Differential Gene Expression of Eph Receptors and Ephrins in Benign Human Tissues and Cancers. *Clinical Chemistry, 50*(3), 490-499. doi: 10.1373/clinchem.2003.026849

Haramis, A.-P. G., & Perrakis, A. (2006). Selectivity and Promiscuity in Eph Receptors. *Structure, 14*(2), 169-171. doi: http://dx.doi.org/10.1016/j.str.2006.01.005

Harbott, L. K., Marston, D. J., & Nobes, C. D. (2004). Ephrin-Regulated Contact Repulsion of Growth Cones. In M. P. P. C. Anne Ridley (Ed.), *Cell Motility* (pp. 61-74).

Harris, A. K. (1976). Is cell sorting caused by differences in the work of intercellular adhesion? A critique of the steinberg hypothesis. *Journal of Theoretical Biology, 61*(2), 267-285. doi: http://dx.doi.org/10.1016/0022-5193(76)90019-9

Herath, N. I., & Boyd, A. W. (2010). The role of Eph receptors and ephrin ligands in colorectal cancer. *International Journal of Cancer, 126*(9), 2003-2011. doi: 10.1002/ijc.25147

Herath, N. I., Spanevello, M. D., Doecke, J. D., Smith, F. M., Pouponnot, C., & Boyd, A. W. (2012). Complex expression patterns of Eph receptor tyrosine kinases and their ephrin ligands in colorectal carcinogenesis. *European journal of cancer (Oxford, England : 1990), 48*(5), 753-762.

Himanen, J., Chumley, M., Lackmann, M., Li, C., Barton, W., Jeffrey, P., . . . Nikolov, D. (2004). Repelling class discrimination: ephrin-A5 binds to and activates EphB2 receptor signaling. *Nat Neurosci, 7*, 501 - 509.

Holtfreter, J. (1939). Tissue affinity, a means of embryonic morphogenesis. Arch. Exp. Zellforsch, 23, 169-209.

Hwang, Y.-S., Lee, H.-S., Kamata, T., Mood, K., Cho, H. J., Winterbottom, E., . . . Daar, I. O. (2013). The Smurf ubiquitin ligases regulate tissue separation via antagonistic interactions with ephrinB1. *Genes & Development, 27*(5), 491-503. doi: 10.1101/gad.208355.112

Iwamasa, H., Ohta, K., Yamada, T., Ushijima, K., Terasaki, H., & Tanaka, H. (1999). Expression of Eph receptor tyrosine kinases and their ligands in chick embryonic motor neurons and hindlimb muscles. *Dev Growth Differ, 41*, 685 - 698.

Jørgensen, C., Sherman, A., Chen, G. I., Pasculescu, A., Poliakov, A., Hsiung, M., . . . Pawson, T. (2009). Cell-Specific Information Processing in Segregating Populations of Eph Receptor Ephrin–Expressing Cells. *Science, 326*(5959), 1502-1509. doi: 10.1126/science.1176615

Kao, T.-J., & Kania, A. (2011). Ephrin-Mediated cis-Attenuation of Eph Receptor Signaling Is Essential for Spinal Motor Axon Guidance. *Neuron, 71*(1), 76-91.

Keller, R., Davidson, L., Edlund, A., Elul, T., Ezin, M., Shook, D., & Skoglund, P. (2000). Mechanisms of convergence and extension by cell intercalation. *Philosophical Transactions of the Royal Society of London. Series B: Biological Sciences, 355*(1399), 897-922. doi: 10.1098/rstb.2000.0626

Keller, R., Keller, M., Cooper, M., Danilchik, P., Tibbetts, P., & Wilson. (1989). Cell intercalation during notochord development inXenopus laevis. *The journal of experimental zoology, 251*(2), 134-154.

Kemp, H. A., Cooke, J. E., & Moens, C. B. (2009). EphA4 and EfnB2a maintain rhombomere coherence by independently regulating intercalation of progenitor cells in the zebrafish neural keel. *Developmental Biology, 327*(2), 313-326.

Kida, Y. S., Sato, T., Miyasaka, K. Y., Suto, A., & Ogura, T. (2007). Daam1 regulates the endocytosis of EphB during the convergent extension of the zebrafish notochord. *Proceedings of the National Academy of Sciences, 104*(16), 6708-6713. doi: 10.1073/pnas.0608946104

Kim, S. H., Yamamoto, A., Bouwmeester, T., Agius, E., & Robertis, E. M. (1998). The role of paraxial protocadherin in selective adhesion and cell movements of the mesoderm during Xenopus gastrulation. *Development, 125*(23), 4681-4690.

Klein, R. d. (2004). Eph/ephrin signaling in morphogenesis, neural development and plasticity. *Current Opinion in Cell Biology, 16*(5), 580-589.

Kraft, B., Berger, C. D., Wallkamm, V., Steinbeisser, H., & Wedlich, D. (2012). Wnt-11 and Fz7 reduce cell adhesion in convergent extension by sequestration of PAPC and C-cadherin. *The Journal of Cell Biology, 198*(4), 695-709. doi: 10.1083/jcb.201110076

Krens, S. F. G., Möllmert, S., & Heisenberg, C.-P. (2011). Enveloping cell-layer differentiation at the surface of zebrafish germ-layer tissue explants. *Proceedings of the National Academy of Sciences, 108*(3), E9-E10. doi: 10.1073/pnas.1010767108

Krieg, M., Arboleda-Estudillo, Y., Puech, P. H., Kafer, J., Graner, F., Muller, D. J., & Heisenberg, C. P. (2008). Tensile forces govern germ-layer organization in zebrafish. *Nat Cell Biol, 10*(4), 429-436.

Kumar, S. R., Scehnet, J. S., Ley, E. J., Singh, J., Krasnoperov, V., Liu, R., . . . Gill, P. S. (2009). Preferential Induction of EphB4 over EphB2 and Its Implication in Colorectal Cancer Progression. *Cancer Research, 69*(9), 3736-3745. doi: 10.1158/0008-5472.can-08-3232

Kury, P., Gale, N., Connor, R., Pasquale, E., & Guthrie, S. (2000). Eph receptors and ephrin expression in cranial motor neurons and the branchial arches of the chick embryo. *Mol Cell Neurosci, 15*, 123 - 140.

Landsberg, K. P., Farhadifar, R., Ranft, J., Umetsu, D., Widmann, T. J., Bittig, T., . . . Dahmann, C. (2009). Increased Cell Bond Tension Governs Cell Sorting at the Drosophila Anteroposterior Compartment Boundary. *Current Biology, 19*(22), 1950-1955. doi: http://dx.doi.org/10.1016/j.cub.2009.10.021

Laplante, C., & Nilson, L. A. (2011). Asymmetric distribution of Echinoid defines the epidermal leading edge during Drosophila dorsal closure. *The Journal of Cell Biology, 192*(2), 335-348. doi: 10.1083/jcb.201009022

Lee, H.-S., Mood, K., Battu, G., Ji, Y. J., Singh, A., & Daar, I. O. (2009). Fibroblast Growth Factor Receptor-induced Phosphorylation of EphrinB1 Modulates Its Interaction with Dishevelled. *Molecular Biology of the Cell, 20*(1), 124-133. doi: 10.1091/mbc.E08-06-0662

Lee, H.-S., Nishanian, T. G., Mood, K., Bong, Y.-S., & Daar, I. O. (2008). EphrinB1 controls cell-cell junctions through the Par polarity complex. *Nat Cell Biol, 10*(8), 979-986. doi: http://www.nature.com/ncb/journal/v10/n8/suppinfo/ncb1758_S1.html

Lou, X., Li, S., Wang, J., & Ding, X. (2008). Activin/nodal signaling modulates XPAPC expression during Xenopus gastrulation. *Developmental Dynamics, 237*(3), 683-691. doi: 10.1002/dvdy.21456

Luu, O., David, R., Ninomiya, H., & Winklbauer, R. (2011). Large-scale mechanical properties of Xenopus embryonic epithelium. *Proceedings of the National Academy of Sciences, 108*(10), 4000-4005. doi: 10.1073/pnas.1010331108

Maître, J.-L., Berthoumieux, H., Krens, S. F. G., Salbreux, G., Jülicher, F., Paluch, E., & Heisenberg, C.-P. (2012). Adhesion Functions in Cell Sorting by Mechanically Coupling the Cortices of Adhering Cells. *Science, 338*(6104), 253-256. doi: 10.1126/science.1225399

Maître, J.-L., & Heisenberg, C.-P. (2011). The role of adhesion energy in controlling cell–cell contacts. *Current Opinion in Cell Biology, 23*(5), 508-514. doi: http://dx.doi.org/10.1016/j.ceb.2011.07.004

Manning, M. L., Foty, R. A., Steinberg, M. S., & Schoetz, E.-M. (2010). Coaction of intercellular adhesion and cortical tension specifies tissue surface tension. *Proceedings of the National Academy of Sciences*. doi: 10.1073/pnas.1003743107

Marquardt, T., Shirasaki, R., Ghosh, S., Andrews, S. E., Carter, N., Hunter, T., & Pfaff, S. L. (2005). Coexpressed EphA Receptors and Ephrin-A Ligands Mediate Opposing Actions on Growth Cone Navigation from Distinct Membrane Domains. *Cell, 121*(1), 127-139. doi: 10.1016/j.cell.2005.01.020

Marston, D. J., Dickinson, S., & Nobes, C. D. (2003). Rac-dependent trans-endocytosis of ephrinBs regulates Eph-ephrin contact repulsion. *Nat Cell Biol, 5*(10), 879-888.

Monier, B., Pelissier-Monier, A., Brand, A. H., & Sanson, B. (2010). An actomyosin-based barrier inhibits cell mixing at compartmental boundaries in Drosophila embryos. *Nat Cell Biol, 12*(1), 60-65. doi: http://www.nature.com/ncb/journal/v12/n1/suppinfo/ncb2005_S1.html

Monier, B., Pélissier-Monier, A., & Sanson, B. (2011). Establishment and maintenance of compartmental boundaries: role of contractile actomyosin barriers. *Cellular and Molecular Life Sciences, 68*(11), 1897-1910. doi: 10.1007/s00018-011-0668-8

Moore, S.W., Keller, R.E., & Koehl, M.A. (1995). The dorsal involuting marginal zone stiffens anisotropically during its convergent extension in the gastrula of Xenopus laevis. Development, 121(10), 3131-3140.

Nagel, M., Tahinci, E., Symes, K., & Winklbauer, R. (2004). Guidance of mesoderm cell migration in the Xenopus gastrula requires PDGF signaling. *Development, 131*(11), 2727-2736. doi: 10.1242/dev.01141

Ninomiya, H., David, R., Damm, E. W., Fagotto, F., Niessen, C. M., & Winklbauer, R. (2012). Cadherin-dependent differential cell adhesion in Xenopus causes cell sorting in vitro but not in the embryo. *Journal of cell science, 125*(8), 1877-1883. doi: 10.1242/jcs.095315

Park, E. C., Cho, G.-S., Kim, G.-H., Choi, S.-C., & Han, J.-K. (2011). The involvement of Eph–Ephrin signaling in tissue separation and convergence during Xenopus gastrulation movements. *Developmental Biology, 350*(2), 441-450. doi: 10.1016/j.ydbio.2010.12.012

Pasquale, E. B. (2004). Eph-ephrin promiscuity is now crystal clear. *Nat Neurosci, 7*(5), 417-418.

Passante, L., Gaspard, N., Degraeve, M. l., FrisÃ©n, J., Kullander, K., De Maertelaer, V., & Vanderhaeghen, P. (2008). Temporal regulation of ephrin/Eph signaling is required for the spatial patterning of the mammalian striatum. *Development, 135*(19), 3281-3290.

Phillips, H. M. (1978). Liquid-Tissue Mechanics in Amphibian Gastrulation: Germ-Layer Assembly in Rana Pipiens. *American Zoolology, 18*(1), 81-93. doi: 10.1093/icb/18.1.81

Rohani, N., Canty, L., Luu, O., Fagotto, F., & Winklbauer, R. (2011). EphrinB/EphB Signaling Controls Embryonic Germ Layer Separation by Contact-Induced Cell Detachment. *PLoS Biol, 9*(3), e1000597. doi: 10.1371/journal.pbio.1000597

Shih, J., & Keller, R. (1992). Cell motility driving mediolateral intercalation in explants of Xenopus laevis. *Development, 116*(4), 901-914.

Solanas, G., Cortina, C., Sevillano, M., & Batlle, E. (2011). Cleavage of E-cadherin by ADAM10 mediates epithelial cell sorting downstream of EphB signaling. *Nat Cell Biol, 13*(9), 1100-1107. doi: http://www.nature.com/ncb/journal/v13/n9/abs/ncb2298.html#supplementary-information

Steinberg, M. S. (1970). Does differential adhesion govern self-assembly processes in histogenesis? Equilibrium configurations and the emergence of a hierarchy among populations of embryonic cells. *J. Exp. Zool., 173*, 395–434.

Steinberg, M. S. (2007). Differential adhesion in morphogenesis: a modern view. *Current Opinion in Genetics & Development, 17*(4), 281-286.

Theil, T., Frain, M., Gilardi-Hebenstreit, P., Flenniken, A., Charnay, P., & Wilkinson, D. G. (1998). Segmental expression of the EphA4 (Sek-1) receptor tyrosine kinase in the hindbrain is under direct transcriptional control of Krox-20. *Development, 125*(3), 443-452.

Townes, P. L., & Holtfreter, J. (1955). Directed movements and selective adhesion of embryonic amphibian cells. *Journal of Experimental Zoology, 128*(1), 53-120.

Ulrich, F., Ulrich, M., Krieg, E.-M., Schötz, V., Link, I., Castanon, V., . . . Heisenberg. (2005). Wnt11 Functions in Gastrulation by Controlling Cell Cohesion through Rab5c and E-Cadherin. *Developmental Cell, 9*(4), 555-564.

Walsh, R., & Blumenberg, M. (2011). Specific and shared targets of ephrin A signaling in epidermal keratinocytes. *J Biol Chem, 286*(11), 9419-9428. doi: 10.1074/jbc.M110.197087

Wang, H., Chen, Z., & Anderson, D. (1998). Molecular distinction and angiogenic interaction between embryonic arteries and veins revealed by ephrin-B2 and its receptor Eph-B4. *Cell, 93*, 741 - 753.

Watanabe, T., Sato, Y., Saito, D., Tadokoro, R., & Takahashi, Y. (2009). EphrinB2 coordinates the formation of a morphological boundary and cell epithelialization during somite segmentation. *Proceedings of the National Academy of Sciences, 106*(18), 7467-7472. doi: 10.1073/pnas.0902859106

Wei, S.-Y., Escudero, L. M., Yu, F., Chang, L.-H., Chen, L.-Y., Ho, Y.-H., . . . Hsu, J.-C. (2005). Echinoid Is a Component of Adherens Junctions That Cooperates with DE-Cadherin to Mediate Cell Adhesion. *Developmental Cell, 8*(4), 493-504. doi: http://dx.doi.org/10.1016/j.devcel.2005.03.015

Winklbauer, R., & Damm, E. W. (2012). Internalizing the vegetal cell mass before and during amphibian gastrulation: vegetal rotation and related movements. *Wiley Interdiscip Rev Dev Biol, 1*(2), 301-306. doi: 10.1002/wdev.26

Winklbauer, R., & Keller, R. (1996). Fibronectin, mesoderm migration, and gastrulation in Xenopus. *Developmental Biology, 177*(2), 413-426.

Winklbauer, R., & Kwang, W. J. (2009). Chapter 5 Cell Adhesion in Amphibian Gastrulation *International Review of Cell and Molecular Biology* (Vol. Volume 278, pp. 215-275): Academic Press.

Winklbauer, R., & Luu, O. (2009). Frizzled-7-dependent Tissue Separation in the Xenopus Gastrula *Wnt Signaling* (pp. 485-492).

Wu, Q., Wu, G., Lind, H.-C., Aasheim, F., Micci, I., Silins, C., . . . Suo. (2007). The EPH Receptor Bs (EPHBs) Promoters are Unmethylated in Colon and Ovarian Cancers. *Epigenetics, 2*(4), 237-243.

Wybenga-Groot, L. E., Baskin, B., Ong, S. H., Tong, J., Pawson, T., & Sicheri, F. (2001). Structural Basis for Autoinhibition of the EphB2 Receptor Tyrosine Kinase by the Unphosphorylated Juxtamembrane Region. *Cell, 106*(6), 745-757. doi: http://dx.doi.org/10.1016/S0092-8674(01)00496-2

Xu, Q., Alldus, G., Holder, N., & Wilkinson, D. G. (1995). Expression of truncated Sek-1 receptor tyrosine kinase disrupts the segmental restriction of gene expression in the Xenopus and zebrafish hindbrain. *Development, 121*(12), 4005-4016.

Xu, Q., Mellitzer, G., & Wilkinson, D. G. (2000). Roles of Eph receptors and ephrins in segmental patterning. *Philosophical Transactions of the Royal Society of London. Series B: Biological Sciences, 355*(1399), 993-1002.

Zhou, Jian, Kim, Hye Young, Wang, James H.-C., & Davidson, Lance A. (2010). Macroscopic stiffening of embryonic tissues via microtubules, RhoGEF and the assembly of contractile bundles of actomyosin. Development, 137(16), 2785-2794. doi: 10.1242/dev.045997

Zimmer, G., Rudolph, J., Landmann, J., Gerstmann, K., Steinecke, A., Gampe, C., & Bolz, J. (2011). Bidirectional EphrinB3/EphA4 Signaling Mediates the Segregation of Medial Ganglionic Eminence- and Preoptic Area-Derived Interneurons in the Deep and Superficial Migratory Stream. *The Journal of Neuroscience, 31*(50), 18364-18380. doi: 10.1523/jneurosci.4690-11.2011